RESISTIVITY TESTING
OF
PILED FOUNDATIONS

BY

WILLIAM JOHN McCARTER

B.Sc.

A thesis submitted for the Degree of

Doctor of Philosophy

UNIVERSITY OF EDINBURGH

1981

DECLARATION

I hereby declare that the following thesis has been composed by me, that the work has been carried out by myself and that it has not been presented in any previous application for a higher degree.

ABSTRACT

An investigation has been undertaken of an electrical resistance technique for use as a non-destructive testing method in Civil Engineering, with particular reference to fault-detection in concrete load-bearing piles.

The problems facing the piling contractor and Engineer with regard to pile construction and pile selection for a load-testing programme are described. Present non-destructive pile testing techniques are critically reviewed and the role of the non-destructive test in relation to pile selection for load-testing examined. Several electrical methods are examined and an earth-resistance technique selected for detailed study.

The work reported is both theoretical and experimental. A number of electrical analogue experiments has been designed to confirm and illustrate the application of the theoretical analysis and methodology of fault detection. In addition, experimental programmes have been undertaken to identify and study the factors which determine the electrical properties of concrete and soil.

From the experimental and field results obtained using the earth-resistance technique it is shown that a determination of the integrity of a pile-soil system can be made.

ACKNOWLEDGEMENTS

The author wishes to thank Professor A.W. Hendry, Head of the Department of Civil Engineering and Building Science, and Professor J.H. Collins, Head of the Department of Electrical Engineering, for placing the facilities of their respective Departments at his disposal.

The author is particularly grateful to Dr. M.C. Forde and Dr. H.W. Whittington for their supervision. Their suggestions, criticism and constructive comments have been invaluable in the preparation of this thesis.

Robert Matthew, Johnson-Marshall and Partners are to be thanked for providing access to the I.B.M. site at Greenock.

The author is indebted to fellow students Simons and Campbell for undertaking some of the experimental work; the Librarian, Mrs. V. Thomson for tracking down many obscure references and Mrs. C.A. Laurence who typed this thesis with very creditable speed and accuracy.

The author wishes to express his thanks to his parents for their help, patience and encouragement at all times.

The financial support of the Department of Education for Northern Ireland is gratefully acknowledged.

LIST OF CONTENTS

The Text is divided into Chapters and Sections. Sections are numbered decimally within each Chapter; the numbers given to Figures indicate to which Chapter or Appendix they belong, but are not related to the Section numbers.

PAGE

CHAPTER 5 THE ELECTRICAL PROPERTIES OF CONCRETE

CHAPTER 1

INTRODUCTION

1.1 Foundations Types

The foundation of a structure is defined as that part of the structure in direct contact with the ground and which transmits the load of the structure to the ground. There are, basically, four types of foundation used for Civil Engineering purposes, these being:

(a) isolated or pad foundations, which are usually provided to support individual structural columns. They can take the form of a square, circular or rectangular slab of uniform thickness, or they may be stepped or haunched to distribute the load from a heavily loaded column. Various forms of pad foundations are shown in Figure 1.1.

(b) continuous or strip footings, which are normally used for load-bearing walls or when it is necessary to control the magnitude of differential settlements between columns supported on individual pad footings. This type of foundation would also be used, from a purely economic point of view, when columns are so closely spaced that individual pad foundations would almost touch each other. (Fig. 1.2).

(c) raft foundations are used on soils of low bearing capacity or when the loads are so large that continuous footings would occupy close to 50% of the projected area of the building. (Fig. 1.3).

(d) piled foundations are used when the ground conditions cannot support pad, strip or raft foundations. Piled foundations derive their load carrying capacity from either end-bearing and/or

skin friction components of resistance. The use of piles overcomes a number of design difficulties which are briefly mentioned in the next section. (Fig. 1.4)

The final selection of any particular type of foundation depends on the site in question and the type of structure or building to be constructed. Selection of the correct type of foundation is important since this will ultimately affect the stability and settlement characteristics of that particular structure.

1.2 Piled Foundations

Every building or structure must ultimately transfer its load into the ground to the extent that the stress the foundation transmits into the soil is less than the permissible bearing capacity of that particular soil. The upper layers of the earth's surface do not always provide the required degree of firmness and the load from the structure must be transmitted to the lower firmer layers. The use of piles is one means of accomplishing this quickly and economically.

The use of piles not only obviates shear failure but overcomes a number of problems which the foundation engineer may be confronted. It is not surprising that many thousands of piles are used in the United Kingdom, in fact, two million linear metres of piles are constructed annually (1). Piles can be used to:

(a) reduce overall settlement,

(b) reduce differential settlement,

(c) absorb lateral loads and moments,

(d) provide support through water,

(e) provide support from a limited area,

(f) allow early construction on compacted fill,

(g) absorb fluctuating loads, and

(h) underpin.

If a piled foundation is chosen, then the next problem is the selection of the most appropriate pile type. The selection of the most appropriate pile type (2) (Fig. 1.5) for any given set of circumstances listed above depends on many variables, particularly the type of subsoil, which will dictate whether the pile be either skin-friction or end-bearing.

Other variables that have to be taken into account in pile selection are:

(a) the topography of the site,

(b) the location of the site in relation to noise and nuisance effects,

(c) speed of construction,

(d) transport and materials,

(e) the size and form of the proposed structure, and,

(f) cost of pile installation.

If the above variables are not considered during the design stage then difficulties can arise during the construction phase.

1.3 The Problem of Pile Integrity

Engineers cannot readily assure themselves that piled foundations

conform to design dimensions, that the concrete conforms to design specifications, and, in the case of skin-friction piles, that the pile-soil system is as anticipated. In the case of cast-in-situ piles, problems of integrity can arise due to unforeseen subsoil conditions and/or undetected poor quality workmanship. The incidence of such faults as complete voids, overbreak, necking and poor quality concrete cannot be completely eliminated even by using experienced contractors and good supervision. The detection of soft-spots, which reduce the load carrying capacity of skin-friction piles, cannot be completely assured with conventional site investigations.

The conventional approach of load-testing piles has the advantage of yielding the bearing capacity of the pile under test and a load-deformation curve, but has the major disadvantage of costing about £1,000 - £5,000 per pile. In consequence, only a small proportion of a pile population would be load tested.

An alternative approach is to test the piles using a non-destructive technique which is less expensive, quick and can be applied to every pile on a given site. Suspect piles thus detected could be subjected, selectively, to traditional load-tests. It would also be advantageous if the non-destructive test method could be undertaken as soon as possible after the pile has been constructed, thereby allowing corrective measures to be taken in the event of a defective pile being found.

When an Engineer, on site, accepts that a piled foundation conforms completely to specification, and that every pile is continuous and homogeneous, he must be aware of the consequences if he makes a mistake. It could be catastrophic even if only a few piles were

defective as this would lead to excessive settlement and perhaps complete failure of the structure.

There are several incidences of such failures, one being of a five-storey office block in Canada, which, when nearing completion, tilted 25 cm. On probing, discontinuities in the piles were discovered and the building had to be demolished and reconstructed (3).

In a building in New York similar defects developed, but fortunately the defective piles were discovered before construction of the superstructure and remedial measures were taken, thus preventing a potentially serious structural collapse. Althogether 32 piles out of a total of 1,500 were found to be defective, in some cases the length of the discontinuity exceeding 10 metres. All completed piles were rejected and the contract was delayed by one year (3).

At the John Hancock Center in Chicago several defective piles were discovered by core-drilling, the discontinuities exceeding 5 metres (4, 5).

Construction of the Esso oil refinery at Fawley, Southampton suffered severe delay and additional cost when the foundation of one of the largest oil storage tanks in Europe settled excessively when undergoing a water-loading test. Failure was due to a combination of bad workmanship and lack of appreciation of the variations in the subsoil (6).

1.4 The Approach Adopted

The work described in this thesis examines a non-destructive testing

technique for determining pile integrity. Research has been directed towards the development on an electrical earth-resistance technique to fulfil the above requirements. The earth-resistance technique has been referred to by Bobrowski et al (3) when it was used on a site in London. This is the only reported use of this technique on site. No experimental or theoretical justification of the method has been published, although it showed promise (7,8).

The work describing the earth-resistance technique was both theoretical and experimental. Experimental programmes were undertaken to verify theoretical predictions of the variables involved.

Finally, an alternative methodology for pile testing, based on a combination of electrical resistance, non-destructive testing, and conventional load-testing is developed.

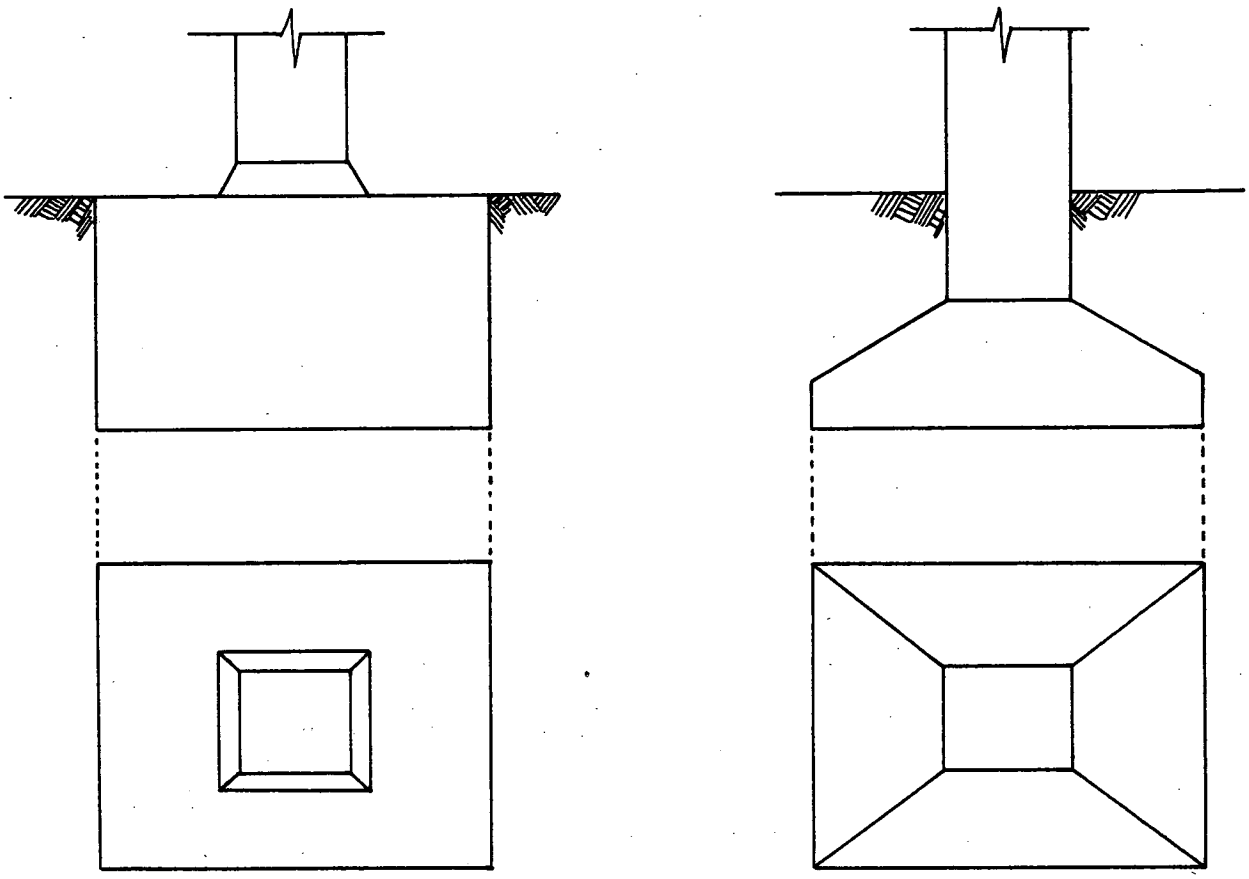

FIG. 1.1 Types of Pad Foundation

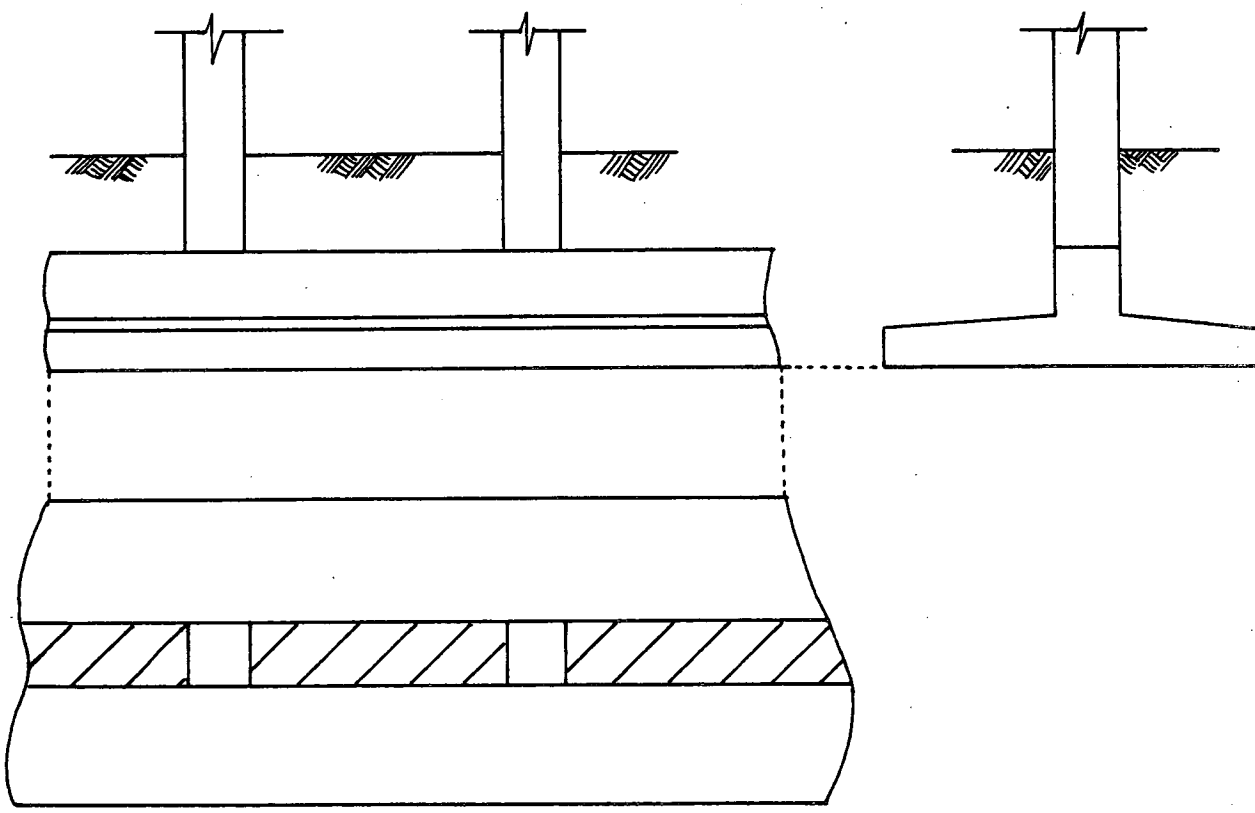

FIG. 1.2 Continuous or Strip Foundation

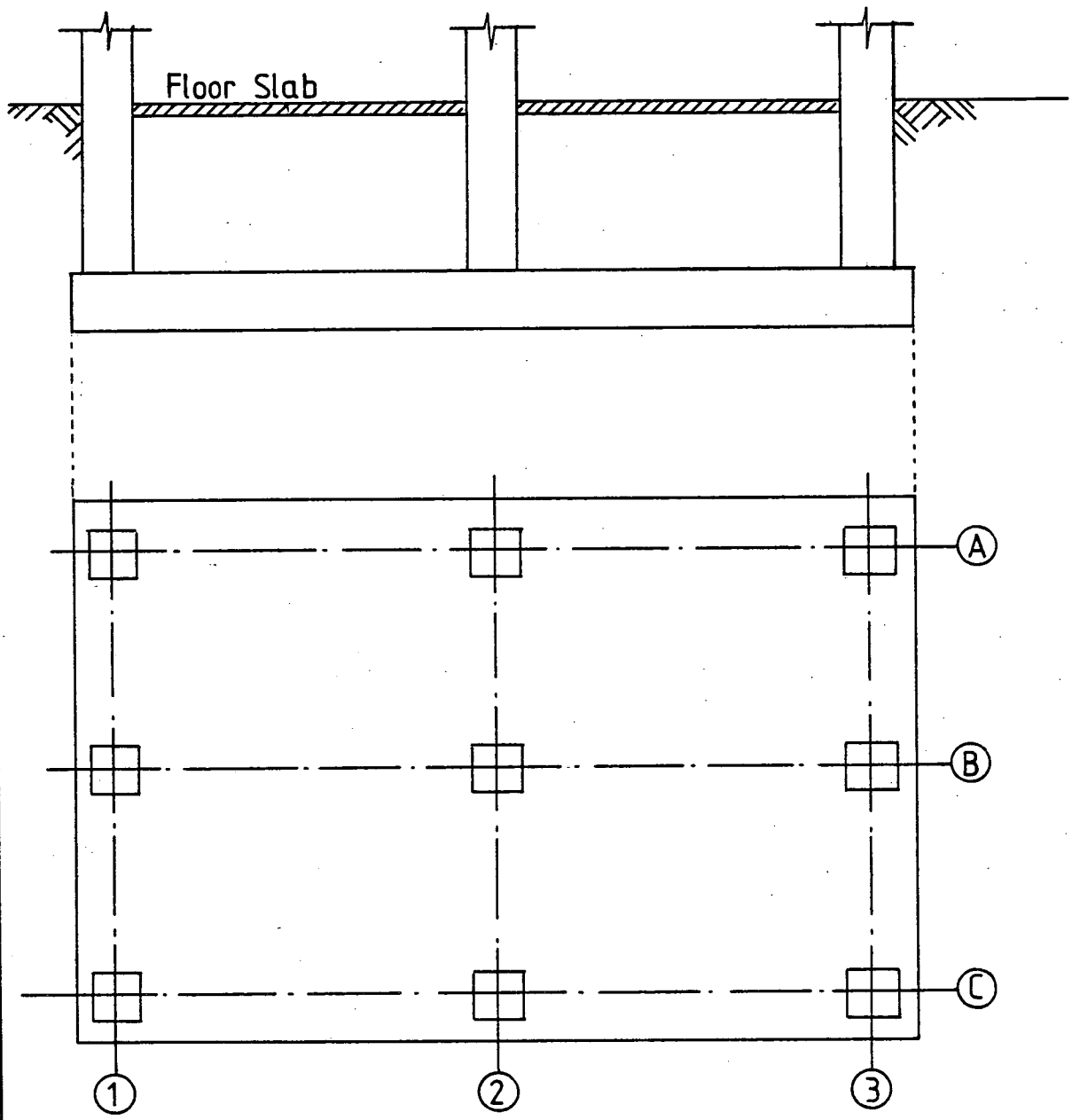

FIG. 1.3 Raft Foundation

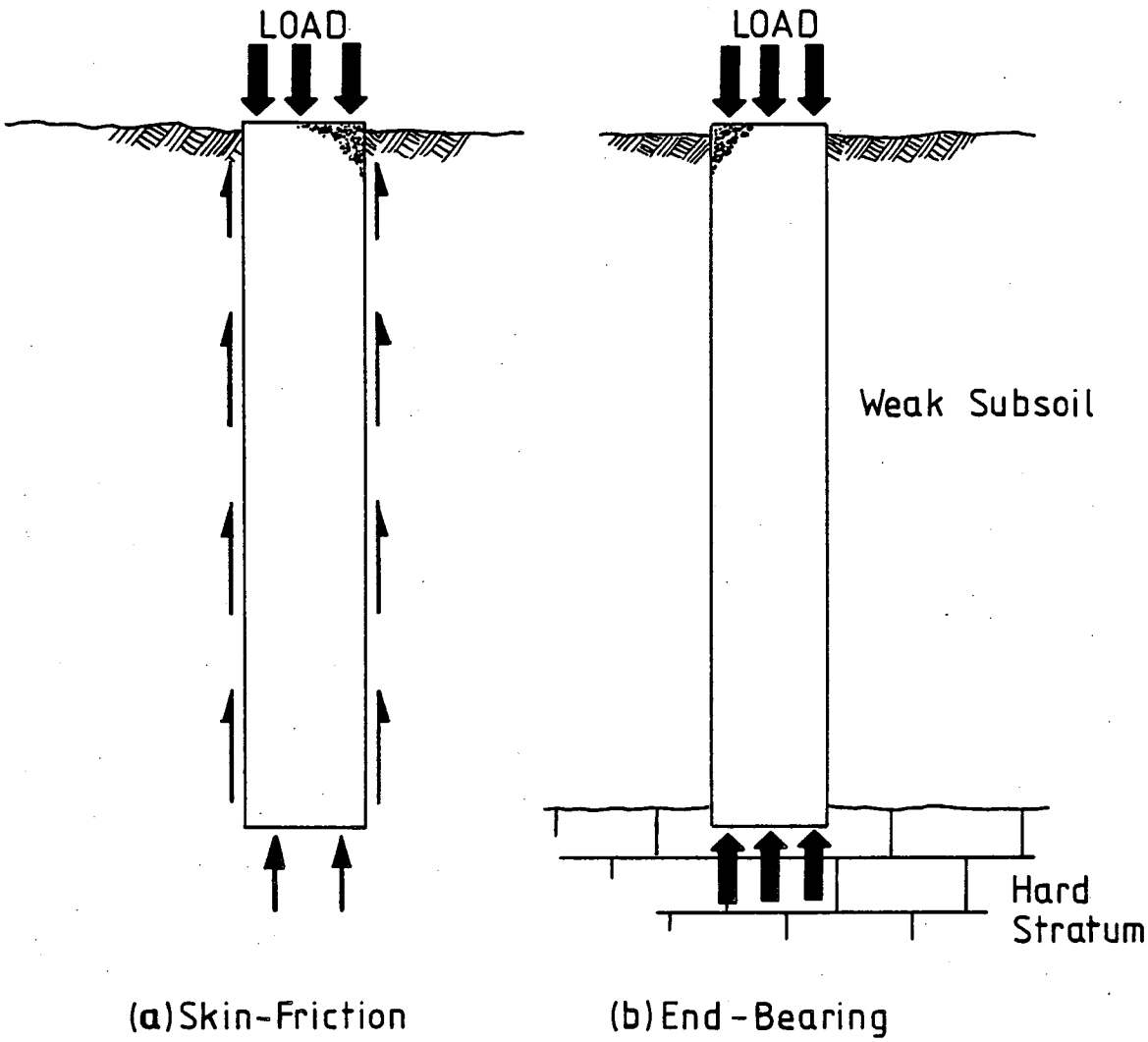
LOAD
LOAD
Weak Subsoil
Hard
Stratum
(a) Skin-Friction
(b) End-Bearing

FIG. 1.4

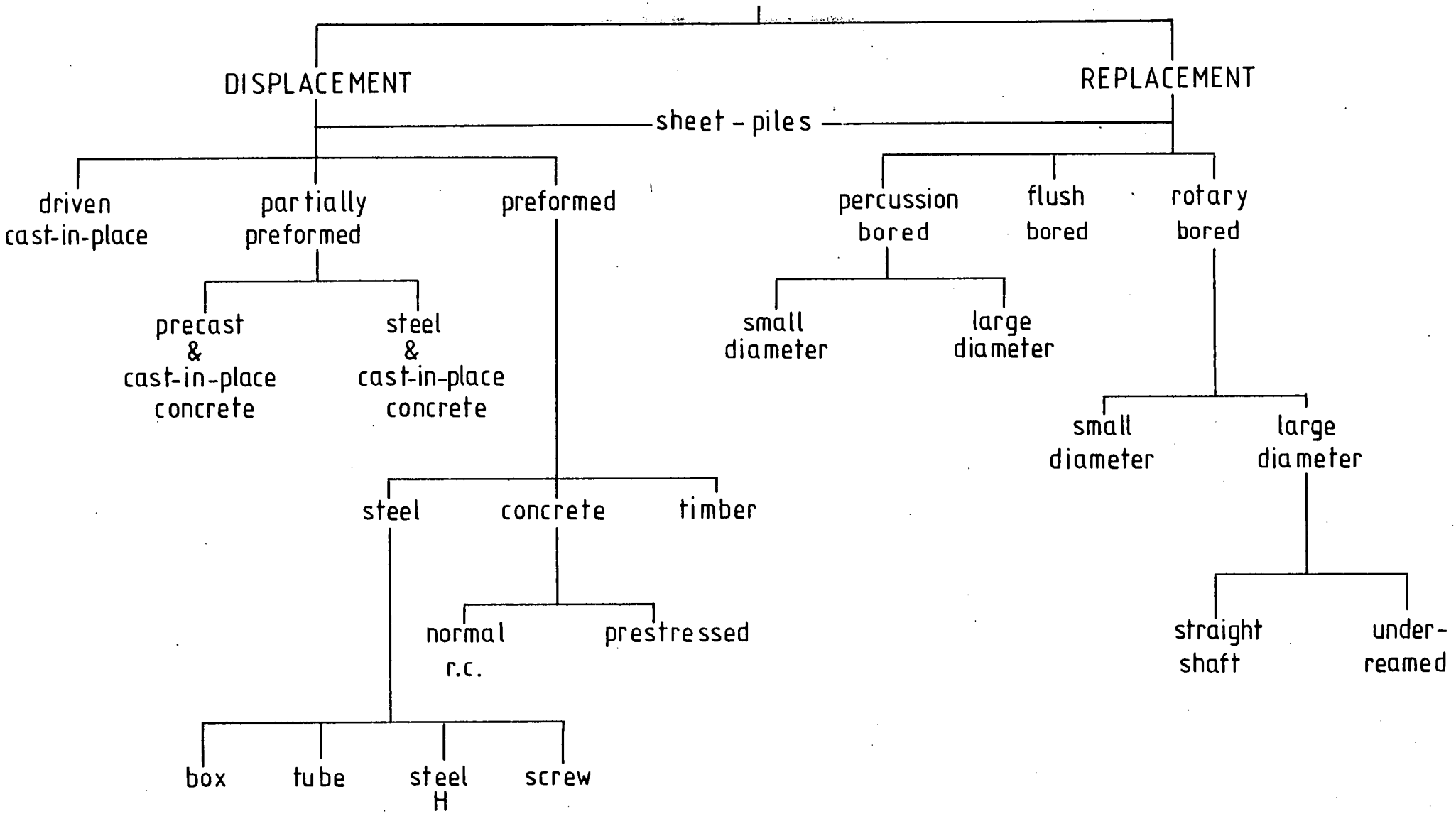

FIG. 1.5 Types of Piles in common use[2]

CHAPTER 2

A GENERAL REVIEW OF PILE TESTING

2.1 Introduction

Unlike most other structural members, a pile, once placed, cannot be seen. Visual inspection of piles is impracticable therefore methods of testing the integrity or quality of the pile in the ground are required. There are two aspects of pile quality to consider:

(a) the load-bearing capacity of the pile - soil system viz. the pile design. This is usually checked by preliminary load tests which are constructed prior to the main contract, and,

(b) the structural soundness of the pile as a load-bearing unit, which is currently checked by contract working load tests.

It is during the latter when non-destructive integrity tests may be advantageously employed.

2.2 Constructional Faults Associated With Piled Foundations

Two variables are concerned in the evaluation of the integrity of a piled foundation - the structural homogeneity and continuity of the pile itself and the nature of the soil surrounding the pile. Examination of the soil will have been undertaken at the site investigation stage of the contract and, consequently, there will be some appreciation of the local variation over the site. However, due to the random nature with which boreholes are selected, it is possible for problems such as weak clay pockets to go undetected.

This section identifies the constructional problems associated with

piled foundations.

2.2.1. The Precast Pile

One of the principal problems associated with precast piles is unseen breakage in the buried portion of the pile due to driving. Damage is caused either by compressive or tensile failure of the concrete. In the case of compressive failure, crushing or shearing of the pile shaft will result for a pile which is seated on a hard stratum. When the pile deviates from alignment, breakages due to tensile bending forces can result with the lower portion of the pile projecting at an oblique angle.

Precast concrete piles which consist of units jointed together (e.g. Herkules) are even more susceptable to deviation from vertical alignment. In such circumstances the pile may break up into separate units with a complete loss of bearing capacity.

With driven piles, however, the driving log should provide corroborative evidence of irregularity of the soil as well as any damage to the pile shaft itself. It is with cast-in-situ piles that most problems occur.

2.2.2. The Cast-In-Situ Pile

Cast-in-situ piles are usually constructed using a shell and auger or auger boring techniques. The auger excavates the soil from the pile bore and a steel cylindrical casing stops the sides of the pile bore from collapsing. Drilling continues to the required depth with the casing advancing to that depth. A reinforcing cage is then lowered down the pile bore and the shaft concreted, the casing being withdrawn during the concreting process. It is during the extraction of the

temporary casing and during the initial setting period that most faults occur.

2.2.2.1 Shaft Separation

One of the most serious problems associated with the extraction of the temporary casing is complete separation of the pile shaft. This can occur when a low-slump concrete is specified and/or when the period of time between placing the concrete and extraction of the temporary casing is in excess of two hours (1). If these conditions exist, then the frictional forces between the casing and the concrete during extraction may be of such magnitude that the concrete and the reinforcing cage may be lifted and complete shaft separation will occur at the bottom edge of the casing. If the reinforcing cage is securely embedded in the lower portion of the concrete shaft, only the concrete outside the shaft is lifted.

2.2.2.2 Overbreak

Overbreak is another serious problem which can affect pile preformance and is the removal of material outside the nominal pile periphery and results in local cavitation when the casing is withdrawn. Overbreak during the formation of the pile bore is thought to be responsible for more defects than almost any other cause (1).

Overbreak usually occurs when drilling through unstable or weak water-bearing strata. When the auger advances through the strata there exists the possibility of sidewall collapse into the pile bore. As the casing advances, the cavity is, effectively, sealed off when the

concrete is being poured. This cavity can become filled with ground-water and, if such a situation exists, the effect can be detrimental to the pile shaft.

During extraction, as the bottom edge of the casing reaches the elevation of the water filled cavity, the concrete can flow into the cavity mixing with the water thereby creating a weak section in the pile shaft. If the concrete has a low workability then, with the casing withdrawn, a temporarily stable column of concrete will remain. The ingress of water into the concrete can cause segregation with the annulus of concrete outwith the reinforcement slumping into the cavity. The water may penetrate the body of the pile shaft and a complete water filled discontinuity can occur. Plate 1 illustrates such a defect.

2.2.2.3 Honeycombing

Once the casing is completely withdrawn, the concrete is still relatively weak, and infiltration of ground-water under a sufficient hydraulic gradient can cause serious problems to the pile shaft during this initial setting period. What usually results, under these circumstances, is that the fines viz. fine aggregate and cement are washed out leaving severely weakened concrete. This is commonly called honeycombed concrete (9) . Plate 2 illustrates the effect of ground-water.

2.2.2.4 Reinforcement Detailing

The serious defects resulting from concrete containment by dense reinforcement cages warrants consideration, especially when used in conjunction with a low-workability concrete. When the above are

specified in a contract, the concrete may fail to flow out through the gaps in the reinforcement cage, the result of which is a pile whose reinforcement has little or no cover. Furthermore, the forces induced in the vertical steel rods and the horizontal binders by the pressure of the concrete can rupture the reinforcement cage with the result that, a reinforcement cage, which initially projected above cut-off level, disappears (1) . When such events occur there is the temptation by site operators to compensate for the loss of starter bars by individually pushing vertical rods into the concrete. (Plate 3).

2.2.2.5 Waisting Of The Pile Shaft

Waisting or necking of the concrete in the pile shaft can occur due to soil pressure on the relatively weak, liquid concrete, resulting in a reduction or even elimination of the concrete cross-sectional area (10) .

2.2.2.6 Mix-Design Specification

Unsuitable mix-design results in many unforeseen difficulties for the piling contractor, several have already been mentioned; however, yet another difficulty that can arise by a rigid specification of a low-slump concrete is one of compaction. Inadequate densification of the concrete results in arching with the result that voids and air pockets develop within the concrete.

Another cause of defective piles which cannot be ruled out is defective concrete being delivered or batched on site. The cause of

bad concrete may be due to a mixup in design mixes, i.e. a low strength mix substituted, accidentally for a required high strength design mix. The cause may also be an error at the batch plant in the proportions of cement, sand and gravel or water. In the case of drier mixes, site operators may be tempted to add water to facilitate and speed up compaction of the concrete.

2.2.2.7 Inadequate Supervision

Piles which do not conform to design dimensions either through misunderstanding or lack of supervision cannot be completely ruled out.

2.3 Pile Quality Control Testing

In the case of displacement piles, an indication of the soundness of the pile can be gained from the record of driving resistance and the set at full driving depth. For replacement piles, it is the usual practice to carry out a limited number of contract load-tests which will usually disclose any gross defects and will also verify the load-bearing characteristics of the pile-soil system.

2.3.1 Load Testing

Load-tests are generally performed by simply jacking against kentledge placed over the pile head or against anchor piles sunk on either side of the pile under test. (Fig. 2.1) This is the traditional method of proving the structural integrity of piled foundations. As already mentioned, testing covers two distinct stages in the evaluation of a piled foundation,

(a) test suitability of pile design in the particular soil, and

(b) test workmanship.

As part of the design phase, several test piles will be constructed on a site, usually where the ground conditions are considered to give minimum bearing capacity, or where any other particular problems are present. These piles are then loaded to a specified multiple of the working load. Successful loading confirms bearing capacity and settlement under load. At this stage the pile design, if necessary, may be modified.

There is little alternative to these expensive preliminary load tests, but it forms an essential contribution to the design process. Throughout the piling operation contract load-tests are carried out on constructed working piles to,

(a) confirm preliminary load test results in proving design suitability, and,

(b) check on the quality of pile construction.

Load tests on working piles may be selected using random or grid sampling techniques or where difficulty has been encountered during installation. Typically, only 0.5% to 5.0% of a pile population would be load tested, with a realistic figure being about 1%, and selection is usually random despite what may appear to be a considered choice (11).

Load tests suffer from the major disadvantages that,

(a) they are expensive and time consuming,

(b) because of (a) only a few piles are usually tested and this number is often not large enough to give statistically significant results,

(c) because of (b) load tests can be regarded as measuring the performance of the test piles only and do not serve to locate faulty piles,

(d) test piles are seldom loaded up to failure,

(e) they are seldom carried out in such a way that the relative contributions of end resistance and skin-friction can be determined,

(f) they yield no information on the dimensions of the pile in the ground and only confirm that the pile is structurally strong enough to carry the test load without giving any measure of concrete quality,

(g) more care may be taken by the contractor in installing piles that are preselected for testing so that results can be misleading, and,

(h) the pile is often discarded after test and not included as part of the foundation.

There is thus a need in the construction industry for the development of less expensive test methods which will help in assessing the quality of the pile in the ground.

2.3.2. The Integrity Test

The integrity, or Non-Destructive Test (N.D.T.), is a tool which can be used by the Engineer in appraising some aspect of the quality of the pile and should, therefore, be regarded more as a means of quality control than a complete substitute for load-testing. Nonetheless, the main advantage of a N.D.T. is that if such a test could be used to check every pile on site (blanket testing) then it could help in assessing the relative preformance of every pile. Furthermore, the integrity test could be used as a complementary test with informed selection for load-testing. A practical implication of such an idea would mean that the Engineer, on site, can formulate a more rational approach to any quantative testing programme.

A N.D.T. has to meet certain requirements before being considered viable for use in the field, it must be:

(a) easy to operate,
(b) give reliable results which can be easily interpreted,
(c) relatively inexpensive so that it can be used on the total pile population,
(d) cause no delay on site, and,
(e) require no instrumentation to be incorporated within the pile or prior preparation to the pile head.

Techniques which can yield information relating to the pile-soil system would be valuable as the overall behaviour of the pile is also a function of the interaction between the pile and the subsoil in which it is constructed. A pile may be constructed to specification but

fail due to the nature of the context around the pile not shown up at the site investigation stage of the contract.

If an integrity test could be used on the total pile population, then piles which give anomalous results could be selected for further quantitative investigation. If the integrity test results can be obtained in numerical or graphical form then results can be compared visually without resorting to detailed mathematical analysis. In this way the distribution of test results would give an indication of the relative performance of all the piles permitting a much better appreciation of the integrity of the entire population.

Characteristic similarity in the results obtained from a particular group or groups of piles on site should also be recognised; for example, the recognition of a particular pattern common to all or most of the piles. Significant departures from the general trend may give indications that the pile is suspect. It is to be emphasised that irregularity in itself is not a sign of a defective pile, but only when the irregularity occurs in one, or a few of the piles, and not in the group as a whole. If a pile gives a markedly different response, it should, in the first instance, be compared with the neighbouring piles. This will immediately show whether the characteristic is one of the site rather than one of the individual pile.

System calibration using results from known non-defective piles (i.e. preliminary test piles) may also be advantageously employed and, in this way, relative integrities can be assessed. Figure 2.2 (12) shows how non-destructive testing techniques may be incorporated into pile testing procedure.

2.3.3 Discussion - Philosophy of Testing and the rôle of the Integrity Test

The assurance of product quality in the building industry has long been a problem to both contractors and consultants. As uncertainties are unavoidable in the design and planning of engineering projects, inspection and standards of acceptance are necessary in order to ensure some minimum level of performance of the product. To this end, load-tests have been developed to check pile design and construction. If this test is too stringent it may needlessly increase the cost of the pile, but if too lax, the quality of the pile may be well below the minimum required.

Working load-tests usually involve testing a small sample out of a large number of piles. The information obtained from this sample is then used to make generalisations about the population from which the sample was obtained viz. the ratio of sound to defective piles in this test sample is then used by the Engineer to give an idea of the number of defective piles expected in the total pile population. Obviously the larger the sample the closer the predicted result will approach the actual, but as this will be both expensive and time consuming the Engineer has to decide - what piles to test and how many to test. This is a particularly pertinent question when the pile population is large.

If several defective piles are present in a large population the chances of selecting a defective pile by traditional methods would be small. (See Appendix I) The test sample might well contain only sound piles, which would then imply that the remainder of the population is sound.

If defective piles are included in this test sample then doubts are immediately raised about the integrity of the entire population and the situation thus becomes even more uncertain. One would require to establish whether the entire population was defective or whether the load-test hit on the one defective pile. Clearly more tests would have to be conducted before construction proceeded. Money spent on proving that a pile can take a specified multiple of its working load is expensive and of finite value since the successful loading of one pile yields almost no information about its neighbour. However, if it is felt the pile has doubtful integrity then the expense would be justified.

2.4 A Review Of Present Integrity Testing Methods

Over the last few decades many new methods of integrity testing have been developed. The techniques available are reviewed and discussed in this section under the following headings:

(a) Excavation,
(b) Exploratory boring and drilling,
(c) Closed circuit television methods,
(d) Acoustic methods,
(e) Radiometric methods,
(f) Sonic Echo Method,
(g) Dynamic response methods,
(h) Integral compression test,
(i) Electrical methods.

2.4.1 Excavation

As its name implies, inspection of a pile by excavation entails clearing soil from around the pile head, usually by means of a mechanical digger. This method, although not strictly an integrity test, would only be contemplated if the top few metres were thought to be unsound. This method is inconvenient and can cause delays in the construction programme especially if a battered excavation has to be used and pumping is required to remove water from the excavation. Excavation would only be used in exceptional circumstances such as a dispute over a foundation failure.

The obvious advantage of excavation is that reliable evidence as to the condition of the exposed part of the pile is obtained, but suffers from the disadvantages that,

(a) it is expensive, and costs escalate below depths of 1.2m when temporary support is required,
(b) the method is not suitable for blanket testing, and
(c) it cannot be used for skin friction piles.

2.4.2 Exploratory Coring and Drilling

Drilling by rotary percussion equipment can be used for integrity testing. By carefully monitoring the rate of progress of the drilling bit and the colour and quantity of the flushing media, indications as to the homogeneity of the pile shaft can be deduced (10, 11, 13). The main advantages of drilling are,

(a) the full length of the pile may be examined, and,

(b) the drill holes may be utilised for further tests e.g. T.V. inspection.

Disadvantages of rotary percussive drilling are that,

(a) the drilled hole will only detect defects in its path and to inspect a pile adequately several holes would have to be drilled,

(b) difficulties are encountered in maintaining a plumb drilling line, and,

(c) the cost can be high, approximately £20/metre (11) .

More information can be obtained from coring the pile shaft albeit more expensive than drilling. The core obtained is adequate in itself to detect voids or breaks and in addition, a direct assessment of the concrete in the pile may be made. As with drilling, difficulty in maintaining a vertical alignment and speed of drilling (0.5 metre/hour) are major drawbacks. The cost of coring is about £60/metre.

Blanket testing of a pile population by these methods would be prohibitively expensive, and testing would necessarily have to be selective in nature.

2.4.3 Closed-Circuit Television Methods and Caliper Logging

On a site where extensive percussion drilling has been carried out, a proportion of the holes may be selected for television scanning, perhaps for confirmation of an existing defect or where the extent of the

discontinuity is very small.

The disadvantages of television inspection are,

(a) only defects intersected by the drilled hole are viewed and detected,

(b) treatment of cloudy, water filled drill holes with flocculating agents may lead to delays, and,

(c) considerable distortion of an irregularity can occur as the television camera is very close to the walls of the drill hole.

In addition to using the drilled hole for T.V. inspection, it may also be used for caliper logging. In this case the diameter of the drill hole should be between 50mm and 200mm. A probe with three arms set at 120^{o} apart is lowered down the borehole, while a pen recorder traces the diameter of the drilled hole via potentiometers with a surface read-out. In this way defects of a moderate size may be detected.

Closed circuit television methods and caliper logging are only used in conjunction with, rather than as an alternative to, coring. Typical costs are in the range of £1 to £5/metre (11) in addition to the cost of drilling the inspection hole.

2.4.4 Acoustic Methods - Sonic Coring

This method has been developed by the Centre Experimental de Recherche et d'Etudes du Bâtiment et des Travaux Publics (C.E.B.T.P.) and consists of testing the continuity of the concrete in the pile shaft by

sonic transmission between several vertical tubes cast into the pile at the time of construction (14, 15, 16) . Three tubes, usually made of metal or plastic, are placed in a triangle with only two tubes being used at any one time. Transducers are lowered down the tubes and a sonic pressure wave is transmitted from one transducer and received by the other, the transmitter and receiver being raised and lowered together. The tubes are filled with water to provide contact between the transducers and the wall of the tube and to ensure an acoustic coupling. (Fig. 2.3 (a)).

The time of transmission between the tubes depends on the distance between the tubes and the modulus of elasticity of the material through which the sonic pulse travels. Since the velocity of sound is greater in good concrete than it is in poor concrete, and is reduced in varying degrees by soil, water and air discontinuities, variations in the nature of the material through which the pulse passes will be revealed. With this method, the full length of the pile is scanned and a high accuracy of pinpointing faults achieved (3, 17) .

The disadvantages of the sonic coring method are,

(a) it will detect only those defects located along the path of the sonic wave (Fig. 2.3 (b)), thus defects located outwith the direct path may go undetected,

(b) a reluctance from piling contractors to cast inspection tubes into the piles at the time of construction (18), and,

(c) the cost of the pile is increased by approximately £20/metre for

3 metal tubes.

Testing of a large pile population by this technique would have to involve preselection as blanket testing would be expensive.

2.4.5 Radiometric Methods

A drawback in a number of integrity testing methods is the delay in waiting for the concrete to achieve suitable strength before any test can be carried out. Methods based on nuclear radiation may be used on fresh concrete but, as with sonic coring, guide tubes must be cast into the pile at the time of construction. They, thus, suffer from the disadvantage of pre-selection - or the provision of tubes in all piles.

Two general methods are possible; gamma ray backscattering using a single tube cast into the pile or neutron or gamma ray transmission using a twin tube method. Neutron transmission varies with moisture content of the media through which it is transmitted and is, therefore, sensitive to clay inclusions in the pile shaft. Gamma ray transmission responds to changes in density of the medium through which it passes, but a strong source is required for transmission across a pile using a twin tube method. The gamma-ray backscatter method, in which a relatively weak source is used, has been most widely used in piling applications.

This system is described by Preiss and Caisserman (19) and the arrangement of equipment used by them is shown in Figure 2.4. A radius of about 100-150mm around each vertical hole may be examined by this method and a density profile, based on this number of photons back-

scattered, can be obtained.

The disadvantages of radiometric techniques are that,

(a) to inspect a pile several tubes may have to be provided at a cost of approximately £8/metre/tube, (11) and,

(b) the method would only be suitable for preselective testing.

2.4.6 Sonic Echo Method

This technique entails transmitting a sonic wave impulse down the longitudinal axis of the pile (20-23) . The pile head is struck by a hammer blow and a transducer, mounted on top of the pile, responds to the impulse via surface waves (Rayleigh waves) developed at the pile head and later registers the arrival of the reflected wave from the pile base or discontinuity, if one exists.

The trace is usually displayed on an oscilloscope and photographed. A typical system is shown in Figure 2.5 (22, 23). The time interval between the initial impulse at the pile head and the reflected signal, t_c, is measured, and, knowing the velocity of sound in concrete, V_c, an apparent pile length can be calculated ($V_c.t_c$). The signal is attenuated very quickly in concrete, hence the depth may be limited. To make the method effective for lengths in excess of 10 metres it is necessary to have a transducer placed at the bottom of the pile (3) which would increase costs.

Some difficulty in interpretation of the trace records has been reported, especially when strong surface waves develop and mask the reflected signal.

Signal processing techniques could possibly be used to eliminate much of this unwanted noise (24, 25). On average 20-30 piles/day could be tested at a cost of about £5/pile.

2.4.7 Dynamic Response Methods

In dynamic methods, a vibration or shock is applied to the pile and the frequency response of the pile is monitored over a selected frequency spectrum. Early attempts at dynamic testing have been reported by Dořák (26), but perhaps the most widely used dynamic method is that which has been developed by C.E.B.T.P. in France (15, 16, 27) - the vibration method.

In the C.E.B.T.P. method the pile is vibrated using an electrodynamical vibrator placed on the prepared and level pile head. A constant amplitude, sinusoidal input current is supplied by a sine wave generator, the frequency of which may be varied from 20 to 1,000 Hz. A velocity transducer, mounted separately on the pile head, is used to monitor the vertical velocity of the head (Fig 2.6 (a)). The signal from this transducer gives a measure of the mechanical admittance of the pile head i.e. the velocity of the pile head divided by the applied force. A signal proportional to the mechanical admittance is plotted on an X-Y recorder against frequency of vibrator. A typical response curve is shown in Figure 2.6 (b). Reflections from the pile base, or discontinuities, produce peaks of resonance which are equally spaced at intervals of frequency $\Delta f = V_c/2L$, where V_c is the velocity of wave propagation in concrete. By assuming values for V_c, the length may be estimated; also, the mean value of mechanical admittance in the resonant portion gives an indication of the pile cross-sectional area,

if an average concrete density is assumed. Gardner and Moses (28) give details of the application of the vibration technique and also give some guidance on the interpretation of the test results.

A shock technique employing a series of hammer blows to the top of the pile head and employing the same theory as the above method, has been developed by Higgs (29) of C.E.P.T.B. Fast Fourier analysis methods are used and the response curve obtained is similar to that obtained by the vibration technique.

Advantages of the method are that,

(a) the method does not require preselection,

(b) under suitable conditions it is possible to compute pile length or distance to a major discontinuity. In certain circumstances, pile/soil stiffness at low stresses may be estimated.

Disadvantages of the vibration method are that,

(a) prior preparation to the pile head is required a few days before the test,

(b) it is not suitable for piles which are founded in soils that are very stiff laterally due to their high damping effect,

(c) the length to diameter ratio of the pile should not exceed 20,

(d) analysis of results requires skilled interpretation and piles with large overbreaks have been found to produce anomolies (13),

(e) the cost of the test is about £50/pile.

2.4.8 Integral Compression Test

A method of integrity testing which applies the full working load to the pile has been proposed by Moon (30). In principle, the method is that of applying a compressive force over a length of the pile by the stressing of internally cast (and recoverable) rods or cables. If the pile is significantly weakened by any form of fault this becomes apparent by a downward movement of the top of the pile in the case of a fault nearer the top; or by a greater elongation of the stressing element than that due to stressing alone, indicating an upward movement of a lower section in the case of faults nearer the base. Figures 2.7 (a) and (b) illustrate the method.

The advantage of this technique is that the pile is stressed to a realistic level so that the effect of discontinuities is appraised in a practical way. However, the disadvantages are that,

(a) the method is expensive and is estimated to add 12% onto the cost of the pile, (in 1972 a 400 tonne test on a 13.7 metre pile was quoted by Moon to cost £66), and,

(b) the provision of internally cast ducts or sheathing for the prestressing cables may involve pre-selection of the piles to be tested.

2.4.9 Electrical Methods for Integrity Testing

The electrical methods discussed in this section are, essentially, standard geophysical techniques which are used for near surface geology determination. For example, geophysical techniques have been applied

to Civil Engineering site investigation (31, 32) in the determination of the depth to bedrock (33, 34, 35). The objective of this section is to show how these techniques can be adapted to test the integrity of a pile-soil system and to show the relative merits of each technique.

There are four possible electrical methods (3, 11, 36), all have the common feature of forming a circuit between the pile reinforcement and an electrode placed outwith the pile. They are,

(a) Spontaneous Polarisation or Self Potential.

(b) Earth-Resistivity.

(c) Induced Polarisation.

(d) Earth-Resistance.

2.4.9.1 Self-Potential

The self-potential method differs from the other electrical methods in that no electrical field is applied to the pile-soil system. Measurement is made on the natural potential difference which will generally exist between the pile reinforcement and another electrode placed in the ground. (Fig. 2.8) These potentials will be partly fluctuating and partly constant and are due to such phenomena as electro-filtration, pH differences and electro-osmosis. For example, the reinforcement acquires a potential against the concrete (37), and the contact between the concrete and the ground will also produce an e.m.f. due to the differing electrical properties of the two media in contact with each other (38).

The measurement of self potentials are relatively simple. Referring to Figure 2.8, any millivoltmeter with a sufficiently high input impedance may be connected between the reinforcement and an electrode driven into the ground. This electrode must be of the non-polarizable (N.P.) type as ordinary metal stakes are not satisfactory since electrochemical action at their contact with the ground tends to obscure the natural potentials associated with the pile.

Perhaps the single, main disadvantage of the method is that slowly varying natural earth currents can mask the potential one is trying to measure. Also, the need for non-polarising electrodes is another disadvantage as they are cumbersome to use in the field. Difficulty in theoretical analysis, quantification and interpretation of the results would be a problem and would virtually preclude this method.

2.4.9.2 Earth-Resistivity

This method is based on the standard Wenner (39) 4 - electrode array used in geophysical exploration. Referring to Figure 2.9, a current is applied between the pile reinforcement and electrode C_1, while the resulting potential distribution on the ground is measured between a second pair of inner, potential electrodes (P_1P_2). The potential measured at the ground surface will be indirectly related to the pile-soil system. However, the exact relationship between the variables would be difficult to ascertain.

Faults, either in the pile itself or in the composition of the soil around the pile, will alter the potential distribution on the surface near the pile head. Since the measuring electrodes (P_1P_2) are

placed outwith the pile periphery anomalies may go undetected. Space requirements of the electrode arrangement make this method unattractive.

2.4.9.3 Induced Polarisation

This method can best be explained by reference to Figure 2.10 (a). A single direct current pulse (Fig. 2.10 (b)), or a series of square wave pulses separated by equal time intervals during which no current flows (Fig. 2.10 (c)), is supplied to the system via the reinforcement, R, and an electrode, B, placed in the ground. Following the termination of the current, or during the time when no current is flowing, the relaxation voltage is measured across R and M. It will quickly drop to a value V_{max}, and after this initial drop the voltage will decay over a period of time (40) . The magnitude of this voltage at any time, t, or its integral over a period of time is then taken to indicate the degree of polarisation of the pile-soil system. If a series of pulse amplitudes is used for each pile then one could obtain a response spectrum for that pile. It is visualised that defective piles would be represented by having different decay rates from non-defective piles.

To obtain measurable decay rates, however, the electrode spacings would have to be large. At such spacings deep geological features could affect results and anomalies go undetected. There are also practical difficulties if the site is restricted and there is a limited amount of space around the pile head. Furthermore, theoretical analysis of the situation would be extremely complex. As with the self potential

method, stray earth currents can affect results, and non-polarising electrodes are required.

2.4.9.4 Earth-Resistance

This method was chosen for detailed study. There are several possible methods for measuring the earthing resistance of a pile which are discussed in the next chapter. A theoretical analysis, relating the resistance measured at the ground surface and the physical dimensions of the pile in the ground, is also developed in the next chapter. This particular technique has several advantages over the other electrical methods described, these being,

(a) an approximate theoretical analysis is possible, hence, the interrelationship between the system variables can be deduced, and the effect of changing, say, pile dimensions, quantatively assessed. Such analysis is not possible with the other methods.

(b) stray earth-currents can be eliminated by instrumentation design. These earth-currents can, as already indicated, affect the self-potential and induced-polarisation results,

(c) space requirements for electrodes can be adapted for the particular site,

(d) non-polarising electrodes need not be used.

2.5 Discussion

Many of the integrity tests described in section 2.4 suffer from the disadvantage of having to cast tubes in the pile at the time of construction or prior preparation to the pile head. This, in turn, means that any integrity testing programme using such methods requires pre-selection of the pile. Extra care may be taken by contractors in installing piles that are pre-selected for testing so that results could be misleading. Drilling or coring, although not requiring guide tubes, is too expensive and time consuming to be contemplated for testing every pile on a given site. Of the present available techniques, sonic echo and shock methods seem best suited to blanket testing and need only a minimal amount of preparation to the pile head. However, with these methods there has to be a time interval of several days between casting the pile and testing. There is thus scope for the development of methods which could be used on freshly cast piles and, generally speaking, a need in the construction industry for the ... 'development of relatively simple, reliable and inexpensive methods of establishing the structural integrity of piles, with particular reference to methods which do not require special means of instrumentation to be incorporated in the piles at the time of construction. Over-sensitivity of equipment should be discouraged, since the existence of minute defects in piled foundations is inevitable' (1).

Due to the expense involved with any load-testing programme non-destructive tests may be advantageously employed. The use of integrity tests, in conjunction with load-tests, would help give the

Engineer, on site, a better appreciation of,

(a) possible piles for working load-tests, and,

(b) the relative integrities of the piles not load-tested.

Appreciating the problems of both the Engineer and the contractor the approach detailed in section 2.3.2 is more logical than the present state of the art. From the Engineer's point of view, he will have a better knowledge of the relative performance of every pile.

2.6 Summary

This Chapter has outlined the problems that can be encountered during the construction of a piled foundation. Defects in piled foundations will only be eliminated by good site practice and supervision during concrete pours coupled with selection of the correct pile type for the particular site. Nonetheless, there is always the possibility of faults occurring and some form of testing is essential.

The present non-destructive testing techniques outlined nearly always require some form of preselection and there is thus a growing interest in the development of methods not suffering from such an inherent disadvantage. Four experimental electrical methods, based on standard geophysical techniques, are described showing possible measurement procedures and adaption for pile integrity testing. The merits and demerits of these electrical techniques are assessed and the earth-resistance method selected for detailed study.

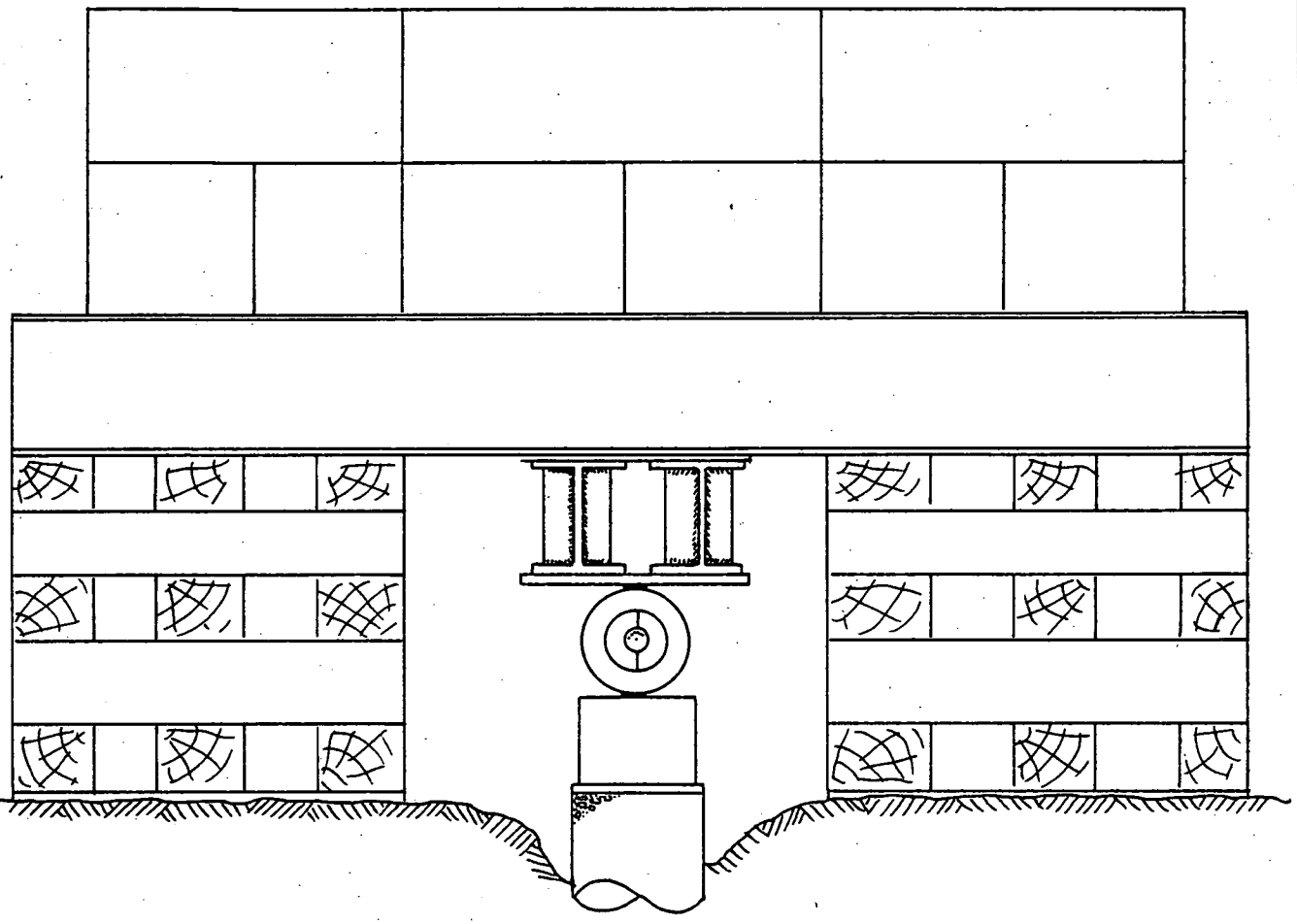

(a)

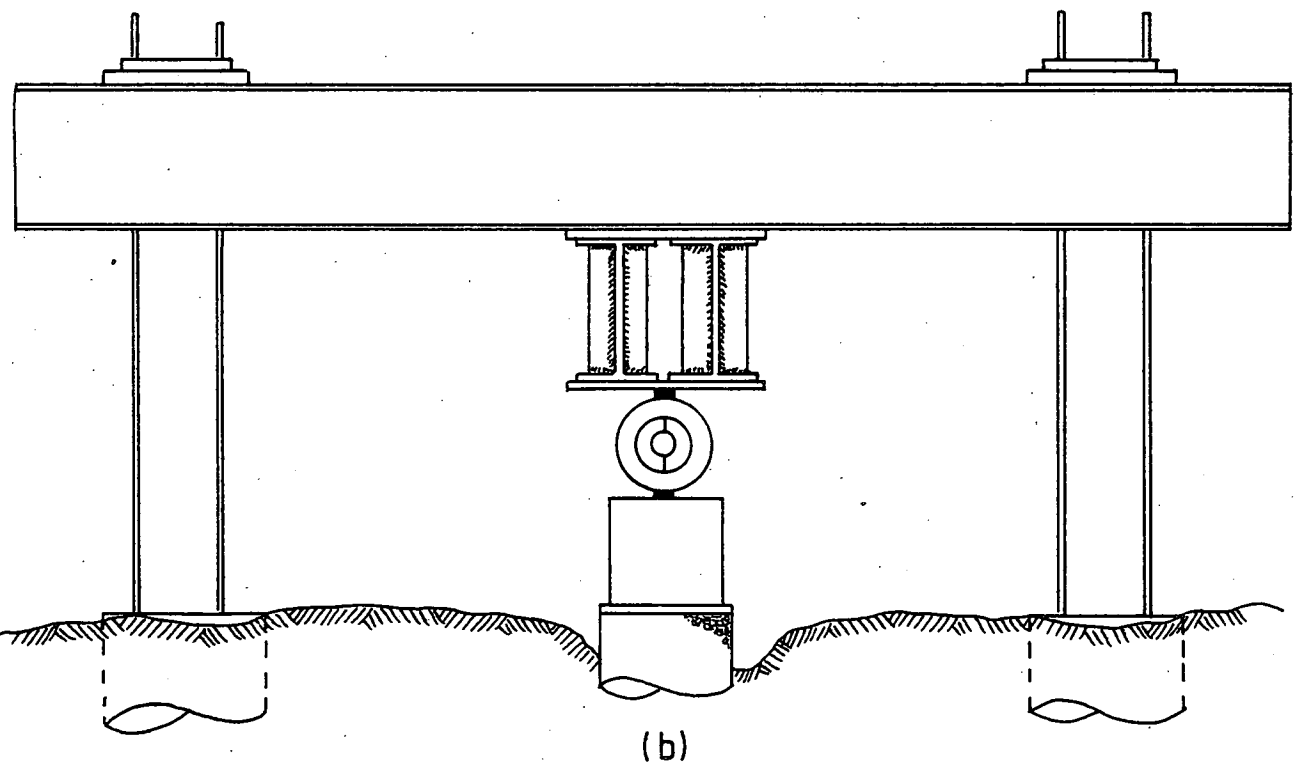

(b)

FIG. 2.1 (a) Kentledge Reaction System and
(b) Anchor Pile System

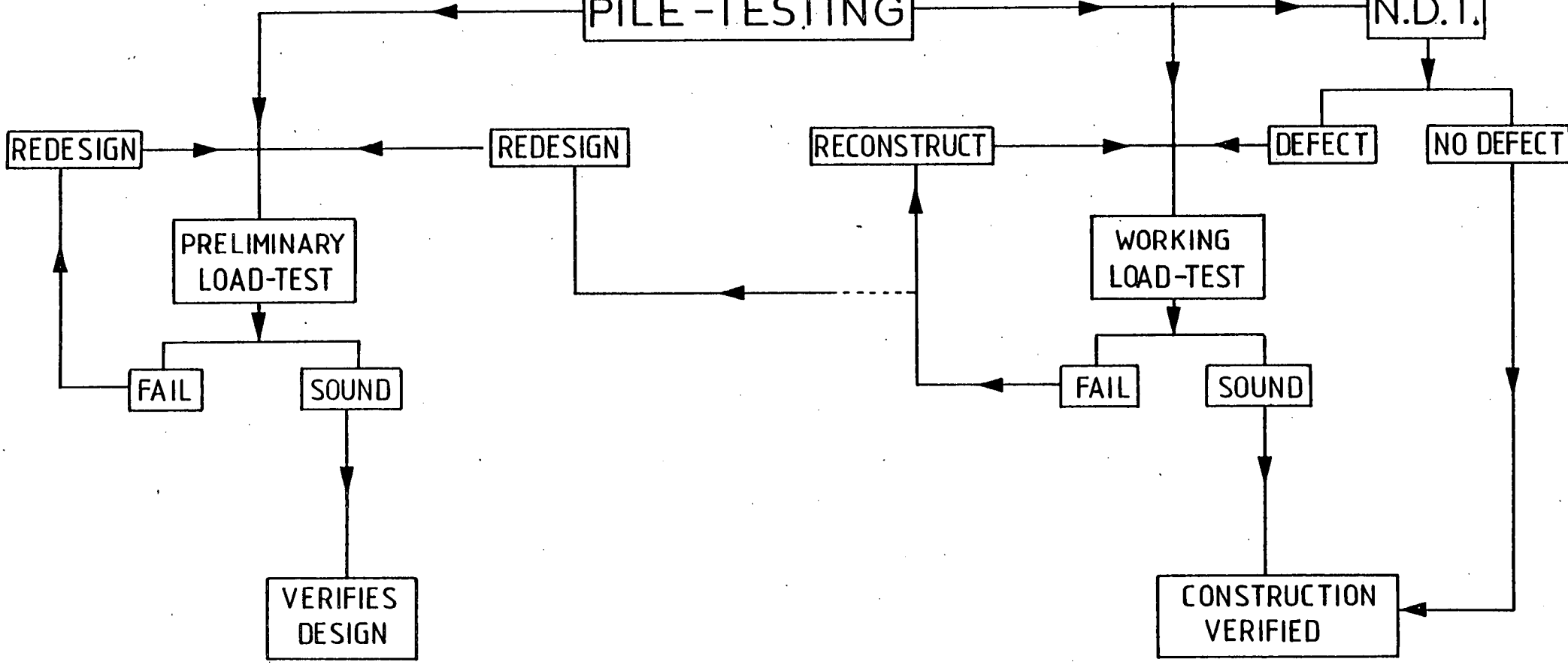

FIG. 2.2 Sequences involved in Pile Testing

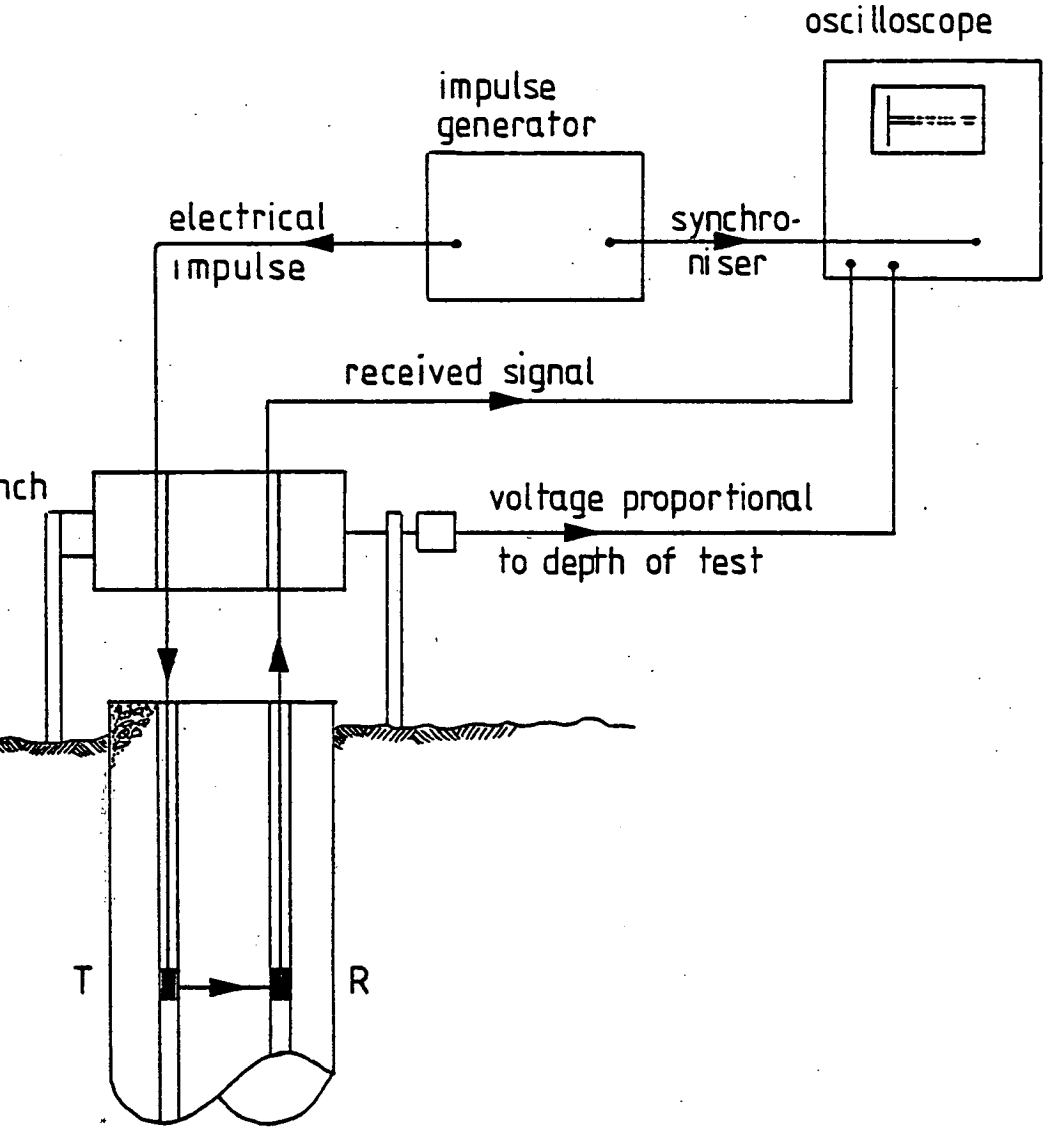

(a) General arrangement of sonic coring apparatus

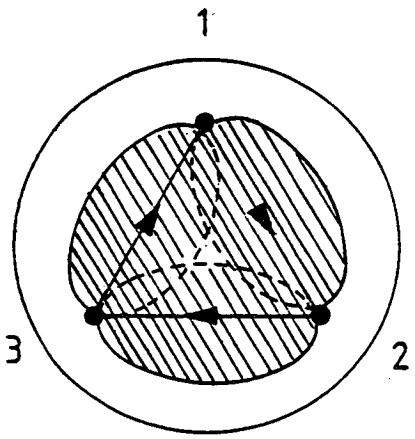

(b) Path of sonic wave and zones of influence in the case of three tubes

FIG. 2.3 The Sonic Coring Method

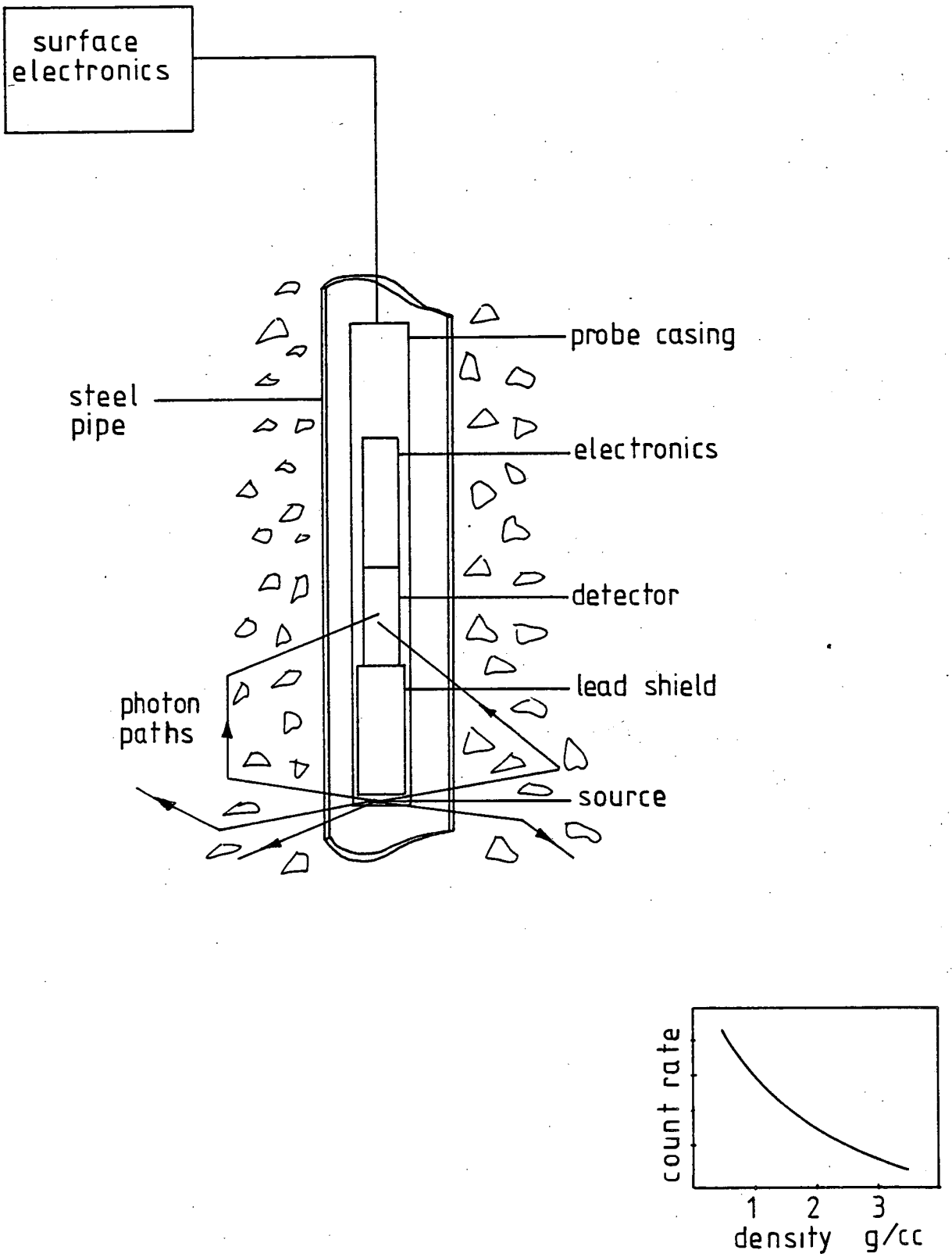

FIG. 2.4 The Gamma Ray Backscatter Method

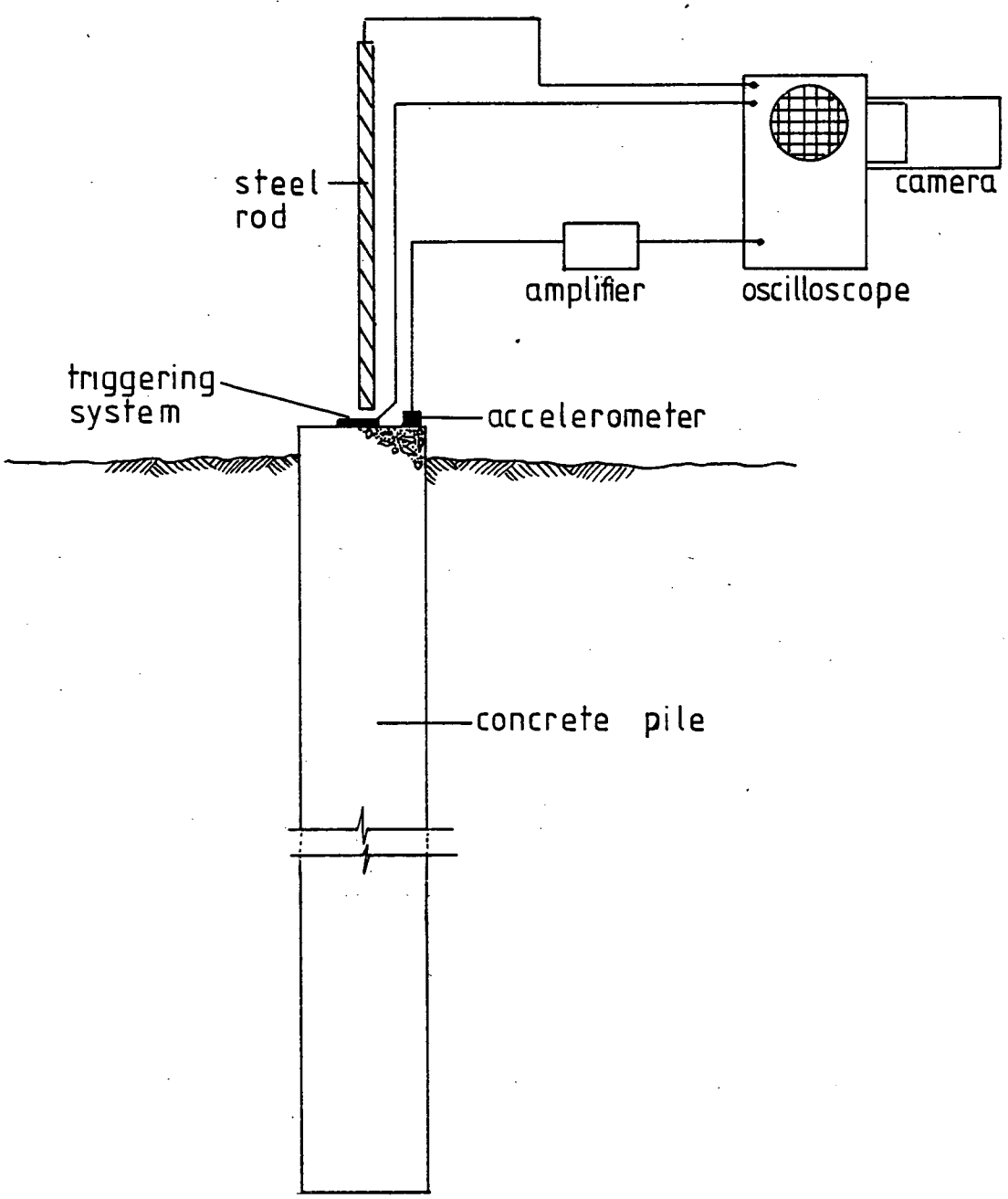

FIG. 2.5 Schematic diagram of Sonic Echo Method

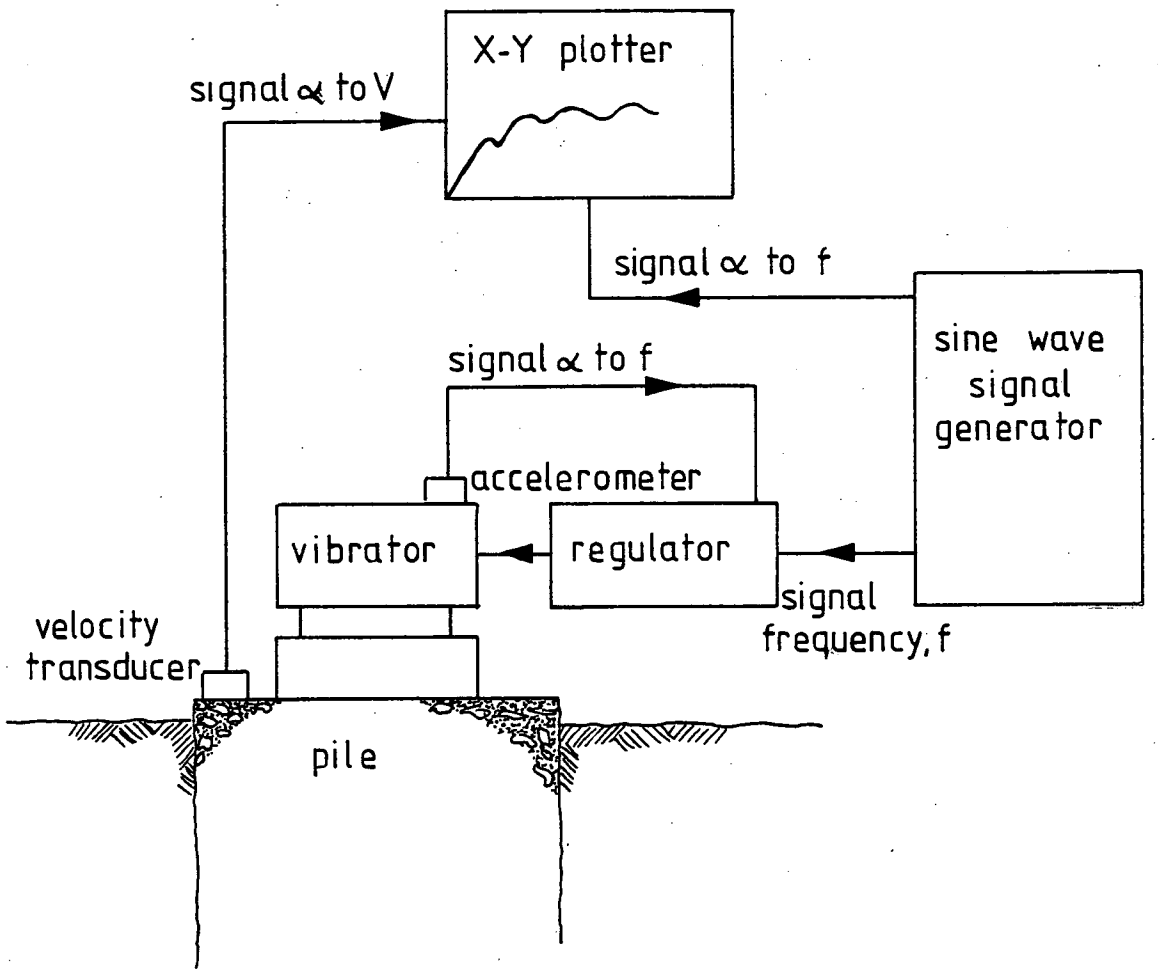

(a) Schematic diagram of the vibration method

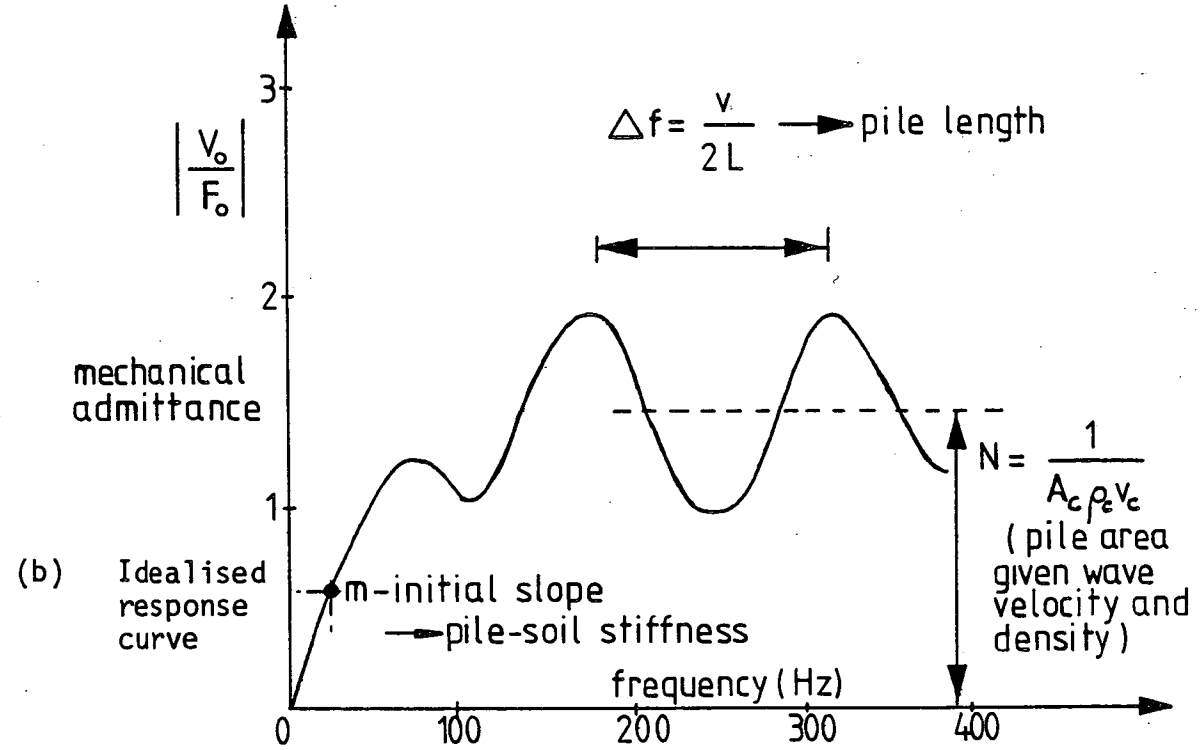

(b) Idealised response curve

FIG. 2.6 The Vibration Method

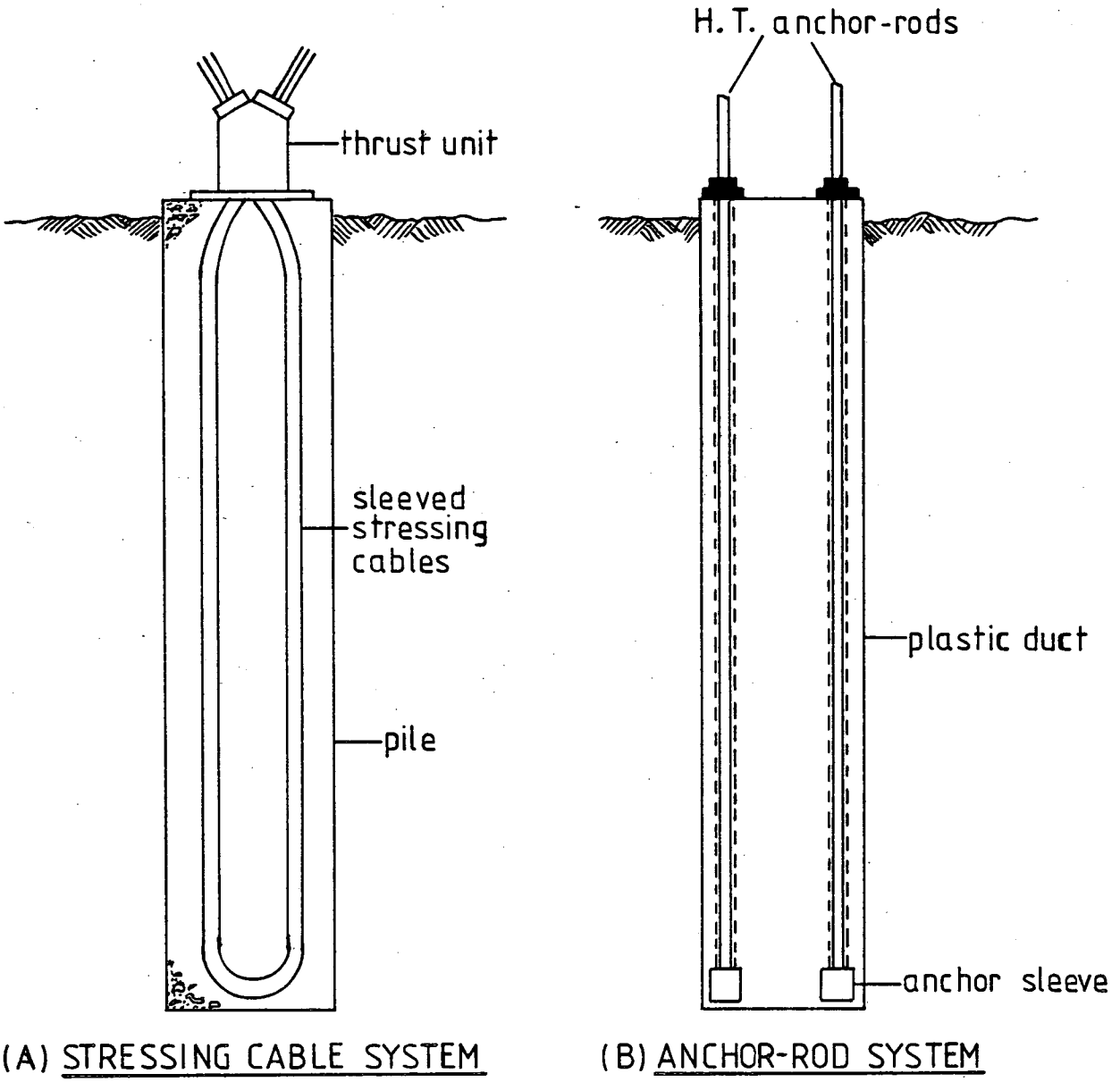

FIG. 2.7 The Integral Compression Test

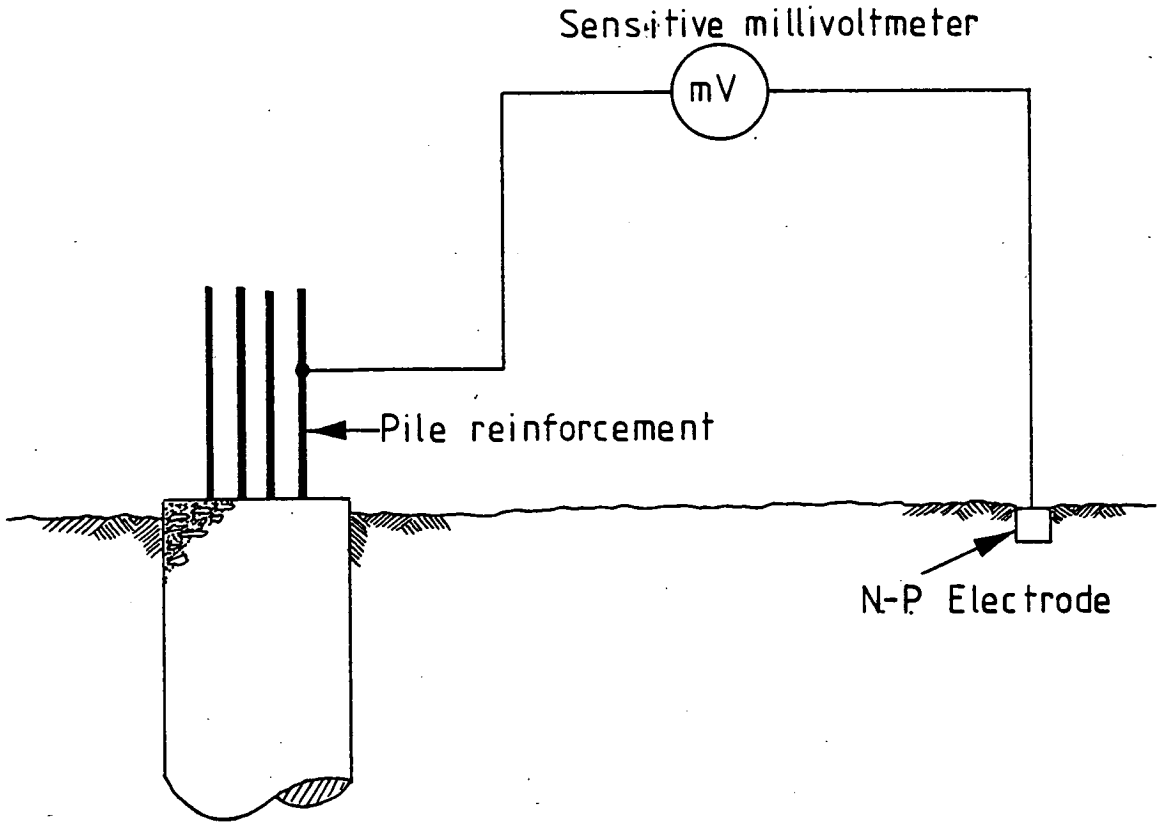

FIG. 2.8 The Self-Potential Method

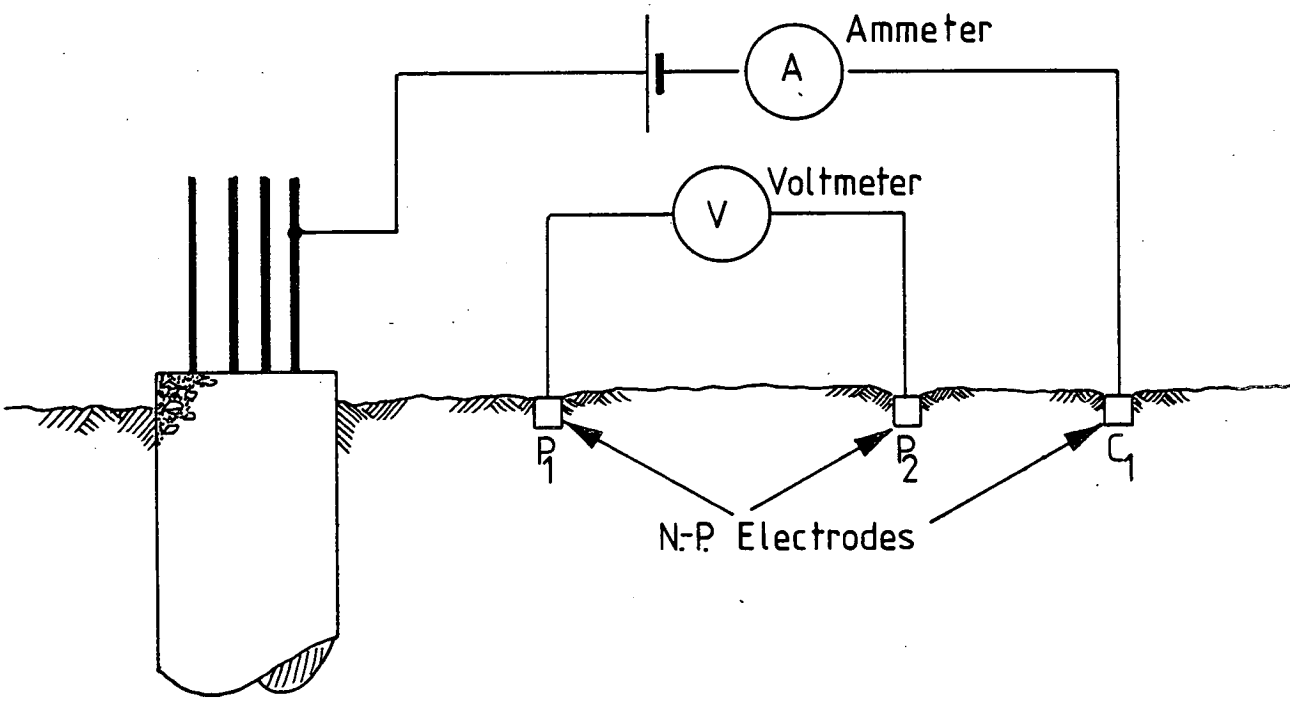

FIG. 2.9 The Earth-Resistivity Method

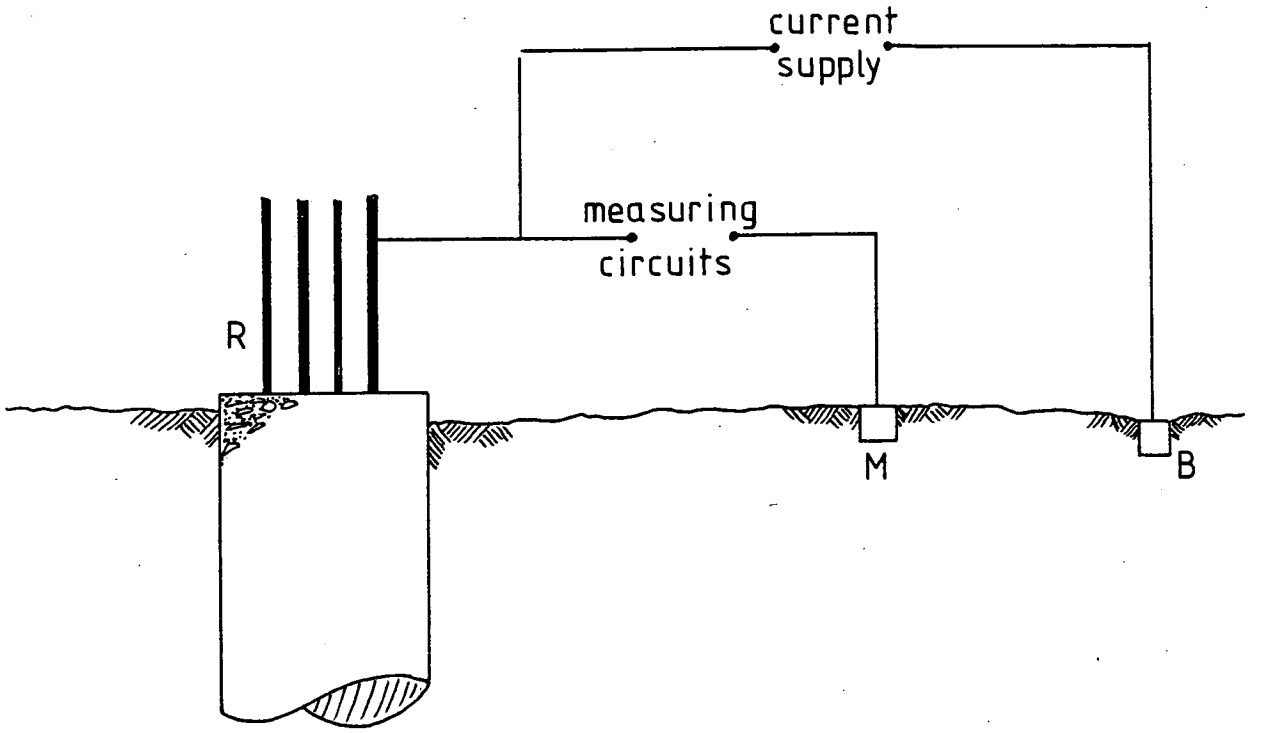

(a)

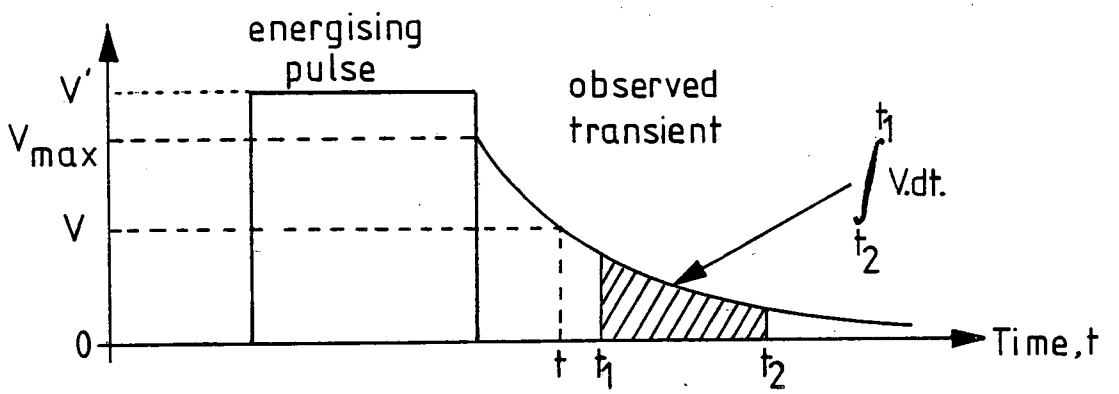

(b)

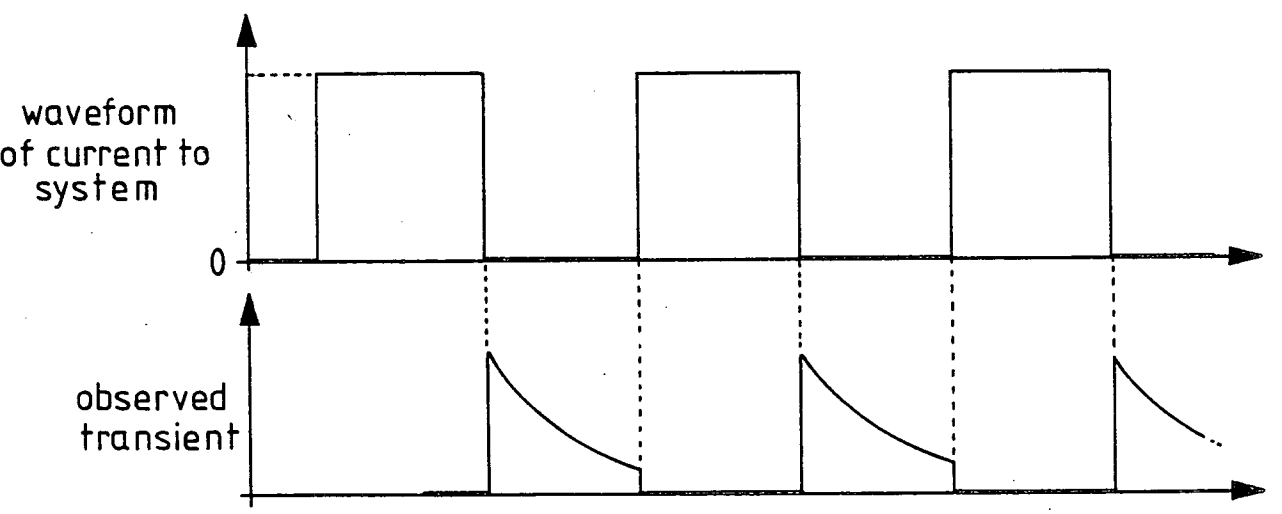

(c)

FIG. 2.10 Induced Polarisation

PLATE 1

Defective piles caused by overbreak

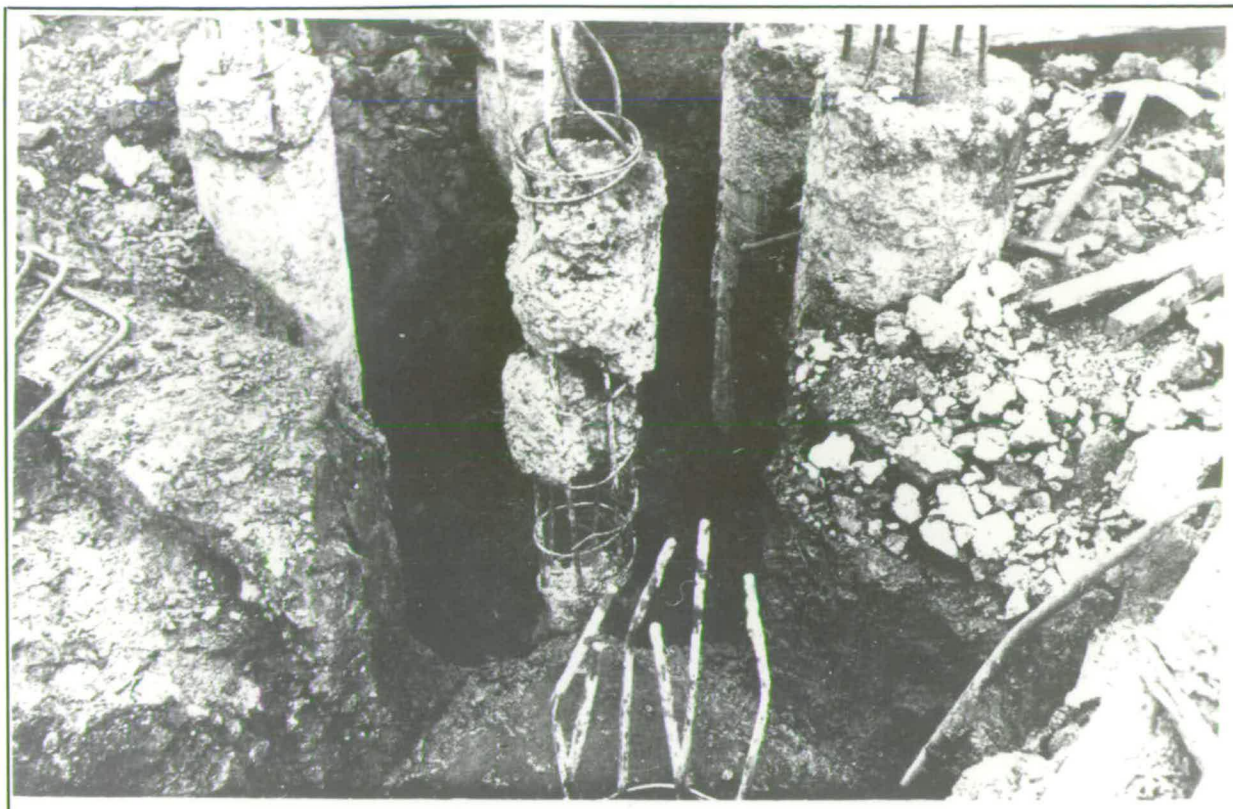

PLATE 2

Effect of groundwater on pile shaft

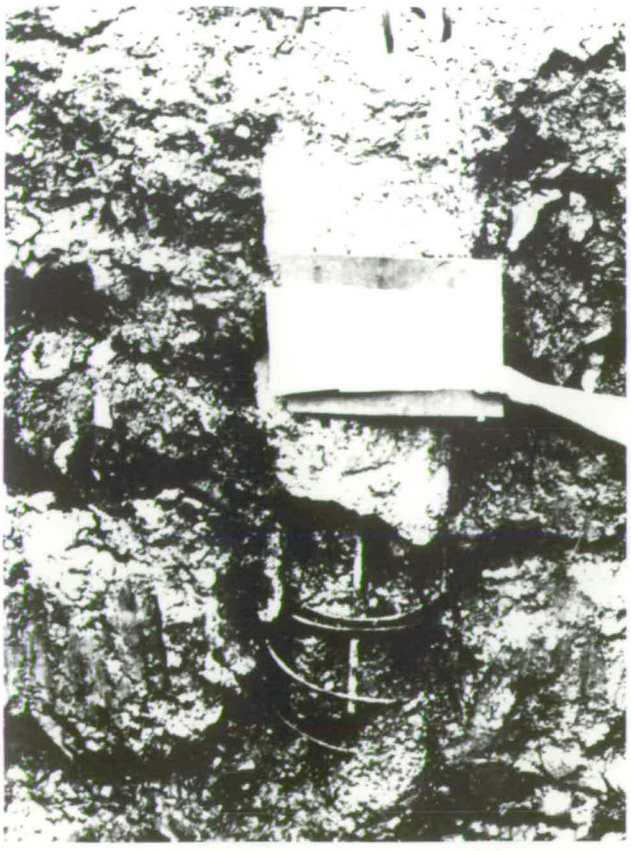

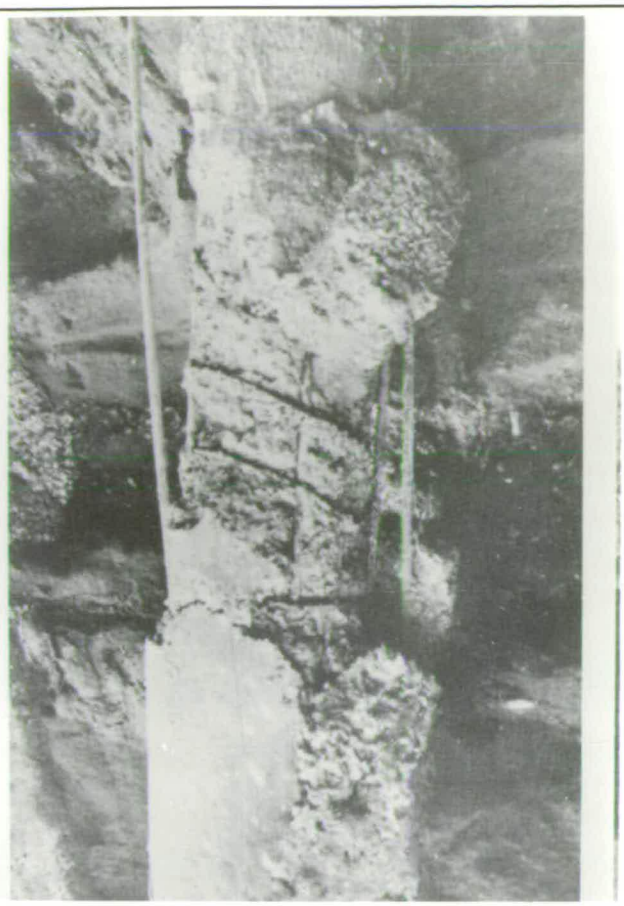

PLATE 3

Starter bars added after loss of main reinforcement

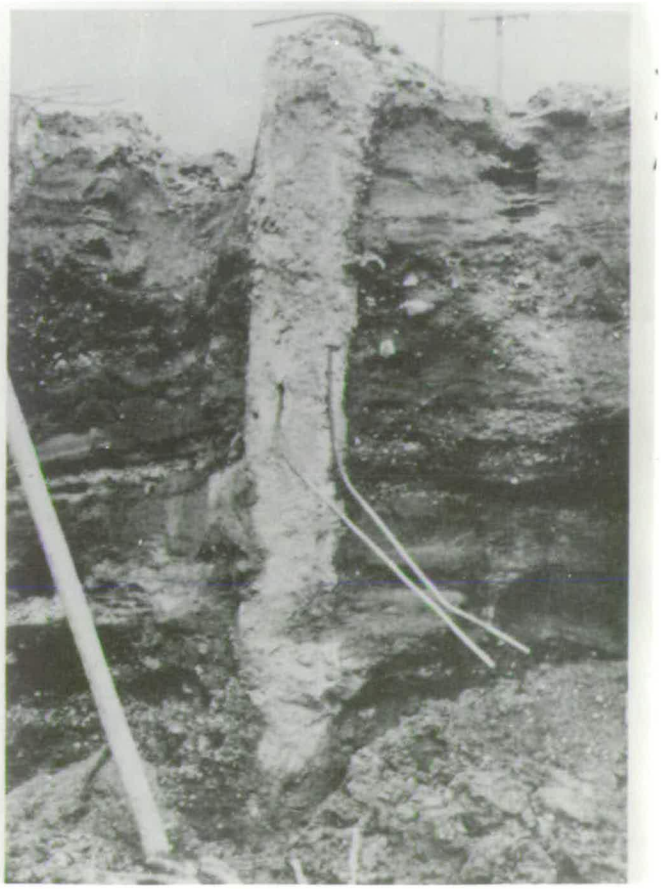

CHAPTER 3

THE PILE AS AN EARTH ELECTRODE

3.1 Introduction

This chapter deals with the earth resistance method of integrity testing as used in the field and shows how the variables of the pile-soil system are interrelated. A theoretical approach to earthing-resistance is possible with certain assumptions but it is expected that the solution involved will be, at best, approximate because of interaction effects which cannot be taken completely into account. However, even an indication of the variations to be expected and how the earthing resistance is related to the physical dimensions of the pile in the ground would be a useful contribution to the present knowledge of this particular branch of non-destructive testing.

3.2 Measurement of the Earthing-Resistance of a Pile

There are three possible methods (41, 42, 43) for obtaining the earthing resistance of a pile, which are described below.

3.2.1 Test With a Known Earth

This is, perhaps, the simplest way in obtaining the necessary measurement and entails finding the combined resistance of the pile under test and an electrode of known or negligible resistance as illustrated in Figure 3.1.

The main disadvantage to this comparatively simple method is finding an auxiliary electrode of known resistance - one possibility is water supply system - and this may not be available on an isolated site. Another disadvantage is that piles will be scattered over a site at

varying distances from R_0 and, consequently, large variations in resistance would occur due to the increase in the mass of earth between R_x and R_0. Anomalous results could also be due to deep geological features and not related to the integrity of the pile being tested.

3.2.2 Triangulation or Three-Point Method

A logical extension of the method described above is to insert two auxiliary electrodes into the earth and to measure the combined resistances between pairs of electrodes and to deduce from these the pile resistance. This is illustrated in Figure 3.2 where X is the pile under test and A and B are the auxiliary electrodes.

Then,

$$\begin{aligned} R_1 &= X + A \\ R_2 &= X + B \\ R_3 &= A + B \end{aligned} \qquad \ldots\ldots (3.1)$$

hence,

$$X = {}^1/_2 \cdot (R_1 + R_2 - R_3) \qquad \ldots\ldots (3.2)$$

The main disadvantage to this method is that the effect of any observational or experimental error is magnified by the form of equation (3.2). It is almost certain that A and B will be large compared with X, so any errors in R_1, R_2 or R_3 may produce very large errors in the calculated value of X; in fact, experimental errors could produce a negative value for X. This method cannot be considered reliable.

3.2.3 The Fall of Potential Method

This method is shown schematically in Figure 3.3. X is the pile under test and P and C are two auxiliary electrodes placed at suitable distances from X. A known current is passed between the pile and a return electrode, C, and the potential drop between X and P is measured. If the current is I and the potential drop V, the quotient, V/I, will give the earthing resistance of the pile for that particular position of electrodes. This method was employed to facilitate earth-resistance measurement. Instrumentation requirements and operation, precautions and field procedure are described in the next chapter.

3.3 The Nature of a Pile-Electrode Resistance

In order to examine the nature of such an electrode consider Figure 3.4, where the reinforcing cage is buried in a medium of resistivity ρ_1. The total earthing resistance can be divided into four parts,

(a) the resistance of the reinforcement itself,
(b) the contact resistance between the surface of the reinforcement and medium of resistivity ρ_1,
(c) the resistance due to medium of resistivity ρ_1, and
(d) the resistance of the earth immediately surrounding the pile.

The resistance due to (a) can, for practical purposes, be neglected. The contact resistance, or interface polarisation impedance, has been found to be negligible (41) and the main part of the electrode resistance is due to the concrete around the pile reinforcement and the soil around the pile viz. the two factors which determine pile integrity.

The problem resolves itself into two parts. First, to calculate the earthing-resistance of the reinforcement if it were buried in a semi-infinite medium of resistivity ρ_1; and secondly, to calculate an additional resistance representing the disturbing effect of the medium resistivity ρ_2.

3.3.1 Preliminaries

For the purpose of quantitative interpretation, the pile-soil system is regarded as consisting of regions of approximately constant resistivity separated by plane interfaces. For a proper appreciation of the problem it is necessary, therefore, to understand the behaviour of current flowing in such a system and how this affects the distribution of potential.

In dealing with the particular problem a starting point is the evaluation of the potential about a single-point, current source, P, in an infinite medium. (Fig. 3.5) This can be done using Ohm's Law which can be written as,

$$\underset{\sim}{E} = \rho \underset{\sim}{J} \qquad \ldots\ldots (3.3)$$

where, $\underset{\sim}{E}$ is the potential gradient, $\underset{\sim}{J}$ the current density and ρ is the resistivity of the medium.

If the current is assumed to be steady, then the total current flowing into any closed region must equal that flowing out. The flux of current for any closed region must, therefore, be zero for any closed surface which does not include any sources of current, i.e.

$$\int_S \int \underset{\sim}{J}.\underset{\sim}{n}\, dS = 0 \qquad \ldots\ldots (3.4)$$

where $\underset{\sim}{n}$ is the unit vector along the normal to the element dS and $\underset{\sim}{J}$ is the current density vector whose direction is along the line of flow of electric current. This equation can be put in the form (44),

$$\text{div } \underset{\sim}{J} = 0 \qquad \ldots\ldots (3.5)$$

Combining (3.3) and (3.5) obtains,

$$\text{div } \underset{\sim}{J} = \frac{1}{\rho} \text{ div } \underset{\sim}{E} = 0 \qquad \ldots\ldots (3.6)$$

E is defined as the potential gradient and is represented, mathematically as,

$$\underset{\sim}{E} = -\left(\underset{\sim}{i}\frac{\partial V}{\partial x} + \underset{\sim}{j}\frac{\partial V}{\partial y} + \underset{\sim}{k}\frac{\partial V}{\partial z}\right) = -\text{ grad } V \qquad \ldots\ldots (3.7)$$

where V is the scalar potential and $\underset{\sim}{i}$, $\underset{\sim}{j}$, and $\underset{\sim}{k}$ are unit vectors at right angles to each other; hence if ρ is constant, then,

$$\text{div } E = \text{divgrad } V = 0 \qquad \ldots\ldots (3.8)$$

or,

$$\frac{\partial^2 V}{\partial x^2} + \frac{\partial^2 V}{\partial y^2} + \frac{\partial^2 V}{\partial z^2} = 0 \qquad \ldots\ldots (3.9)$$

Thus, in a homogeneous electric conduction field, the potential, V, at any point in the medium can be solved by using Laplace's Equation and appropriate boundary conditions.

3.3.2 Solution of Laplace's Equation as applied to a Pile-Soil System

Consider Figures 3.6 (a) and (b) where the reinforcement is injecting a current - I per unit length into a medium of resistivity ρ_1. The problem resolves itself into a calculation of the potential at the surface of the reinforcement and then applying Ohm's Law to calculate the earthing-resistance. The reinforcement is represented by a line source.

Consider a small element, dh, which can be assumed to be a point source, O, in the medium at depth h, from the surface of the earth. (Fig. 3.6 (c)) Let this be the centre of a system of cylindrical co-ordinates t, z (θ is eliminated due to symmetry). As shown in the last section, the potential at any point in the medium must satisfy Laplace's Equation, which, in cylindrical co-ordinates, can be written as,

$$\frac{\partial^2 V}{\partial r^2} + \frac{1}{r} \cdot \frac{\partial V}{\partial r} + \frac{\partial^2 V}{\partial z^2} = 0 \qquad \ldots\ldots (3.10)$$

Using Fourier's method to find a solution to (3.10), assume that a solution can be found in the form of a product of two functions, each of which depends on only one variable, i.e.

$$V = f(r) . \phi(z) \qquad \ldots\ldots (3.11)$$

If (3.11) is now substituted into (3.10) and divided by $f(r) . \phi(z)$, then,

$$\frac{f''(r)}{f(r)} + \frac{1}{r} \cdot \frac{f'(r)}{f(r)} + \frac{\phi''(z)}{\phi(z)} = 0 \ldots\ldots (3.12)$$

Equation (3.12) can be separated into two independent relationships,

$$\frac{\phi''(z)}{\phi(z)} - \lambda^2 = 0 \qquad \ldots\ldots (3.13)$$

$$\frac{f''(r)}{f(r)} + \frac{1}{r} \cdot \frac{f'(r)}{f(r)} + \lambda^2 = 0 \qquad \ldots\ldots (3.14)$$

The solution to (3.13) may contain terms in $e^{-\lambda z}$ and $e^{+\lambda z}$, while the solution to (3.14) is the solution to Bessel's Equation of order zero, the solutions being $Jo(\lambda r)$ and $Yo(\lambda r)$ (45) . The function $Yo(\lambda r)$ tends to become infinite when r is small, and, since this is not acceptable for points on the z axis, then all terms in the solution to equation (3.14) which contain $Yo(\lambda r)$ must have zero co-efficients. The complete solution to (3.12) can contain only two types of terms, namely $Jo(\lambda r)e^{-\lambda z}$ and $Jo(\lambda r)e^{+\lambda z}$, together with any

linear combination of these functions. Since λ can vary continuously, the potential at any point in the medium can be conveniently written as (46),

$$V = \frac{I\rho_1}{4\pi}\cdot\left[\int_0^\infty Jo(\lambda r)e^{-\lambda z}.d\lambda + \int_0^\infty A(\lambda)Jo(\lambda r)e^{-\lambda z}.d\lambda + \int_0^\infty B(\lambda)Jo(\lambda r)e^{+\lambda z}.d\lambda\right] \quad \ldots\ldots (3.15)$$

The boundary conditions for the particular problem are,

(a) as z tends to infinity, the potential, V, must approach zero. This immediately implies that $B(\lambda) = 0$, and,

(b) at the surface of the earth the potential gradient is zero, i.e. at $z = -h$, $\frac{\partial V}{\partial z} = 0$ giving $A(\lambda) = e^{-2\lambda h}$.

Hence, the potential at any point, in a semi-infinite, homogeneous medium due to a point source, O, at depth, h, from the surface, can be written as,

$$V = \frac{I\rho_1}{4\pi}\cdot\left[\int_0^\infty Jo(\lambda r)e^{-\lambda z}.d\lambda + \int_0^\infty Jo(\lambda r)e^{-\lambda(z+2h)}.d\lambda\right] \quad \ldots\ldots (3.16)$$

Using the Weber-Lipschitz integral identity for the Bessel Function then,

$$V = \frac{I\rho_1}{4\pi}\cdot\left((r^2+z^2)^{-\frac{1}{2}} + (r^2+[2h+z]^2)^{-\frac{1}{2}}\right) \quad \ldots\ldots (3.17)$$

The potential on the surface of the reinforcement is assumed to be uniformly distributed, with the mean potential, Vm, over the full reinforcement being equal to the potential at the upper extremity of the reinforcement (Fig. 3.7). In the case of reinforcement of radius, a, and length, l, the potential at point P due to a small element of the reinforcement at depth h, is obtained by putting $r = a$ and $z = -h$, giving

$$V = \frac{I\rho_1}{2\pi} \cdot (a^2+h^2)^{-\frac{1}{2}} \quad \ldots\ldots (3.18)$$

The current, I, in the above expression is the current flowing from a small element, dh, of the reinforcement, hence the total potential at point P due to the full reinforcement is given, by,

$$Vm = \frac{I\rho_1}{2\pi} \cdot \int_0^l \frac{dh}{(a^2 + h^2)^{\frac{1}{2}}} \qquad \ldots\ldots (3.19)$$

Thus,

$$Vm = \frac{I\rho_1}{2\pi} \cdot \text{Sinh}^{-1}(l/a) \qquad \ldots\ldots (3.20)$$

If l is large in comparison to a, then (3.20) simplifies to,

$$Vm = \frac{I\rho_1}{2\pi} \cdot \log_e \frac{2l}{a} \qquad \ldots\ldots (3.21)$$

The total current on the reinforcement is l.I. hence using Ohm's Law,

$$Vm = l.I.R_\infty \qquad \ldots\ldots (3.22)$$

where R_∞ is the earthing resistance of the reinforcement buried in medium of resistivity ρ_1. Combining (3.22) and (3.21) gives,

$$R_\infty = \frac{\rho_1}{2\pi l} \cdot \log_e \frac{2l}{a} \qquad \ldots\ldots (3.23)$$

The next stage of the calculation is to evaluate the effect of the soil.

3.3.3 Disturbing Effect of Soil

A simple approach to calculate the additional potential due to the disturbing effect of the soil around the pile is to use geometric optics. An analogy may be drawn between the way in which the current travels through the earth and the way light rays travel through space. For example, the density of current flowing from a point source varies as the inverse square of the distance. Light rays behave similarly, with the intensity decreasing as the square of the distance travelled. In setting up the optical analogue, current sources are replaced with light sources and the planes separating regions with different resisti-

vities are replaced with semi-transparent mirrors - in this case the pile-soil interface and the ground surface - air interface. At the boundary between the two media the following two conditions must be satisfied:

(1) the potential must be continuous across the boundary, and,
(2) the normal component of current flow through the boundary must be continuous.

In order to calculate the potential of the surface of the reinforcement it is first necessary to calculate the potential due to itself in medium of resistivity ρ_1 (Section 3.3.2), and adding to it the disturbing potential due to the soil of resistivity, ρ_2.

At this point several assumptions have to be stated:

(a) only the reinforced section of the pile contributes to the response, which immediately means that medium of resistivity ρ_1 continues to an infinite depth, hence reflections from the base can be neglected. (This assumption would appear to be justified from laboratory experiments).

(b) the cross-section of the pile is assumed to be square with sides of length equal to the diameter of the pile. This effectively gives four mirrors.

(c) as in section 3.3.2, the current distribution on the reinforcement is assumed uniform.

It is first necessary to replace the arrangement of Figures 3.4 by a completely symmetrical arrangement as shown in Figure 3.8 (a) in which there is a medium of resistivity ρ_1 and thickness, 2p, sandwiched between two semi-infinite media of resistivity ρ_2. The reinforcement is combined with its image above the surface of the earth, giving a source of length 2l and carrying a current I per unit length.

The first three images are shown in Figure 3.8 (a). The first pair M_1 and M_1' are both at a distance 2p from the centre of the source and the current on these two images is taken as kI per unit length, where k is the 'reflection coefficient' and is numerically equal to $(\rho_2-\rho_1)/(\rho_2+\rho_1)$ (47). The second pair of images are M_2 and M_2' at a distance 4p from the centre of the source, and the current on these will be k^2I. Similarly the n^{th} pair of images will be at a distance 2np from the centre of the source and the current on these images will be k^nI. Considering the problem in three dimensions, the images shown in Figure 3.8 (b) will exist with the current on the general image $k^{(n+m)}I$.

With reference to Figure 3.9, the potential of the reinforcement due to the images can now be approximated. The potential, δV_0, at point O on the reinforcement due to an element of current, dy, on the image, is, from equation (3.17) and considering an infinite medium,

$$\delta V_0 = \frac{\rho_1 k^{(n+m)} I dy}{4\pi\left((2mp)^2+(2np)^2+y^2\right)^{\frac{1}{2}}} \qquad \ldots\ldots (3.24)$$

Hence the total potential, V_0, at O due to the full image is,

$$V_0 = \frac{\rho_1 I k^{(n+m)}}{4\pi} \cdot \left[\int_0^{2l-x} \left((2mp)^2+(2np)^2+y^2 \right)^{-1/2} dy + \int_0^{x} \left((2mp)^2+(2np)^2+y^2 \right)^{-\frac{1}{2}} dy \right] \qquad \ldots\ldots (3.25)$$

Equation (3.26) must be multiplied by 4 since there are four images.

Integrating,

$$V_0 = \frac{\rho_1 I k^{(n+m)}}{\pi} \cdot \left[\text{Sinh}^{-1}\left(\frac{2l-x}{A}\right) + \text{Sinh}^{-1}\left(\frac{x}{A}\right) \right] \quad \ldots\ldots (3.26)$$

where $A = [(2mp)^2 + (2np)^2]^{\frac{1}{2}}$. $\ldots\ldots (3.27)$

Now this is the potential of a small element, dx, of the reinforcement due to one image, hence the total potential, V_T, at point O due to all the images is,

$$V_T = \frac{\rho_1 I}{\pi} \cdot \sum_{n=0}^{\infty} \sum_{m=1}^{\infty} K^{(n+m)} \cdot \left[\text{Sinh}^{-1}\left(\frac{2l-x}{A}\right) + \text{Sinh}^{-1}\left(\frac{x}{A}\right) \right] \ldots\ldots (3.28)$$

and the mean potential, V_m, of the full reinforcement (Fig.3.10) will be,

$$V_m = \frac{I\rho_1}{2\pi l} \cdot \sum_{n=0}^{\infty} \sum_{m=1}^{\infty} K^{(n+m)} \cdot \int_0^{2l} \left[\text{Sinh}^{-1}\left(\frac{2l-x}{A}\right) + \text{Sinh}^{-1}\left(\frac{x}{A}\right) \right] dx$$

$\ldots\ldots (3.29)$

Proceeding with the integration yields,

$$V_m = \frac{\rho_1 I}{2\pi l} \cdot \sum_{n=0}^{\infty} \sum_{m=1}^{\infty} K^{(n+m)} \cdot \left[4l \, \text{Sinh}^{-1}\left(\frac{2l}{A}\right) - 2(4l^2+A^2)^{\frac{1}{2}} + 2A \right] \ldots\ldots (3.30)$$

This can be written,

$$V_m = \frac{2\rho_1 I}{\pi} \cdot \sum_{n=0}^{\infty} \sum_{m=1}^{\infty} K^{(n+m)} \cdot \left[\text{Sinh}^{-1}\frac{l}{B} - \left(1 + \frac{B^2}{l^2}\right)^{\frac{1}{2}} + \frac{B}{l} \right] \ldots\ldots (3.31)$$

where $B = [(mp)^2 + (np)^2]^{\frac{1}{2}}$.

Equation (3.31) can be written,

$$V_m = \frac{2\rho_1 I}{\pi} \cdot \sum_{n=0}^{\infty} \sum_{m=1}^{\infty} K^{(n+m)} \cdot \left[\log_e \frac{1+\sqrt{(1+C^2)}}{C} - (1+C^2)^{\frac{1}{2}} + C \right]$$

$\ldots\ldots (3.32)$

where $C = \left[\left(\frac{mp}{l}\right)^2 + \left(\frac{np}{l}\right)^2 \right]^{\frac{1}{2}}$ and depends on the ratio p/l alone.

The total current on the reinforcement is 2II and the potential is given by equation (3.32), hence, using Ohm's Law, the additional resistance, R_a, due to the soil is,

$$R_a = \frac{Vm}{2\Pi I} = \frac{\rho_1}{\pi l} \cdot \sum_{n=o}^{\infty} \sum_{m=1}^{\infty} K^{(n+m)} \cdot \left[\log_e \left(\frac{1+\sqrt{(1+C^2)}}{C} \right) - (1+C^2)^{\frac{1}{2}} + C \right] \quad \ldots\ldots (3.34)$$

The total resistance to earth of the pile is the sum of equations (3.34) and (3.23) i.e.

$$R_\infty = \frac{\rho_1}{2\pi l} \cdot \left[\log_e \frac{2l}{a} + 2 \cdot \sum_{n=o}^{\infty} \sum_{m=1}^{\infty} K^{(n+m)} \cdot \left[\log_e \left(\frac{1+\sqrt{(1+C^2)}}{C} \right) - (1+C^2)^{\frac{1}{2}} + C \right] \right] \quad \ldots\ldots (3.35)$$

Equation (3.35) can be put in the form

$$R_\infty = \frac{\rho_1}{2\pi l} \cdot (R + R_a) \quad \ldots\ldots (3.36)$$

Where R_a is the second term within the outside brackets in equation (3.35) and represents the disturbing effect of the soil. R_a was calculated using the EMAS 2980 computer and a graph of R_a against p/l is shown in Figures 3.11 (a) and (b) for various values of reflection coefficient, k. The series is convergent for $-1.0<k<1.0$.

From the foregoing analysis it can be seen that the resistance measured at infinity on the ground surface is related to the physical dimensions of the pile in the ground; the electrical resistivity of concrete, and indirectly related, through the reflection coefficient, to the electrical resistivity of the soil. The variation of resistance with distance from the pile is shown in Figure 3.12, with the return

current electrode being placed at infinity. The resistance, R_x, measured on the ground surface will also be functionally related to R_∞, so this resistance reading must be a measure of the integrity of the pile in the ground.

The questions that still have to be resolved are,

(a) what is the effect of the mutual resistance of the current return electrode when it is placed at a more practical distance from the pile and the effect this has on the shape of the earth-resistance curve.

(b) what effect has a defective pile on earthing-resistance.

(c) how is this resistance measured in the field.

3.3.4 Effect of Mutual Resistance of Current Electrode

It is emphasized that the foregoing analysis is based on the return current electrode being placed an 'infinite' distance from the pile. In practice this would not be possible and, in fact, undesirable as deep geological features would affect the resistance readings and also only the soil in the immediate vicinity of the pile is of interest as this will determine its bearing capacity. Considering the problem when the current electrode is placed at a more practical distance from the pile, the mutual resistance of the electrodes will have a definite influence on the shape of the earth-resistance curve for the pile.

The potential at any point between the pile and the return electrode can be theoretically calculated. Even though only an approximate

solution can be found it is felt that some analysis would be useful.

A relationship can be obtained by considering Figure 3.13 in which the reinforcement is buried in a medium of resistivity ρ_1. The potential V_∞, at O due to a total current I' entering at O has been calculated in section 3.3.2 (Eq. 3.21), and that due to the current leaving at C is V_{oc}, so that the total potential at O is,

$$V_\infty - V_{oc} \qquad \ldots\ldots (3.37)$$

The potential at P due to the current I' entering at E is V_{op} and due to the current leaving at C is V_{pc}, hence the total potential at P is,

$$V_{op} - V_{pc} \qquad \ldots\ldots (3.38)$$

Accordingly, the total potential difference, V_d, between E and P is,

$$V_d = (V_\infty - V_{oc}) - (V_{op} - V_{pc}) \qquad \ldots\ldots (3.39)$$

If the return current electrode can be regarded as a point 'sink' on the ground surface, then the potential at any point from it can be calculated by equation (3.18). Therefore,

$$V_d = \frac{I'\rho_1}{2\pi l} \log_e \frac{2l}{a} - \frac{\rho_1 I'}{2\pi(h-a)} - V_{op} + \frac{\rho_1 I'}{2\pi(h-d)} \qquad \ldots\ldots (3.40)$$

V_{op} can also be obtained by using equation (3.18) viz.,

$$V_{op} = \frac{I'\rho_1}{2\pi l} \int_0^l \frac{dx}{(d^2+x^2)^{\frac{1}{2}}} \qquad \ldots\ldots (3.41)$$

i.e. $$V_{op} = \frac{I'\rho_1}{2\pi l} \cdot \log_e \left[\frac{l}{d} + \sqrt{\left(\left(\frac{l}{d}\right)^2 + 1\right)} \right] \quad \ldots\ldots (3.42)$$

Hence,

$$V_d = \frac{I'\rho_1}{2\pi} \cdot \left[\frac{1}{l} \cdot \log_e\left(\frac{2l}{a}\right) - \frac{1}{l} \cdot \log_e \left[\frac{l}{d} + \left(\left(\frac{l}{d}\right)^2 + 1\right)^{\frac{1}{2}} \right] - \left[\frac{1}{(h-a)} - \frac{1}{(h-d)} \right] \right] \quad \ldots\ldots (3.43)$$

In terms of the resistance, R_d at any point,

$$R_d = \frac{\rho_1}{2\pi l} \cdot \left[\log_e \frac{2l}{a} - \log_e \left[\left(\frac{l}{d}\right) + \left(\left(\frac{l}{d}\right)^2 + 1\right)^{\frac{1}{2}} \right] - \left[\frac{1}{(h-a)} - \frac{1}{(h-d)} \right] \right] \quad \ldots\ldots (3.44)$$

and for the actual situation Figure 3.13 could be regarded as a general image injecting a current $K^{(n+m)}\ I'$, so that,

$$R_d = \frac{\rho_1}{2\pi l} \cdot \left[f_1\left(\frac{l}{a}, k, \frac{p}{l}\right) - f_2\left(\frac{d}{l}, \frac{p}{l}, k\right) - f_3\left(k, \frac{a}{l}, \frac{h}{l}, \frac{p}{l}\right) + f_4\left(k, \frac{h}{l}, \frac{d}{l}\right) \right] \quad \ldots\ldots (3.45)$$

or simplifying,

$$R_d = \frac{C\rho_1}{l} \cdot f\left(k, \frac{p}{l}, \frac{l}{a}, \frac{d}{l}, \frac{h}{l}\right) \quad \ldots\ldots (3.46)$$

Where f represents a functional relationship between the terms inside the bracket. The effect of mutual resistance of the return electrode on the earth-resistance curve is shown in Figure 3.14. It should be noted that as this curve passes through an infinite number of points, there must exist one point on this curve which is numerically equal to the true earthing resistance of the pile (Point A), or, put in mathematical terms the fractional error, $(R_d - R_\infty)/R_\infty$ is reduced to zero. Furthermore, all the terms inside the bracket in equation (3.46) are

non-dimensional so modelling methods could be advantageously employed with the full scale resistance the same as the model resistance multiplied by the length ratio, and resistivity and all other ratios being kept constant.

3.3.5 The Reflection Coefficient

The reflection coefficient, k, is an important quantity in expression (3.35), and it varies between +1 and -1. If the soil were a perfect insulator i.e. $\rho_2=\infty$, then k = +1, and if the soil were a perfect conductor i.e. $\rho_2 = 0$, then k = -1. Now,

$$k = (\rho_2 - \rho_1)/(\rho_2 + \rho_1) = \frac{\frac{\rho_2}{\rho_1} - 1}{\frac{\rho_2}{\rho_1} + 1} \qquad \ldots\ldots (3.47)$$

and so depends on the ratio ρ_2/ρ_1 alone. A graph of ρ_2/ρ_1 and ρ_1/ρ_2 corresponding to various values of k is shown in Fig. 3.15. For large ρ_2/ρ_1 and ρ_1/ρ_2 ratios, small changes in ρ_2 (i.e. soil resistivity) have little effect on the value of the reflection coefficient, k, the significance of this being that small fluctuations expected in soil resistivity over a given site will not appreciably affect resistance readings. If, however, there is a large variation in ρ_2, then the resistance will be adversely affected, as, for example, the occurrence of a weak water-bearing clay pocket. To obtain a large resistivity contrast ratio the pile should be tested when the resistivity of the concrete, ρ_1, is relatively low viz. after pouring. Conversely, when the resistivity of the concrete is much greater than the surrounding soil, then, similarly small changes in soil resistivity will not alter the reflection coefficient to any great extent. This latter point may have importance to pre-cast concrete piles.

3.3.6 Effect of Defect on Pile Resistance

It is immediately apparent that the resistivity of concrete (ρ_1) has a major influence on the resistance measured on the ground surface as this term is outside the bracket in equation (3.35). This has been the subject of investigation in Chapter 5 of this thesis. It is also apparent that changes in pile dimensions will also have a marked influence on the observed resistance.

In order to calculate the effect of, say, defective concrete or a soil inclusion over part of the pile shaft, then, owing to the change in resistivity of the material surrounding the reinforcement it is no longer possible to assume that the current flows uniformly from the reinforcement along its length. A reasonable assumption would be that the current density on the reinforcement will be inversely proportional to the resistivity of the medium in direct contact with the reinforcement (Fig. 3.16).

Let J_1 and J_3 be the current per unit length; J_1 in the non-defective concrete and J_3 in the defective concrete, then,

$$J_1\rho_1 = J_3\rho_3 \qquad \ldots\ldots (3.48)$$

and,

$$J_3h + J_1(1-h) = I' \qquad \ldots\ldots (3.49)$$

Where I' is the total current on the reinforcement. Solving these equations gives,

$$J_1 = \frac{I'\rho_3}{\rho_1 h+\rho_3(1-h)} \qquad \ldots\ldots (3.50)$$

$$J_3 = \frac{I' \rho_1}{\rho_1 h + \rho_3 (1-h)} \qquad \ldots\ldots (3.51)$$

The potential of the reinforcement would now have to be recalculated using the above current densities resulting from the defect. Suffice to say that a defective section in the pile will ultimately alter the resistance measured on the surface of the earth, depending on the ratio ρ_1/ρ_3. For large/small ρ_1/ρ_3 ratios, the current densities will be altered and the difference in resistance readings appreciable, but as this ratio approaches unity the current densities will not alter significantly.

3.4 Summary

The purpose of this Chapter has been to present some of the theoretical aspects of earthing resistance which will assist in making realistic measurements in the field. To accomplish this objective certain assumptions have been made, although these simplifications will not affect the basic principles. A better understanding of this technique can now be appreciated and the analysis will assist in showing the interrelationship between the system variables, and the effect on resistance when any of the parameters are changed.

The effect of defects on the resistance has been discussed from a qualitative point of view as a rigorous mathematical treatment would be complex. It should be emphasised that the acceptance or rejection criteria for a pile is not based on the deviation of the theoretical value from the measured value but on the relative displacement of earth-resistance curves between neighbouring piles. In other words, predetermined values of resistance are not required, it is the relative

magnitudes between piles on a site that are of greater significance.

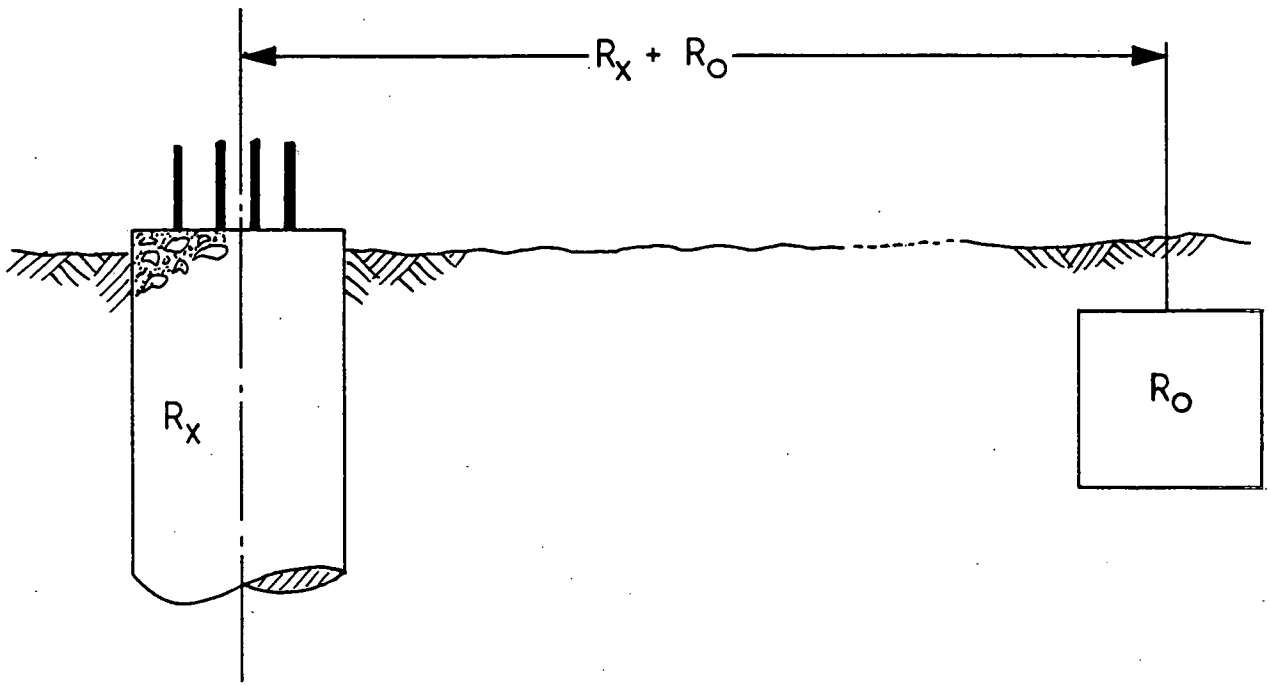

FIG. 3.1 Test with known earth

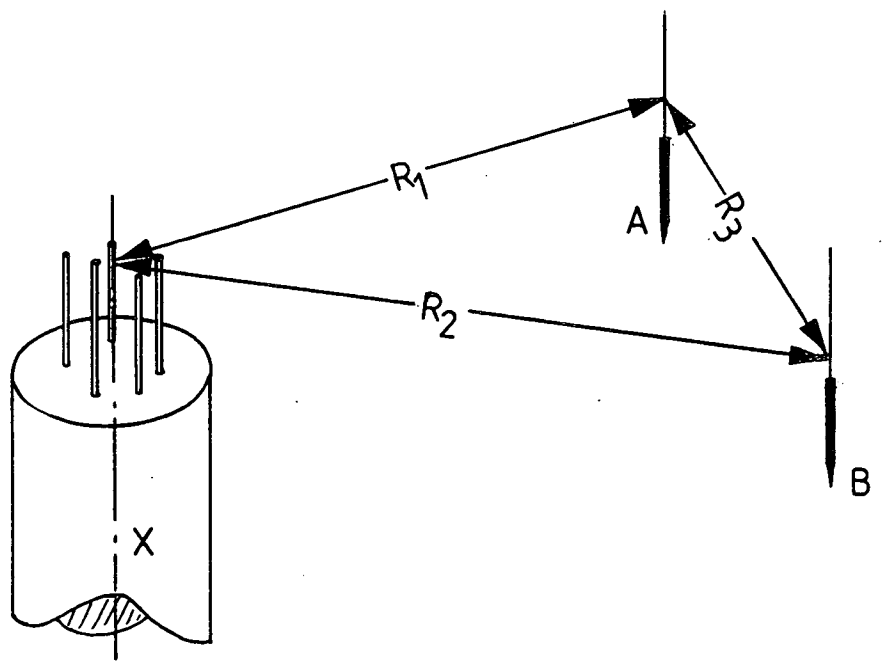

FIG. 3.2 Triangulation Method

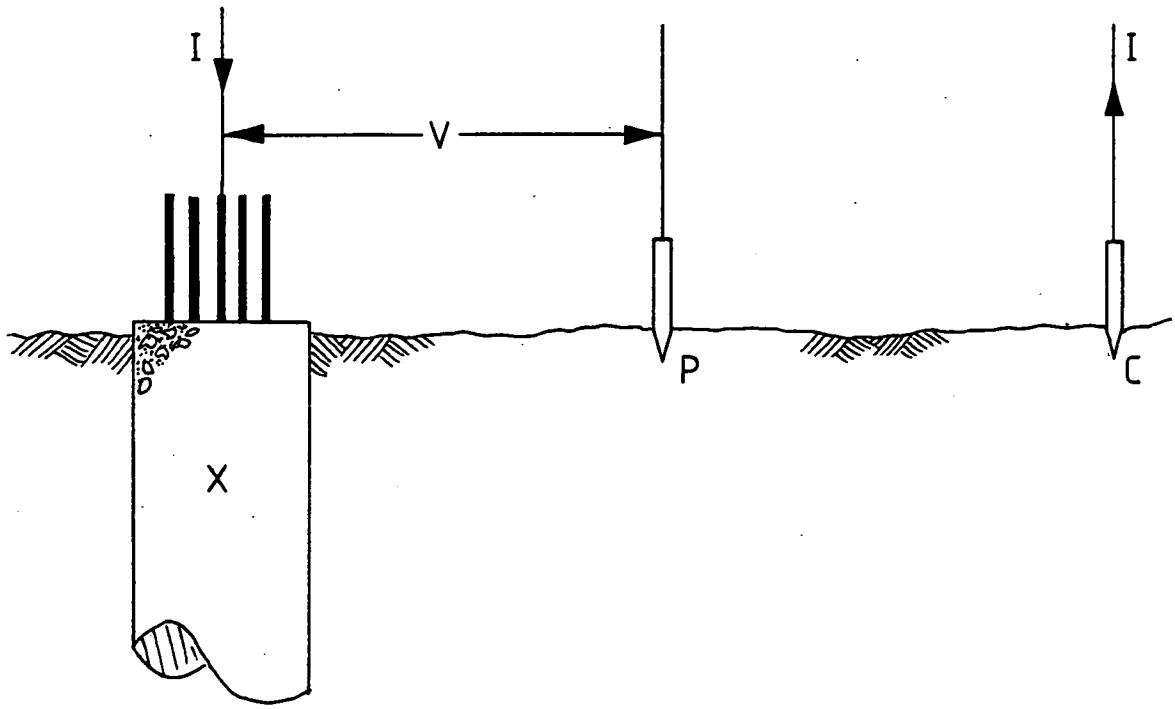

FIG. 3.3 Fall-of-Potential Method

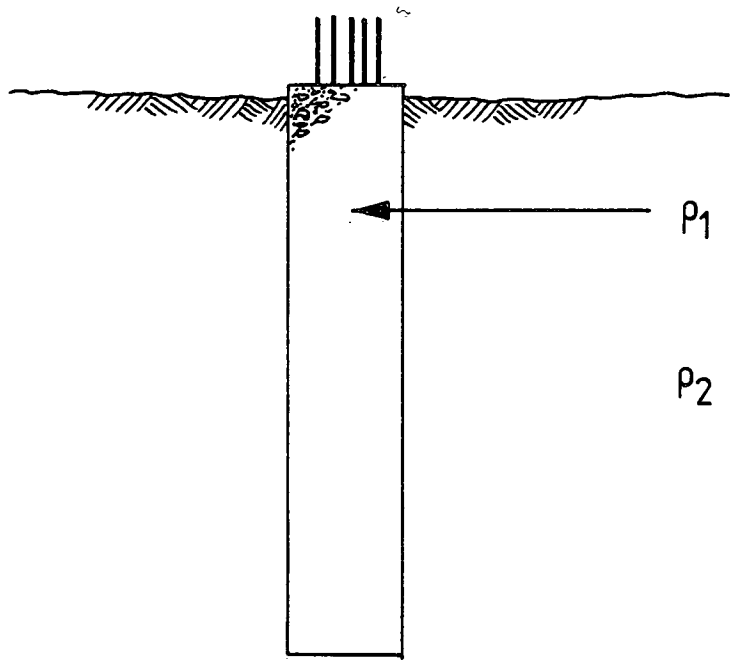

FIG. 3.4 Components of electrical resistance

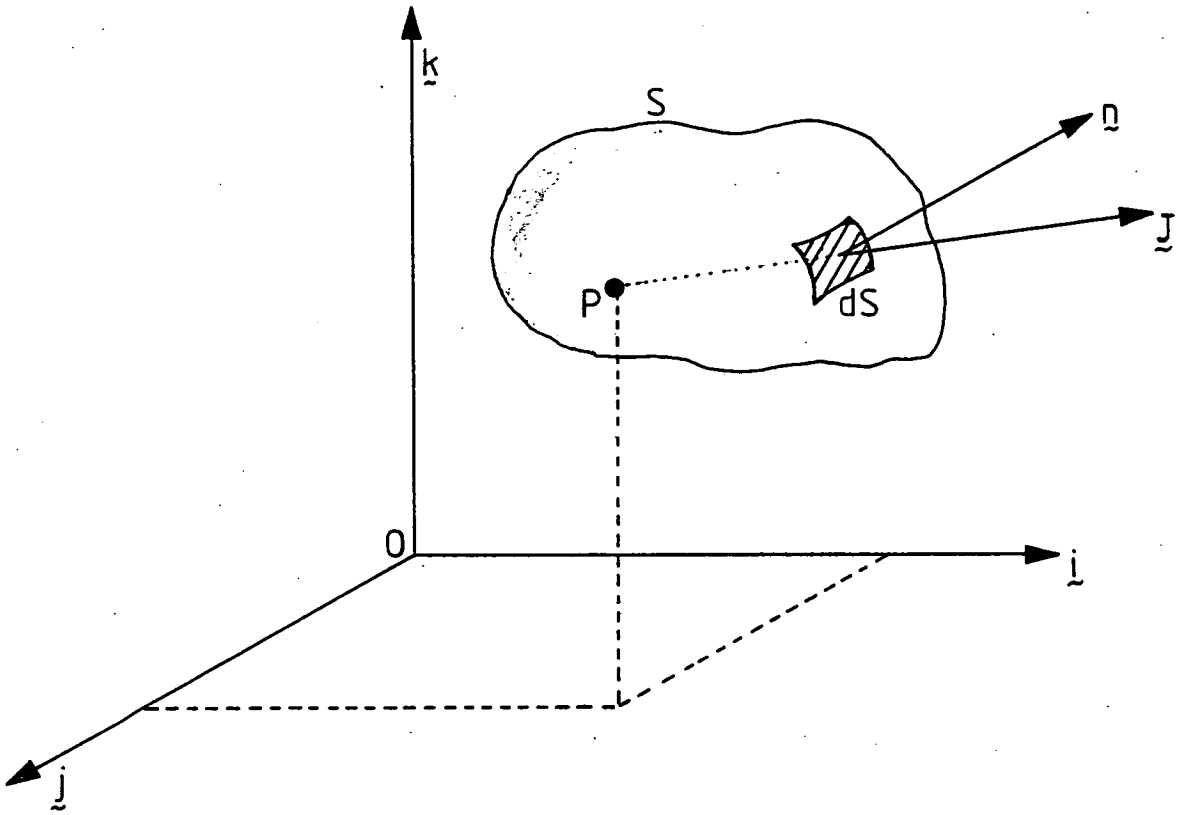

FIG. 3.5 Current flow in an infinite medium

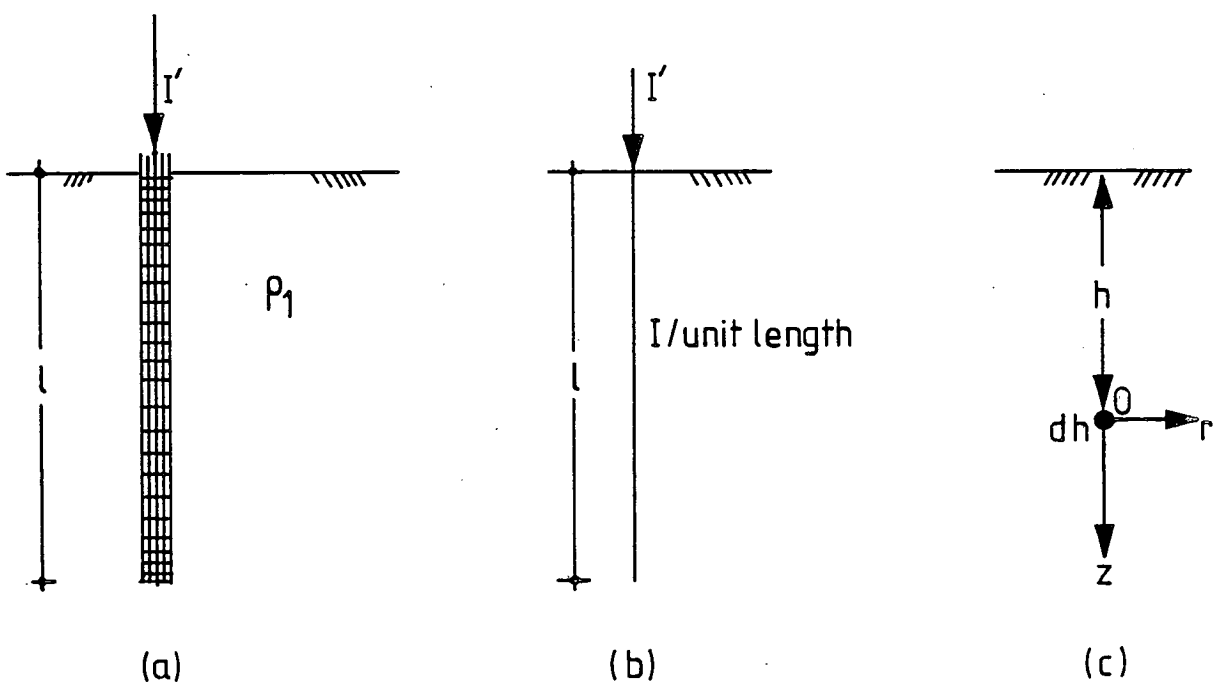

FIG. 3.6 Reinforcement in a semi-infinite medium

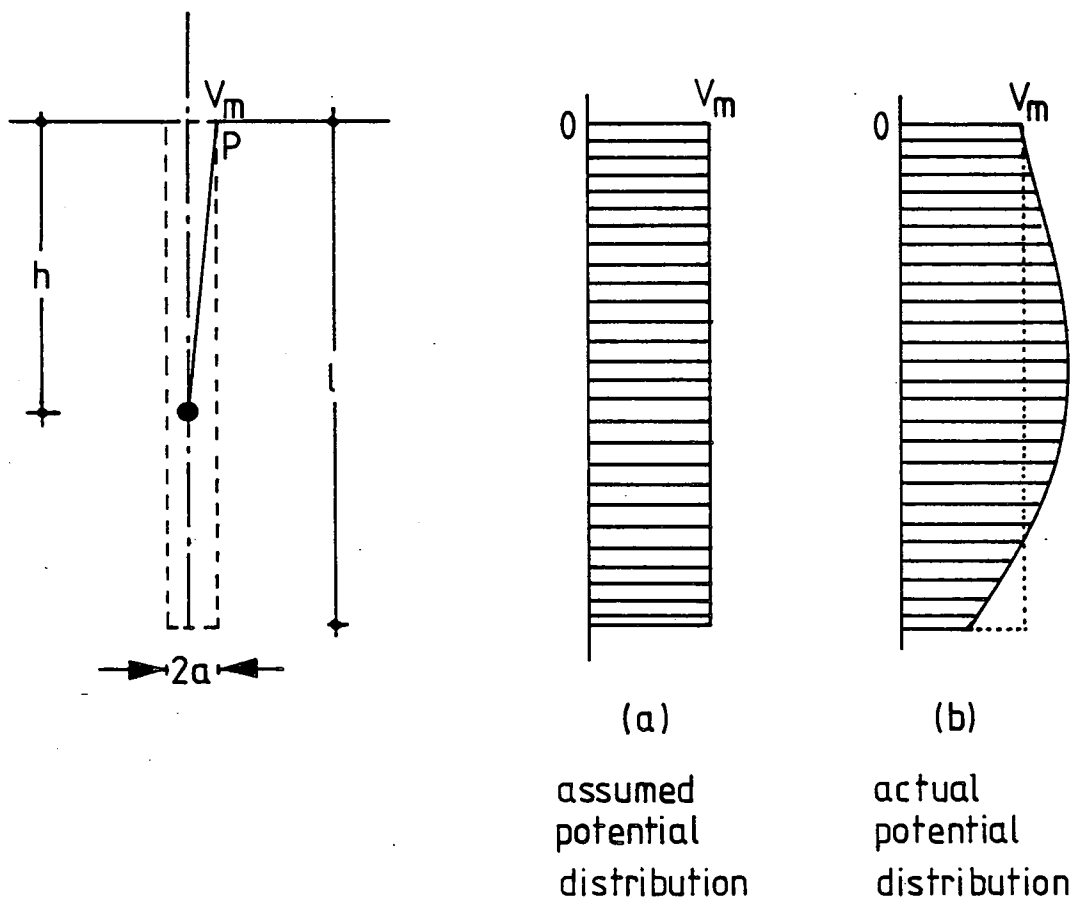

FIG. 3.7 Potential Distribution on reinforcement

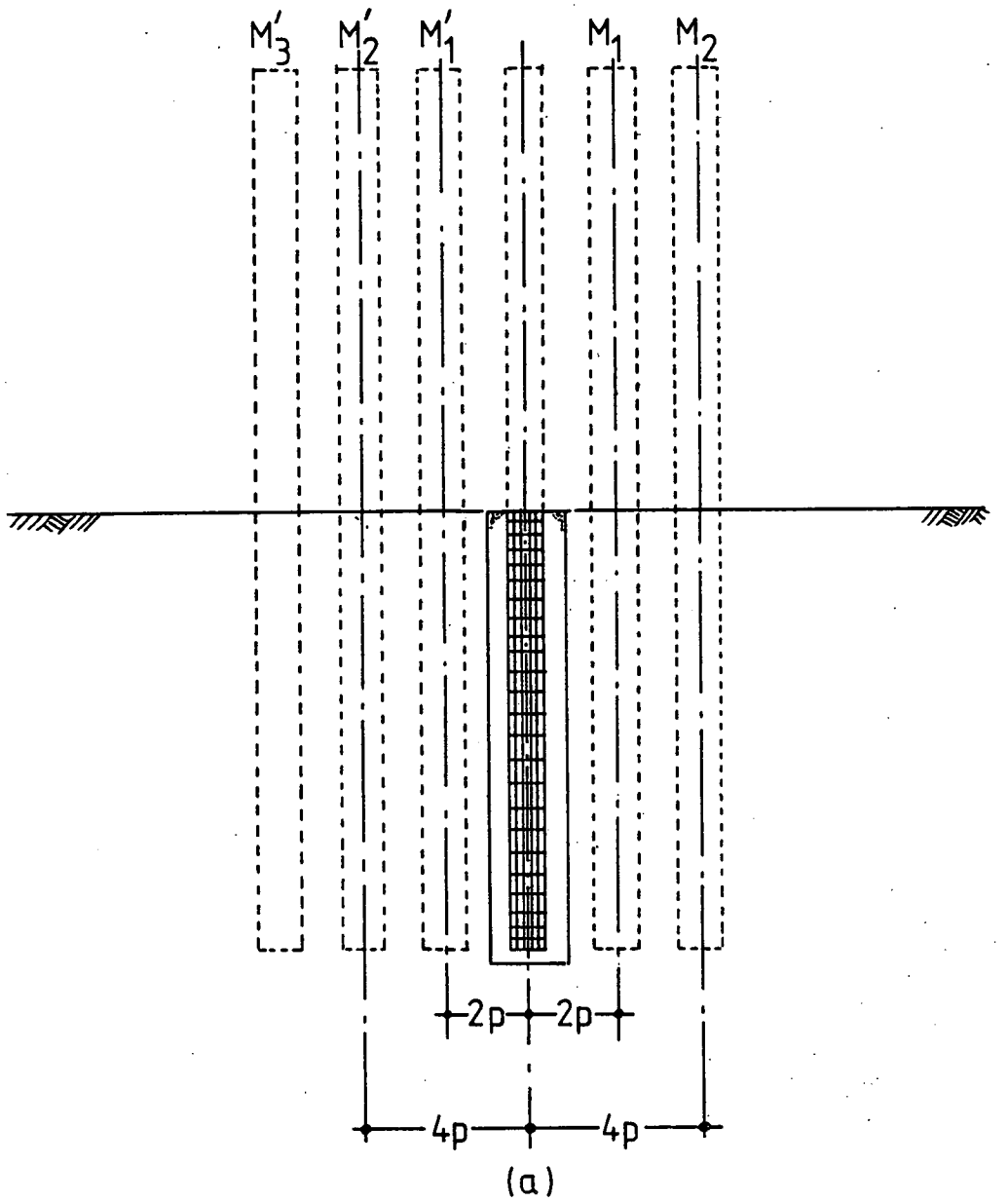

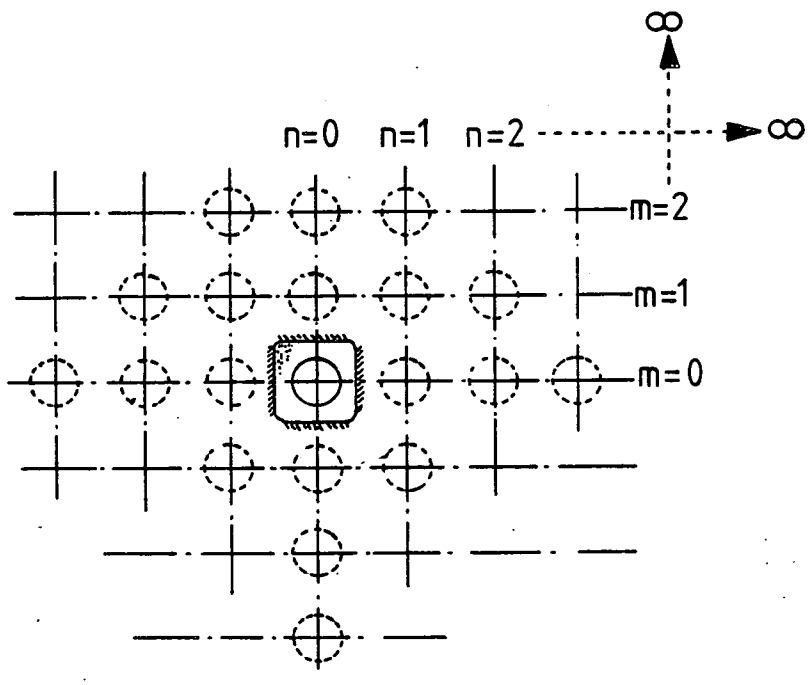

FIG. 3.8 Images formed at reflections between boundaries

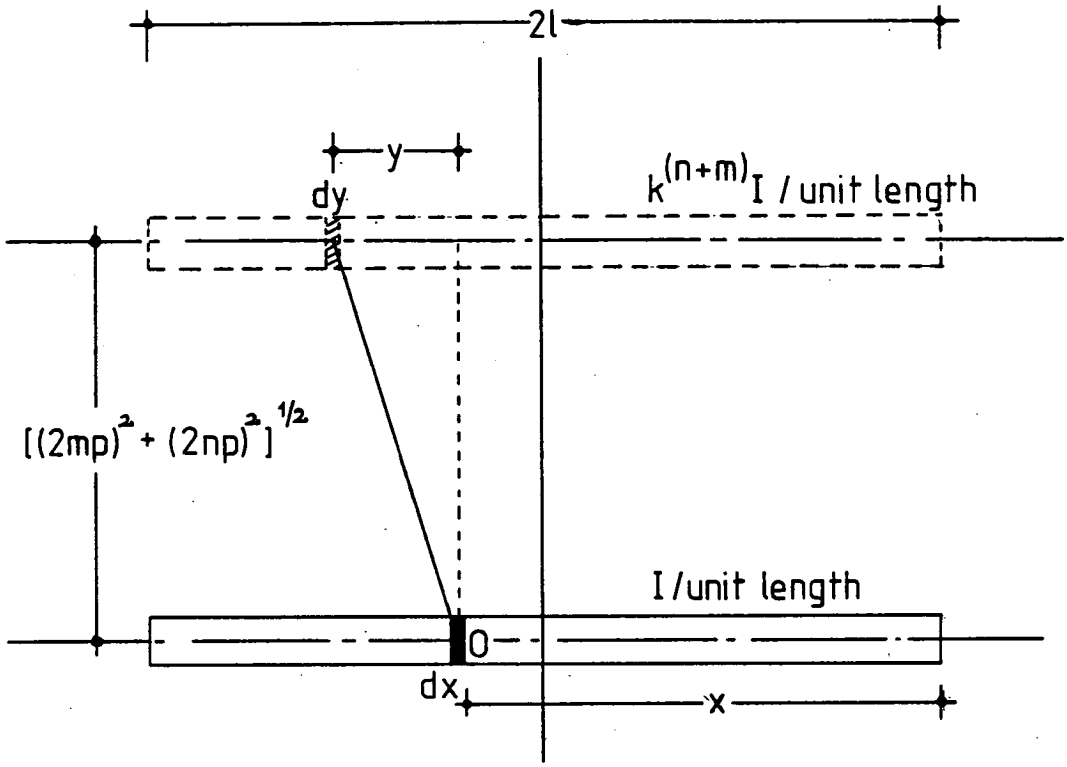

FIG. 3.9 Potential on reinforcement due to image

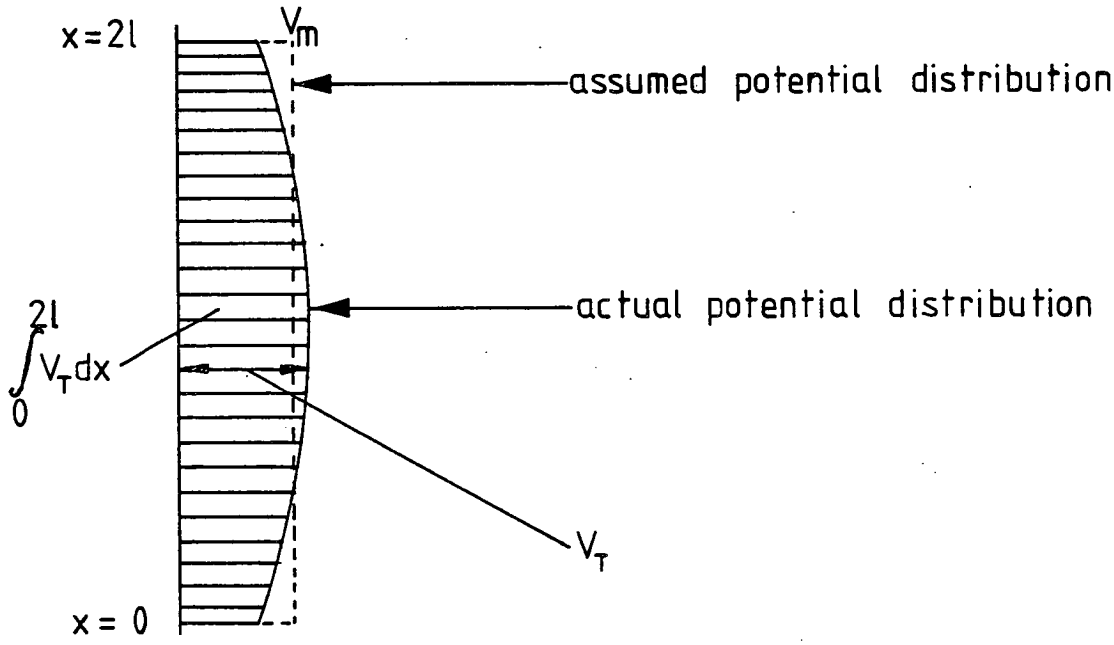

FIG. 3.10 Potential distribution on reinforcement

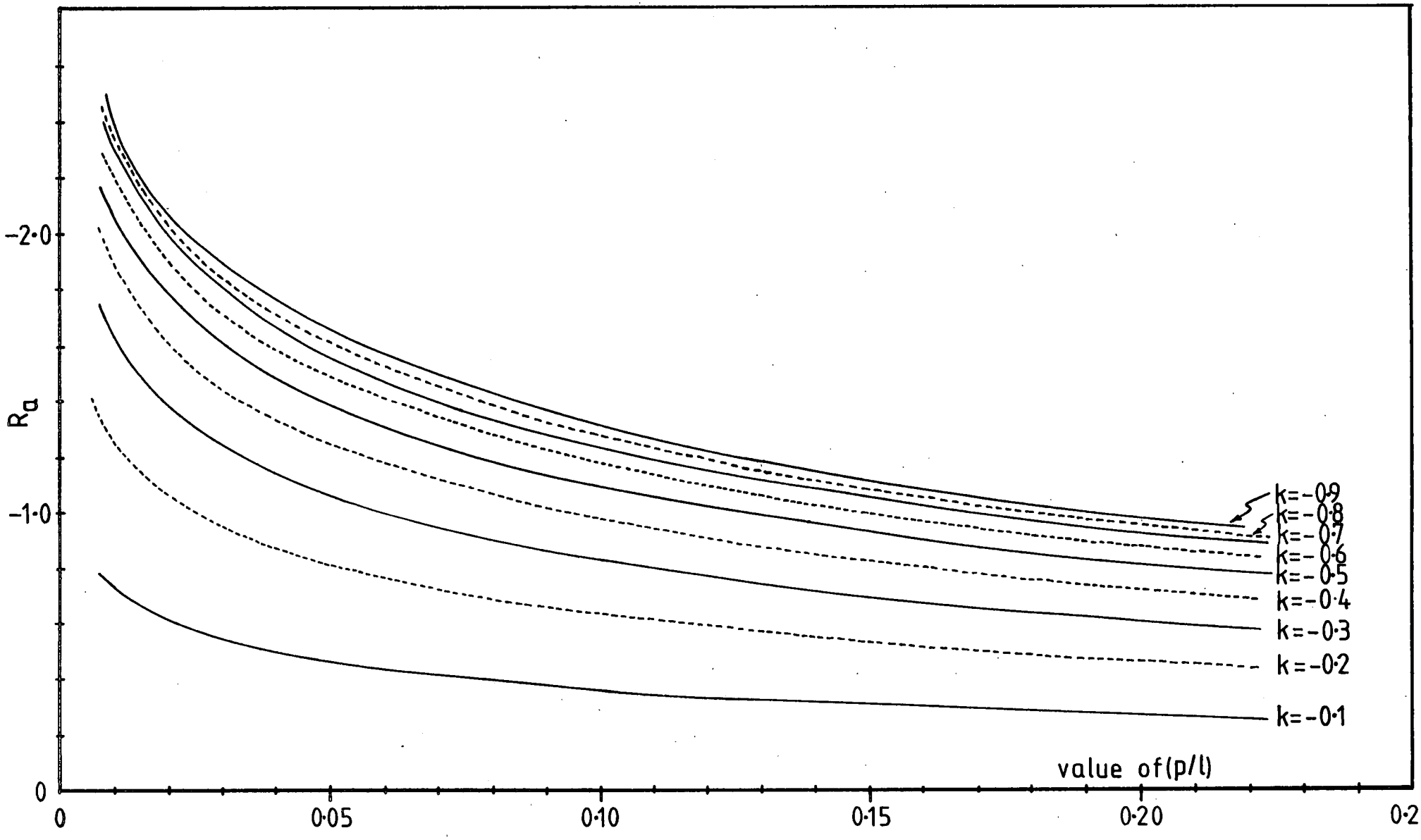

FIG. 3.11 (a) Value of function R_a for negative values of k

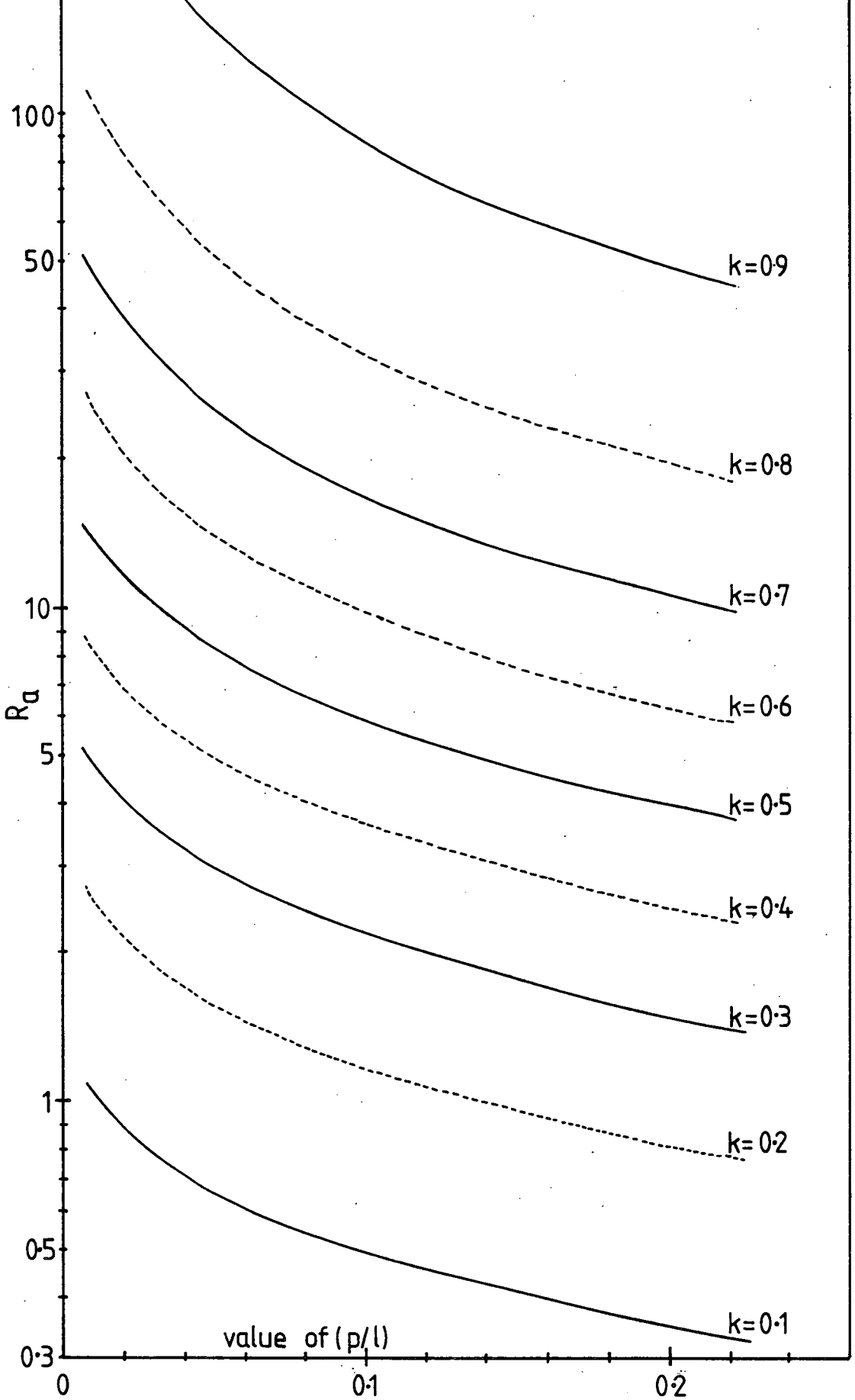

FIG. 3.11 (b) Values of function R_a for positive values of k^a

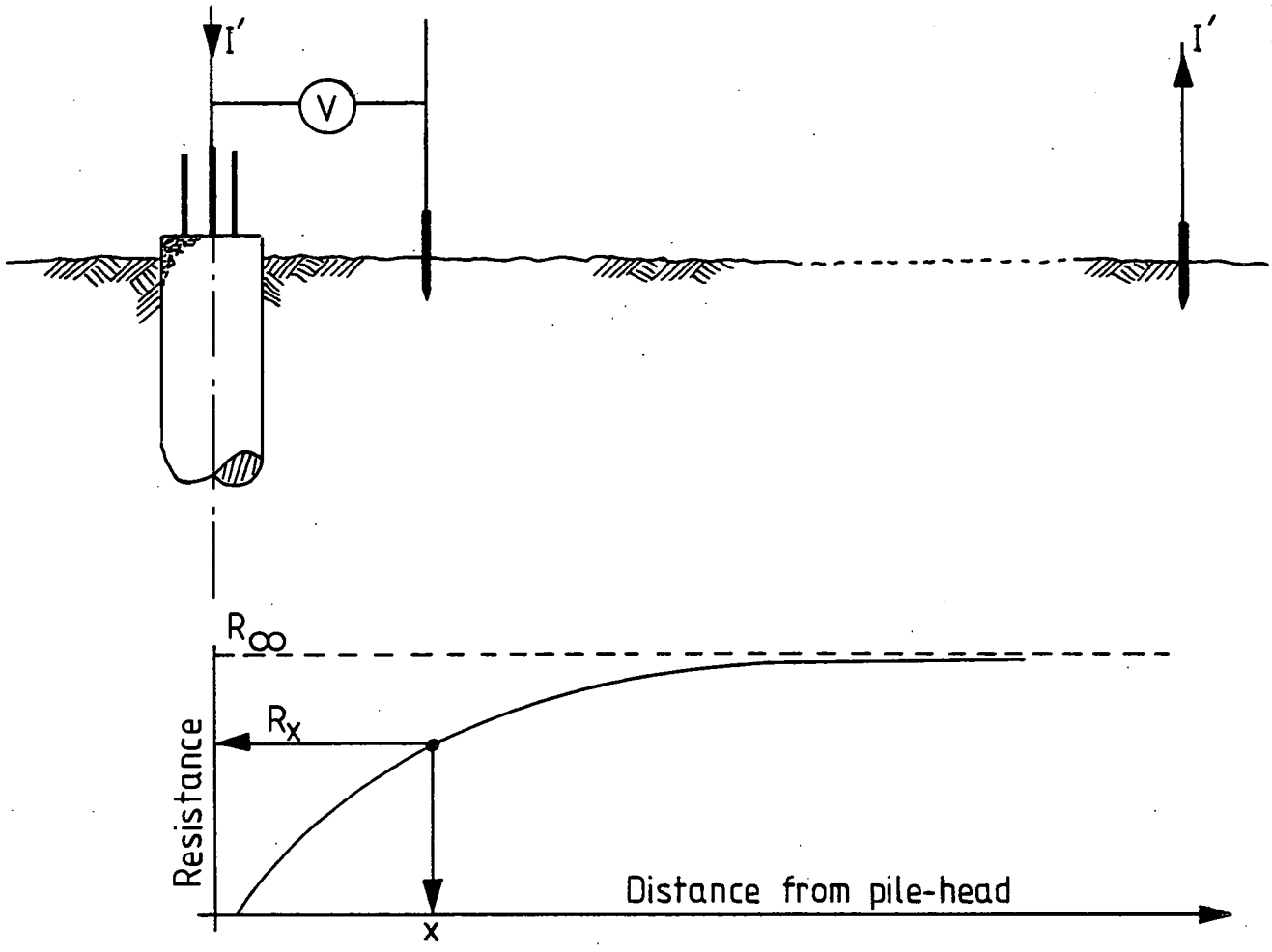

FIG. 3.12 Variation of resistance with distance from pile

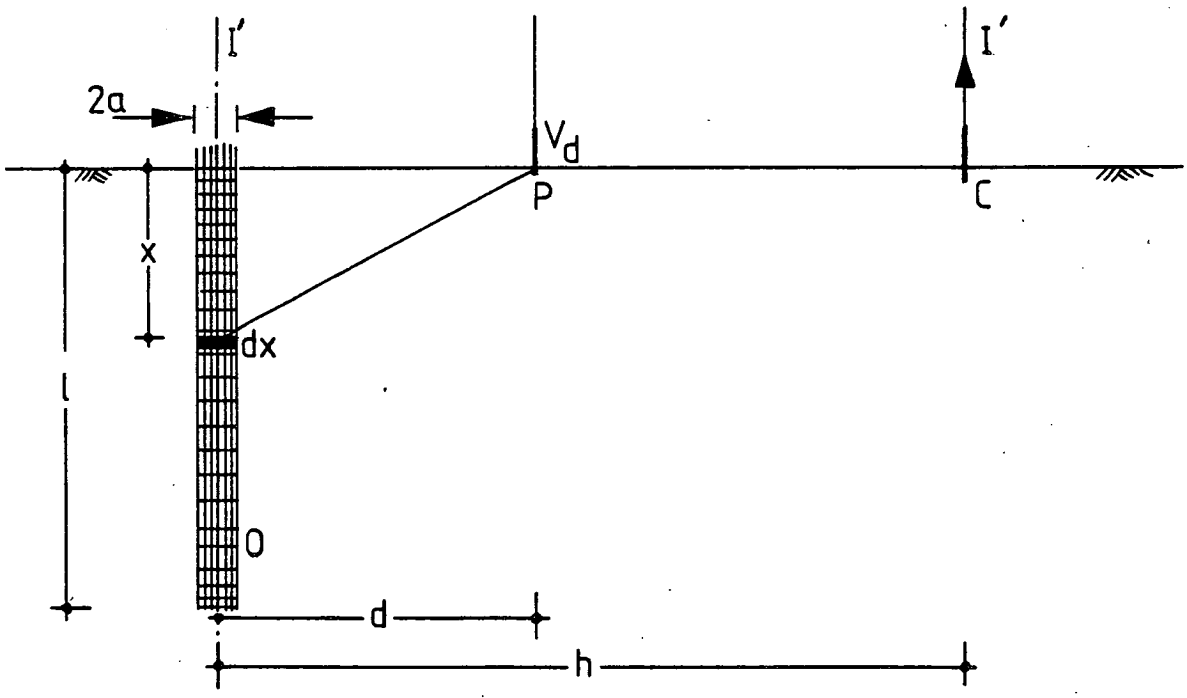

FIG. 3.13 Calculation of potential on surface of earth

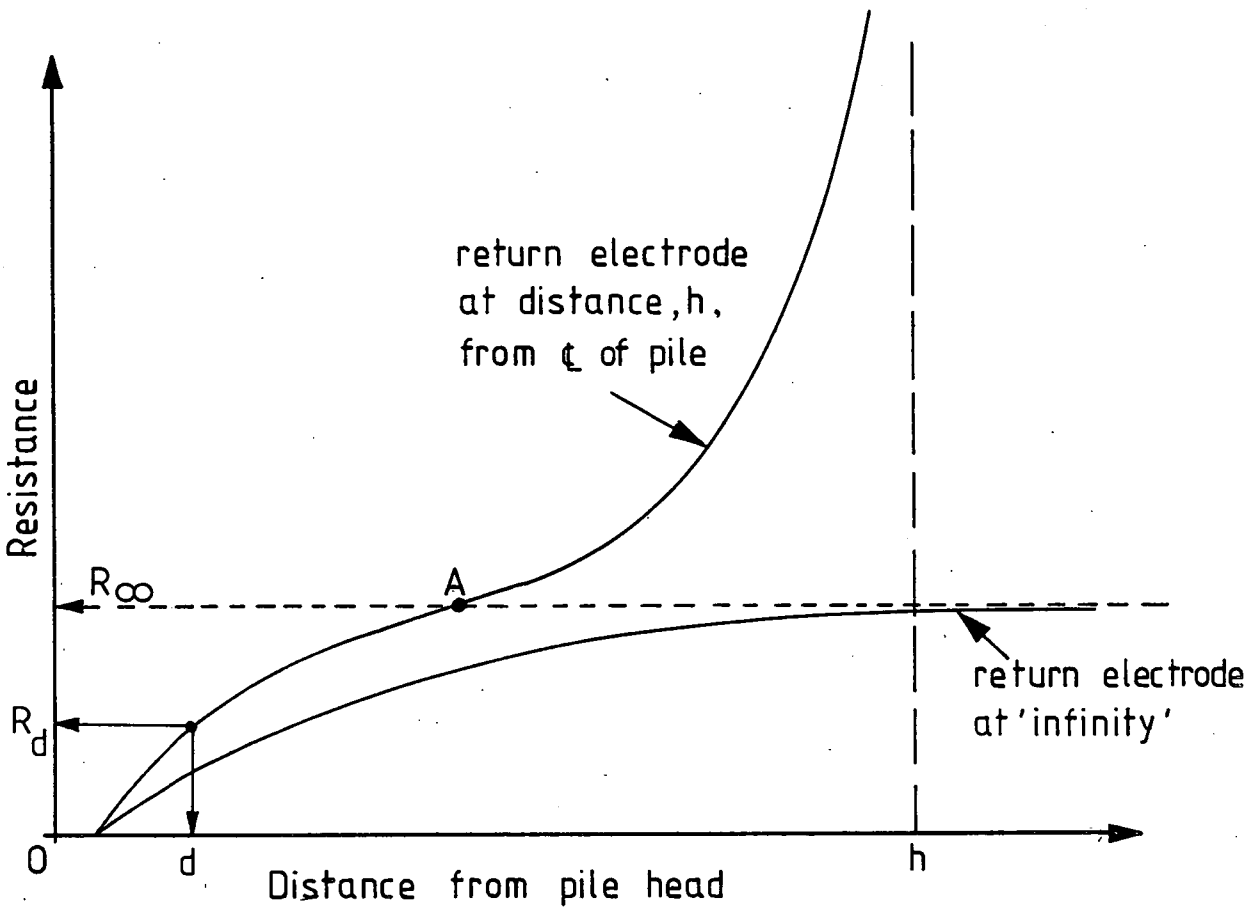

FIG. 3.14 Effect of mutual resistance of return electrode

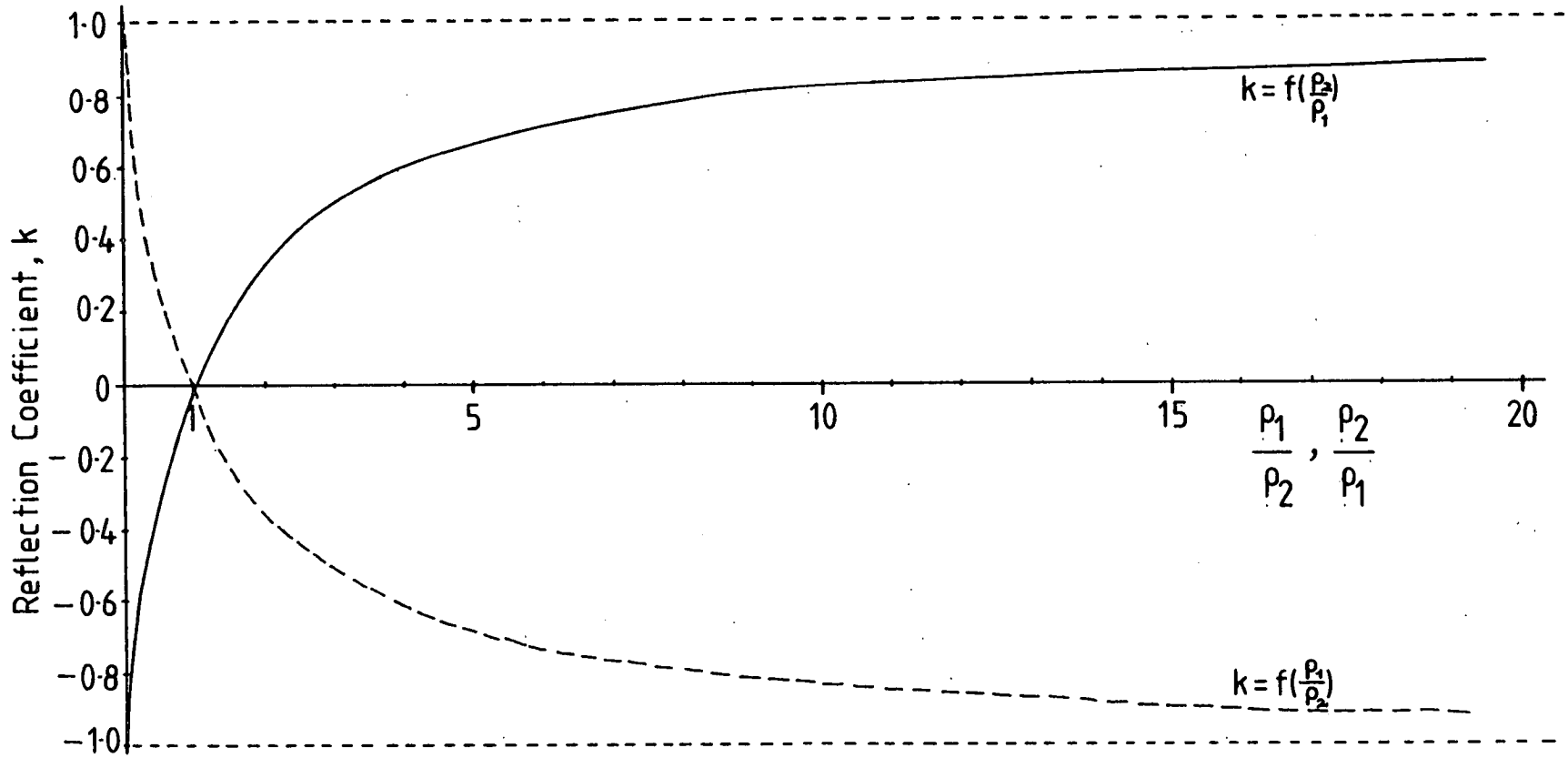

FIG. 3.15 Graph of Reflection Coefficient, k

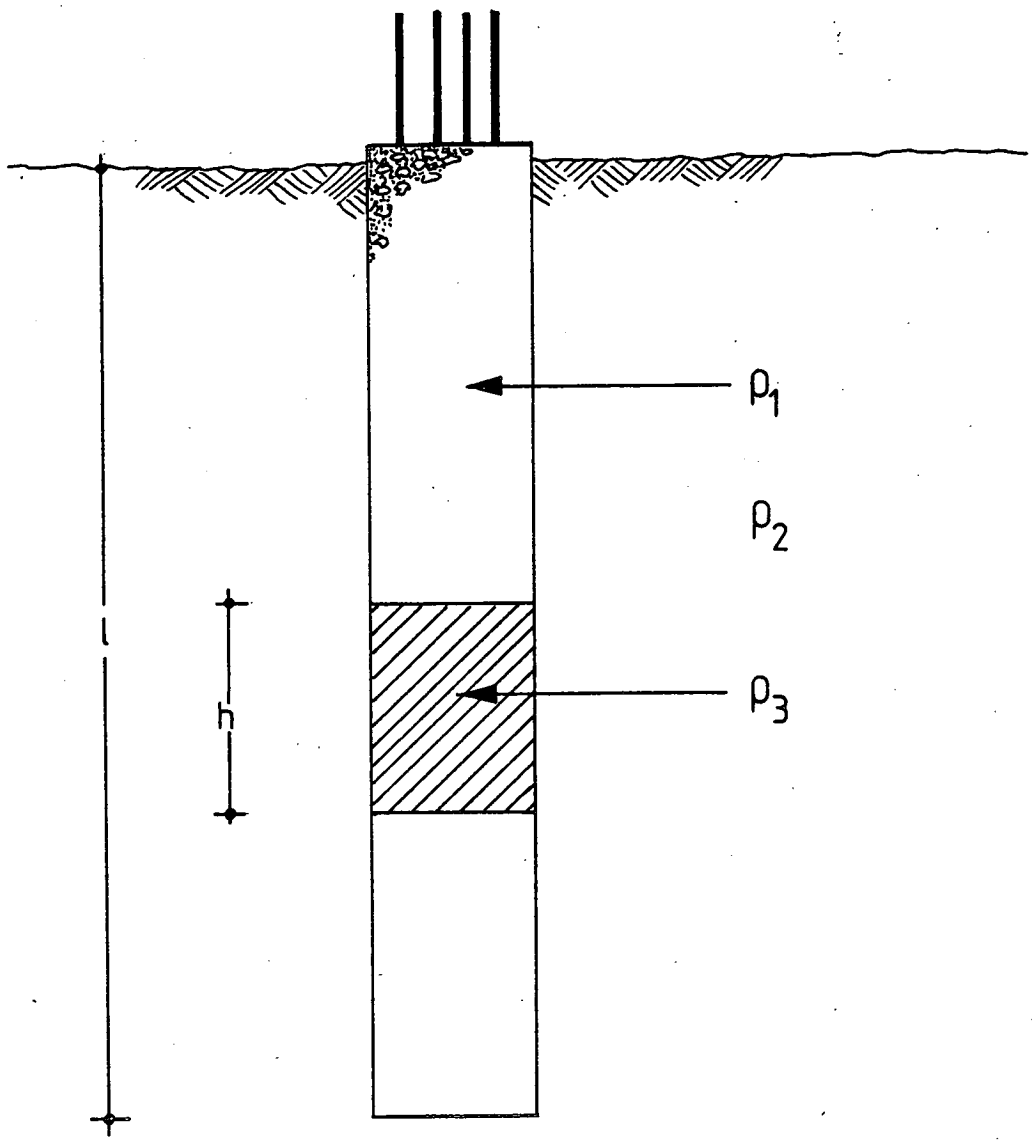

FIG. 3.16 Effect of pile defect

CHAPTER 4

INSTRUMENTATION

4.1 General Considerations

In order that any instrument be considered viable for use in the field there are several physical requirements which must be satisfied. The instrument must be as light-weight and portable as possible and it must be sufficiently robust to withstand rough treatment. The instrument must be self contained, i.e. possess its own internal power source and be easy to operate in the field. The need for portability and self containment cannot be overemphasised as methods which require an 'external' power supply and have power leads running across the site have obvious disadvantages.

These, then, are the physical specifications that any instrumentation must satisfy. However certain electrical requirements must also be satisfied.

4.2 Electrical Requirements

4.2.1 Elimination of Stray Potentials

At first sight it would appear that the resistance, R, of the pile can be obtained by simultaneous observations of the current, I, and the potential, V. Referring to Fig. 4.1, current from a source B, such as a bank of batteries, is supplied to the ground via two electrodes (the pile reinforcement acting as one electrode) and its value measured by means of an ammeter, A. The potential drop between the reinforcement and a point outwith the nominal pile periphery is measured by means of a voltmeter, V - the resulting quotient, V/I, being the resistance for that particular position of potential electrode. However, the measured potential will not be that resulting from B alone.

Induced polarisation phenomena which occur in the volume of earth around the electrodes and at the electrodes themselves can cause serious errors in measurement of earth-resistance if direct-current is used. Direct current measurements are also affected by slowly varying natural earth and telluric currents and by stray alternating currents of power frequency (50-60 Hz.). Steps must be taken to eliminate such potentials from earth-resistance measurements.

In connection with geophysical prospecting, Wenner (39) employed alternating current to remove polarisation effects at the measuring electrodes and Gish and Rooney (48) used synchronous commutation to achieve the same ends. As natural earth-currents tend to be unidirectional they, also, are eliminated when alternating current (a.c.) is used. All modern geophysical instruments employ either a.c. or commutated current to facilitate resistance measurements and many instruments based on these principles are available (Table 4.1). It is important that the operating frequency of the instrument is not the same as power frequency (50-60 Hz.) and also the frequency should be as low as possible as ground inductance and capacitance and more complex frequency effects (e.g. skin effect) become increasingly more important at higher frequencies (46, 49).

4.2.2. Elimination of Current and Potential Electrode Resistance

When measurements are being made, good grounding of the auxiliary electrodes is essential to reduce contact resistance to a minimum. This resistance may vary over quite a large range - from fractions of an ohm in moist clayey soils to as high as tens of thousands of ohms in dry sandy soil.

The effects of electrode resistance (and electrode contact resistance) can best be removed by making the measurement with a high impedance device and, traditionally, potentiometric devices have been used for this purpose (49, 50), since their input impedance at balance is, theoretically, infinite. In a typical commercial instrument which employs a potentiometric measuring device (schematically shown in Fig. 4.2), the voltage drop across the measuring electrodes (P_1,P_2) is compared with that across an internal, variable resistance placed in series with the current electrodes (C_1,C_2). Since the same current, I, flows through both resistance R and through the pile-soil system (represented by a resistance X), then, at balance the voltage V_R, is equal to that present between the measuring electrodes, V_X. The instrument may therefore be calibrated to read directly in ohms.

With such an arrangement the resistances of the various electrodes can have no effect on the balance condition. Letting the electrode resistances be simulated by resistors in series, then, the resistances of the current electrodes are included in the main circuit and thus are factors affecting the value of the current I. Since, however, R and X are carrying the same current, the balance condition is unaffected by changes in I. The resistances of the potential electrode are in series with the galvanometer, G, and since, at balance, no current is flowing in this circuit, these resistances have no effect, at least theoretically, on the balance condition.

4.3 The A.B.E.M. Terrameter

Electrical earth-resistance measurements were carried out using the A.B.E.M. Terrameter which fulfilled all the requirements mentioned

above. The Terrameter is usually employed in electrical resistivity surveying but was adapted for electrical earth-resistance measurements. For this, binding posts C_1 and P_1 are coupled together and connected to the pile reinforcement (Fig. 4.3); P_2 and C_2 being connected to auxiliary electrodes placed outwith the nominal pile diameter.

The Terrameter is contained in two lightweight watertight metal cases each measuring 400 x 150 x 200 mm / and having a combined weight of about 15kg. (See Plate 4). One case - the V-box - contains the measuring circuits, while the other - the G-box - contains the power supply. With reference to Fig. 4.3, which shows a schematic layout of the instrument, the current is supplied by a transistorised oscillator, E, and a powertransformer, T, producing a very low frequency square-wave alternating current (4Hz). The Terrameter employs a combined null-balance and resistance-comparator system of measurement and for details of circuitry reference may be made to the maker's handbook (51).

The special features of the Terrameter are its sensitivity and high instrumental accuracy, $\pm$ 3% for readings as low as 0.01 ohm, and $\pm$ 10% for readings of 0.003 ohm.

4.3.1 Mode of Operation

The V-box contains an amplifier A, a meter M, and a potentiometer R. A switch connects A and M to either the coupled potential electrodes X, or the potentiometer R. In position X, the potential difference between P_1 and P_2 is connected through the amplifier to the meter, M. The amplifier gain is adjusted until a deflection of, say, 60-70 scale

divisions, is obtained; switching to the XR position then connects the amplifier and meter to the potentiometer. The potentiometer is adjusted until the deflection on M is the same as that when the switch is in the X position. The comparison is checked by switching between X and XR positions as it is usually necessary to perform some fine adjustments to the reference potentiometer until both readings are exact. The reading on the potentiometer is then multiplied by the appropriate scaling factor, the resulting figure being the earthing-resistance of the pile for that particular position of P_2 and C_2.

To obtain a full earth-resistance curve for the pile, auxiliary electrode P_2 is inserted at several points between the pile and current electrode, C_2, with resistance readings being taken at these points. (Current electrode, C_2, is not moved during this operation.)

4.3.2 Auxiliary Electrodes, Connectors and Cables

One particular advantage in using alternating current is that one can forego the use of non-polarising electrodes, and, instead, galvanised steel stakes are quite adequate. The stakes used were approximately 600mm. in length and had a T-cross-section which ensured good contact with the ground (Plate 4). The stakes were either hammered or pushed into the ground at the required points for measurement. Pre-measured points were marked on the stakes so that the depth the electrodes were inserted into the ground was the same for all measurement points. In order to speed-up field procedure, bayonet plugs were employed throughout, both in connecting the cables to the Terrameter and the electrodes.

A precaution that has to be taken when using a.c. is to avoid the use of multi-core cables as errors can be introduced due to electromagnetic coupling between the current and potential leads. Individual, lightweight cables were used thus eliminating any coupling effects. Electromagnetic coupling between the V and G boxes can also occur if they are placed close to each other. However, this can be avoided by placing the boxes about one metre apart (51).

Connections to the pile reinforcement were by means of heavy duty crocodile clips (Plate 4), four being sufficient to ensure a reasonable contact. The only preparation to the pile is to clean any concrete etc., from the reinforcement with a wire brush/emery paper to obtain a good electrical connection.

4.3.3 Elimination of Lead Resistance

Generally speaking, lead resistance is not important. Normally when measurements are being made on the pile, one current and one potential electrode are joined and connected to the reinforcement by means of the crocodile clips (Fig. 4.4(a)). In this case the resistance of the lead is included in the measurement and if the pile resistance is low, the lead resistance may be an appreciable part of the whole. It can either be measured or separate leads run from the potential and current terminals as in Figure 4.4(b). In the latter case the resistance of the lead is not included in the measurement.

Lead resistance will only be a problem if the cables from C_1 and P_1 are long. By placing the boxes close to the pile head as part of field procedure then the leads from C_1 and P_1 can be reduced to a minimum

and the arrangement in Figure 4.4(a) used. Furthermore, as only the relative magnitudes of resistances between piles are required rather than accurate determinations, then, as long as the length of leads are kept the same for all the piles, lead resistance can be neglected.

4.3.4 Instrument Checks

Before any results were obtained, and periodically during field and laboratory work, the instrument was tested to check that the values indicated were correct. This was done using a standard resistance (R) whose value was accurately determined using a Wheatstone Bridge. The Terrameter was wired as an ohm-meter for this check, (Fig. 4.5) by coupling binding posts P1, C1 and P2, C2 and connecting the standard resistor between P1 and P2.

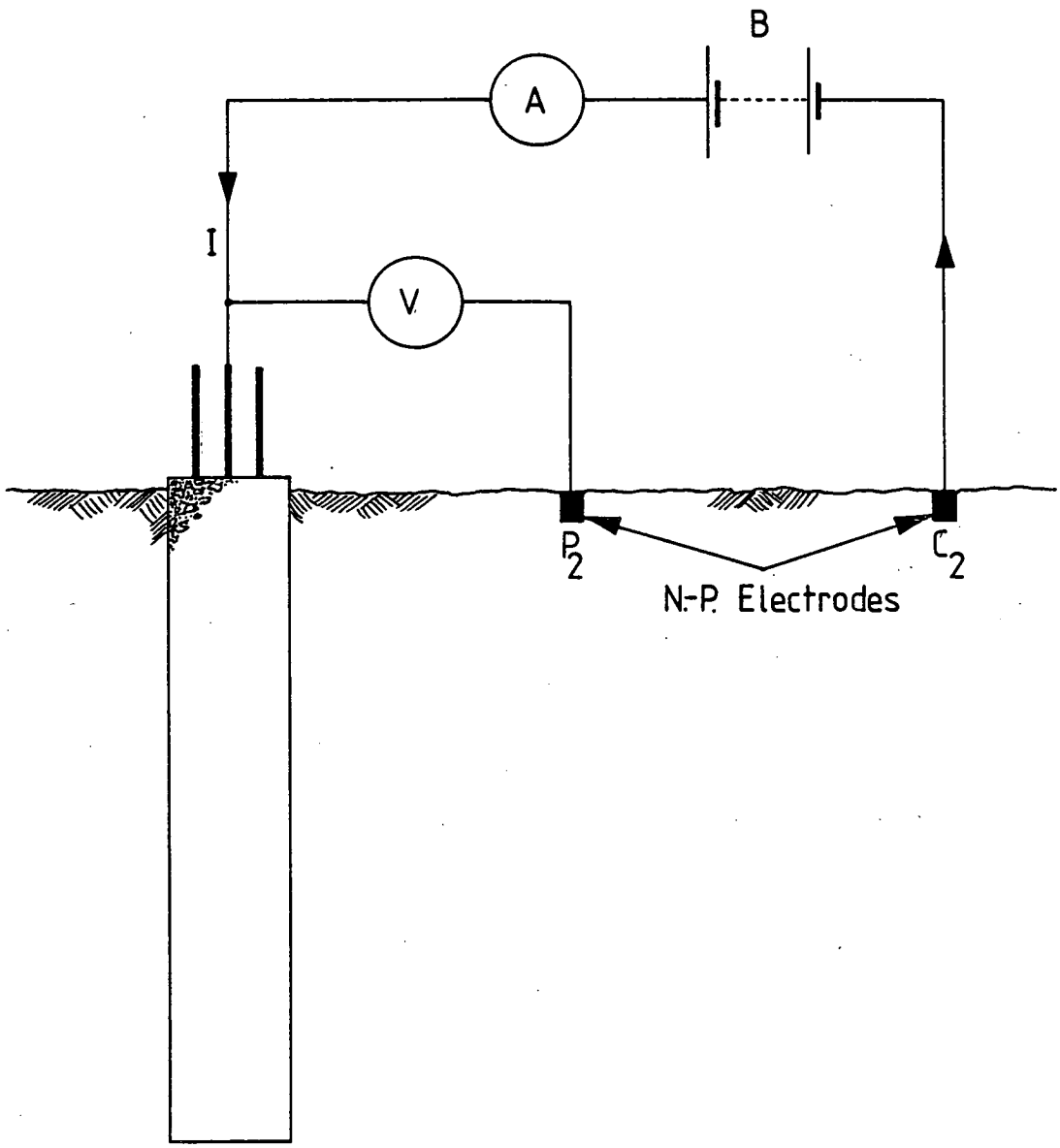

FIG. 4.1 Simplified arrangement for measuring the earthing resistance of a pile

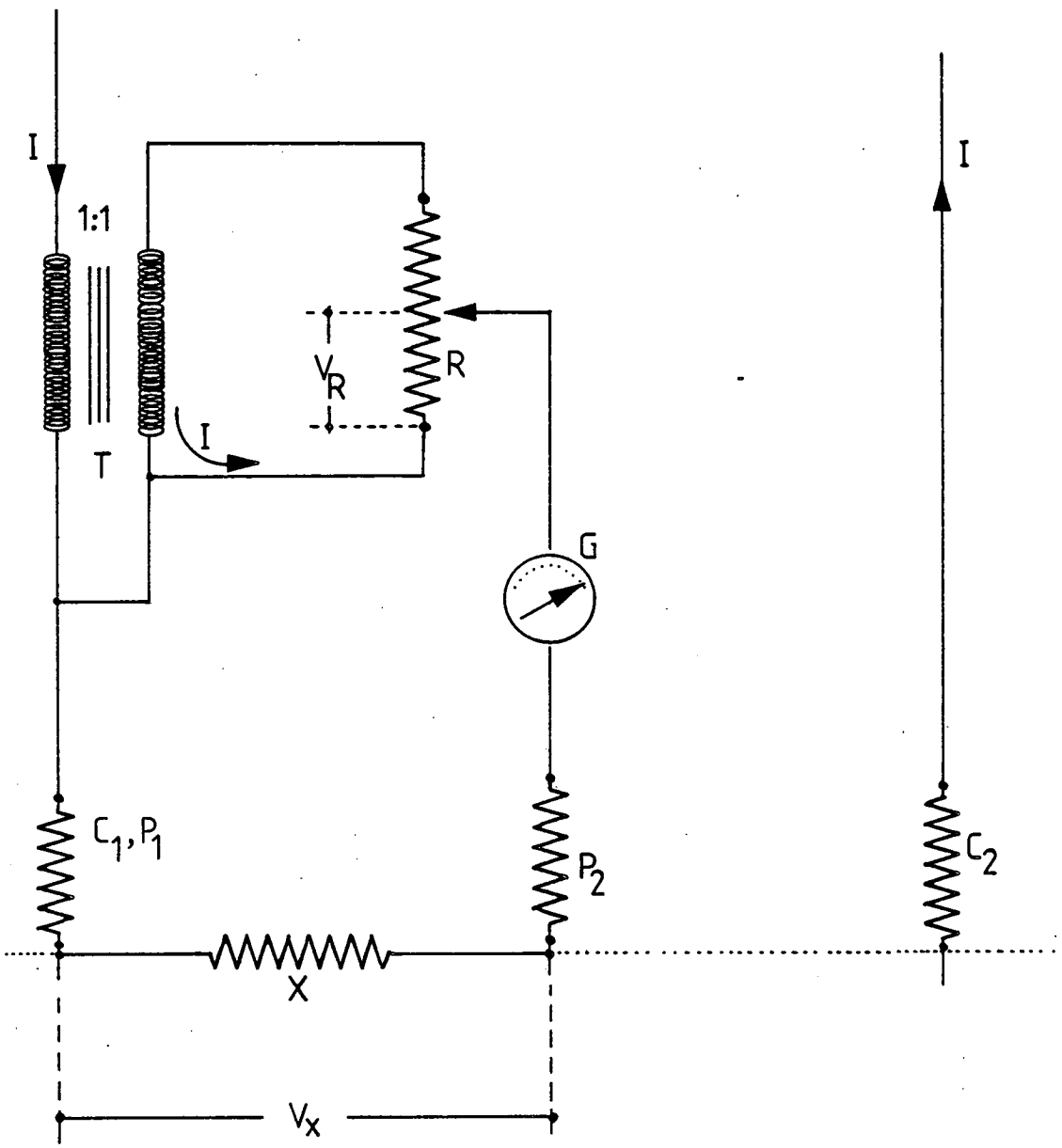

FIG. 4.2 Potentiometric system of measurement

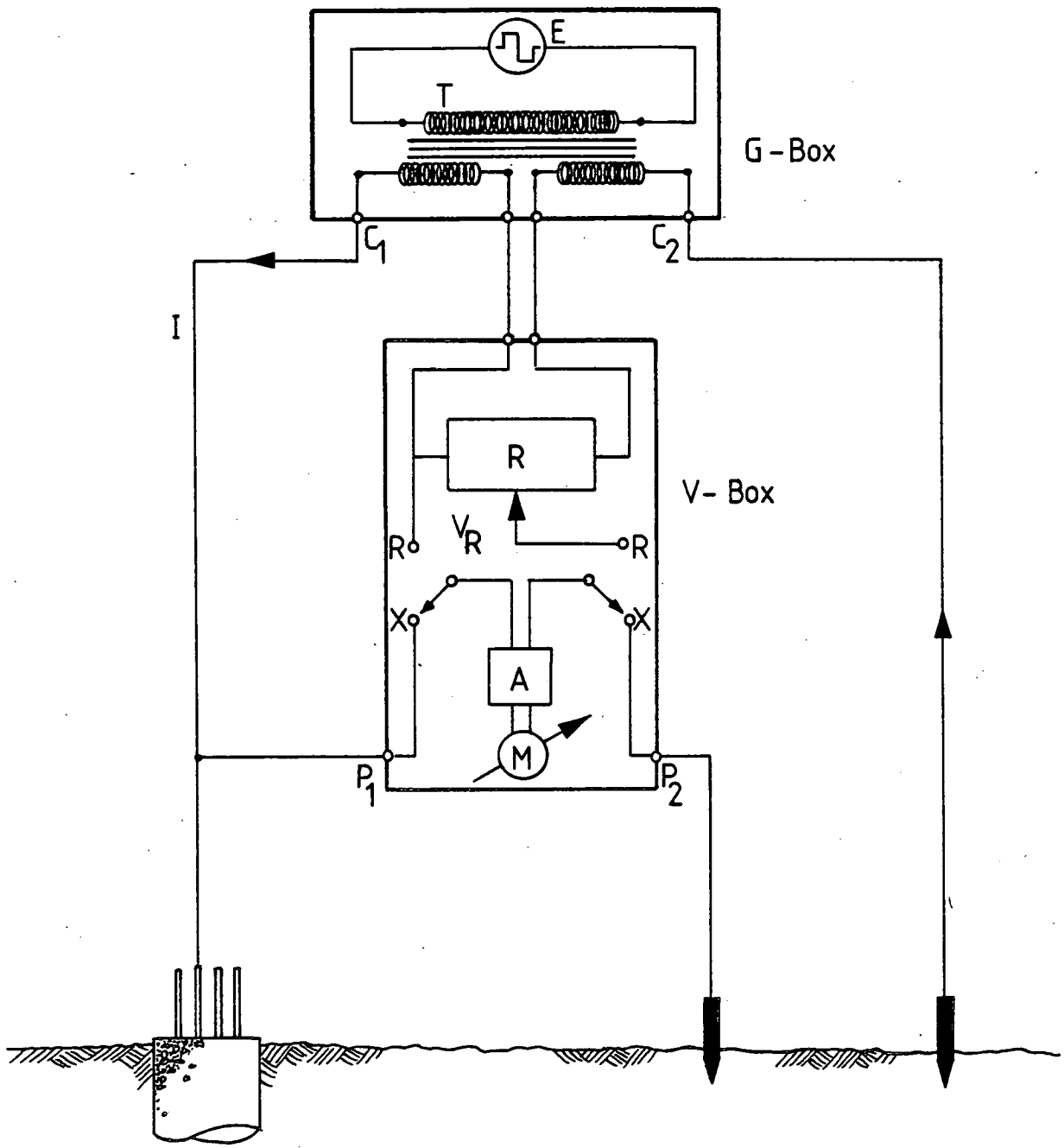

FIG. 4.3 Schematic layout of Terrameter

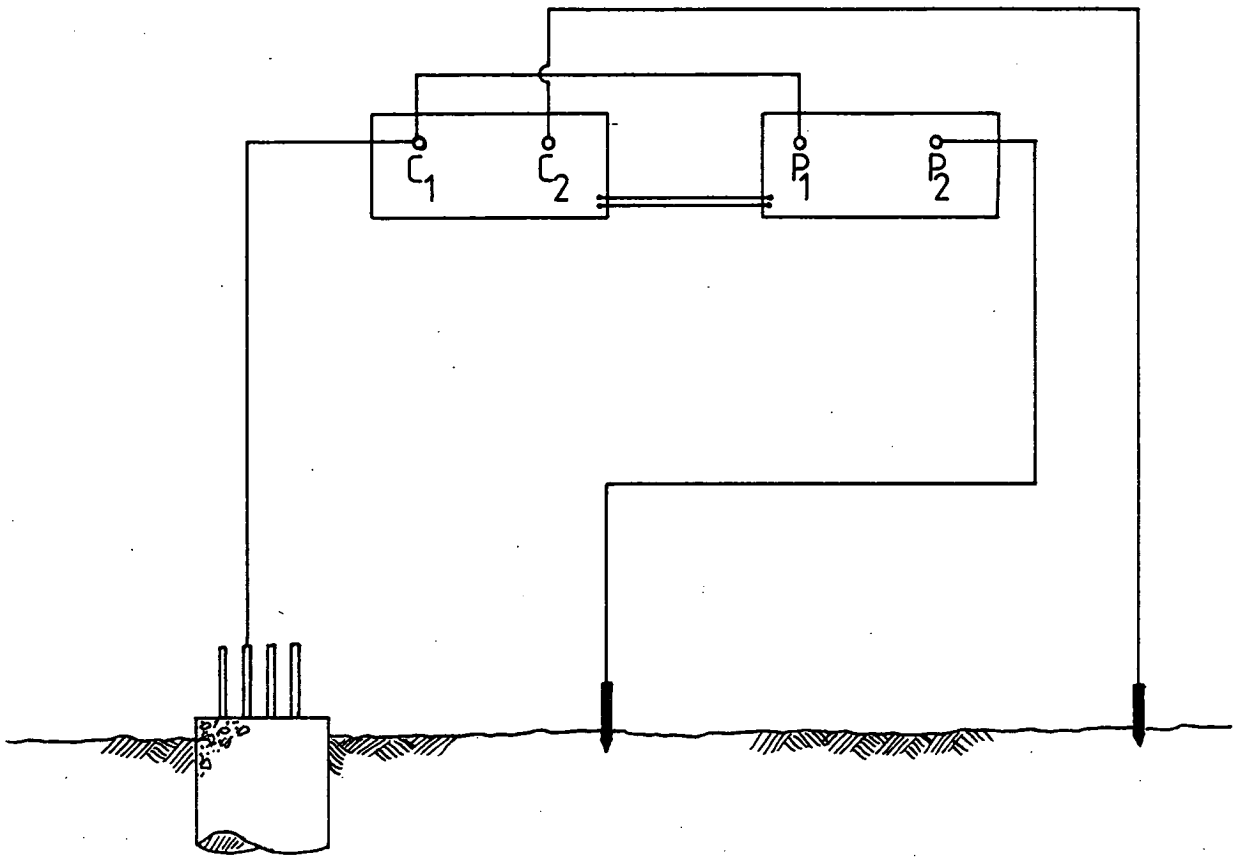

(a)

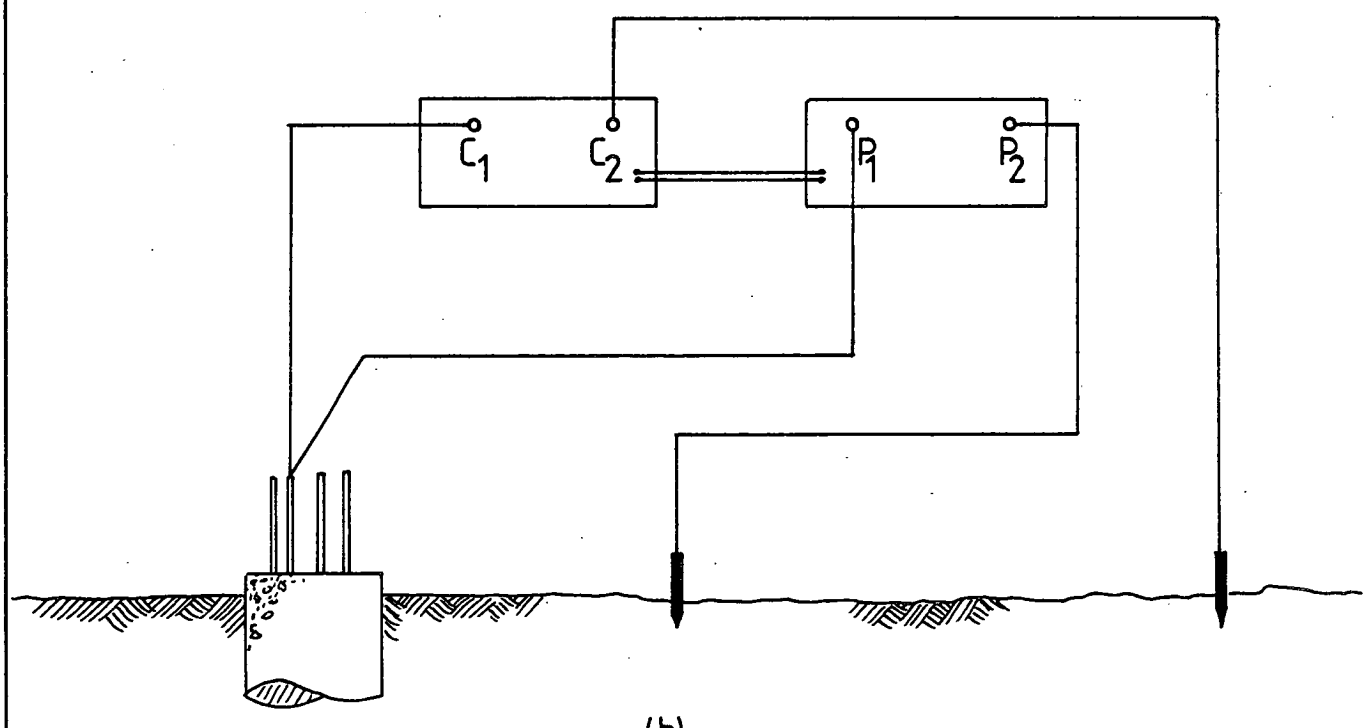

(b)

FIG. 4.4 Elimination of lead resistance

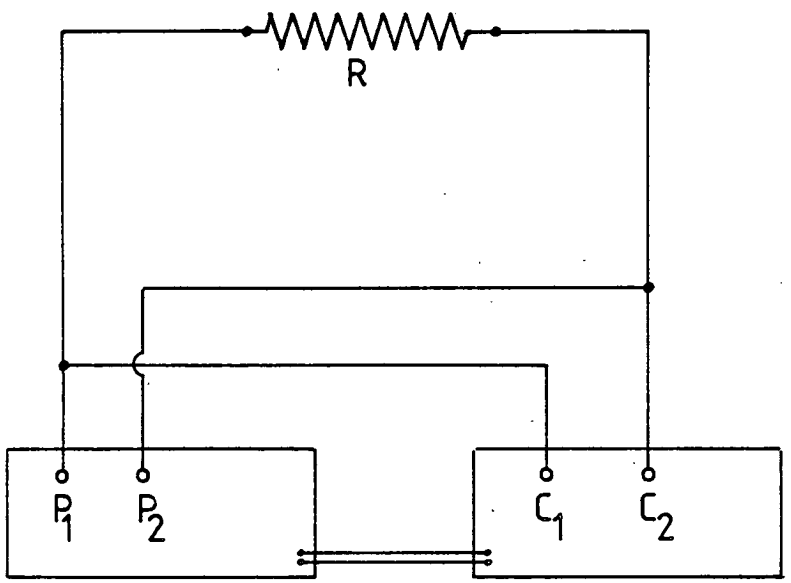

FIG. 4.5 Wiring arrangement for instrument checks

Instrument	Operating Frequency (Hz.)	Measuring Range (Ω)
Tellohm Soil Resistance Meter	110	0 - 10,000
Geohm Earth Tester	108	0 - 5,000
Norma Earth-Resistance Meter	125	0 - 5,000
Geophysical Meggar Earth Tester	20	0 - 1,000
A.B.E.M. Terramter	4	0 - 10,000
The Earth Tester	150	0 - 1,000

TABLE 4.1

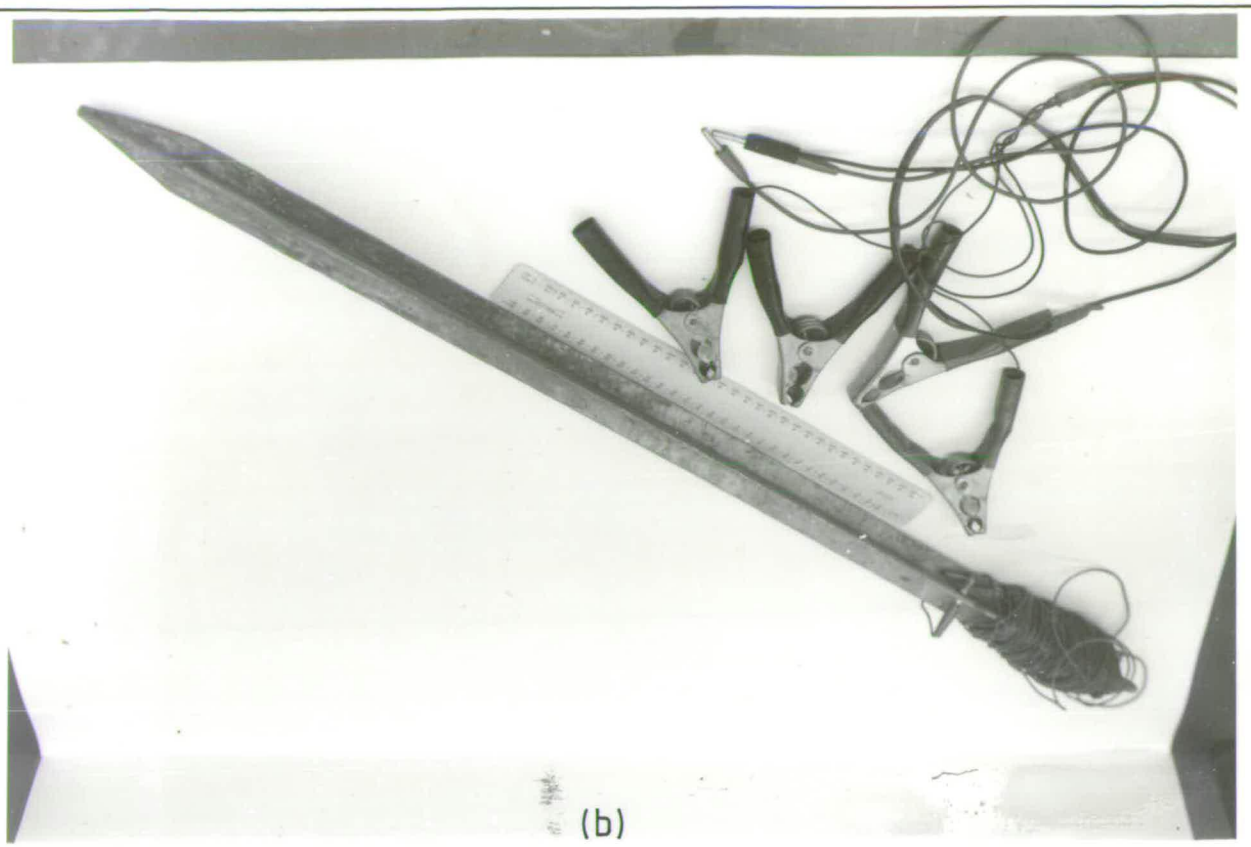

(b)

PLATE 4

(a) A.B.E.M. Terrameter & (b) Electrodes & Connectors

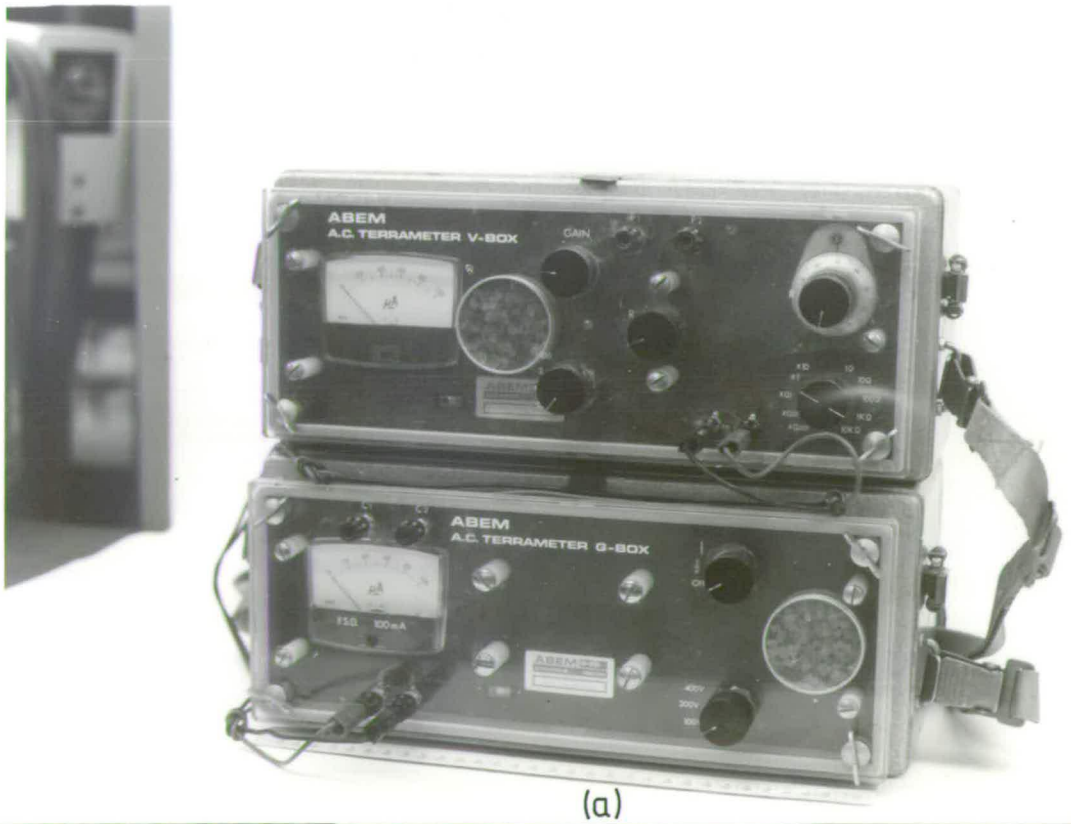

(a)

CHAPTER 5

THE ELECTRICAL PROPERTIES OF CONCRETE

5.1 Introduction

The foregoing analysis in Chapter 3 has been important in that it has highlighted the interrelationship between the system variables which determine the earthing-resistance of a reinforced concrete pile. The electrical resistivity of concrete has a major influence on the overall earthing resistance of the pile. The influence of, for example, mix-ratios, environment and time, on the resistivity of concrete are essential for an accurate assessment of field tests. These form the subject matter of this Chapter.

Comparatively little work has been undertaken on the electrical properties of cements and even less on concretes, especially on the variation of electrical resistivity during the initial setting stages and subsequent hardening process. The characteristics of cement vary considerably throughout the setting process and consequently, the relative importance of such factors as polarisation and capacitance changes with the age of the concrete. Furthermore, the electrical properties may not be constant throughout the specimen of concrete for the following reasons:

(a) concrete itself is a heterogeneous material,
(b) stratification occurs during placing, and
(c) subsequent dry-out takes place preferentially from the exposed surfaces resulting in a moisture gradient from the centre to the exposed face of the concrete.

The present work has been concentrated on the measurement of the electrical properties of concretes of different mixes and water cement

ratios, these mixes being typical of those used in concrete structures. Comparative data on specimens of neat cement pastes, mortars and concretes made with different types of cement was also obtained. Investigation has been made of the variation of electrical resistivity of concrete during the initial setting period (i.e. first 24 hours) and throughout the hardening process.

Considerable progress has been made in relating the physical and mechanical properties of concretes to the corresponding properties and volume fractions of the constituent aggregate and hardened cement paste (e.g. elastic modulus, shrinkage, creep and Poisson's Ratio), but as yet, a similar pattern of interrelated behaviour has not been established for electrical resistivity characteristics. The experimental data obtained is examined closely in an attempt to assess how the electrical resistivity for cement pastes, mortars and concretes is affected by mix-proportions, the water-cement ratio and temperature of the specimens. From this examination an electrical and theoretical model for the conduction of current through concrete is proposed.

5.2 Review of Previous Work

Previous work has mainly been undertaken on cement pastes and has been directed towards obtaining information about the changes in electrical resistance during the first twenty four hours of the setting process.

Among the earlier workers in this field were Baire (52), Petin (53), Kind (54), and Dorsch (55). The latter, working with cement pastes of different types of cements, found that the electrical resistivities were in reverse order to the lime contents of the cements tested.

The same author also showed that in the short period covered by his tests, a decrease in the water-cement ratio from 0.30 to 0.25 corresponded to an increase in resistivity of approximately 20 percent.

Boast (56) also investigated conductometric methods for studying the setting phenomena during the first three hours and tried to correlate conductivity of sand mortars with their 28 day compressive strength. It is of interest to note that he was unable to find a general relation between the resistivity of the mortar and its 28 day strength.

Michelson (57) attempted to investigate the beginning and end of setting by considering the galvanic currents generated in any paste between two different metals. On voltage time graphs the beginning is given by the point at which constant section of curve commences to slope upwards and the end by the point corresponding to maximum voltage. A similar effect was also noticed by Aschan (58). Jesser (59), who considered setting and hardening as an electrostatic phenomena, studied the e.m.f. of galvanic elements in various cements in connection with the colloidal nature and change in the paste.

Calleja (60) published curves showing the variation in electrical resistance of Portland cement pastes setting under adiabatic conditions and indicated that over a range of frequencies from 40-20,000 Hz, the resistance of the paste decreased only slightly, the maximum decrease being about 10 percent.

The Division of Building Research C.S.I.R.O. (Australia) reported that the resistivity, between pools of mercury, for a block of air-dry portland cement paste lies between 2.5 and 50 kΩ-m (61), and Maguire

and Olen (62), using a guard-ring technique found that concretes (with siliceous aggregate), after oven drying at 96°C for one day had resistivities exceeding 100 MΩ-m at 700V. The same authors gave resistivities of 6.54-11.4 KΩ-m for mature concretes which were not artifically dried.

The resistivities (during storage in air) of neat Portland cement and gravel concretes made with slag cement and Portland cement were investigated by Decoux and Barree (63). The resistivity of specimens of neat Portland cement was much less than that of concrete; furthermore the addition of sodium chloride, calcium chloride, magnetic iron oxide or iron turnings appreciably decreased the electrical resistivity. Cigna (64) found that mortar containing calcium chloride had a resistivity some 15 times lower than a similar mortar without calcium chloride. Ohama (65) and Yamada (66) have also given some data on electrical resistivities in connection with work on the electrical heating of concrete, whilst Spencer (67) has investigated the relationship between electrical resistance and moisture content in mass concrete.

Hammond and Robson (68) undertook a limited study on the a.c. and d.c. electrical properties of different cements and concretes and found that the resistivities of high alumina cement specimens were 10-15 times higher than the Portland cement specimens, whereas there was negligible difference between the resistivities of Rapid Hardening Portland Cement and Ordinary Portland Cement specimens. (Possibly due to the varying lime contents between O.P.C. and H.A.C.). They also indicated that for concrete subjected to a.c. the capacitative reactance is much larger than the resistance at all ages; in consequence, most current flows

through the latter and the power factor is nearly unity.

The resistivity of cement pastes with pozzolana additive was investigated by Ganin (69) in the U.S.S.R., the specimens being sealed and stored at room temperature.

Monfore (70) concluded that conduction through moist concrete is essentially electroytic, with a resistivity of about 100 Ω-m; this is within the range of semiconductors. On the other hand, the resistivity of concrete may be increased manyfold by air-drying, and upon over drying at 105°C has a resistivity of about 1000 MΩ-m, which means that concrete is a reasonably good insulator. The effect of prolonged moist storage on the resistivity of mortar, and cement paste specimens was investigated by Monfore; however so few data points exist that no general trends as to the shape of the resistivity versus time graph can be deduced. He also found that the majority of admixtures added to cement pastes generally cause a decrease in the resistivity of the paste at early ages, but, as the paste matures some show a moderate increase in resistivity.

Henry (71) found that the electrical resistivity of concrete increases with age and decreases with an increase in salinity of mixing water. This latter conclusion was of greater significance in concretes with high water cement ratios than in high strength concretes.

Farrar (72) used "Marconite" to reduce substantially the electrical resistivity of concrete while Nikkannen (73) used finely divided bituminous material to increase the resistivity of concrete, and, in cases where static electricity is undesirable and a decrease in the

insulation resistance of concrete is required, satisfactory results could be achieved by the addition of acetylene carbon black (2 to 3% by weight of cement).

Hancox (74) has given some data on the electrical conductivity of cement pastes, which was used in the determination of the mean pore radius of cement paste.

The available literature has revealed very little data directly relevant to the author's area of interest.

5.3 Concept of Resistivity of a Material

Resistivity is a fundamental property ofaparticular material which characterizes that material almost as completely as its density. The relationship between resistivity and resistance can be explained with reference to Figure 5.1. The electrical resistivity of any material is defined as the resistance, in ohms, between opposite faces of unit cube of that material. Thus, if R is the resistance of a block of concrete having a length, L metres, and a cross-sectional area, A metres^2, then the resistivity, ρ, is expressed by the formula.

$$\rho = \frac{RA}{L} \quad \Omega\text{-m} \qquad \ldots\ldots (5.1)$$

Resistivity, being a fundamental property of the material, is independent of the volume, whereas resistance depends upon the shape and size of the specimen. The conductivity of a material is defined as a reciprocal of its resistivity, i.e.

$$\sigma = {}^1/_{\rho} \quad \text{Siemens } m^{-1} \qquad \ldots\ldots (5.2)$$

5.3.1 Temperature Coefficient of Resistivity

Concrete exhibits a negative temperature coefficient of resistivity (70, 73), hence the electrical resistivity of such a material at a temperature, t, can be related to its resistivity at a reference temperature, Θ, by the formula.

$$\rho_t = \rho_\Theta / (1 + \alpha(t-\Theta)) \qquad \ldots\ldots (5.3)$$

Where ρ_t is the resistivity at t^oC, ρ_θ is the resistivity at θ^oC and α is the temperature coefficient of resistivity of the material.

Another way of expressing the resistivity, ρ, of concrete at a certain temperature, T is by means of the Hinrichson-Rasch Law which is applicable to most refractory materials, i.e.

$$\log_e \rho = \frac{B}{T} + C \qquad \ldots\ldots (5.4)$$

where B and C are constants, and T is in degrees absolute. If ρ_1 and ρ_2 are the resistivities of the concrete at temperature T_1 and T_2 in degrees absolute, then,

$$\log_e \rho_1 = \frac{B}{T_1} + C \quad \ldots\ldots (a)$$

$$\log_e \rho_2 = \frac{B}{T_2} + C \quad \ldots\ldots (b) \qquad \ldots\ldots (5.5)$$

Subtracting results in,

$$\log_e (\rho_1/\rho_2) = B.\left(\frac{1}{T_1} - \frac{1}{T_2}\right) \qquad \ldots\ldots (5.6$$

or,

$$\rho_1 = \rho_2 e^{B\left(\frac{1}{T_1} - \frac{1}{T_2}\right)} \qquad \ldots\ldots (5.7)$$

5.4 Conduction Paths through Concrete

Concrete may be considered as a composite of various sized aggregate particles in a matrix of Portland cement paste. To explain the possible conduction paths, the author has drawn on a simplified model of heterogeneous porous media proposed to explain the variation of the electrical conductivity of resin-solution columns with the conductivity of the components (75, 76). This model is an approximation, imparting a simple physical meaning to the more complicated exact solution to the problem.

With reference to Figure 5.2, the conduction of electrical current through the heterogeneous medium of concrete can have three possible paths:

(a) through the aggregate and paste in series,
(b) through the aggregate particles in contact with each other, and,
(c) through the paste itself.

5.4.1 Proposed Model for Conduction

A simplified model proposed by the author (77, 78) for d.c. conduction of current through concrete is shown in Figure 5.3 where parameters x,y, and z represent the fractional cross-section of elements (a), (b) and (c). Of current taking path (a), w represents the portion that travels through aggregate. Parameter x represents a measure of current path through the aggregate and parameter z is a measure of the continuous interstitial path. The resistance of each circuit element,

and the overall resistance of the model can readily be determined by assigning values to the geometrical parameters w, x, y and z, or, conversely, by knowing the electrical resistivities of the constituents of the concrete, the values of w, x, y and z can be deduced. From this, it is then possible to calculate the proportion of current flowing through each circuit element and hence, the relative importance of that particular element.

The electrical resistivity of typical aggregates used in concretes is shown in Table 5.1 (38, 70, 79). From experimental work, the electrical resistivity of moist concrete lies in the region of 25.00-45.00 Ω-m while that of a neat cement paste in the region 10.00-13.00 Ω-m. It can be seen that the resistivities of the aggregate are several orders of magnitude higher than that of the concrete, and will, consequently, result in a high proportion of current being conducted through the cement paste, i.e. through the path of least resistance (Appendix 2).

Extension of the same model to a.c. properties is shown in Figure 5.4. Electrically, a block of concrete may be considered as a network of resistances and capacitances; each path is represented by a parallel circuit of resistor and capacitor. The impedance of each zone can be calculated from the parameters associated with the material forming the zone but, for practical purposes, the d.c. model can also be assumed for a.c., as is explained in section 5.5.

Generalising, the resistivity, ρ_c of a composite such as concrete can be written as,

$$\rho_c = \frac{\rho_p}{\beta\phi} \qquad \ldots\ldots (5.8)$$

where ρ_p is resistivity of the cement paste matrix; ϕ is numerically equal to the fractional volume of the cement paste and β is a reduction factor (0.77 for the example in Appendix 2).

5.4.2 Mechanisms of conduction through Portland Cement Paste

The preceeding section described three different conduction paths through concrete and, from a simplified electrical model, showed that a high percentage of the electrical current is conducted through the paste. This leads to the conclusion that concrete can be considered as composites of non-conductive particles contained in a conductive cement paste matrix. The aim of this section is to identify the possible conduction mechanisms through the paste itself.

Nikkannen (73) has suggested that conduction through moist concrete is essentially electrolytic in nature and tests by Hammond and Robson (68), and Monfore (70) support the view that conduction is by means of ions in the evaporable water in the cement paste, the principal ions being (58), Ca^{++}, Na^{+}, K^{+}, OH^{-}, and SO_4^{--} . Since the amount of evaporable water in a typical cement paste varies from about 60 percent by volume at the time of mixing to 20 percent after full hydration (80), then, the electrical conductivity of the concrete should also be a function of time. Another possible path for current flow is by means of electronic conduction through cement compounds themselves.

The conduction of electric current through the cement paste can be visualised as having two components; one is ionic conductivity through the free evaporable water which will depend on ionic concentration, temperature, and type of ions present in solution; and the other is

electronic conduction through the gel, gel-water and unreacted cement particles, particularly compounds or iron, aluminium and calcium. Since approximately 40 percent of the water (by volume) is bound in varying degrees within the products of hydration, then this path could contribute to conduction through the paste as Wyllie and Gregory (81) suggest that even physically immobile water can conduct.

The electrical conductivity of the paste depends on the changes which both solid and solution phase (i.e. evaporable water) undergo. These changes are closely linked to each other since the composition and concentration of ions in the evaporable water depend on the soluble compounds within the cement particles and residual water available; while the composition and structure of the solid phase depends on the amount of water, both absorbed and chemically combined, within the cement compounds during the hydration process. Hence, it is clear that the two factors mentioned above, which conduct nearly all the current through concrete, are virtually inseparable, as the paste itself is in a constant state of change.

Trying to sub-divide the paste further into the two conduction elements mentioned above would be slightly more speculative in nature as the hydrating cement compounds control the concentration and type of ions present in the evaporable water. Also, physical difficulties detailed below preclude dividing the paste:-

(a) the volume of evaporable water available for conduction at any particular point in time is virtually impossible to quantify as water in a cement paste is fluctuating from free (evaporable) water to adsorbed water, interlayer water and chemically combined

water (82). In fact, there is no technique known to the author for determining, with accuracy, the proportions of water held in the aforementioned states,

(b) it is difficult to determine with any degree of accuracy the electrical resistivity of the evaporable water within the paste. The resistivity of typical mixing water is about 100-150 Ω-m, while that of a mature paste about 13 Ω-m, indicating that the resistivity of the evaporable water may be substantially reduced. It would be wrong to use the initial resistivity of the mixing water for the ionic conduction path.

(c) likewise, it would also be difficult to determine the electrical resistivity of the compounds of hydration.

It is concluded that taking the paste as a whole as having the controlling factor in the overall resistivity of the concrete is not an unreasonable proposition and anything which affects the electrical conductivity of the paste will affect the overall conductivity of the concrete.

5.4.3 Theoretical approach to conduction using Resistivity Formation Factors

For specific arrangements of aggregate of regular geometric shape, it is possible to calculate the resistivity of such a composite. Maxwell (47) has derived a general relation for the conductivity, σ_x, for a composite consisting of a matrix with conductivity, σ_1 in which dispersed spherical particles of conductivity σ_2 are embedded in regular arrangement and in such a manner that their distance is large compared with their radii.

If the total volume of composite is ϕ_x, and the total volume of the particles is ϕ_2 and the ratio $\phi_2/\phi_x = r$, then the following relationship exists:

$$\frac{\sigma_x}{\sigma_1} = \frac{2\sigma_1+\sigma_2-2r(\sigma_1-\sigma_2)}{2\sigma_1+\sigma_2+r(\sigma_1-\sigma_2)} \qquad \ldots\ldots (5.9)$$

Hence, in terms of the matrix volume ϕ, and letting $\phi = 1 - r$ or $r = 1 - \phi$, then,

$$\frac{\sigma_x}{\sigma_1} = \frac{3\sigma_2+2\phi(\sigma_1-\sigma_2)}{3\sigma_1-\phi\ (\sigma_1-\sigma_2)} \qquad \ldots\ldots (5.10)$$

However, if the resistivity of the particles is assumed 'infinite' in comparison to the resistivity of the matrix ($\sigma_2 = 0$), then, from equation (5.10), there results,

$$\frac{\sigma_x}{\sigma_1} = \frac{2\phi}{3-\phi} \qquad \ldots\ldots (5.11)$$

or, since the conductivity is the reciprocal of resistivity, then,

$$\frac{\rho_x}{\rho_1} = \frac{3-\phi}{2\phi} \qquad \ldots\ldots (5.12)$$

where ρ_x is the resistivity of the composite, ρ_1 is the resistivity of the matrix and ϕ is the fractional volume of the matrix. Defining the ratio of the resistivity of the composite to that of the resistivity of the matrix as the Formation Factor, then,

$$F = \frac{\rho_x}{\rho_1} \qquad \ldots\ldots (5.13)$$

Lord Rayleigh (83) also examined the problem of the formation factor of systems of spheres and cylinders and concluded that for spheres, Maxwell's expression gave a value of F, which at low ϕ values, was too small. However, Lord Rayleigh's expressions were extremely complex and were not supported by any experimental data.

Fricke (84, 85), generalised Clerk Maxwell's treatment to obtain an expression, applicable not only to spheres but also to oblate and prolate spheroids. His equation, for the case of non-conducting particles is:

$$F = \frac{(x+1)-\phi}{x\phi} \qquad \ldots\ldots (5.14)$$

where $x = 2$ for spheres and $x < 2$ for spheroids. The greater the axial ratio of the spheroid, the smaller Fricke computed x to be. Some experimental data was adduced by Fricke (84, 85), and by Fricke and Morse (86), to support his mathematical conclusions. For the particular sand that Fricke studied x, in the above expression, is 1.4, hence,

$$F = \frac{(2.4-\phi)}{1.4\phi} \qquad \ldots\ldots (5.15)$$

Slawinski (87) also studied the relationship between F and ϕ for aggregates of spheres, both in contact and dispersed, and derived the empirical formula,

$$F = \frac{(1.3219-0.3219\phi)^2}{\phi} \qquad \ldots\ldots (5.16)$$

As a mortar could be considered as a single size particle system in a conductive cement paste matrix, then the formula given above would relate the resistivity of the mortar to the fractional volume of cement paste matrix and the resistivity of that matrix. The experimental results on mortar specimens (70) and the theoretical formation factors using the Maxwell, Fricke and Slawinski relationships are compared in Table 5.2. The results shown in Table 5.2 agree to within a few per cent with the theoretically calculated value, confirming the present argument that conduction is primarily through the cement paste matrix.

5.4.4 A Modified Archie's Law

The formulae derived are mainly applicable to composites of single particle size in a conductive matrix. Concrete consists of many sizes of particles (aggregate) in a cement paste matrix and the derived formulae may not be applicable to concrete, although they do confirm that conduction is through the cement paste matrix. For concrete a different approach is required.

Archie (88), when investigating the electrical resistivity of consolidated and unconsolidated sandstones, found there existed a relationship between resistivity formation factor, F, and porosity ϕ, of the rock, viz:

$$F = \frac{R_o}{R_w} = \phi^{-m} \qquad \ldots\ldots (5.17)$$

where, R_o = resistivity of the sandstone when filled with water,

R_w = resistivity of the water contained in the sandstone,

ϕ = fractional volume of water contained in the rock,

m = the shape factor.

Pirson (89) found that the exponent m lay between 1.3 for slightly 'cemented' rock and 2.2 for highly 'cemented' rock. The exponent, m, may thus be visualised as a measure of the degree of consolidation of the rock.

Atkins and Smith (90) developed a theoretical approach for the formation factor of a rock consisting of several particle sizes, and showed that by applying Archie's equation sequentially to each of the components of the rock could generalise equation (5.17) which would then apply to

a multi-size particle system, i.e.

$$F = A\phi^{-m} \qquad \ldots\ldots (5.18)$$

where F, m and ϕ are defined above and A is a constant. The relationship was shown to exist by Winsauer et al (91) from a purely empirical standpoint.

Applying equation (5.18) to concrete, F, as defined by the author, would be the ratio of the measured resistivity of the concrete to the resistivity of the cement paste, and ϕ the fractional volume of the paste within the concrete. Thus, if a log-log graph is plotted of formation factor of concrete against the fractional volume of cement paste in that concrete, then a straight line of gradient-m should result. This equation is not unlike equation (5.8) which was developed from the electrical model.

5.5 A.C. Characteristics of Concrete

Ohms Law states that the direct current, I, through a metallic conductor is proportional to the potential, E, applied and inversely proportional to the resistance, R, of the conductor, i.e.

$$I = \frac{E}{R} \qquad \ldots\ldots (5.19)$$

If the conductor is an electrolyte, then the passage of direct current will cause polarization and the establishment of a potential at the electrode/electrolyte interface which opposes the applied potential. To negate this spurious potential alternating current (a.c.) is normally employed.

As stated in section 5.4.1, when a.c. is used a block of concrete can be considered as a complex network of resistances and capacitances with conduction taking place, primarily through the paste. The problem may be simplified by reducing the conduction of alternating current through the paste to that of one through a single capacitance, C, connected in parallel with a resistance, R. The impedance of such a 'lumped system' is expressed as,

$$\frac{1}{Z^2} = \frac{1}{X^2} + \frac{1}{R^2} \qquad \ldots\ldots (5.20)$$

where, z = impedance, ohms.

R = resistance, ohms.

$X = \frac{1}{2\pi f C}$ = capacitative reactance, ohms.

f = frequency of alternating current, Hertz.

C = capacitance, farads.

The effect of the reactance on the total impedance is governed by the relative magnitudes of X and R. When X is of the same order or smaller than R, the effect will be appreciable. The term used in indicating the relative proportions of capacitance and resistance in conducting current is the power factor and, when the material is considered as a capacitor and resistor in parallel, can be expressed as,

$$\text{Power factor} = 1/\sqrt{(1+2\pi f CR)} \qquad \ldots\ldots (5.21)$$

Hammond and Robson (68) showed that, for concrete, the capacitative reactance was so much greater than the resistance and only the resistive element of conduction is contributing to the overall impedance. This implies that the d.c. resistance is very nearly equal to the a.c. impedance. (Within the frequency range of the present study)

This effect was also verified by Monfore (70). Consequently,

for the experiments undertaken, conduction is regarded as purely resistive and reactive effects disregarded, viz. measurement of the capacitative element was not necessary.

5.6 Experimental Procedure

The objective of the experimental programme was to obtain information on the electrical resistivity of moist concrete specimens as a function of,

(a) mix-proportions,
(b) time,
(c) type of cement,
(d) air-voids content, and,
(e) ambient temperature.

The latter was to simulate field conditions. It is to be emphasised that the experimental work undertaken was on moist specimens, i.e. they were not allowed to dry out.

In view of the theory described at the beginning of this Chapter, the results obtained are used to confirm the theoretical deductions.

5.6.1 Test Specimens

The test specimens were 100mm x 100mm x 100mm cubes of the mixes shown in Table 5.3, Ordinary Portland Cement (O.P.C.) being used in all cases. In addition a number of tests were undertaken on concretes made with Sulphate Resisting Portland Cement (S.R.P.C.) and Rapid Hardening

Portland Cement (R.H.P.C.) and a limited number of tests were undertaken on 70mm x 70mm x 70mm mortar cubes, mainly to obtain formation factors for high fractional volumes of paste matrix. All materials were batched by weight. The fine and coarse aggregates for the mortar and concrete specimens were oven dried and allowed to cool before being used. A sieve analysis carried out on the fine aggregate (specific gravity 2.65) showed that it was sand of Grading Zone 3 (92) and the maximum size of coarse aggregate (specific gravity 2.61) was not greater than 13mm. The concrete was mixed using a bench top mixer and vibration-compacted into metal moulds in approximately four 25mm layers. The tops of the moulds were covered with polythene and left for 24 hours. Six specimens were made for each concrete mix ratio at each water cement ratio.

After 24 hours the specimens were demoulded and allowed to cure in a water bath at $23^{o}C$. On demoulding the weights were recorded and Table 5.4 gives a comparison of mean experimental density of the concretes with the theoretical density (absolute volume method (80)).

Since all the concrete specimens could be regarded as well-compacted, an experimental test was carried out on cubes containing a high percentage of air, the air-voids being introduced into the concrete at the time of mixing by using small polystyrene beads. Enough polystyrene was added such that the volume of air in the cubes was increased to 6% and 20%. The mix-proportions used for these voided cubes was 1:2:4 with a water-cement ratio of 0.8. (The volume of air can be calculated by knowing the weight loss between a well-compacted cube and a voided cube and the density of the concrete).

A series of cubes of the mix ratios shown in Table 5.3 were stored outdoors in the ground under 200mm of sand and away from direct sunlight. These cubes were initially allowed to cure for 13 days before being placed outside. A careful check was kept on the weights of these cubes in case there was any evaporation from the cubes. In fact over the test period (3 months), the weights increased by less than 0.1% from their value when taken out of the curing tank, showing that concrete placed in the ground will lose very little water due to evaporation from the exposed cube surfaces.

5.6.2 Choice of Electrodes

Some investigators (64, 68) have measured the electrical resistivity of concrete by embedding rod electrodes into the concrete in such a manner that the current is passed through the interior of the specimen. This electrode configuration would only be used where there is a significant moisture gradient between the surface of the specimen and the inside, as, for example, in the case of a cube being allowed to dry out at elevated temperatures. This is not the case for cubes allowed to cure under water and the moisture gradient is assumed zero between the surface of the cube and its interior. Another objection to the use of embedded electrodes is that it is difficult to evaluate which area should be used for calculating the volume resistivity (Fig. 5.5(a)).

To measure the resistivity with accuracy it is essential that the current traverses the full area of the specimen, which can be ensured by using external plate electrodes the same shape as the surface of the specimen, as shown in Figure 5.5 (b). Using such an arrangement, the

volume resistivity can be calculated using equation (5.1).

The specimens were tested using 100mm x 100mm external brass plate electrodes, these electrodes being placed at opposite faces of the cube. For testing during the initial setting period, i.e. the first 24 hours, the insides of the moulds were lined with polythene, with the electrodes serving initially as two sides of the moulds. To ensure the electrodes were not touching the moulds (as, for example, in the case if the polythene was torn) a resistance meter was attached to the electrodes and the mould. This resistance was infinite in all cases showing that an open circuit existed between the electrode and the mould. Hence the polythene could be regarded as being a very good insulator.

For testing during the hardened state, intimate contact between the electrodes and the specimens was obtained using a liquid cement paste with a water-cement ratio of 0.5. Such a paste has a very low resistivity (~2Ω-m), hence its resistance, $\rho L/A$, was considered negligible in comparison to the resistance being measured. A G-clamp was used to secure the electrodes to the cube. When testing, the specimens were surface dried with blotting paper to ensure that there were no surface conduction effects and that the resistance measured was the volume resistance (Fig. 5.6).

5.6.3 Instrumentation

For reasons already discussed, alternating current was employed for resistance measurements of the specimens. The Terrameter was adapted for use as an ohmmeter by coupling binding posts C1, P1 and C2, P2;

the unknown resistance i.e. the concrete cube, is then connected between P1 and P2 (Fig. 4.5). The Terrameter is operated in the usual manner and the reading obtained is the value of the unknown resistance.

5.7 Discussion of Test Results

All cubes were tested over a 3-4 month period, which was considered long enough to establish any general trends. Long term tests were carried out on some of the cubes for a period in excess of 8 months. For cubes allowed to mature in outdoor conditions, the weather was sufficiently variable to establish the variation of electrical resistivity of concrete under field conditions.

All specimens of the same mix ratios were tested on the same day. The resistivity of the cubes of the same mix proportions and water-cement ratio showed good consistency and the variation in the mean resistivity was less than $\pm$ 3.0%; furthermore there was no measurable difference in resistance between opposite pairs of faces of each cube.

The results from the tests have been given in the form of electrical resistivity versus time graphs:

(a) Figures 5.7 to 5.10 show the development of resistivity of neat-cement pastes and three of the concrete mixes during the first 24 hours of the setting and hardening process,

(b) Figures 5.11 to 5.16 show the increase in resistivity with continuous moist storage at 23^{o}C for the cement pastes and concrete mixes,

(c) Figure 5.17 shows the variation in resistivity with temperature of moist storage,

(d) Figures 5.18 to 5.20 show the variation in the resistivity of concrete with continuous outdoor storage.

(e) Figure 5.21 shows the effect of the type of cement used in the concrete,

(f) Figure 5.22 shows the effect on resistivity of increasing the air content of the concrete, and

(g) Figure 5.23 shows the Formation Factor plotted against fractional volume of paste for all the mixes studied.

5.7.1 Initial Setting Period

During the first 6-8 hours after placing, the electrical resistivity of the concrete specimens increases gradually and only after the concrete sets, does the rate of increase become more rapid, possibly due to reduced ionic mobility as a result of the setting process. The electrical resistivities of the neat cement paste specimens, although much lower than that of concrete, exhibit a slightly different trend during the same period. The resistivity of the paste decreases during the first 5 hours after placing and then increases, quite markedly, in some cases. This decrease could be due to two factors,

(a) the chemical reaction that ensures is exothermic, and as a cement

paste has a negative temperature coefficient of resistivity, an increase in temperature will result in a decrease in resistivity, and

(b) an increase in the number of ions going into solution. (This is perhaps of minor importance as the alkalis in cement dissolve rapidly and becomes saturated with respect to calcium hydroxide and sulphate within a few minutes of mixing (58)).

This decrease in resistivity is not observed in concrete, possibly because the fractional volume of paste is substantially less and the aggregate may tend to act as a heat sink. Furthermore, there is no marked difference in the resistivities of the various neat O.P.C. mixes during the first 10 hours.

5.7.2 Continuous Moist Storage

During the first 20 days of moist storage, the resistivity of the specimens increases rapidly, but after 30 days the rate of increase becomes much less and at this point in time, their electrical resistivity is approximately 90% of their 128 day resistivity.

Since conduction can be regarded as essentially electrolytic in nature, with conduction taking place through the cement paste, the observed initial increase in resistivity is probably due to the reduced amount of evaporable water within the cement paste - this reduction being caused by the continuing hydration process. After about one month the rate of hydration decreases, hence the amount of evaporable water within the cement paste changes little with increasing time.

From an electrical point of view this will mean a levelling off in the resistivity of the specimens, which is borne out by the experimental data. This will in turn mean that for a particular mix at a specified water-cement ratio, the increase of resistivity with time will follow the same general shape as the gain of strength with time curve for concrete as shown in Figure 5.24.

The electrical resistivity of a particular mix ratio is inversely proportional to the water-cement ratio, showing that more evaporable water is available for conduction when the water cement-ratio is increased.

5.7.3 Influence of Temperature of Storage

In order to determine the coefficients α and B in equations (5.3) and 5.7), four cubes were stored in a curing tank at a temperature of $13^{o}C$. These cubes had 1:2:4 mix proportions with a water-cement ratio of 0.8. Figure 5.17 shows the influence of temperature of storage on resistivity - as the temperature decreases, then, from section 5.3.1, the resistivity will increase. This is the case for the concrete cubes stored at $13^{o}C$ and $23^{o}C$; thus, by knowing the resistivities at these two reference temperatures then values for α and β can be computed. From the experimental data an average value obtained for α was $0.022/^{o}C$ and 2130 for B. This value for α should be compared to $0.025/^{o}C$ for most electrolytes (38, 40).

5.7.4 Continuous Outdoor Storage

The resistivity of cubes placed in the ground show a greater variation

than the corresponding mix allowed to cure under constant conditions in a curing tank. Since there was no evaporation of moisture from the cubes, then the difference in resistivity is not attributable to the existence of a moisture gradient between the surface and the interior of the cube.

The reason for the variation can be explained by consideration of equations (5.3) and (5.7). Using equation (5.3) and knowing α, the resistivity, ρ_θ, of the concrete cured under constant conditions (23^oC in this case), and the ground temperature , t, then the resistivity at temperature t, can be calculated. From the experimental work carried out the temperature coefficient of resistivity of concrete is $0.022/^oC$, and values calculated using equation (5.3) show good agreement with those obtained experimentally.

In a similar fashion, equation (5.7) can be used to calculate the resistivity at temperature, T_1, by knowing the constant B and the resistivity of the concrete at reference temperature T_2 (296K). Using the value of B found from experiments (2130), values calculated using equation (5.7) also show good agreement with experimental results.

5.7.5 Influence on resistivity of Cement of Different Types

Figure 5.21 shows the variation in resistivity between a 1:2:4 mix (0.8 water-cement ratio) made with O.P.C., R.H.P.C. and S.R.P.C.

Initially there is little difference between the resistivities of concretes made with the above cements, but as the curing time increases the

difference becomes more apparent, especially for the concrete made with S.R.P.C. There is little difference in resistivity for concretes made with R.H.P.C. and O.P.C. which would be as expected since both cements have a similar chemical composition. A plausible explanation for the slight increase in resistivity for the R.H.P.C. concrete specimens may be due to the rate at which water is absorbed by the cement paste, i.e. the rate of hydration of the paste. Since R.H.P.C. has a higher specific surface than O.P.C. it will absorb a greater amount of water at the initial stages of the hardening process thereby reducing the fractional volume of evaporable water available for conduction. After several weeks the resistivity/time curves for R.H.P.C. and O.P.C. become coincident.

The difference in resistivity between S.R.P.C. and O.P.C. concretes lies in the chemical composition of the cements and hence the ionic concentration in the evaporable water. Possibly the low tricalcium aluminate content as it is similar to O.P.C. in all other respects.

5.7.6. Voided Concrete

As a result of the theory described at the beginning of this Chapter the effect of occluded air voids, resulting from, say, insufficient compaction, can easily be deduced. Air can be regarded as having infinite resistance and, from an electrical point of view, will mean an increase in the fractional volume of non-conductive particles. This will in turn decrease the fractional volume of paste thereby increasing the overall electrical resistivity of the concrete.

From Figure 5.22 the graph is displaced as anticipated, with the resistivities for the voided concrete increasing.

5.7.7 Formation Factors for Concrete

For concretes which were continuously moist cured an overall graph of Formation Factor against fractional volume of paste can be drawn for the complete test period for all the mixes on Table 5.3. (The formation factor for the first day of moist curing has been omitted as thermal equilibrium between the cement paste and concrete/mortar specimens may not exist at this early stage). Drawing the best straight line through the data points in Figure 5.23, results in,

$$F = 1.01\ \phi^{-1.26} \qquad \ldots\ldots (5.22)$$

and has a correlation coefficient of -0.96 remembering that the Formation Factor, F, is the ratio of the resistivity of the concrete to the resistivity of the paste with the same water-cement ratio at the same age. Some general points will be noticed concerning this graph;

(a) as the fractional volume of paste increases the Formation Factor decreases which is in accordance with the theory discussed,

(b) the Formation Factor for a particular mix and water cement ratio remains reasonably constant with time, which is also in agreement with the theory since only the paste is contributing to conduction. It was thought that plotting a similar graph for outdoor storage was not justifiable as conditions were not constant, and,

(c) the graphs and equation may be used in assessing the resistivity

of mixes with fractional volumes of pastes other than those studied. Since the formation factor (at 23°C) can be calculated, then, by making an appropriate temperature correction, the in-situ resistivity of moist cured concrete (or concrete where evaporation of moisture is prevented) may be computed.

Consider the voided concrete specimens with an air content of 6% and 20%. These cubes have a fractional volume of paste of 0.31 and 0.26 respectively. Using the equation above, the Formation Factor for these specimens is 4.38 and 5.47. Hence, for these cubes, the computed resistivities at, 20 days, say (resistivity of paste being 6.50 Ω-m) will be 28.5 Ω-m and 35.6 Ω-m, while the experimental values are 29.4 Ω-m and 35.0 Ω-m respectively (at 23°C).

5.8 General Conclusions

The objective of the work detailed in this Chapter has been to investigate the electrical properties of moist cured concrete as this has a significant influence on the overall earthing resistance of the pile. The results obtained have been useful in quantifying the electrical resistivity of several standard concrete mixes.

Analysis of the results of the large number of tests undertaken on cement paste, mortar and concrete mixes has permitted an electrical model for conduction to be formulated and given some insight into conduction mechanisms through such a heterogeneous medium. From this model explanations as to the variation in resistivity between mixes can be deduced. The cement paste within the concrete, which conducts most

of the current, has an important influence on the overall resistivity of the concrete.

One important conclusion arising out of the study has been that when employing the earth-resistance technique only results from piles tested at the same time after pouring can be realistically compared as the electrical resistivity of the concrete in the pile shaft is continually changing from day to day. Alternatively, if the piles are tested when the resistivity of the concrete is not changing so rapidly, i.e. after one month, then the results from the testing programme will not be significantly affected by several days interval between tests.

The supposition that the electrical resistivity of concrete is relatively low during the first 24 hours after placing has been confirmed by the experimental data, and, for reasons explained in section 3.3.5 it may be advantageous to test the pile at this stage.

Several other main conclusions, listed below, can be drawn from this Chapter:

(1) The experiments undertaken have determined the electrical resistivity characteristics of concrete of different mix proportions and neat cement pastes, and experimental techniques have been developed which allow measurements to be made with relative ease.

(2) The effects of ambient temperature on the value of resistivity have been quantified over a practical working range and relationships are given which can account for the effect a change in ambient

temperature on the resistivity of concrete.

(3) The temporal variation in the resistivity of concrete stored under constant conditions has been established over periods of up to eight months, i.e. to a point where the rate of change of resistivity has become negligibly small.

(4) As the electrical resistivity of aggregate can be regarded as infinite in comparison to the resistivity of the paste, then the resistivity of a concrete mix is almost entirely dependent upon the resistivity and fractional volume of paste within the concrete.

(5) The electrical resistivity of concrete is directly related to the hydration of the cement paste within the concrete. This is confirmed by the fact that the experimental graphs for concrete follow the same trend as those for neat cement pastes, the only difference being that the curves for concrete are displaced upwards. This upward displacement being caused by the reduction in the total volume of paste available for conduction in a concrete.

(6) For a particular mix, the resistivity is inversely proportional to the water-cement ratio viz. as the strength decreases the resistivity decreases (See Table 5.4).

(7) The result of occluded air-voids within the concrete is to increase the electrical resistivity of the concrete.

(8) The electrical resistivity of R.H.P.C. is slightly higher than O.P.C. during the initial hardening period. After approximately three months there is little difference in the resistivities. It could be concluded that cement type will have little effect on the earthing resistance of a pile.

(9) An electrical model was developed which can account for the effects of changing mix proportions, water-cement ratio and air content of concrete. A modified Archies Law would appear to explain the conduction phenomenon.

(10) Concrete placed in the ground loses very little moisture, even when placed close to ground surface.

(11) The resistivity of moist concrete lies in the region of 25-45Ω-m (at $23^{o}C$).

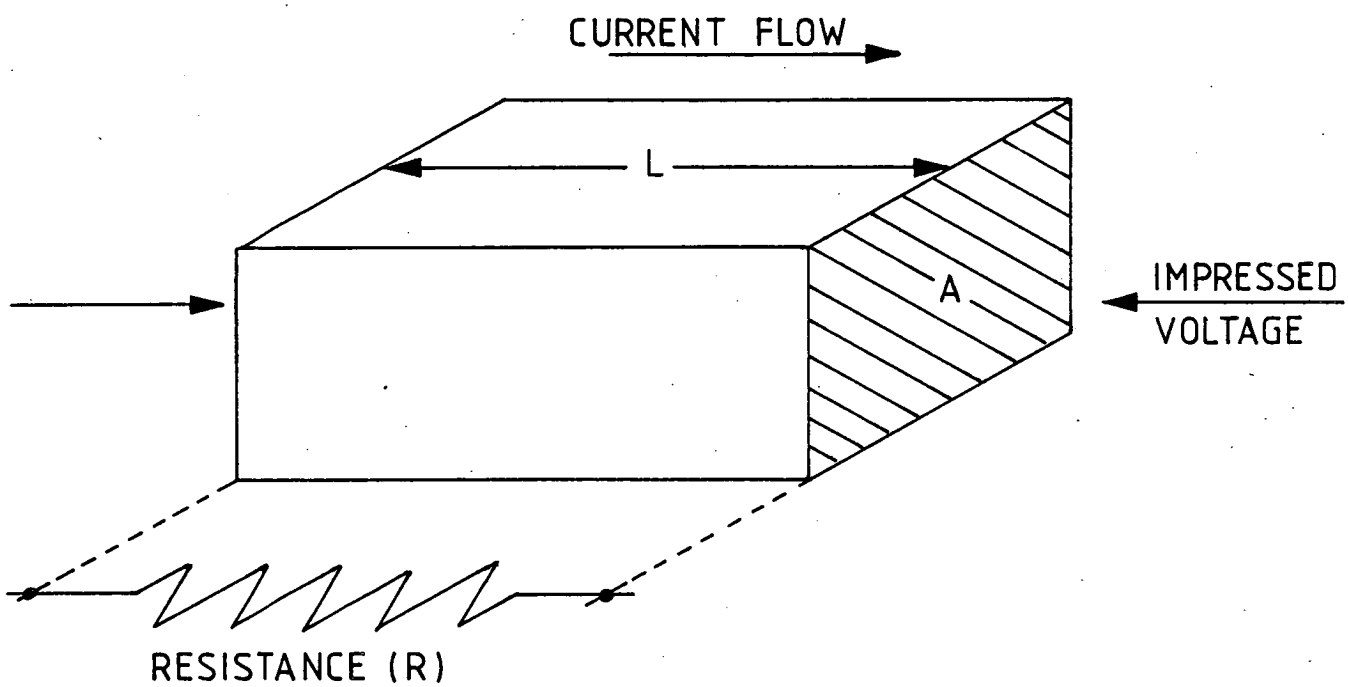

FIG. 5.1 Illustrating the relationship between resistivity and resistance

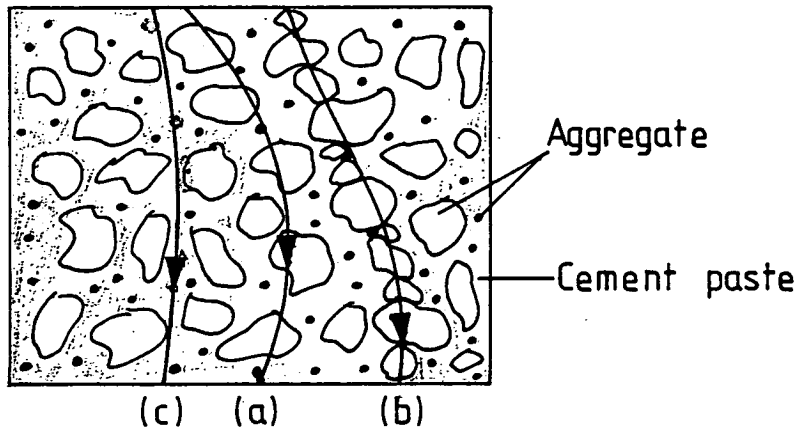

FIG. 5.2 Conduction paths through concrete

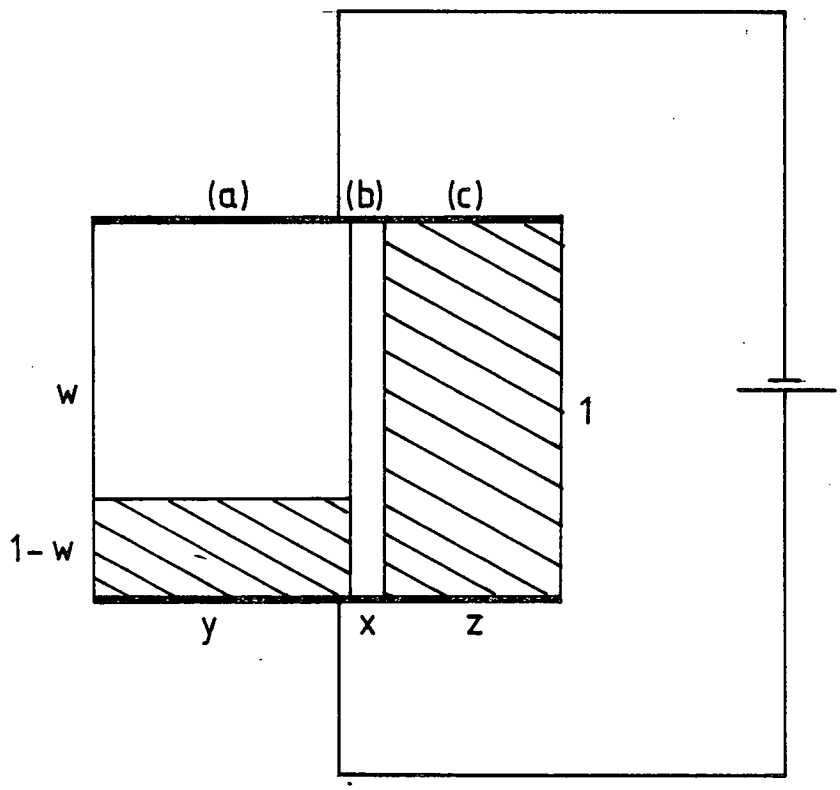

FIG. 5.3 Simplified model for conduction

Rock Type	Resistivity Range (Ω-m)
Granite	$5 \times 10^3 - 1 \times 10^6$
Marble	$5 \times 10^2 - 2.9 \times 10^3$
Gabbro	$1 \times 10^5 - 1.4 \times 10^7$
Limestone	$3 \times 10^2 - 1.5 \times 10^3$
Diorite	1×10^4
Quartz-Porphyrite	3.4×10^2
Serpentine	$5.3 \times 10^2 - 2 \times 10^4$
Slate	$6.4 \times 10^2 - 6.5 \times 10^4$
Hornblende	$3 \times 10^4 - 1.0 \times 10^6$
Sandstone	$1.8 \times 10^2 - 4 \times 10^3$
Syenite	1×10^6
Gneiss	$1.2 \times 10^3 - 2 \times 10^5$
Conglomerate	$2 \times 10^3 - 1.3 \times 10^4$
Quartz	$3.8 \times 10^4 - 1.2 \times 10^{12}$

TABLE 5.1 Resistivities of Typical Aggregates used in Concrete

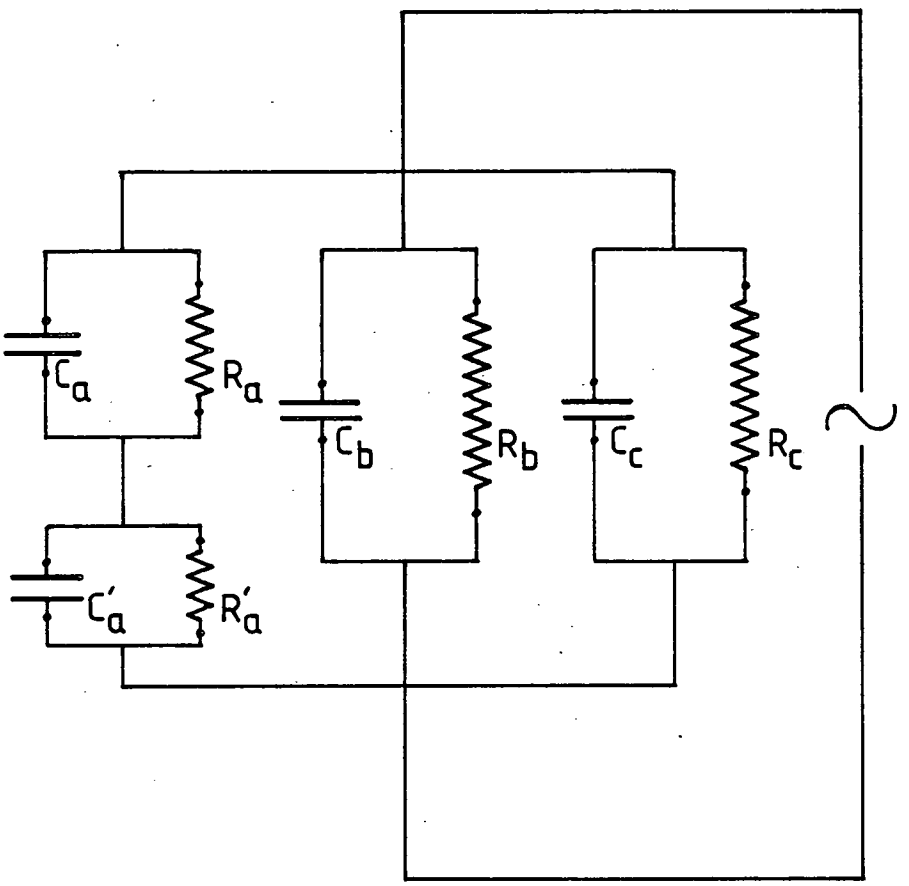

FIG. 5.4 Extension of model to A.C.

Fractional Volume ϕ	Age, Days	Resistivity (70) Ω-cm	Formation Factor, F	Formation Factor, F. (Computed)		
				Maxwell	Fricke	Slawinski
1	3 14 28	757 1071 1154	-	-	-	-
0.654	3 14 28	1430 2030 2200	1.89 1.90 1.91	1.79	1.91	1.89
0.486	3 14 28	2140 3000 3330	2.83 2.80 2.89	2.59	2.81	2.79
0.386	3 14 28	2780 3810 4370	3.67 3.56 3.79	3.39	3.73	3.72

TABLE 5.2 Comparison of Measured and Computed Formation Factors for mortar

Mix Proportions (by Weight) cement = 1			Fractional Volume of cement paste (on demoulding) ϕ	Length of Test Period-Moist Curing (DAYS)	Length of Test Period-outdoor Storage (DAYS)
Coarse Aggregate	Sand	Water			
CEMENT PASTES					
0	0	0.4	1	128	-
		0.5	1	128	-
		0.6	1	128	-
		0.7	1	128	-
		0.8	1	128	-
MORTARS					
0	1	0.6	0.74	7	-
	1.5	0.6	0.64	7	-
	2	0.6	0.56	7	-
CONCRETES					
2	1	0.4	0.380	128	91
2	1	0.5	0.412	128	91
2	1	0.6	0.450	128	91
3	1.5	0.5	0.321	128	91
3	1.5	0.6	0.350	128	91
3	1.5	0.7	0.370	128	91
4	2	0.6	0.285	128	91
4	2	0.7	0.308	128	91
4	2	0.8	0.332	128	91
5	2.5	0.7	0.258	240	-
5	2.5	0.8	0.279	240	-
5	2.5	0.9	0.298	240	-
6	3	0.8	0.245	240	-
6	3	0.9	0.260	240	-
6	3	1.0	0.282	240	-

TABLE 5.3 Summary of mixes studied

Mix Proportions	Water-Cement Ratio	Expt. Density kg/m^3	Calculated Density kg/m^3	Mean 28 day Crushing Strength N/mm^2
1:1:2	0.4	2326	2364	49.6
	0.5	2290	2295	40.6
	0.6	2230	2232	34.9
1:1.5:3	0.5	2349	2369	44.1
	0.6	2335	2317	31.5
	0.7	2244	2269	25.1
1:2:4	0.6	2361	2372	40.8
	0.7	2330	2330	28.6
	0.8	2322	2291	19.6
1:2.5:5	0.7	2336	2371	26.9
	0.8	2318	2337	18.7
	0.9	2300	2304	14.8
1:3:6	0.8	2370	2374	17.0
	0.9	2330	2344	14.8
	1.0	2357	2316	12.3

TABLE 5.4 Comparison of experimental and calculated densities for mixes studied and their crushing strength

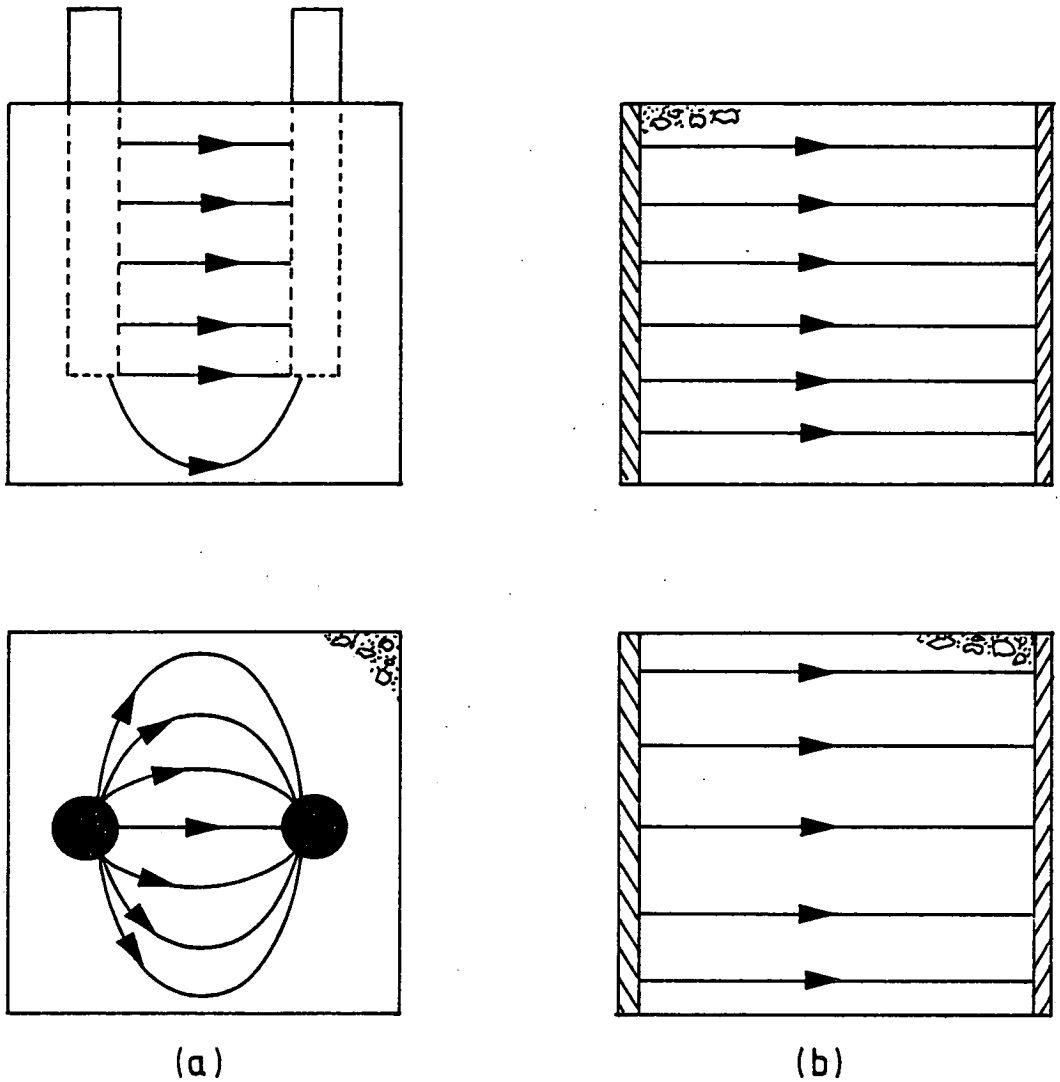

FIG. 5.5 Types of electrodes (a) rod and (b) plate

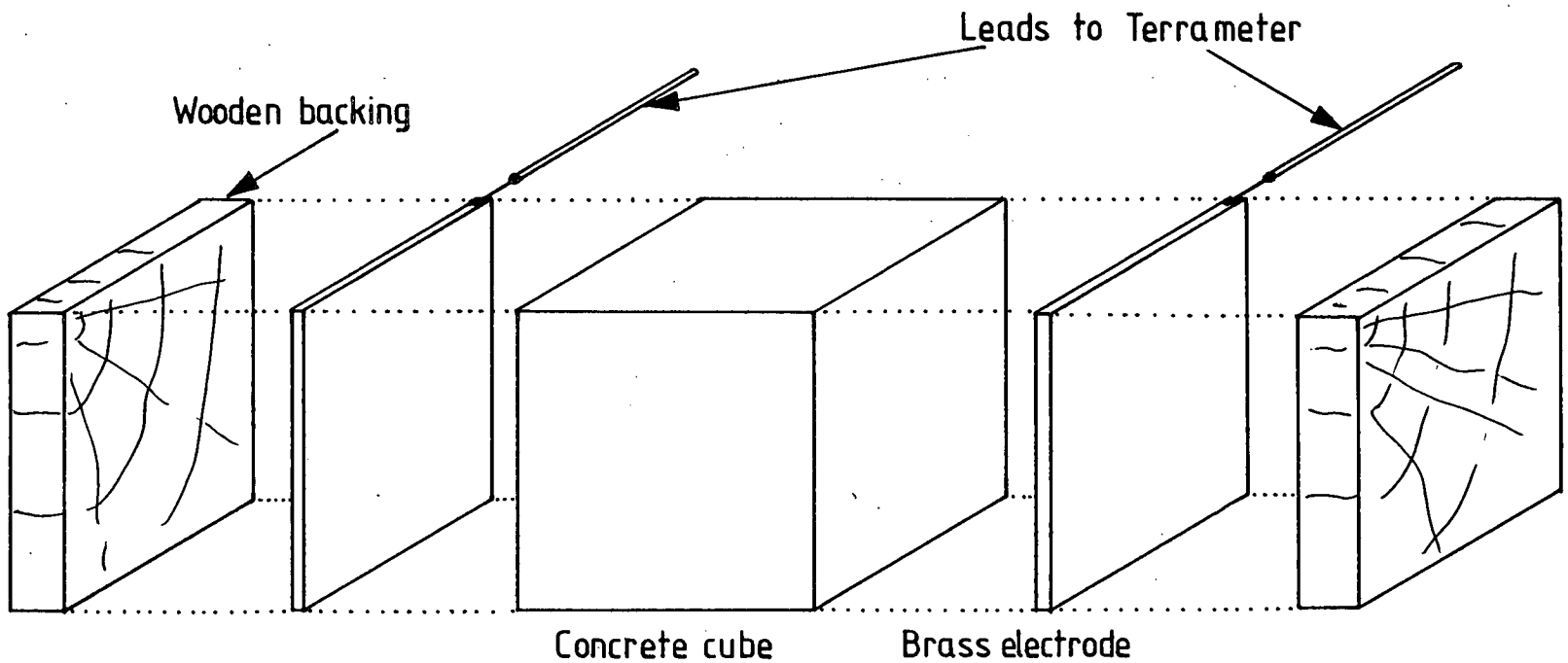

FIG. 5.6 Schematic diagram of testing arrangement

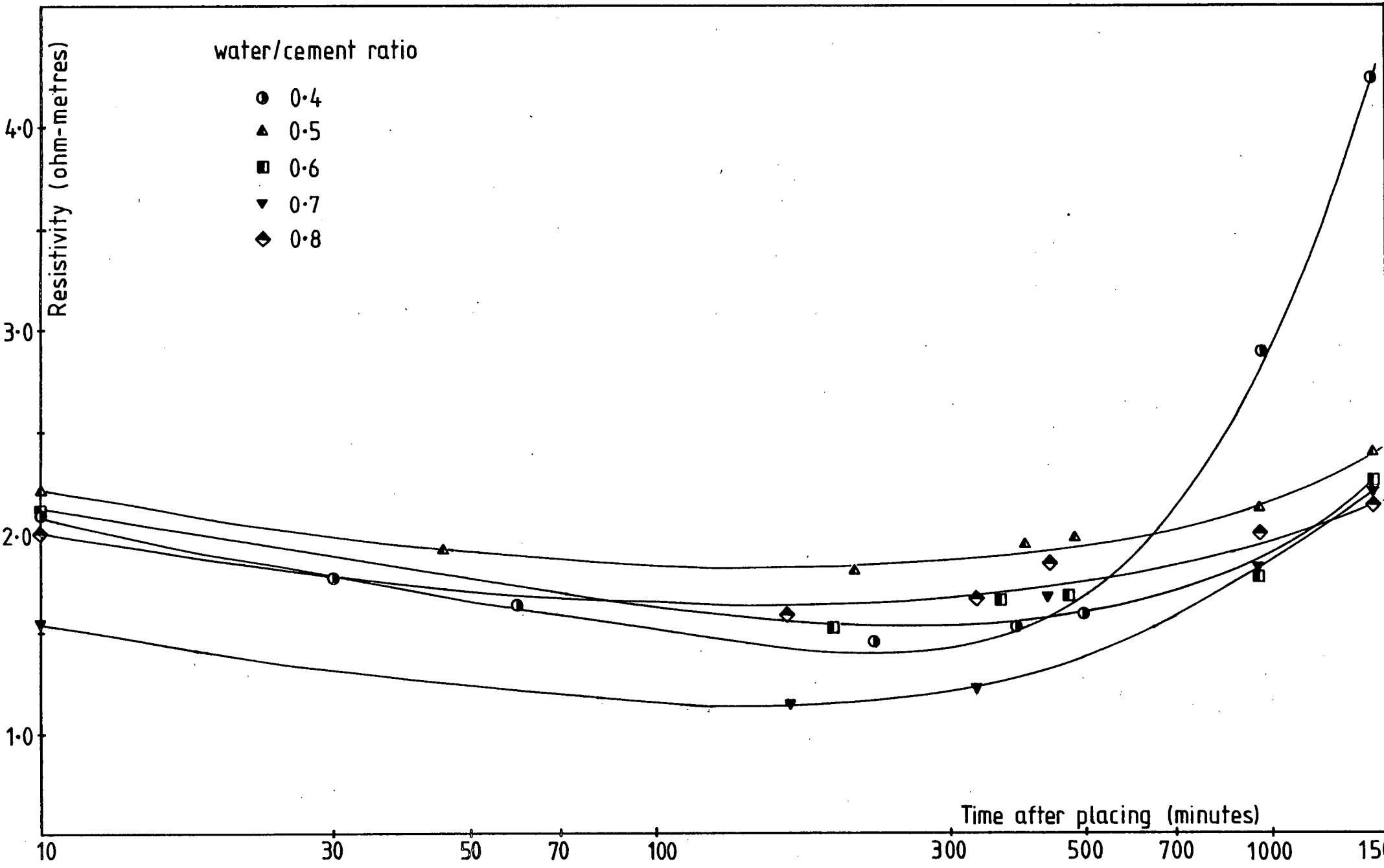

FIG. 5.7 Increase in resistivity during first 24 hours after placing for neat cement pastes

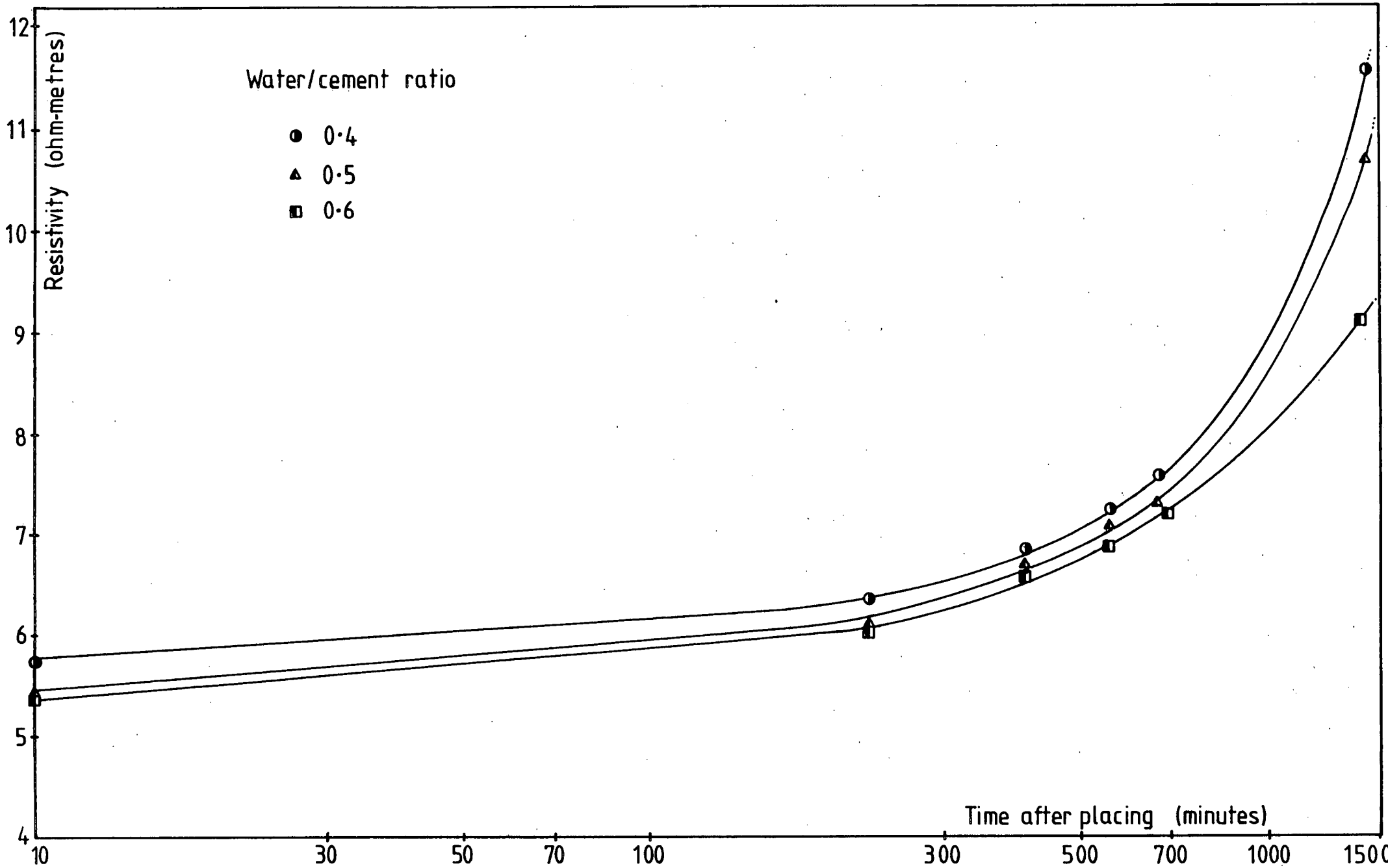

FIG. 5.8 Increase in resistivity during first 24 hours after placing for 1:1:2 mix specimens

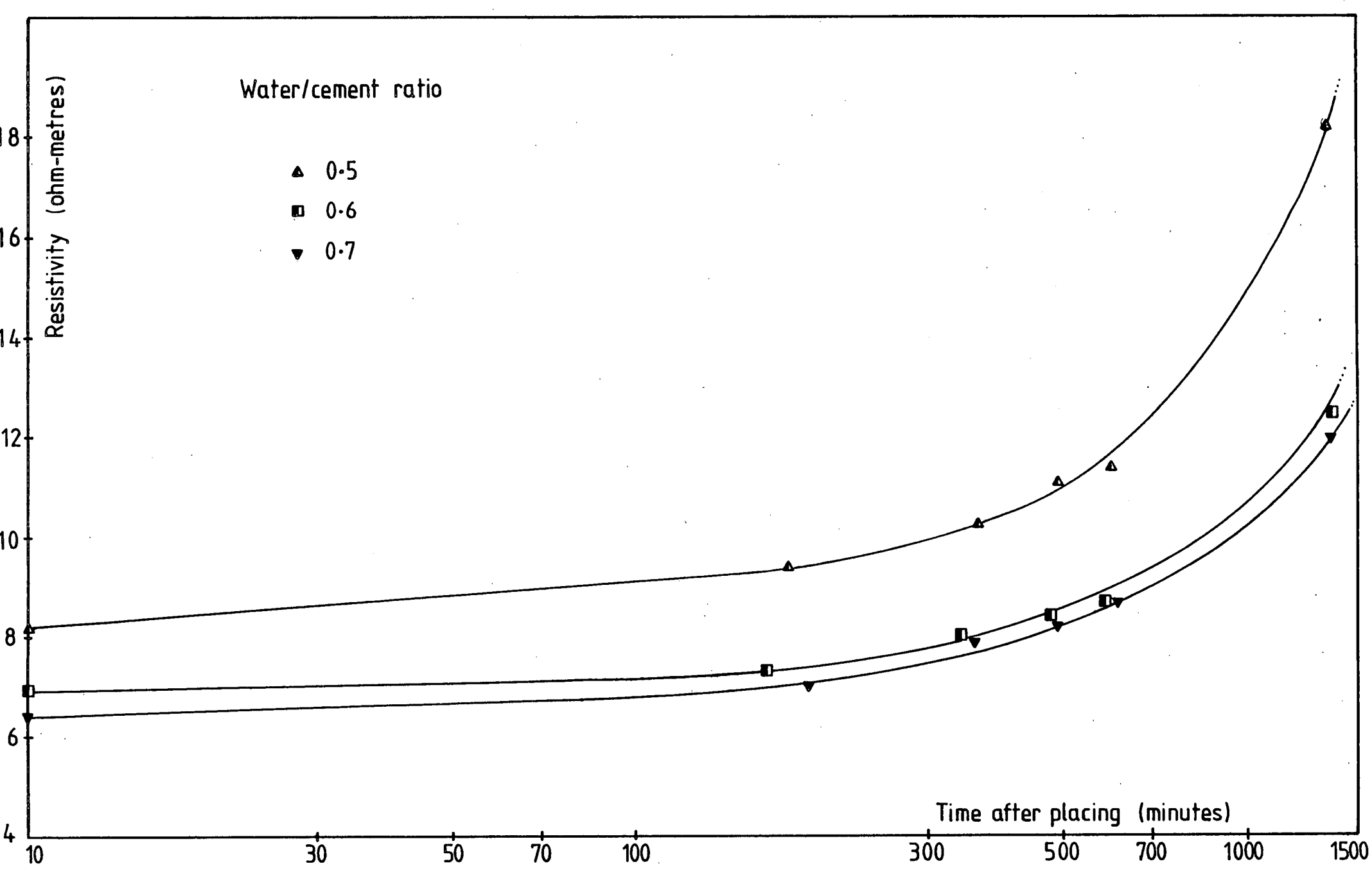

FIG. 5.9 Increase in resistivity during first 24 hours after placing for 1:1½:3 mix specimens

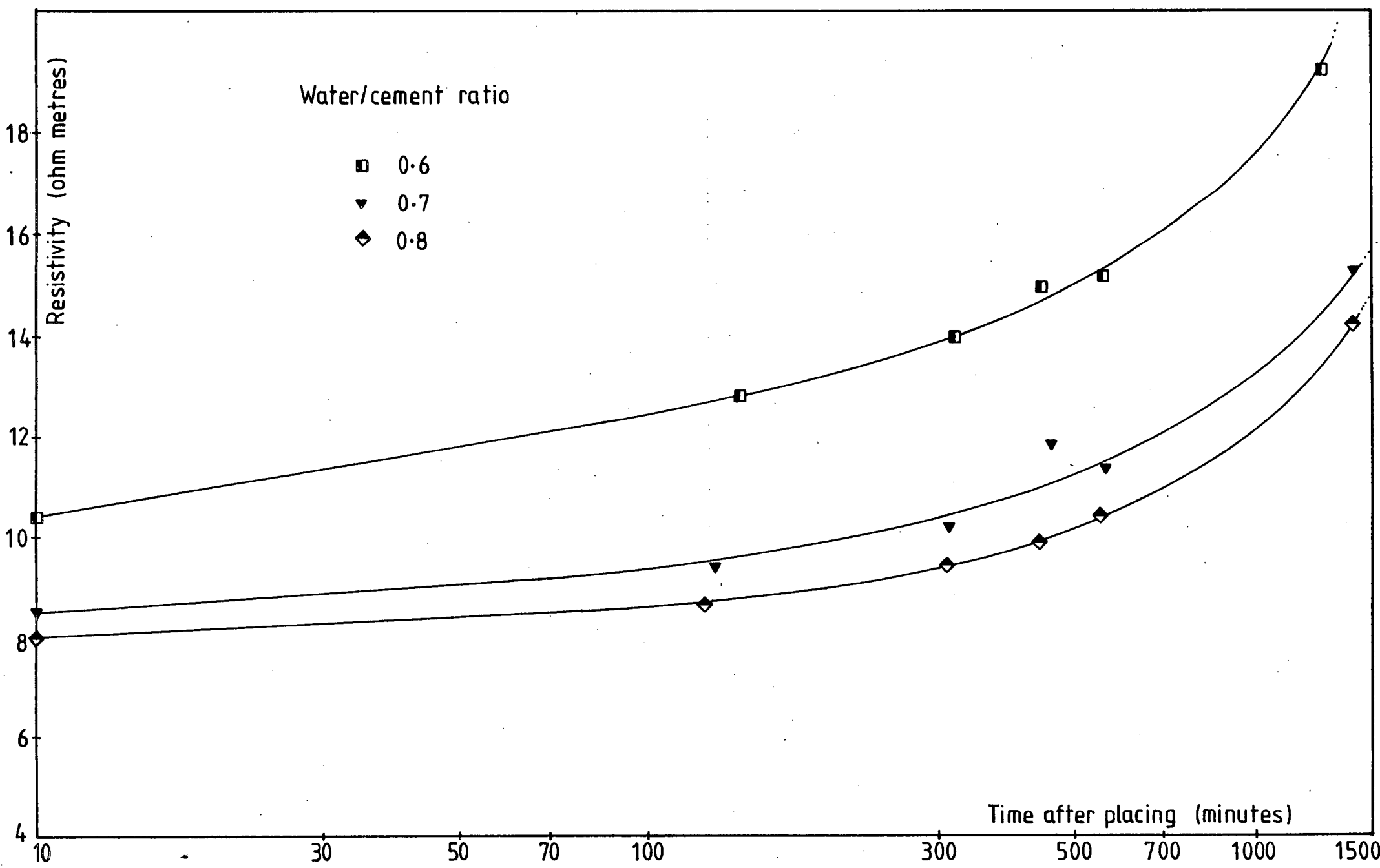

FIG. 5.10 Increase in resistivity during first 24 hours after placing for 1:2:4 mix specimens

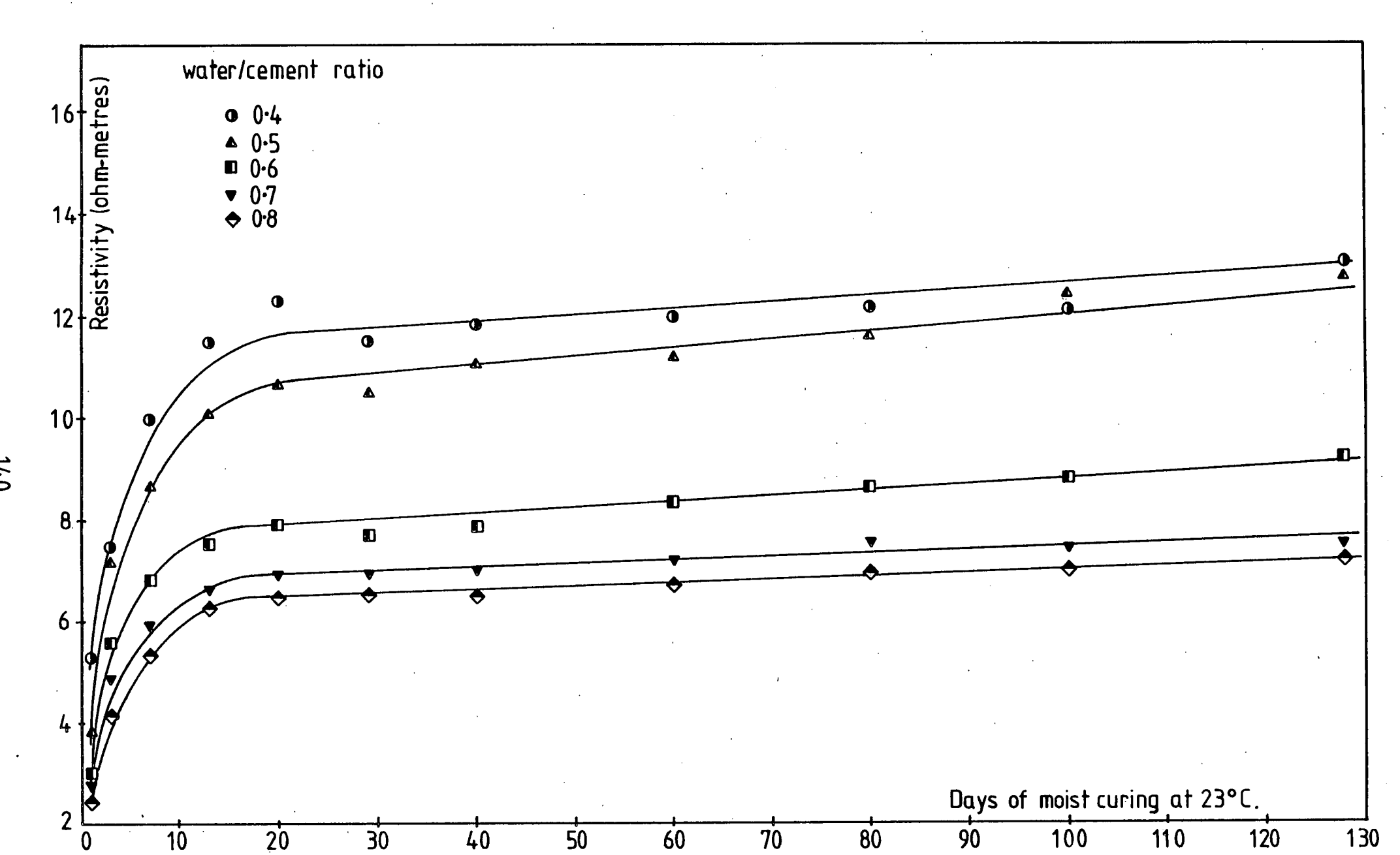

FIG. 5.11 Influence of prolonged moist storage on resistivity of cement paste specimens

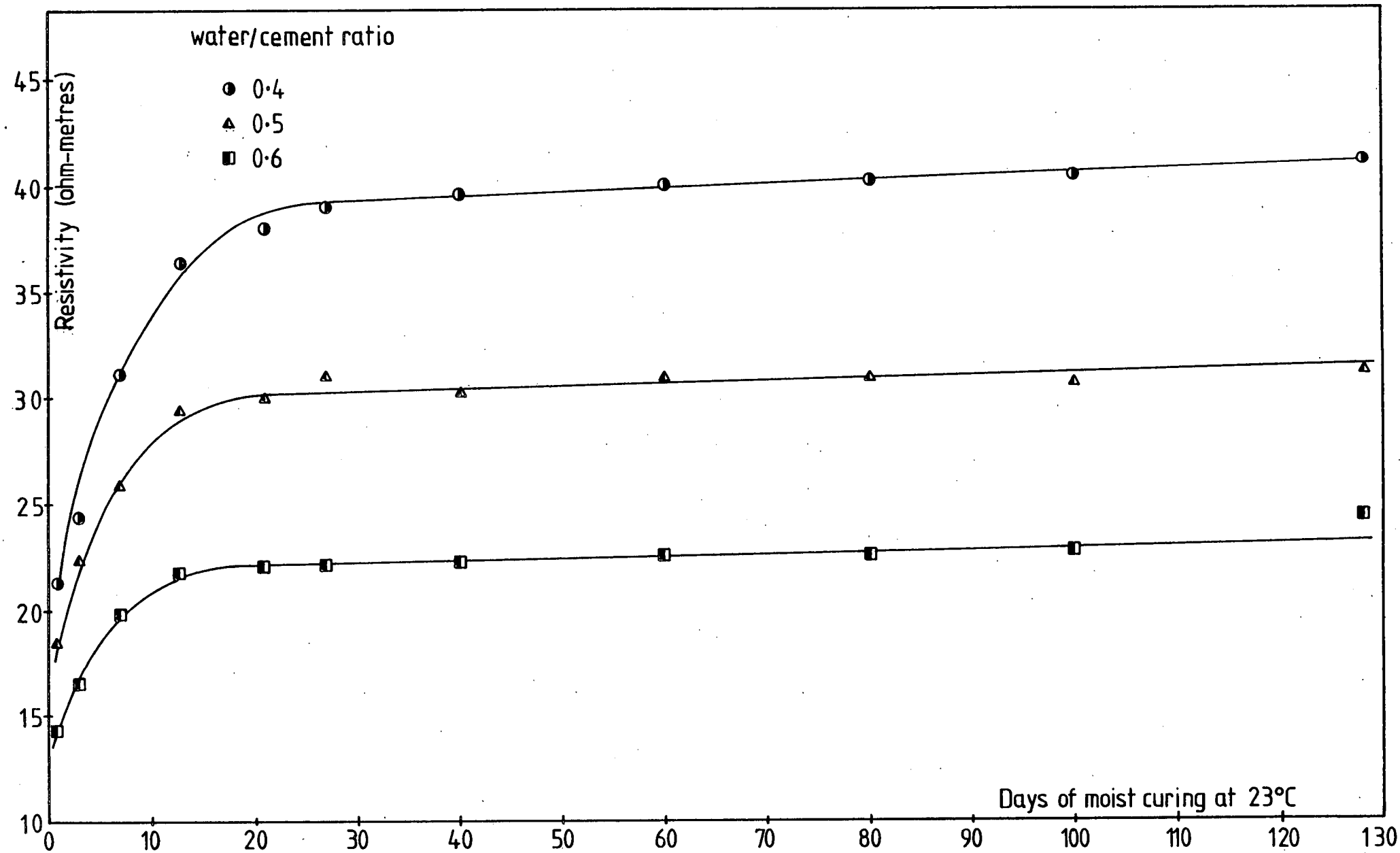

FIG. 5.12 Influence of prolonged moist storage on resistivity of 1:1:2 mix specimens

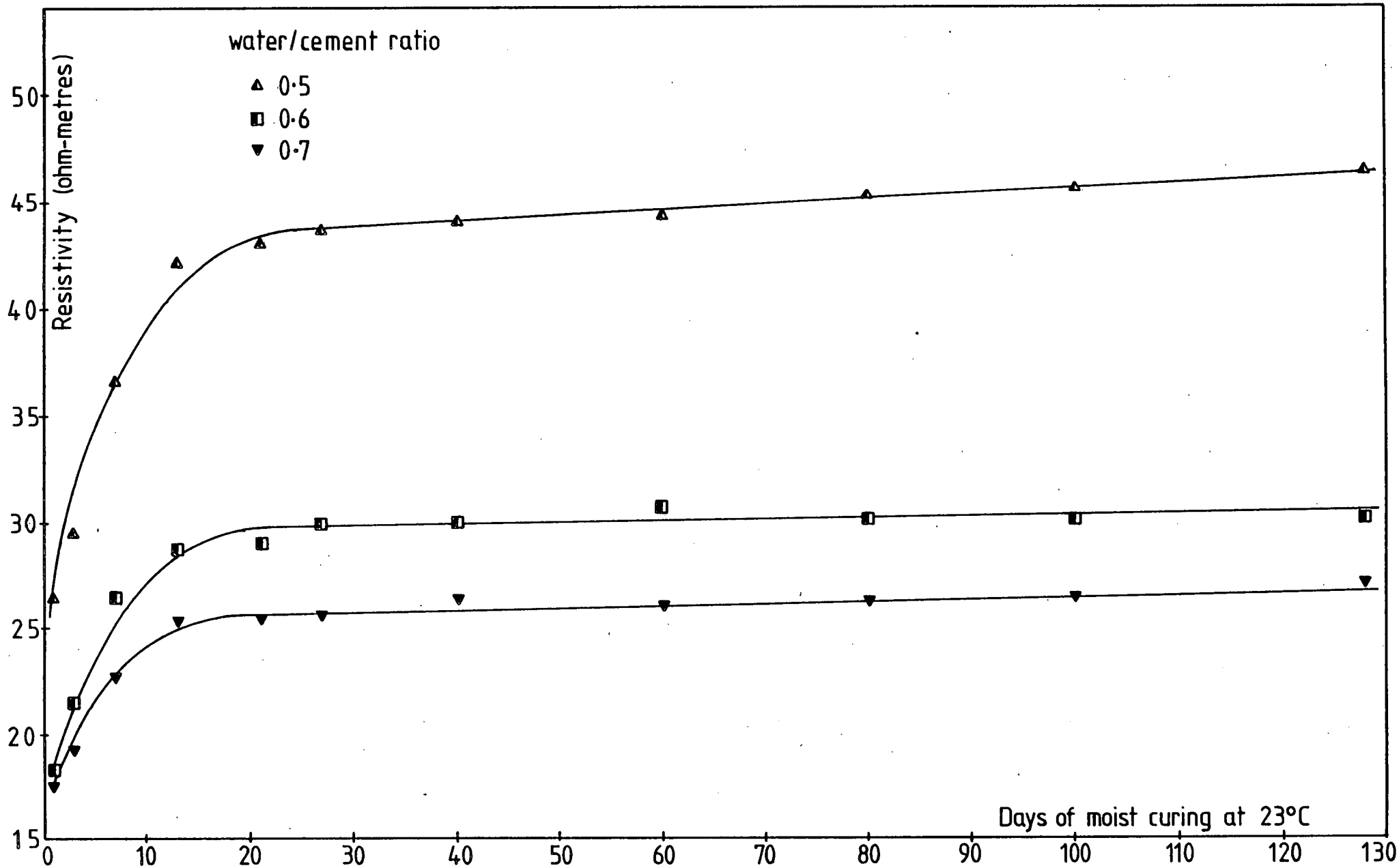

FIG. 5.13 Influence of prolonged moist storage on resistivity of 1:1½:3 mix specimens

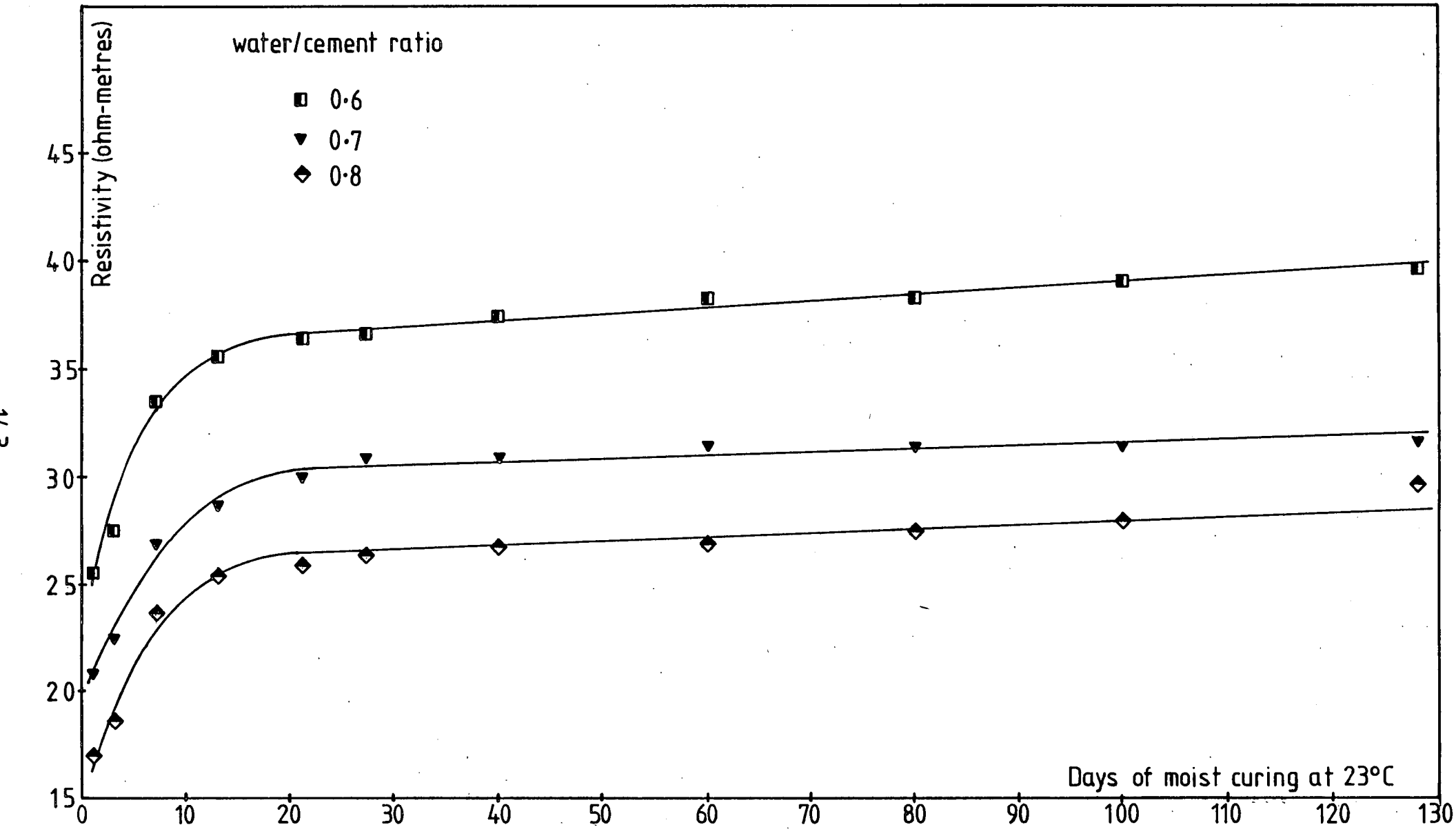

FIG. 5.14 Influence of prolonged moist storage on resistivity of 1:2:4 mix specimens

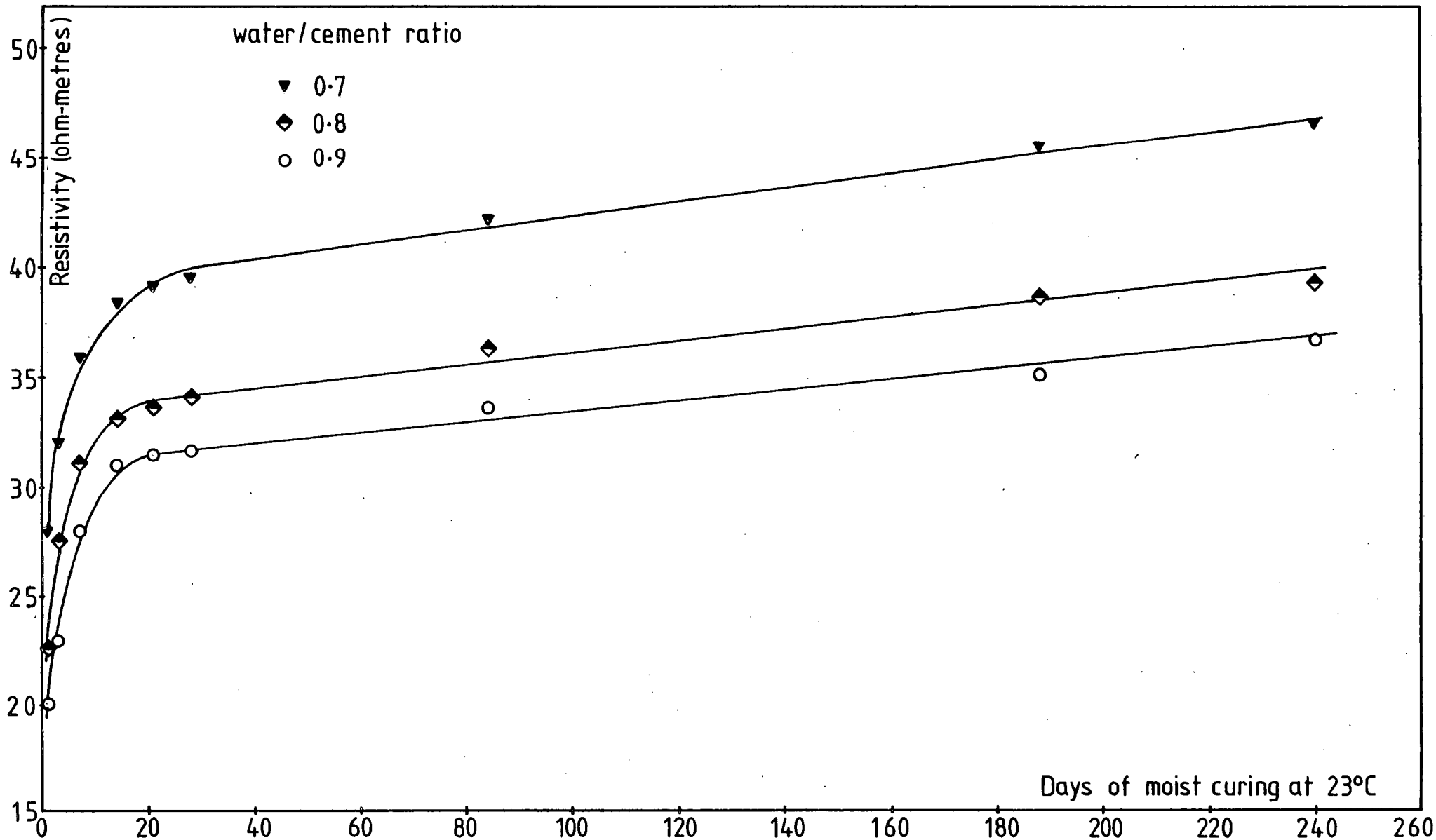

FIG. 5.15 Influence of prolonged moist storage on resistivity of 1:2½:5 mix specimens

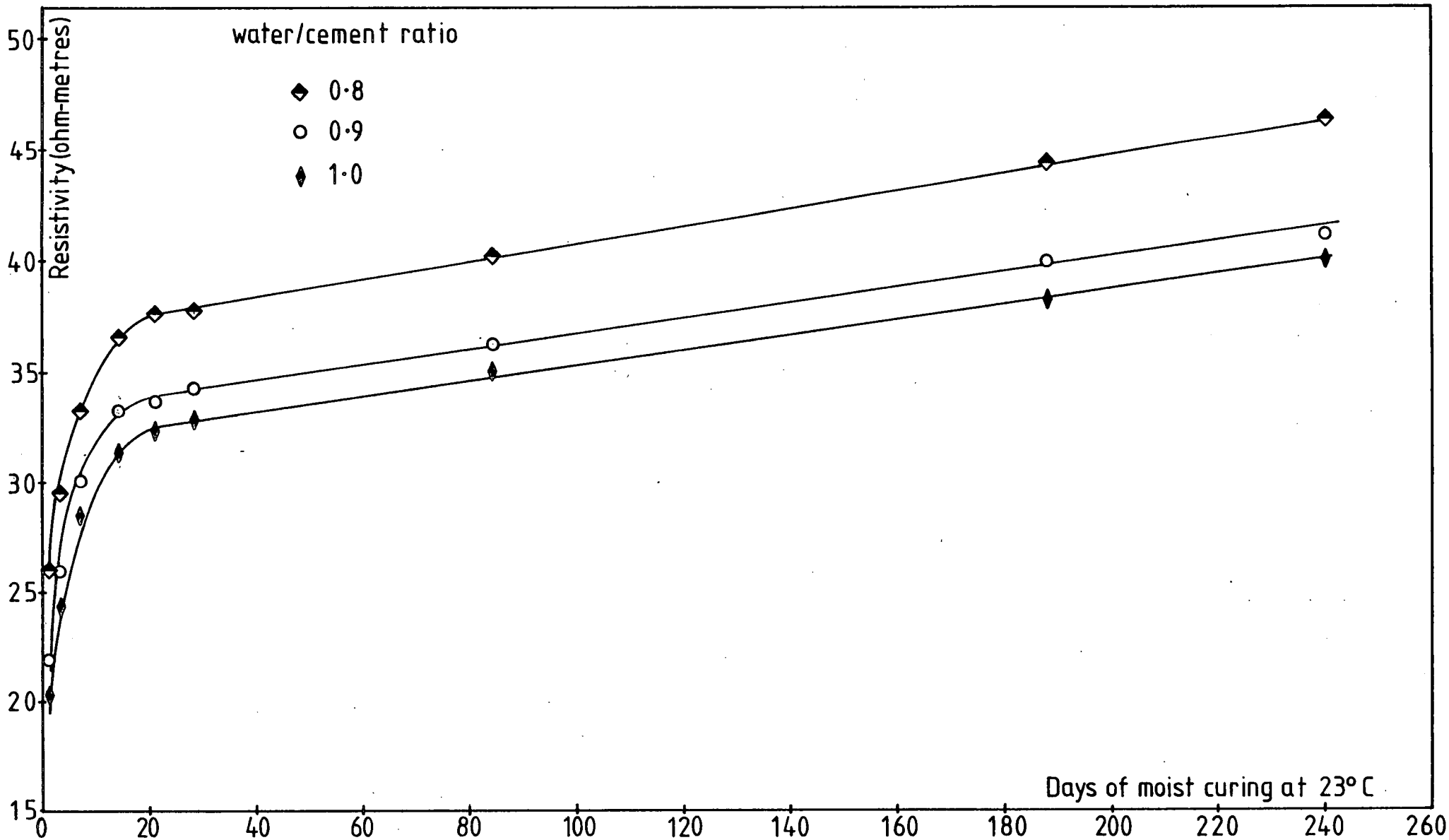

FIG. 5.16 Influence of prolonged moist storage on resistivity of 1:3:6 mix specimens

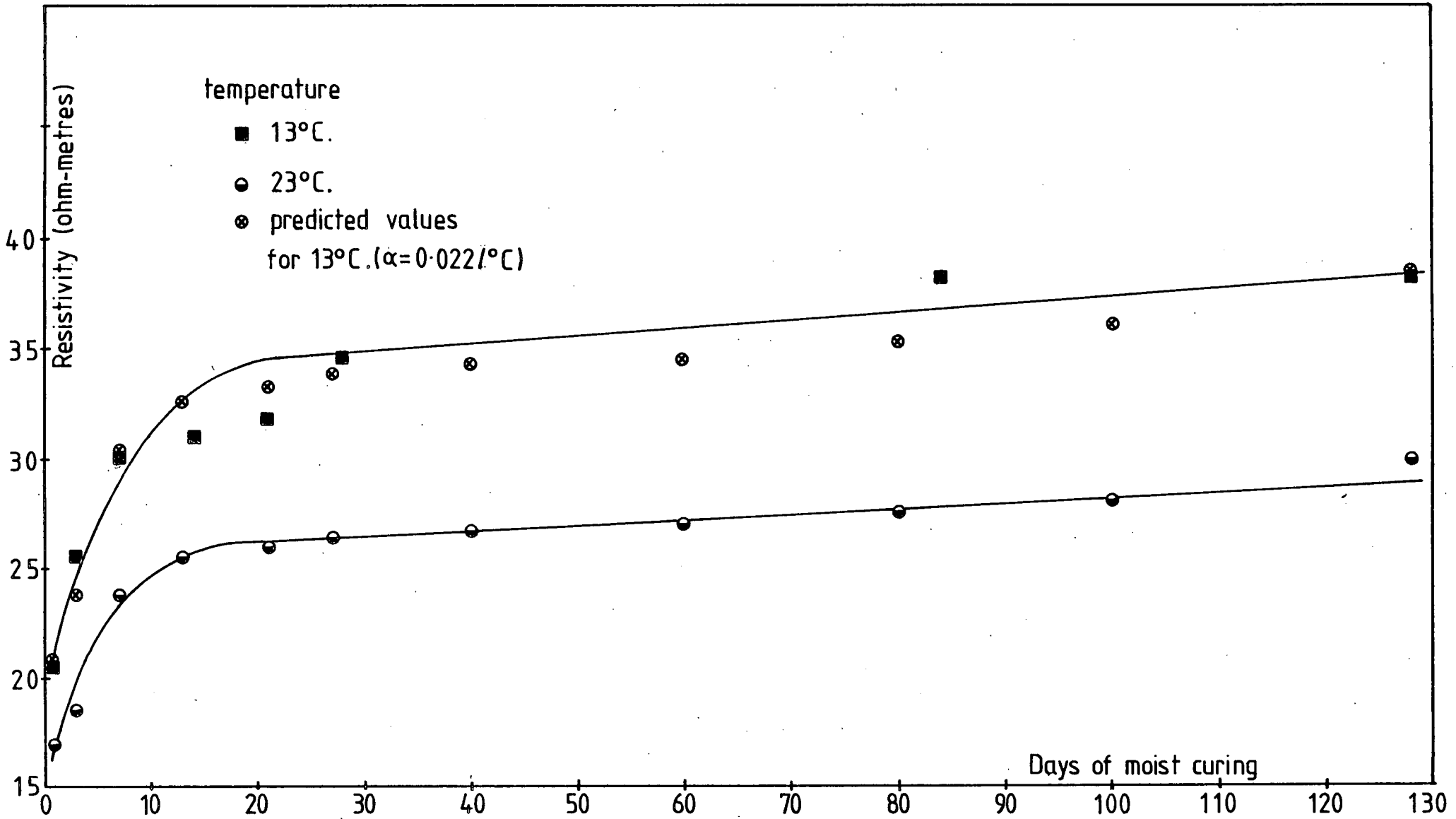

FIG. 5.17 Influence of temperature of storage on resistivity of concrete

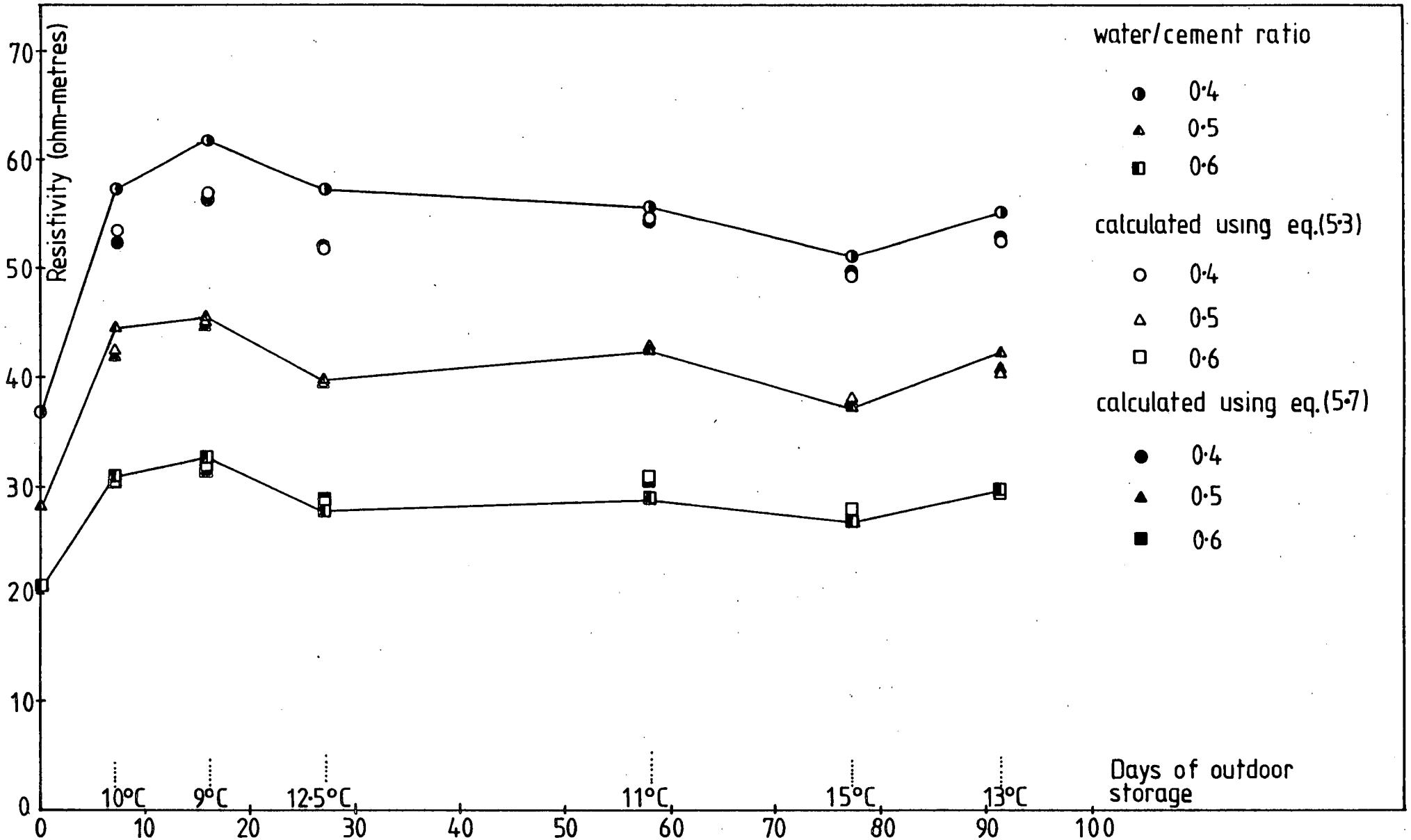

FIG. 5.18 Effect of ambient temperature on resistivity of 1:1:2 mix specimens

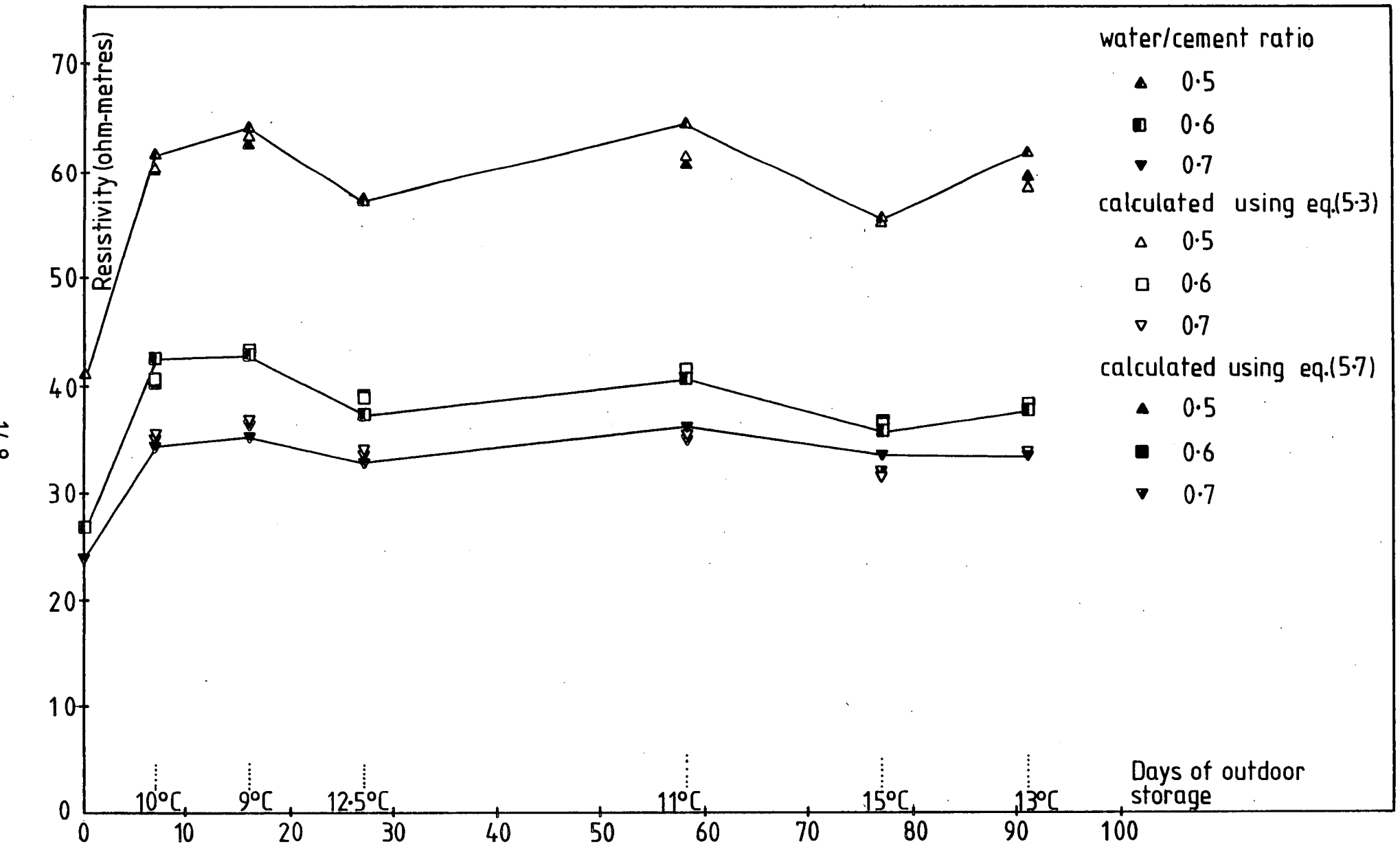

FIG. 5.19 Effect of ambient temperature on resistivity of 1:1½:3 mix specimens

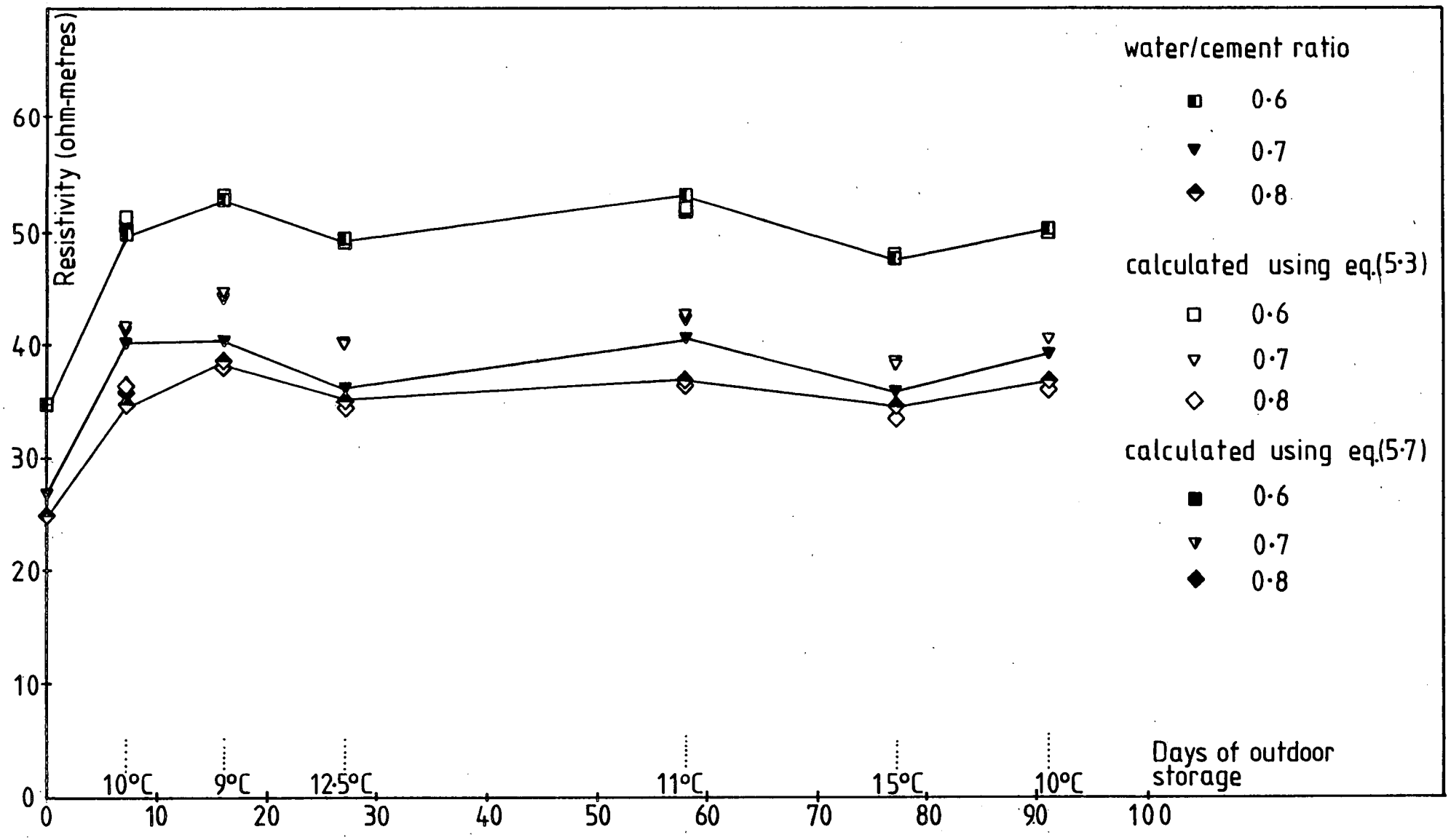

FIG. 5.20 Effect of ambient temperature on resistivity of 1:2:4 mix specimens

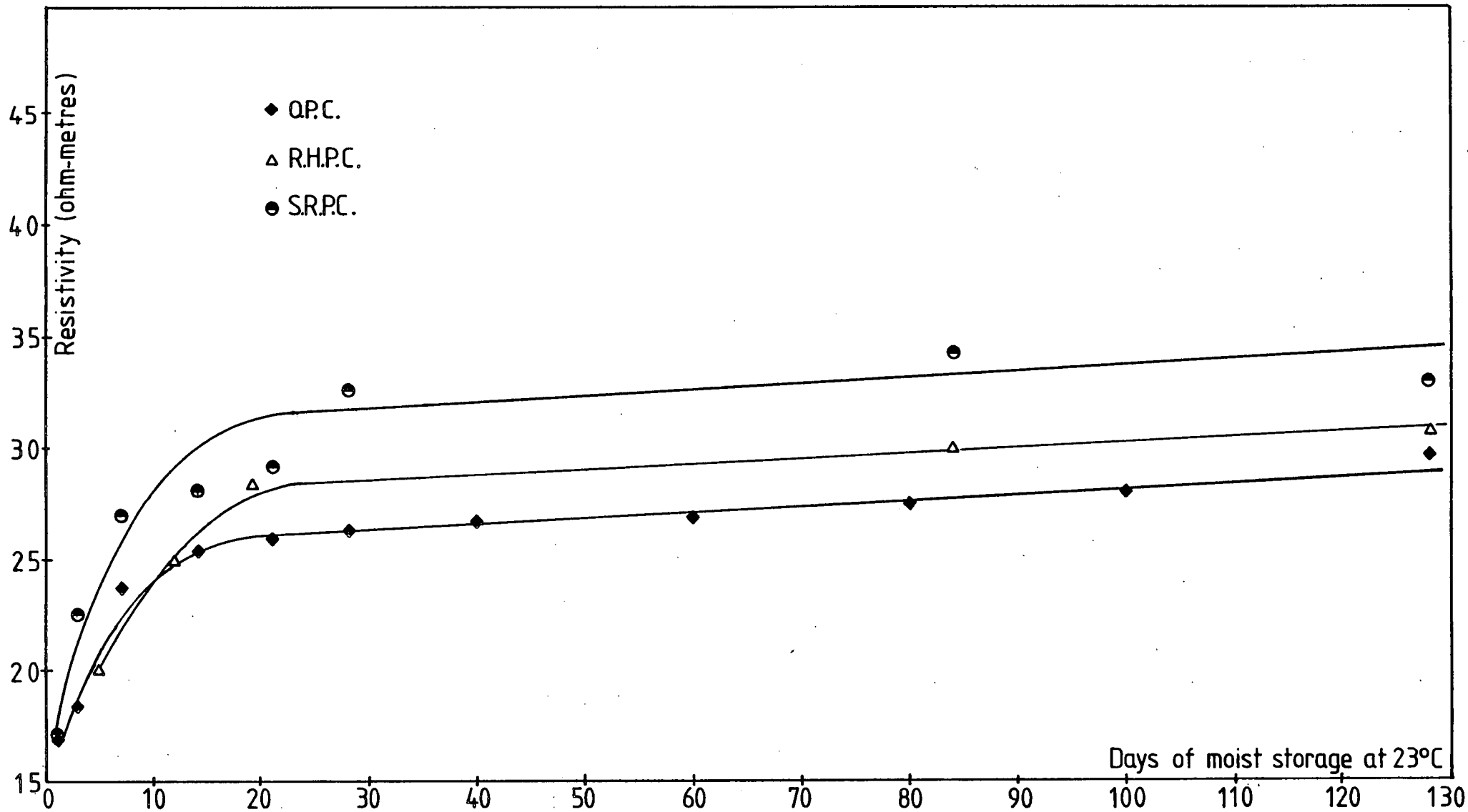

FIG. 5.21 Influence of cement type on resistivity of concrete

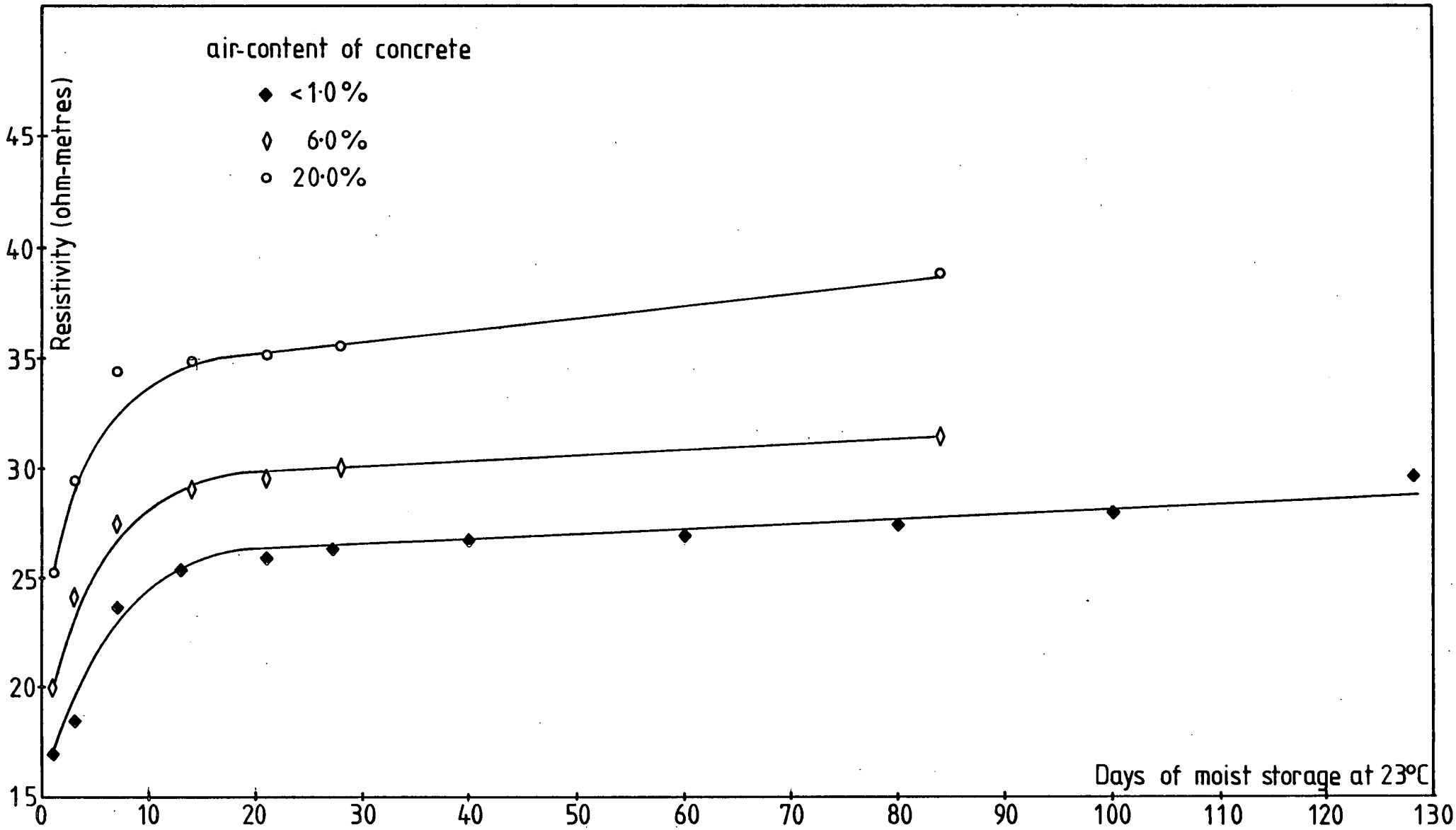

FIG. 5.22 Influence of degree of compaction on resistivity of concrete

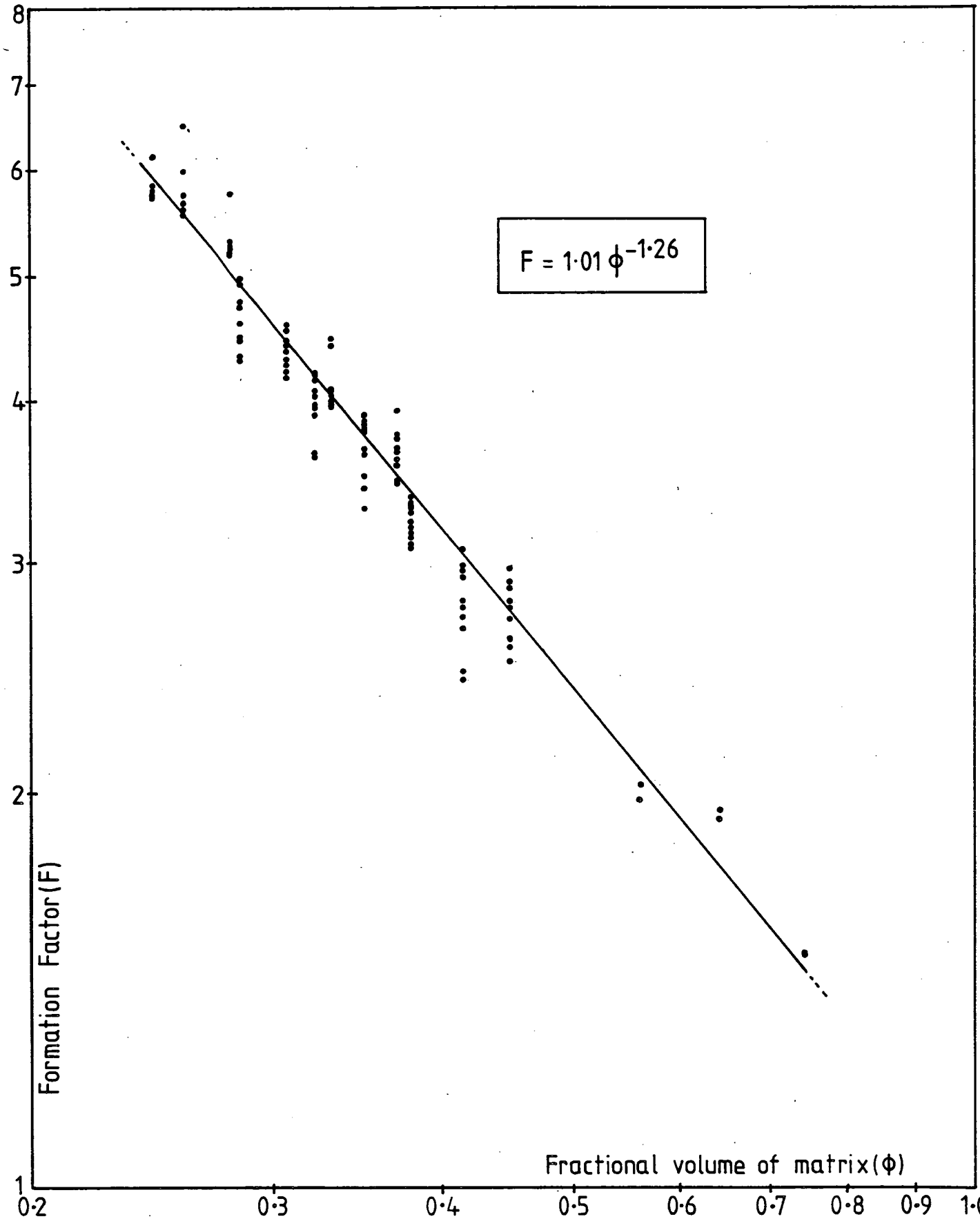

FIG. 5.23 The relationship between Formation Factor and fractional volume of cement paste matrix for continuous moist storage

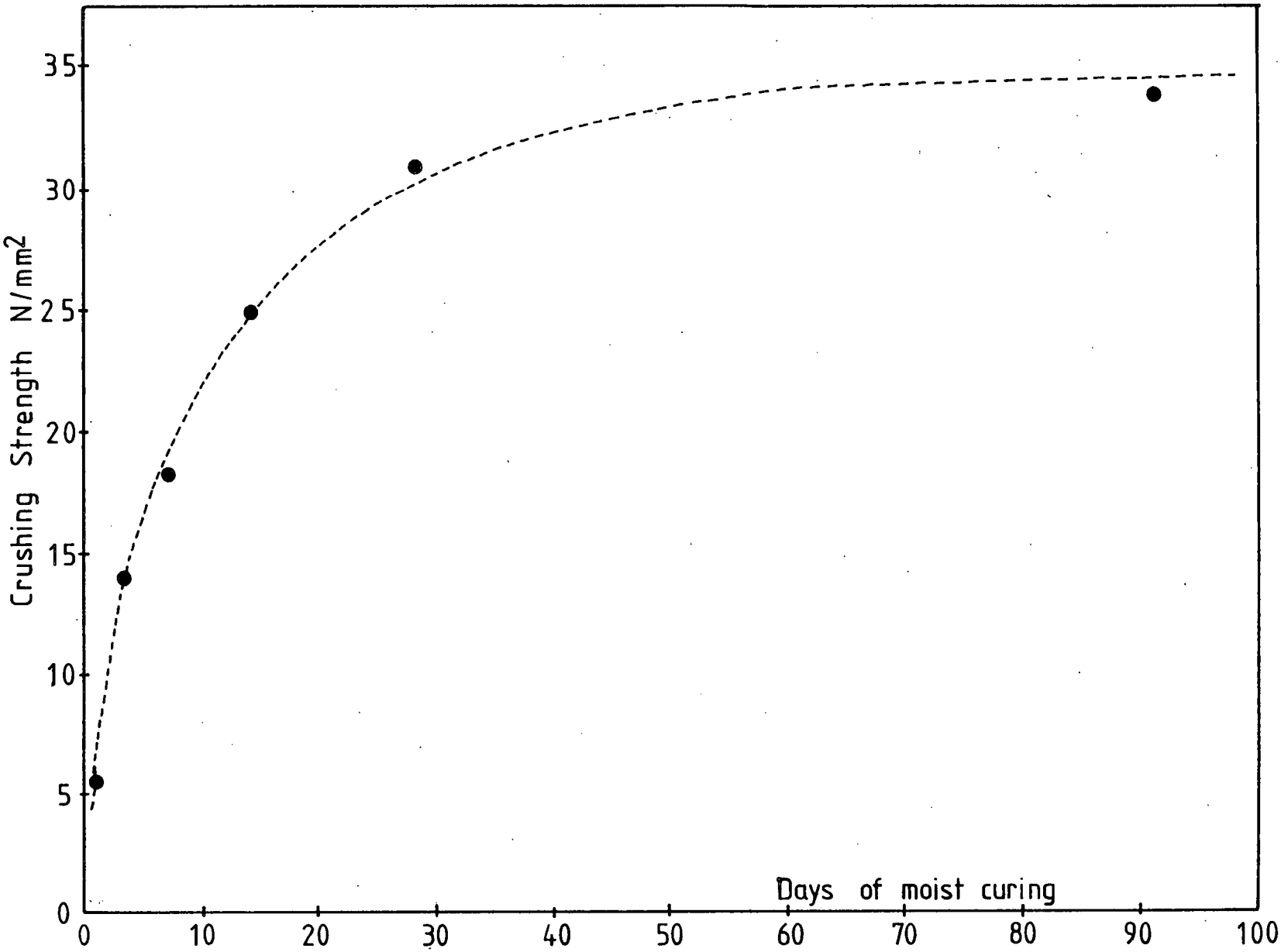

FIG. 5.24 The influence of moist curing on the strength of concrete with a water/cement ratio of 0.5 (80)

CHAPTER 6

THE ELECTRICAL PROPERTIES OF A SOIL-WATER ELECTROLYTE SYSTEM

6.1 Introduction

The objective of this chapter is to investigate the electrical conductivity characteristics of a soil-water electrolyte system. As the earthing resistance of a pile is indirectly related to the electrical properties of the soil surrounding the pile so these warrant consideration.

6.2 Soil Classification

From an engineering point of view, soils can be divided into two types - cohesive soils and non-cohesive soils. For descriptive purposes non-cohesive soils usually comprise coarse grained or granular material, e.g. sand, whereas cohesive material is fine grained, e.g. clay. The concepts of soil microstructure are concerned with very small particles - about 2×10^{-6}m. or smaller as this size of particle is an indirect measure of gravitational and surface bonding forces. It is the clay particles in a soil which develop characteristics such as apparent cohesion and plasticity (93).

The nature of the clay fraction is such that the presence of even a relatively small quantity has a marked effect on the properties of a soil of which it is a constituent. Thus, soils which may contain a high proportion of sand particles (70% to 80%) have noticeable cohesive and plastic properties if as little as 10% of clay is present. A soil need only possess 40% to 50% of clay-size particles to have all the properties of clay in the generally accepted sense.

6.2.1 Theory of Electrical Conduction through Soil

The governing factor which determines the conductivity of a soil is its moisture content (41). However, it must not be assumed that because a lot of water is present, i.e. moisture content is high, the resistivity is necessarily low. A simple experiment with dry sand (non-cohesive material) and distilled water will show that this is not the case.

Since the amount of water present in the soil is a major factor in determining its resistivity, it follows that this resistivity is dependent on the resistivity of the water itself. This, in turn is governed by the concentration of salts dissolved in ground-water. Conduction through soil becomes conduction through the water held in the soil and, thus, will be ionic in nature.

Ionic concentrations will be largely dictated by the clay fraction present in the soil (94). When a dry clay is placed in water, precipitated salts, present on the clay surface, go into solution resulting in an ionic distribution as shown in Figure 6.1. The ions adjacent to the clay surface are tightly bound, while those some distance away are in a truly 'mobile' form.

6.2.2 Previous Experimental Work

The manner in which the resistivity of a soil varies with its moisture content has been the subject of little investigation, McCollum and Logan (95), Higgs (96), and Smith-Rose (97, 98, 99) being the most notable. The first used a red-clay soil which had a

moisture content of about 5% when air-dried, and a resistivity of $2.34 \times 10^4 \Omega$-m. On increasing the moisture content to 22% the resistivity was reduced to 68Ω-m. Higgs used two types of soil found near the National Physics Laboratory (N.P.L.), a top-soil and a sandy-loam.

The manner in which the resistivity of these soils varies with their moisture content is shown in Figure 6.2. It will be noted that at low moisture contents resistivity decreases rapidly with increasing moisture content. The rate of decrease reduces considerably at moisture contents in excess of 15%. Smith-Rose also investigated the electrical conductivity of soils at selected sites near the N.P.L. and confirmed the findings of Higgs and McCollum and Logan (Fig.6.3). These curves illustrate clearly how conductivity tends to a maximum for moisture contents of 20% and over (it should be noted that for Figure 6.3, the conductivity in electrostatic units, $\sigma_{e.s.u.}$, is related to the resistivity, ρ, in ohm-m, by the relationship $\sigma_{e.s.u.} = (1/\rho) \times 9 \times 10^9$).

6.2.3 Discussion - Significance of Degree of Saturation on Resistivity

In considering the influence of water on the resistivity of a soil sample, a simplified model for soil can be envisaged. With reference to Figure 6.4, soils can be divided into a three phase system viz. a solid phase (soil particles), a liquid phase (contained water) and a gaseous phase (air voids). Various relationships between the phases can be derived to define the main physical properties of a soil sample. With reference to Figure 6.4, if W and V are the total weight and volume respectively of a soil sample, and the subscripts, w, s and v refer, respectively, to the water, solid and void phases, the main relationships

that would be of interest when considering their electrical properties are degree of saturation, s, and air-voids ratio, V_a. These are defined as,

$$s = \frac{V_w}{V_v} \qquad \ldots\ldots (6.1)$$

and,

$$V_a = \frac{V_g}{V}$$

The degree of saturation in a soil sample will play an appreciable role in electrical conduction as this dictates the volume of air present in the soil. As the electrical resistance of air can be regarded as infinite, then, referring to Figure 6.5, and using the simplified model for soil, the two soil samples (a) and (b) have identical moisture contents but it would be expected that the samples will have different resistivities due to their differing degrees of saturation/air contents. In the field, soil will exist at varying degrees of saturation. These factors must be taken into consideration for a realistic assessment of the electrical resistivity characteristics of a soil-water electrolyte system.

Previous work has not taken into account the fact that soils, in their undisturbed state, will exist at varying degrees of saturation. Moisture content, alone, cannot be used as a criteria on which to base the resistivity of a soil, i.e. trying to relate laboratory tests on remoulded soils to their in-situ resistivity cannot be based solely on moisture content. A laboratory investigation on remoulded soil samples (which have been mechanically compacted) must investigate resistivity characteristics over a complete range of consistency indices and at varying degrees of saturation/compaction. Even with

laboratory tests, a soil cannot be compacted to the extent that V_a is reduced to 0% (i.e. s = 100%), a realistic figure being 3-15%.

6.3 An Experimental Investigation on Remoulded Clays

A simplified approach adopted by the author to take account of changes in s or V_a of the soil has been to consider the fractional volume of water within the soil, c.f. cement paste in concrete as used in Chapter 5.

A series of experiments was undertaken on remoulded clay samples - Cheshire Clay (12) (liquid limit, w_L = 25%, plastic limit, w_p = 15%) and London Clay (100) (liquid limit, w_L = 65%, plastic limit w_p = 28%). The investigation consisted of measuring the electrical resistivity of these clays as a function of:

(a) Moisture content,
(b) Air-Voids ratio, V_a,
(c) Degree of Saturation, s, and,
(d) Fractional volume of water in the soil.

In this way the electrical resistivity characteristics of undisturbed soils can be assessed.

6.3.1 Sample Preparation

The clay was reduced to powder form by means of a clay mill and then dried in an oven for 24 hours at 108°C. About 600g of the powdered clay was placed in a Winkworth mixer and, with a predetermined

moisture content in mind, the correct mass of distilled water added to the clay and mixed thoroughly. Mixing times varied from about 5 minutes to 30 minutes depending on the moisture content of the sample. After mixing, the samples were left in air-tight plastic bags for 24 hours to allow the water present to equilibrate throughout the sample (at room temperature, 20°C).

The clay was then compacted into plastic tubes having a length of 230mm. and internal diameter 34mm. . A non-conductive material was desirable and plastic was found the most convenient. The mass of the sample was recorded. Both ends of the sample were dressed using a palatte knife to obtain a flat surface and, hence, ensured good electrical contact between the electrodes and the sample. Once the clay had been tested it was recompacted and in this way a series of results could be obtained for different degrees of saturation while the moisture content remained constant.

In order to evaluate the moisture content of the sample accurately, a small amount of clay was extracted from each end of the sample and further small amounts from the middle. The sample was placed in a moisture content tin and dried for 24 hours at 108°C. The moisture content, ω, of the sample could then be determined. By knowing the moisture content, the fractional volume of water in the compacted sample can be deduced,

$$\psi = \frac{\omega . W}{(100+\omega) . V} \% \qquad \ldots\ldots (6.2)$$

where, W = total mass of compacted sample (grms.)

V = total volume of compacted sample (c.c.)

ω = moisture content (%)

ψ = fractional volume of water (%).

The electrical resistivity of the compacted soil sample can be calculated from equation (5.1).

6.3.2 Electrodes, Test Rig and Measuring Equipment

The electrodes were made of brass and had a diameter slightly less than the internal diameter of the tube which contained the sample. In order to measure the electrical resistance of the sample, the electrodes were pressed onto the ends of the sample, and, to make certain of good electrical coupling, a test rig was developed to hold the tube (and sample) in a vertical position (12). With such an arrangement pressure could be applied to the electrodes to obtain intimate electrical contact between the sample and the electrodes. The test rig is shown schematically in Figure 6.6.

As can be seen from Plate 5, the test rig is of simple construction, consisting of a dexian framework mounted on a tufnol base plate. Its overall dimensions are 310 x 310 x 310mm. In the centre of the base plate a cylindrical tufnol block is mounted, onto which a brass electrode can be fitted. The upper electrode mounting is similar in design to the lower one, but has a 115mm. diameter, tufnol loading plate attached onto it. This electrode mounting is detachable thus facilitating the placement and removal of the plastic tubes containing the sample. An electrode similar to that at the base can be attached to the upper electrode mounting.

With the sample in the vertical position in the test rig and the electrodes at either end of the sample a small vertical pressure is

applied via the upper electrode mounting by placing a weight on the loading plate. The electrical resistance of the sample is measured by means of the A.B.E.M. Terrameter wired as per Figure 4.5. After testing the volume of the sample was recorded.

6.4 Discussion of Experimental Results

The experimental data obtained for the two different clays are summarised in Table 6.1. Sample numbers 1-33 are results for Cheshire Clay and numbers 34-47 for London Clay. From these results an overall graph of resistivity versus fractional volume of water, can be drawn for Cheshire Clay (Fig.6.7) and London Clay (Fig. 6.8).

6.4.1 Resistivity versus Fractional Volume of Water

It is immediately apparent that these graphs follow the same general trend as those of Higgs, Smith-Rose and McCollum and Logan. The resistivity drops from almost infinity when the fractional volume of water is zero to a point where increasing the fractional volume of water causesvery little change in the electrical resistivity of the clay. This phenomenon was observed for both clays, with the rate of change of resistivity becoming almost zero when the fractional volume of water is 30% (s is approximately 70%).

Much of the theoretical approach to conduction through a consolidated or unconsolidated porous medium that has been described in Chapter 5 may also be applied to a soil-water electrolyte system. Conduction will be primarily through the fractional volume of water, with the governing equation being (90),

$$\frac{\rho_s}{\rho_w} = A\phi^{-m} \qquad \ldots\ldots (6.3)$$

where, ϕ is the fractional volume of water in the soil; ρ_s, the measured resistivity of the soil, and ρ_w, is the resistivity of the water within the soil. If ρ_w can be regarded as being approximately constant, then,

$$\log [\rho_s] = C - m\log\phi \qquad \ldots\ldots (6.4)$$

where C is a constant. The supposition that ρ_w remains constant is slightly speculative in nature, but it is interesting to plot log-log graphs for the data obtained for Cheshire Clay (Fig.6.9) and London Clay (Fig.6.10). From equation (6.4), the graphs should be straight lines of gradient -m. It is evident from Figures 6.9 and 6.10 that such a logarithmic relationship exists between the fractional volume of water and the resistivity of the soil. (The equations for the lines have been omitted as this is a purely speculative supposition).

6.4.2 Resistivity as a function of V_a and s

From Table 6.1, it can be seen that at a particular moisture content a decrease in air voids ratio, V_a, will result in a decrease in resistivity of the clay. Similarly, as the degree of saturation of the clay increases the resistivity decreases. This gives credence to the discussion in section 6.3, and shows that employing moisture content alone as a criterion in resistivity measurements can be erroneous.

Full compaction (i.e. V_a = 0%) of the remoulded soil sample could not be obtained as was expected.

6.5 Implication of Results to Pile-Testing

Naturallyoccurring, virgin soils (i.e. undisturbed) can be in one of three conditions,

(a) the voids within the soil structure can be completely dry and contain air only (an unusual state),

(b) the voids can be completely saturated with water, and,

(c) the soil can be partially saturated, the voids containing air as well as water.

In its undisturbed state, a soil below the water table will be in a fully saturated condition (s = 100%), furthermore, due to capillary rise, soil lying above the water table will be in an almost fully saturated condition (101-104). In fact, soil below a depth of about 1.0m is not subject to any appreciable fluctuation in degree of saturation due to seasonal variations (99, 103-105).

The experimental data shows that soils recompacted at their natural moisture content ($\simeq w_p$) will have an air voids ratio not exceeding 12%, and hence a change in moisture content above or below its normal value, will not materially change its resistivity.

It could be assumed, therefore, that the resistivity of a soil on a given site will be in a state where an increase in fractional volume of water due to say a fluctuating phreatic surface will not significantly change the reflection coefficient associated with the pile-soil system.

If a pile goes through several layers of soil with resistivities ρ_1, ρ_2, ρ_3.... then the resistivity which determines the reflection coefficient will be an average or apparent resistivity, ρ_a, of all the layers (Fig. 6.11(a)). The subsoil could thus be regarded as being replaced by an equivalent uniform soil of resistivity ρ_a. If the layers remain reasonably constant over a given site then the apparent resistivity will not change appreciably. Testing with a high reflection coefficient will ensure that the resistance readings will not be adversely affected by small fluctuations in subsoil conditions. The reflection coefficient and hence the resistance measured on the ground surface will only be affected by these fluctuations if there is a large resistivity contrast between the layers and the depth of the layer varies appreciably, for example, high resistivity layers, ρ_1 and ρ_3, with a low resistivity layer, ρ_2 (Fig. 6.11(b)). If the depth of the low resistivity layer is increased around a particular pile then the apparent resistivity, ρ_a', of the material around the pile will be altered and this will alter the overall earth-resistance curve for the pile.

In the case of skin-friction piles the Engineer would wish to know of any significant changes in subsoil conditions. The presence of weak layers could thus be detected using the earth-resistance technique. The influence the subsoil conditions around a pile have on the characteristic earth-resistance curve for that pile are investigated in the next Chapter.

Table 6.2 (105) shows the resistivities of typical soils.

6.6 Conclusions

The following conclusions can be drawn from this study.

(i) As the degree of saturation of a soil increases its resistivity decreases.

(ii) As the air-voids ratio increases, the resistivity of the soil increases.

(iii) Clay, and soils which contain a high proportion of clay, will, in their undisturbed state, i.e. fully saturated, have a low resistivity.

(iv) The reflection coefficient will be unaffected by local changes in phreatic surface, as an increase in the degree of saturation of a soil does not materially affect its resistivity. (If the soil is, initially, almost fully saturated - as will generally be the case).

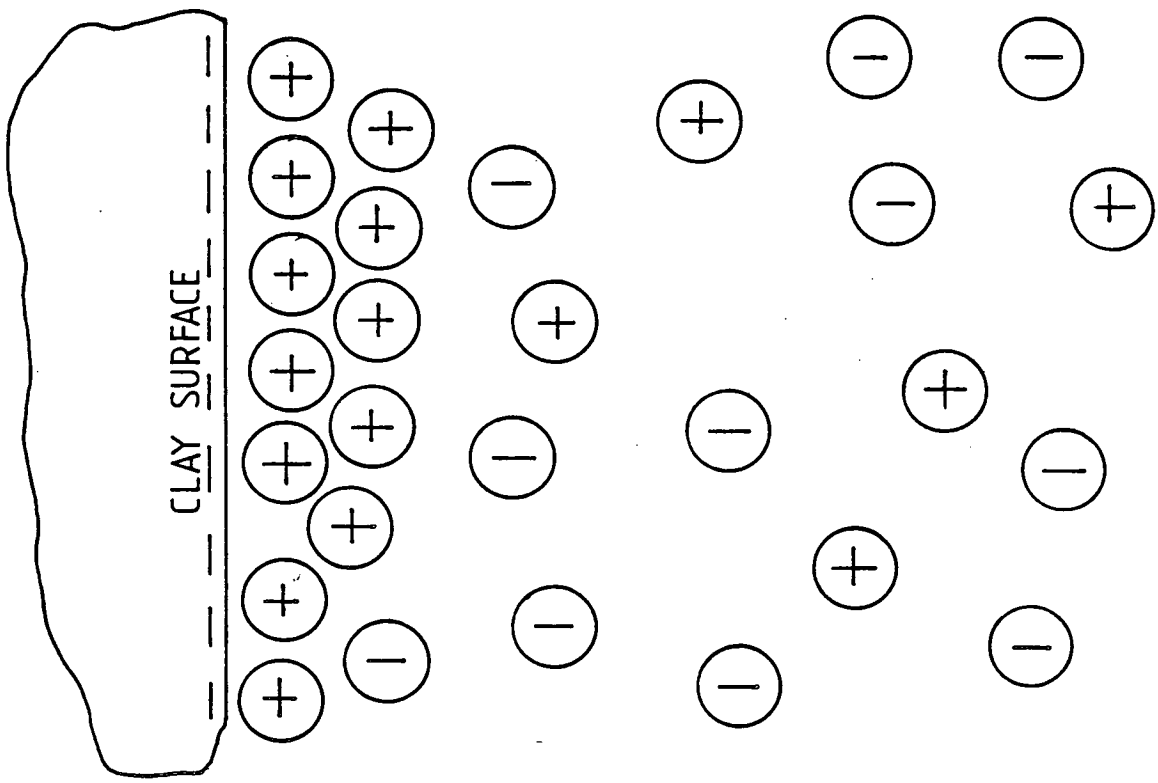

FIG. 6.1 Distribution of ions adjacent to a clay surface

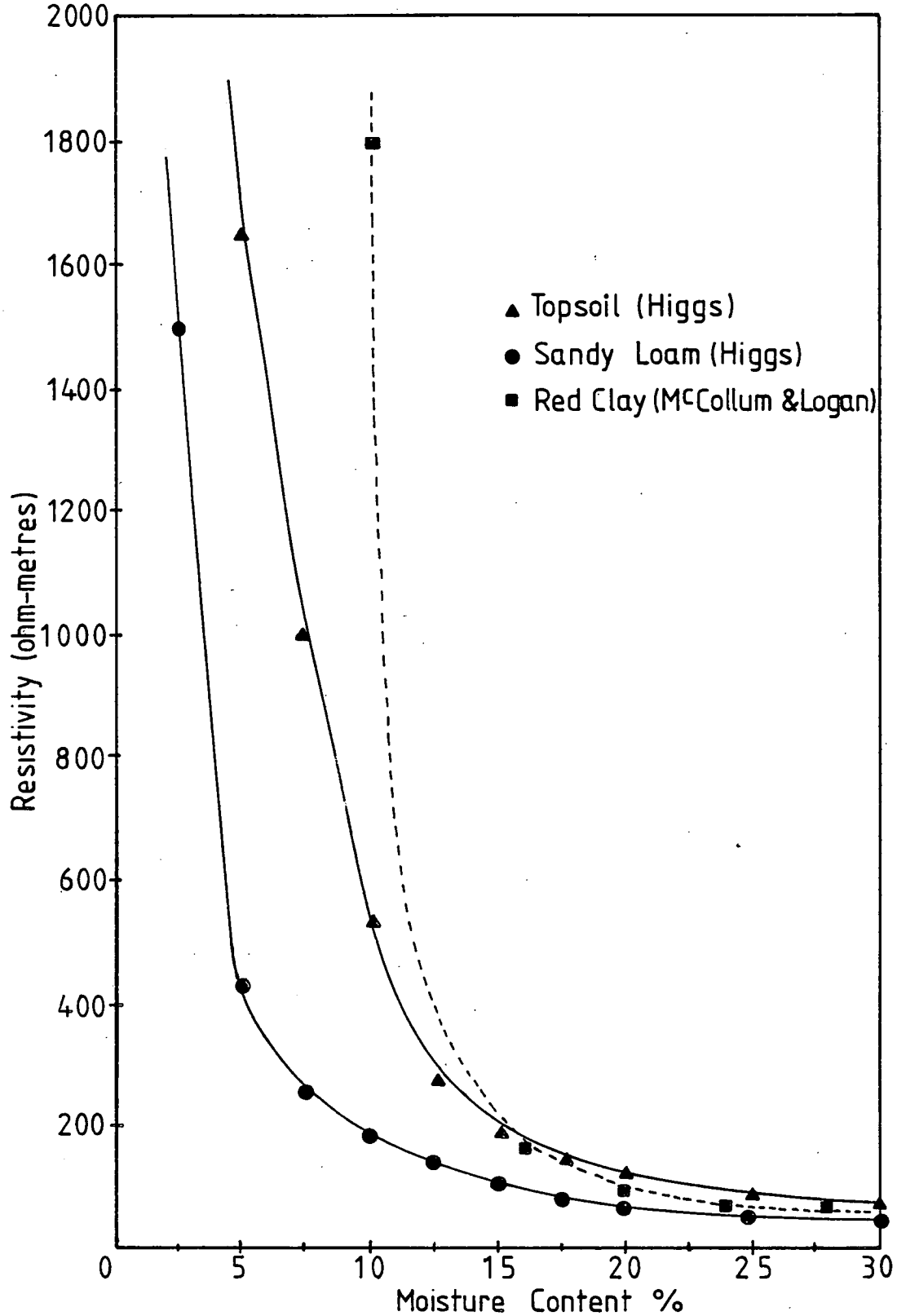

FIG. 6.2 Variation in soil resistivity with moisture content

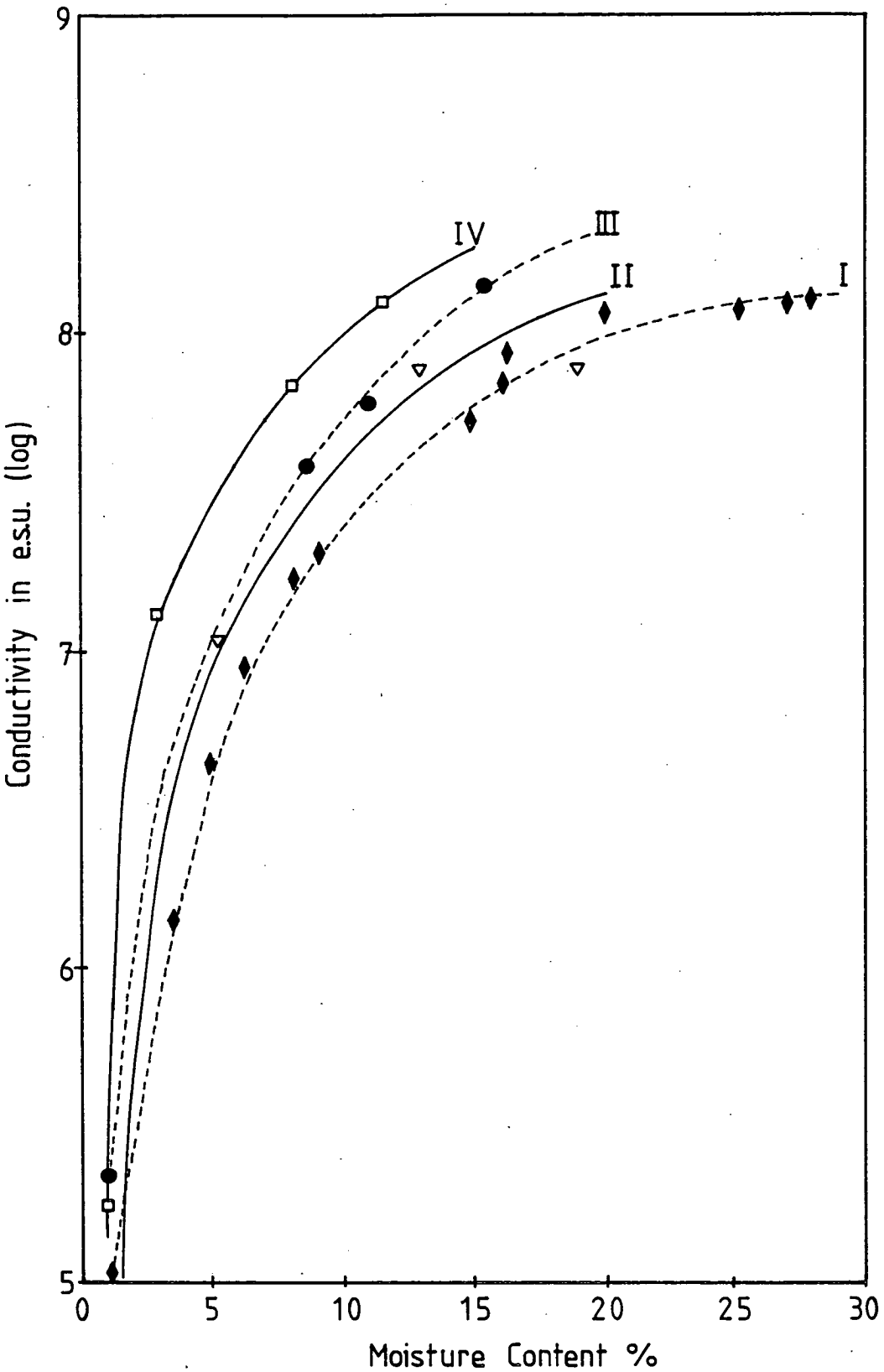

FIG. 6.3 Relation between conductivity and moisture content for soils (after Smith-Rose)

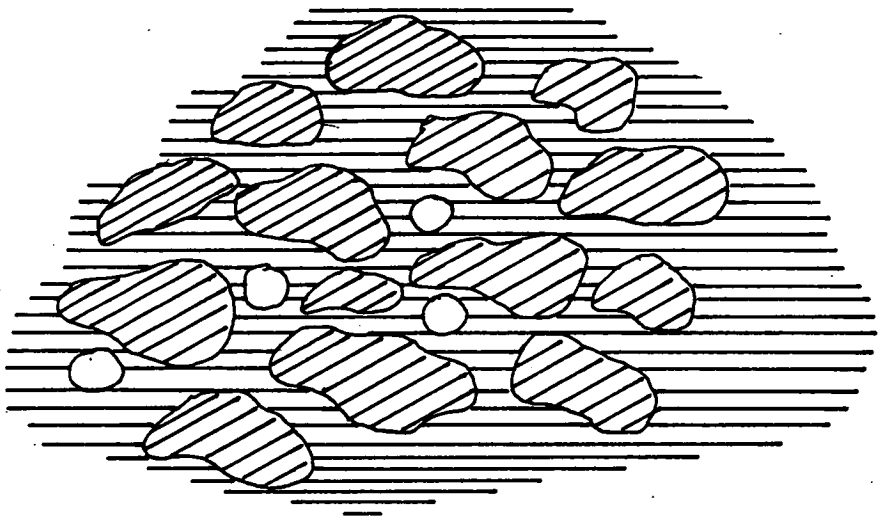

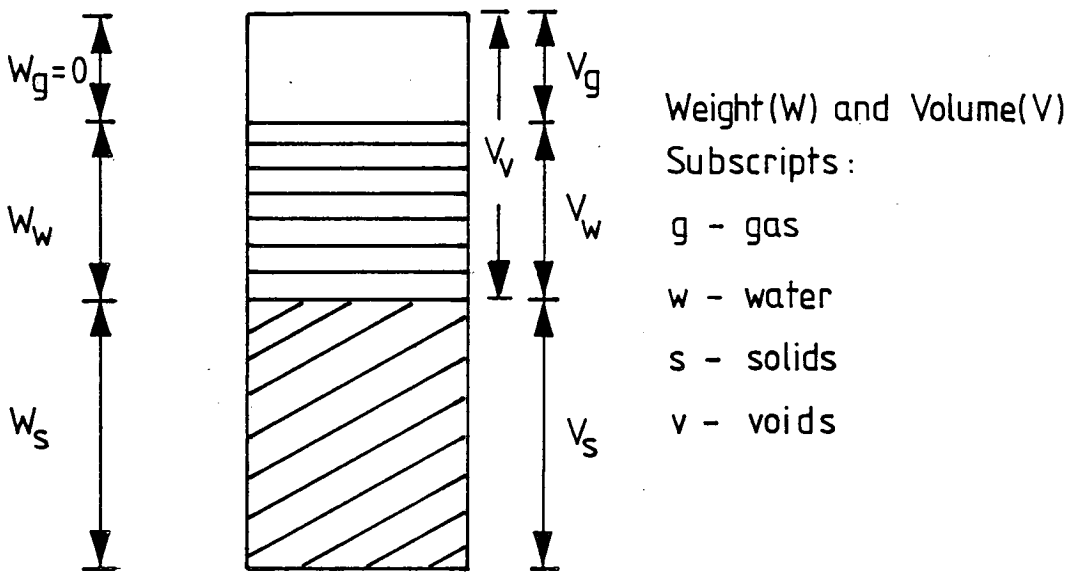

FIG. 6.4 Three phase soil system

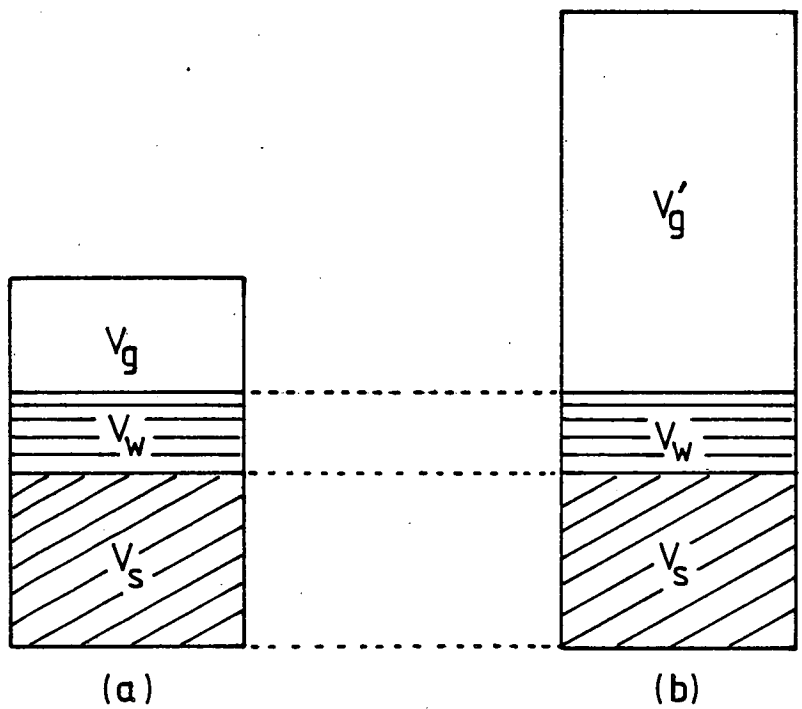

FIG. 6.5 Simplified model for soil

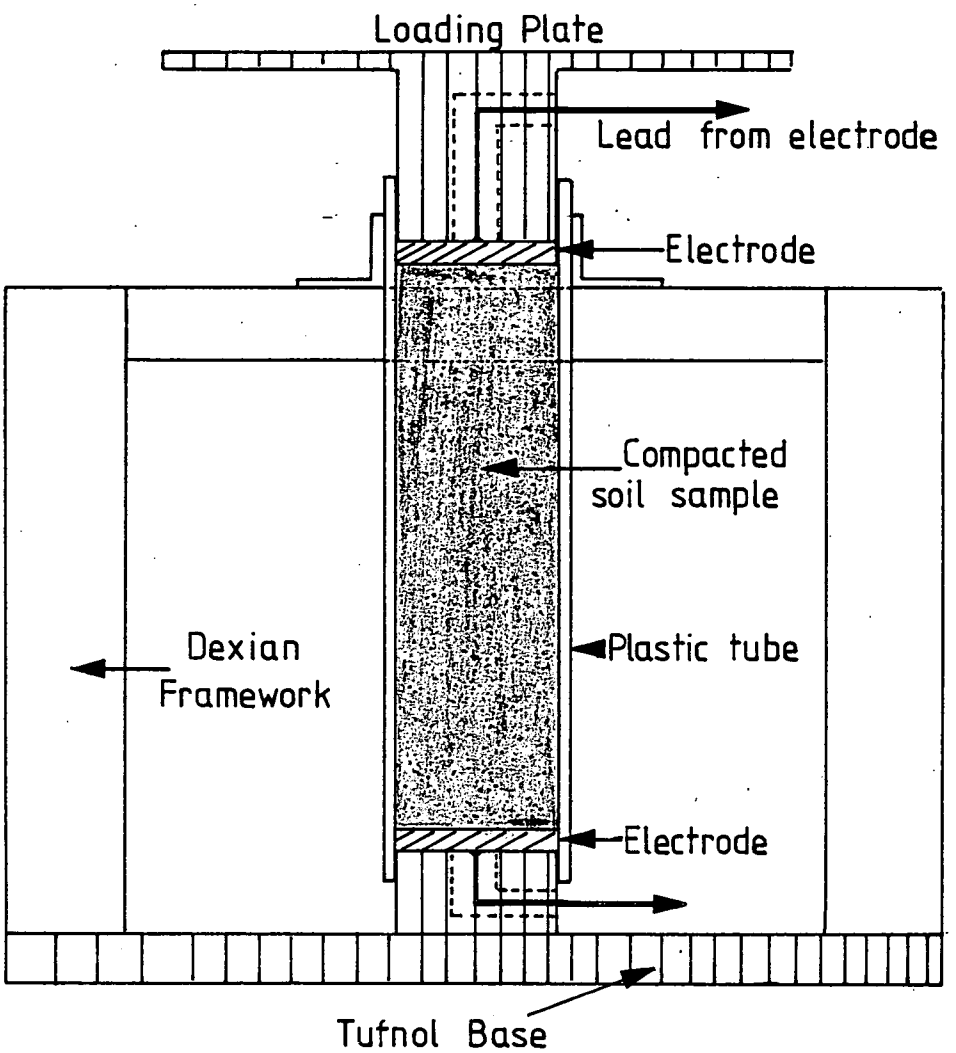

FIG. 6.6 Schematic diagram of Test Rig

PLATE 5

Test-Rig

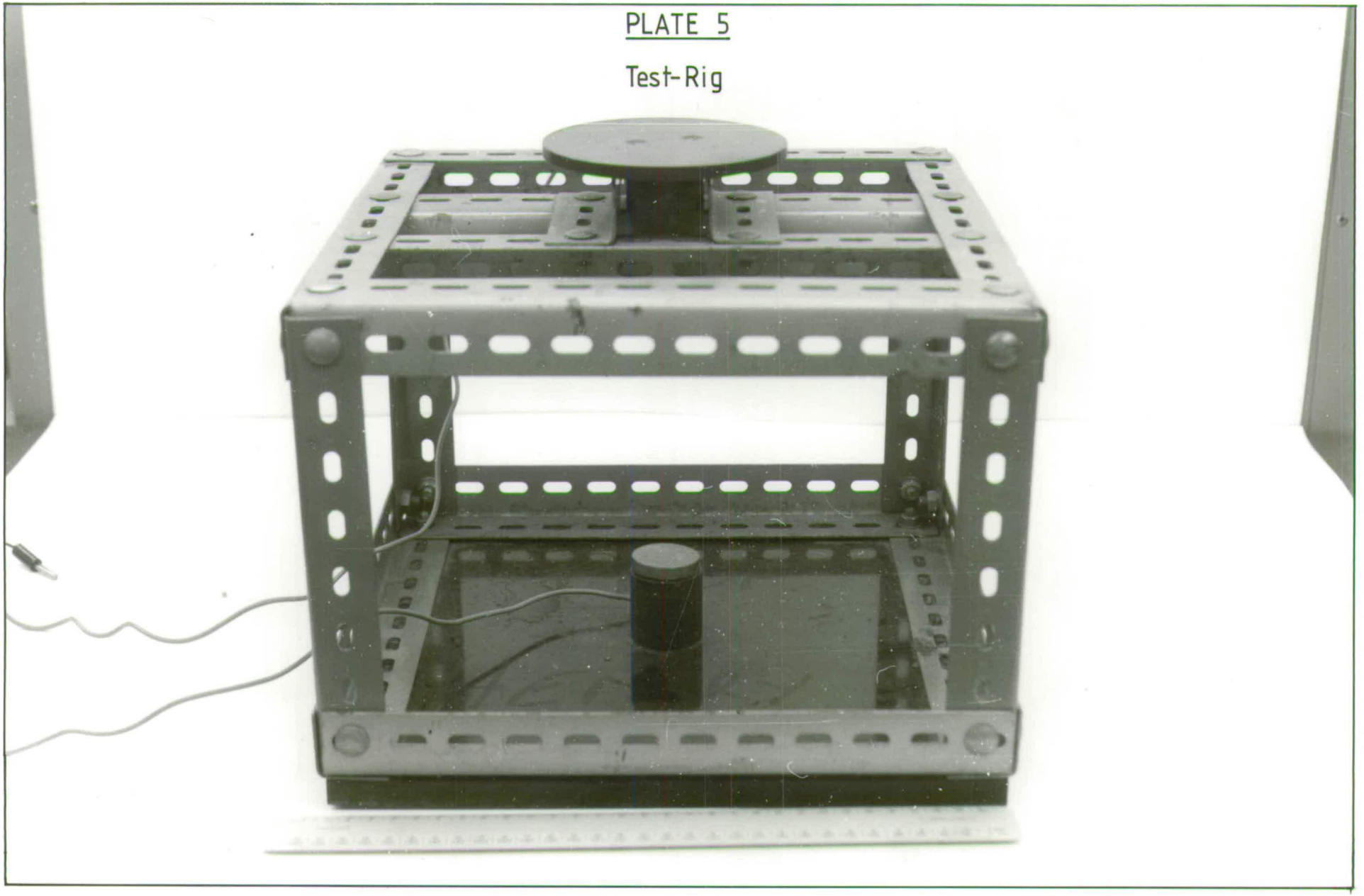

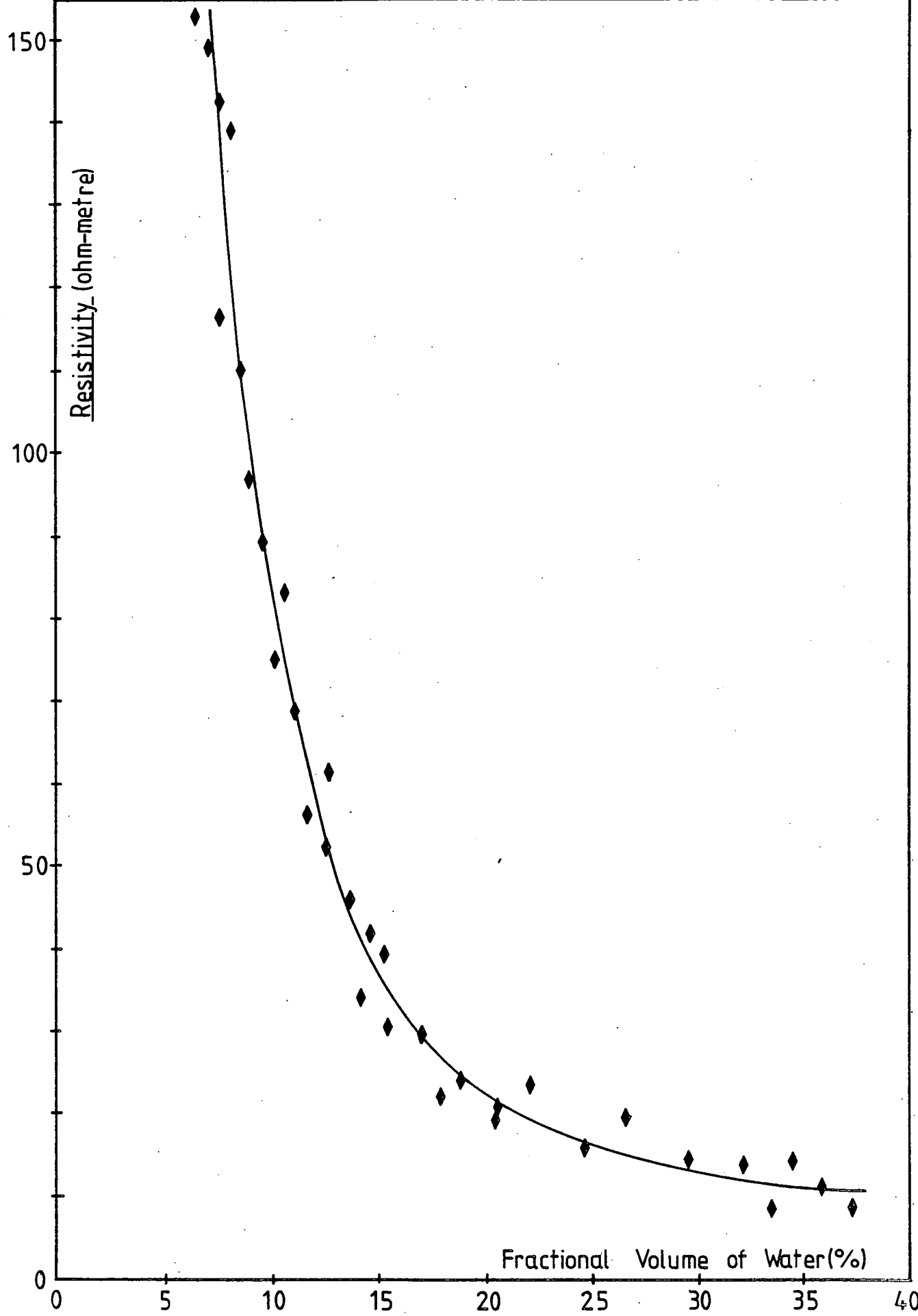

FIG. 6.7 Resistivity characteristics of Cheshire Clay

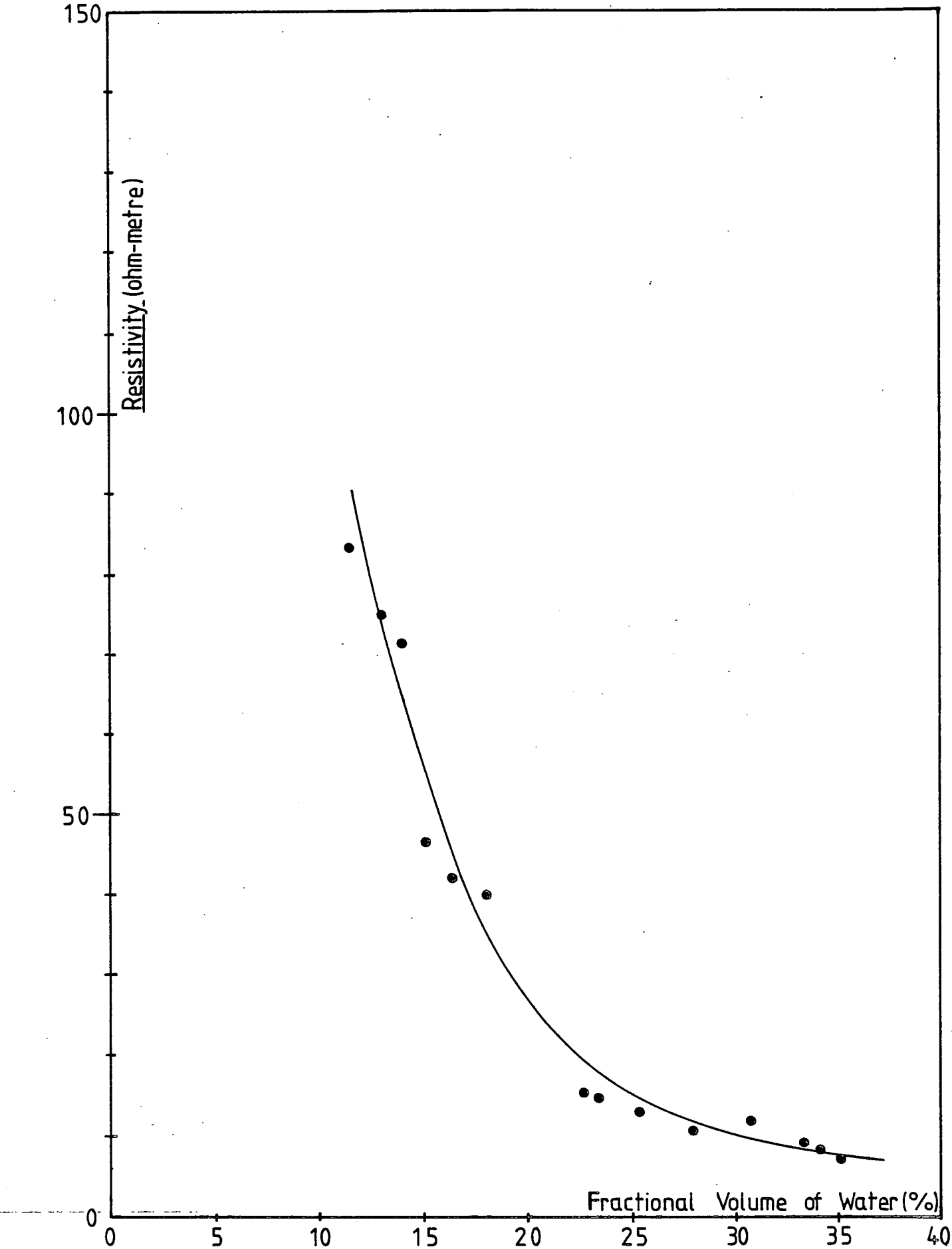

FIG. 6.8 Resistivity characteristics of London Clay

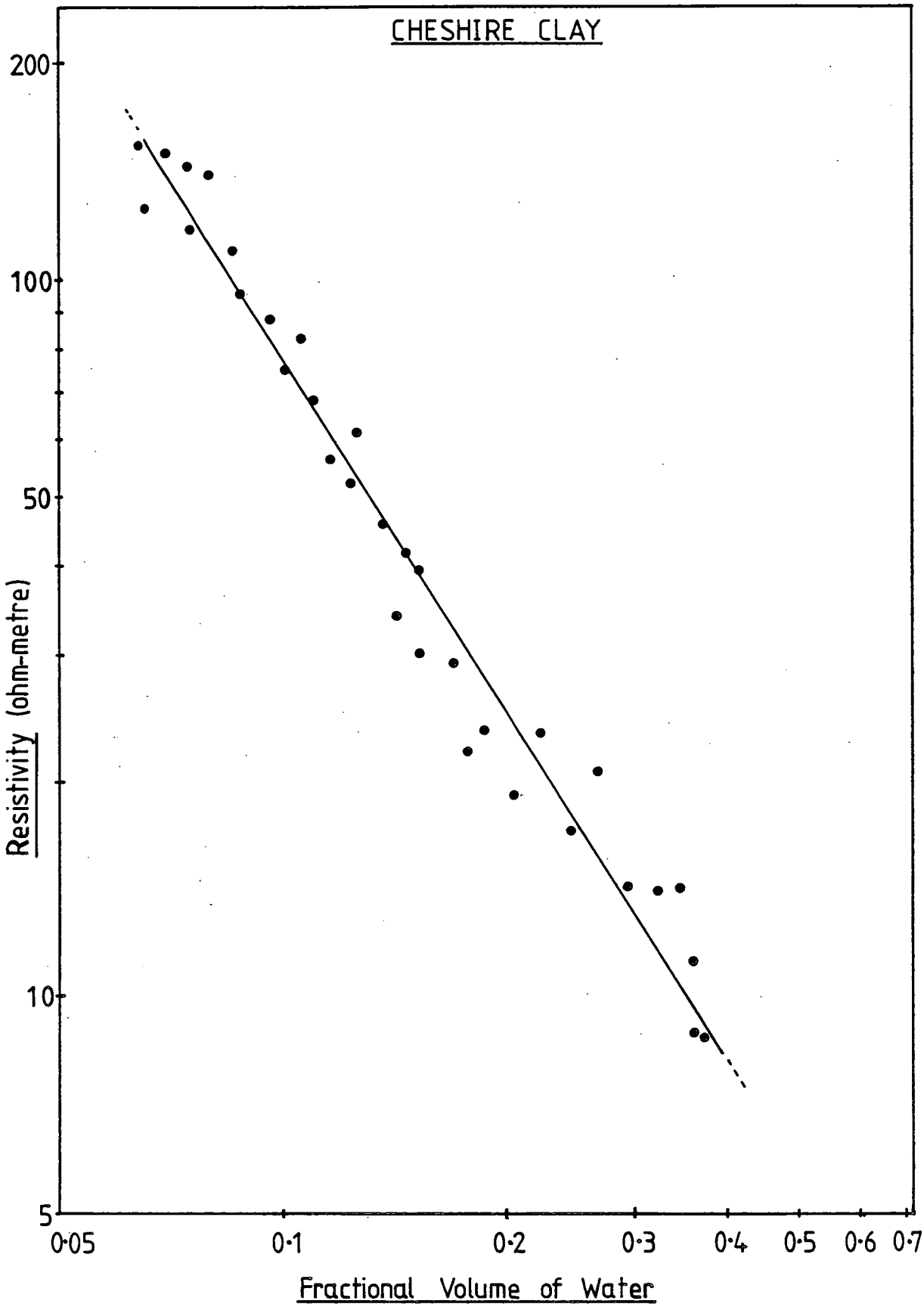
CHESHIRE CLAY
200
100
50
10
5
Resistivity (ohm-metre)
0·05
0·1
0·2
0·3
0·4
0·5
0·6
0·7
Fractional Volume of Water

FIG. 6.9

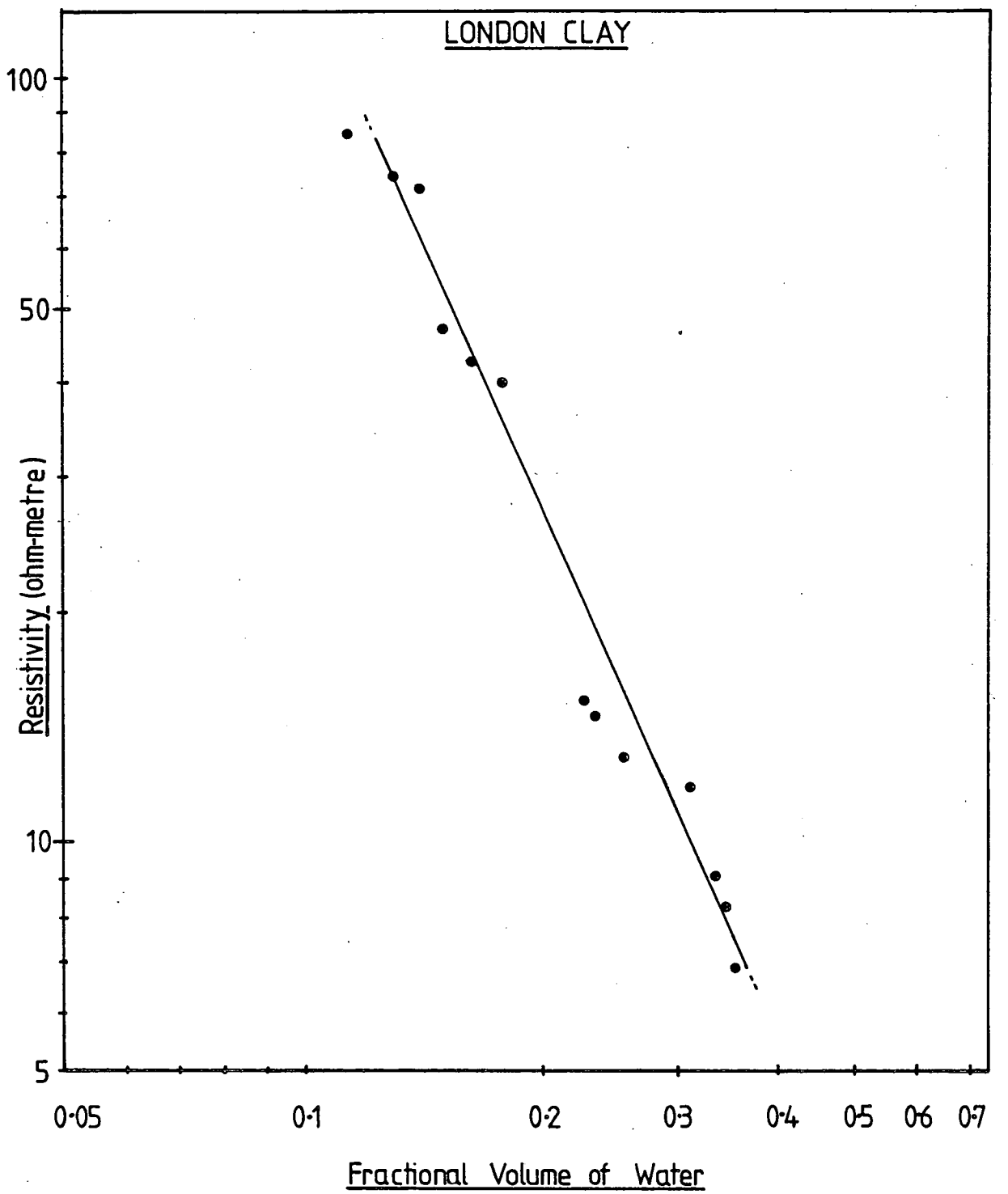
LONDON CLAY
100
50
10
5
Resistivity (ohm-metre)
0·05
0·1
0·2
0·3
0·4
0·5
0·6
0·7
Fractional Volume of Water

FIG. 6.10

Sample No.	Moisture Content (%)	Air-Voids Ratio (%)	Degree of Saturation (%)	Fractional Volume of H_2O (%)	Resistivity Ω-m
1	4.1	36.5	14.8	6.4	153.2
2		30.9	18.3	7.0	149.0
3		24.6	23.0	7.5	142.8
4		20.6	27.8	8.0	139.0
5	4.4	35.4	15.4	6.5	126.5
6		29.0	20.7	7.6	116.1
7		19.5	30.6	8.6	110.1
8	5.5	32.4	21.3	8.8	96.5
9		25.9	27.0	9.6	88.9
10		18.5	36.3	10.6	83.0
11	6.5	32.4	23.4	10.1	74.8
12		27.0	28.8	11.0	68.4
13		15.3	45.3	12.7	61.4
14	7.8	33.9	25.4	11.6	56.3
15		29.2	29.8	12.4	52.0
16		21.9	38.3	13.6	45.9
17		16.6	46.7	14.6	41.5
18		12.5	55.0	15.2	39.3
19	9.2	29.4	32.4	14.1	34.1
20		23.4	39.5	15.3	30.4
21		10.6	62.6	17.8	22.1
22	10.4	22.3	43.3	17.1	29.6
23		14.9	55.6	18.7	23.6
24		7.8	72.3	20.3	19.2
25	13.7	18.4	54.6	22.1	23.5
26		9.6	71.8	24.5	17.0
27		14.4	64.8	26.5	20.8
28		5.0	85.4	29.4	14.4
29	20.3	9.4	77.4	32.2	14.0
30		6.1	84.6	33.3	8.8
31	23.3	11.3	75.1	34.3	14.2
32		7.5	82.6	35.8	11.2
33		4.0	90.2	37.2	8.7
34	7.7	34.0	24.4	11.4	82.9
35		25.0	34.2	13.0	74.8
36		19.0	42.4	14.0	71.3
37	10.0	29.0	34.1	15.1	46.4
38		23.0	42.5	16.4	42.0
39		16.0	52.9	18.0	39.9
40	14.9	21.0	52.3	22.7	15.2
41		19.0	54.8	23.3	14.6
42		12.0	64.7	25.3	12.9
43		3.0	90.1	27.9	10.4
44	20.3	13.0	70.4	30.9	11.8
45		6.0	85.0	33.4	9.0
46		4.0	89.0	34.1	8.2
47		1.0	97.2	35.1	6.8

TABLE 6.1

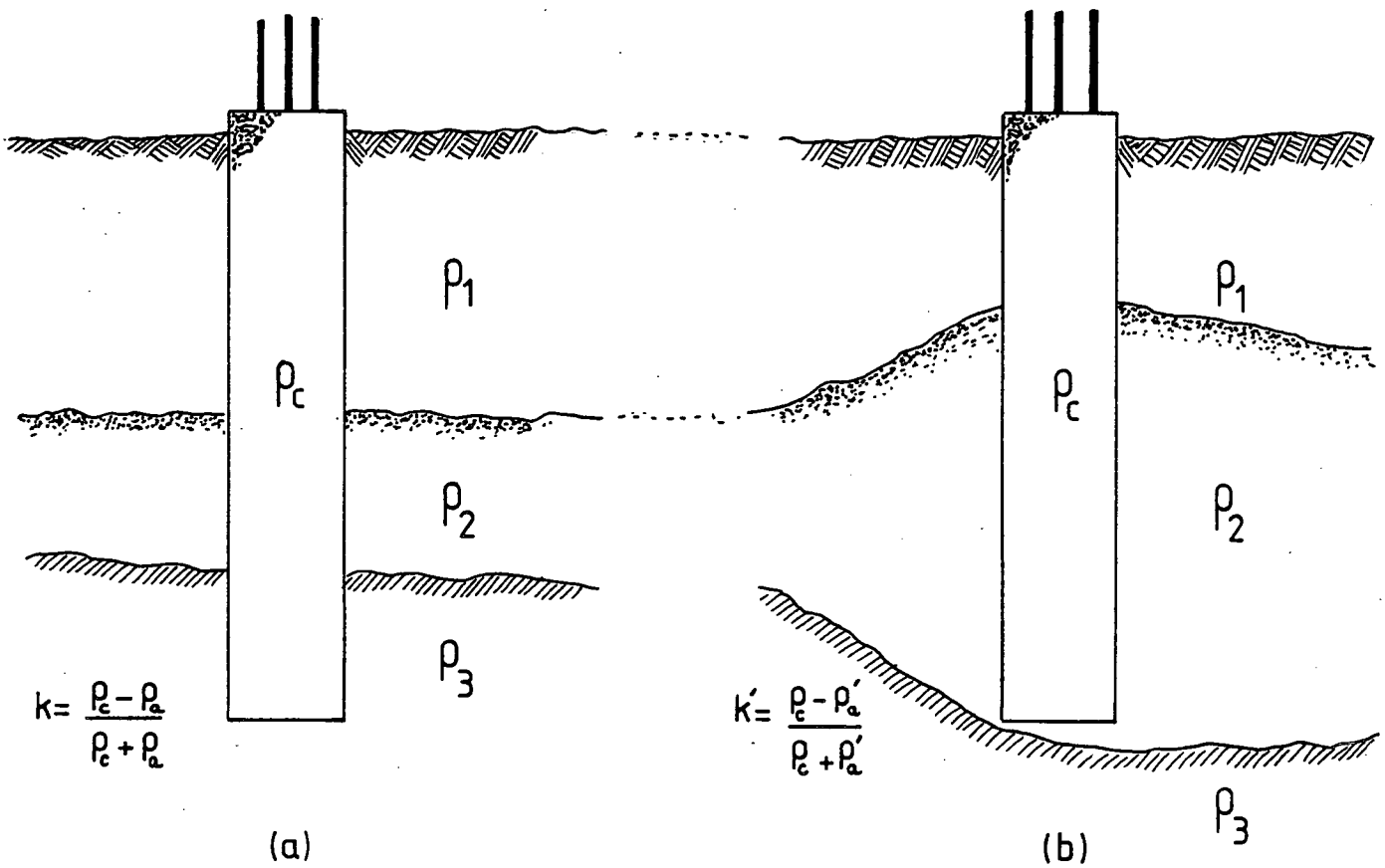

FIG. 6.11 Effect of a layered earth

Resistivity Ω-m	Type of Material
1.5 - 3.0	Moist clayey soils.
3.0 - 15	Moist silty clay and silty soils.
15 - 150	Moist to dry silty and sandy soils.
150 - 300	Well-fractured to slightly fractured bedrock with moist soil filled cracks.
300 - 2500	Slightly fractured bedrock with dry soil filled cracks. Sand and gravel with silt.
2500 +	Massive bedded and hard bedrock. Coarse dry sand and gravel deposits.

TABLE 6.2 Resistivities of different types of material (105).

CHAPTER 7

AN EXPERIMENTAL INVESTIGATION INTO THE EARTH-RESISTANCE OF A PILE-SOIL SYSTEM USING ELECTRICAL ANALOGUES

7.1 Introduction

In the earth-resistance technique electrical analogue and model experiments may be advantageously employed in the determination of the response variations which would occur under fixed conditions. The idealised conditions, made attainable by the use of analogue experiments, often offer a preferable alternative to field experiments with their associated costs and difficulties. They are, generally, simpler and more certain in the determination of the disturbing effects which are associated with pile defects and other anomalies. Observations thus made, may be applied directly to the interpretation of field data, and, in addition, may be used to establish the validity of theoretical predictions. Laboratory experiments can give an indication of the resistance variations to be expected between defective and non-defective piles.

As no experimental data has been published on this integrity testing method then analogue techniques serve as a useful introduction to the methodology of testing and highlight the problems inherent in any attempts at interpretation of field data.

When resistance measurements are to be made on a pile of a certain size and shape, the following questions immediately arise,

(a) at what distance from the pile under test should the current return electrode be placed,

(b) where should the potential reference electrode be placed in relation to the current reference electrode and the pile under

test, and

(c) what effect does the size and shape of the pile under test have on the answers to (a) and (b).

This Chapter attempts to answer the above questions by giving an insight into electric field distribution around a pile.

7.2 Types of Analogue used in the present Study

In theory a full analysis of current flow through porous media should be possible by the use of Laplace's Equation, but, generally, the boundary conditions affecting flow cannot be adequately expressed mathematically because of their complexity. Analogue models help to bridge the gap between theory and practice, but even with these some simplification of real life conditions is necessary. Hence, the usual practical approach requires a balanced blend of theoretical knowledge and empiricism based on experimental judgement assisted by model work.

Analogues are directly relevant to the present study as the governing equation,

$$\frac{\partial^2 V}{\partial x^2} + \frac{\partial^2 V}{\partial y^2} + \frac{\partial^2 V}{\partial z^2} = 0 \qquad \ldots\ldots (7.1)$$

can be conveniently simulated by 2- and 3- dimensional analogues.

A two dimensional representation of the electric field set up around a pile can be conveniently plotted using a conductive-sheet analogue to represent,

$$\frac{\partial^2 V}{\partial x^2} + \frac{\partial^2 V}{\partial y^2} = 0 \qquad \ldots\ldots (7.2)$$

Although not truly representing the 3-dimensional case, nonetheless, it gives some indications of the variations to be expected.

The three-dimensional Laplacian field in single and composite media can be represented more accurately by a conductive liquid or electrolytic tank analogue. Unlike the conductive sheet analogue which shows the distribution of potential (i.e. electric field) around a pile electrode, the electrolytic tank has not been used to plot the field but to obtain earth resistance curves for piles of model dimensions. Each analogue will be dealt with separately.

7.3 The Conductive-Sheet Analogue

When a current is passed through a porous medium between two electrodes, it spreads out and occupies the medium in such a way that the current distribution produces minimum heat. The electric field may be divided into lines of current flow and along each line the potential falls from V_1 at one electrode to V_2 at the other. On each line of flow there is, therefore, a point having a potential V, where V is intermediate between V_1 and V_2, and by joining these points of potential V, an equipotential surface is obtained which cuts the lines of current flow orthogonally. The trace of this surface is known as an equipotential line.

This is the principle of the conductive sheet analogue, with which equipotential lines can be plotted. The application of the conductive-sheet analogue to Laplacian field problems takes three basic steps,

(a) selection of a suitable conductive sheet,

(b) the boundary conditions of the particular field are simulated in the scaled analogue system by means of suitable current sources and sinks, and,

(c) by means of suitable sensing equipment the voltage distribution within the conductive medium is measured and recorded.

As piles are available in a large variety of lengths and diameters, only generalisations can be obtained by plotting the field characteristics around a modelled pile. The following were investigated using this analogue:

(i) the electric field distribution around the reinforcement when buried in a homogeneous earth,

(ii) the effect on the field distribution by encasing the reinforcement in a concrete sheath,

(iii) the field distribution around a pile with partial reinforcement,

(iv) the effect of a fault on field distribution,

(v) the effect of the pile-current electrode distance on (i)-(iv) above.

7.3.1 Resistance Paper - Teledeltos

Conductive sheets of either metal or untreated paper are unsuitable because of their very low and very high resistances respectively. Graphitised paper offers a very acceptable medium for conductive sheet analogues and has a resistivity of the order of several thousand ohms per square. Teledeltos paper, which was originally developed for facsimile telegraphing purposes, is one such commercially available graphitised paper and has a resistivity in the region of 2000 ohms per square.

7.3.2 Simulating a change in medium resistivity

Clearly there are two media to consider, firstly the resistivity of the concrete around the reinforcement, and secondly, the resistivity of the soil surrounding the pile. It should be emphasised that this type of analogue is only convenient for simulating the case when the electrical resistivity of concrete is higher than that of the background medium i.e. negative reflection coefficients only.

Changes in resistivity, to simulate a change in medium, can be achieved by punching holes in the paper. Since the resistance, R, of the paper is given by,

$$R = \frac{\rho . L}{A} \qquad \ldots\ldots (7.3)$$

and by considering a unit square of the paper, punching holes effectively reduces the cross-sectional area for conduction thereby increasing the resistance of the paper. The resistance can also be increased by extending the scaled dimensions of the medium of higher resistivity.

7.3.3 Experimental Procedure

The basic equipment (Figure 7.1) comprises a low voltage d.c. supply obtained from a rectified and smoothed a.c. supply; a potentiometer, P; and a moving-coil galvanometer detector, G. A convenient plotting probe was found to be 4H pencil sharpened at one end to a fine point and the lead exposed at the other end to receive a flexible connection.

7.3.3.1 Application of Boundary Conditions

In most Laplacian field problems the boundary conditions are specified by known potentials along certain boundaries. Non-conducting boundaries (or flow lines) are represented in the analogue by cutting the paper to the required shape of the boundary required, and, for this particular case, the ground surface represents a flow line.

The 100% and 0% equipotential lines are represented in the analogue by painting electrodes on the paper with a conducting paint containing a high percentage of finely divided silver, viz. the pile reinforcement and the return electrode placed outwith the pile.

Connections were made to the painted boundaries by embedding copper wire (22 S.W.G.) into the paint and over the full length of the boundary and using the paint, itself, as an adhesive. (The 'reinforcement electrode' boundary was 300mm long and 10mm wide). A 10mm. wide strip was perforated around the full length of the reinforcement - the resistance of a perforated square being 3840Ω and that of a square of unperforated paper 810Ω giving a resistance ratio

of 4.7:1. To increase the resistance of the paper to the above ratio 60, 0.5mm diameter holes were punched per square centimeter. A fault was simulated by leaving a portion of the paper unperforated.

7.3.3.2 Measurement of Equipotential Lines

The wires from the electrodes are connected to the output terminals of the power supply. The conductivity of the painted 100% and 0% equipotential boundaries are first checked by making sure that, with the probe touching any point on the boundary, balance of the galvanometer is obtained with the potentiometer set at 100% and 0%. This being checked, the potentiometer is then set successively to 90%; 80%; 70%... and the equipotential lines plotted using a null balance technique. With the potentiometer set on say, 60%, the paper is touched with the pencil, which is moved until balance is obtained and in this way the complete field pattern is built up. The current flow lines can be sketched in by hand such that they cut the equipotential lines orthogonally forming 'squares'.

7.3.4 Experimental Results

The results have been reported in the form of equipotential plots around a pile with the current flow lines being omitted for clarity (Figures 7.2-7.12). Its limitations appreciated, this analogue has proved useful in giving some insight into the electric field distribution around a pile. From such an analogue accurate determinations are not possible as the real situation is 3-dimensional, in consequence, results obtained are only qualitative in nature.

7.3.4.1 Discussion of Results

Figures 7.2 and 7.3 show a plot of equipotential lines around the reinforcement which is buried in a homogeneous medium. It is evident that, as the potential lines in the vicinity of the current electrode placed outwith the pile are circular then, this electrode can be regarded as a point sink. This assumption was used in Chapter 3. Furthermore, as the equipotentials in proximity to the return current electrode are closely spaced then this will result in a rapid increase in both field, strength and flux density in this area.

The equipotentials on the ground surface are shown in Figure 7.4. There will exist one equipotential line on the ground surface which is neither concave nor convex. This point would represent the position where the true earthing resistance can be obtained, in other words position A in Figure 3.15, and from the field distribution patterns this point is approximately mid-way between the centre of the pile and the current electrode. When the pile-current electrode distance is increased the potential lines become less distorted, and the rate of change of apparent resistance, with increasing distance from the pile head, decreases.

Referring to Figures 7.5 and 7.6, punching holes in the paper to simulate an increase in resistivity due to the concrete has the effect of moving corresponding equipotential surfaces nearer to the pile. This increases the potential difference between the pile reinforcement and any point outwith the nominal pile periphery. This, in turn, will result in an increase in measured resistance. Only equipo-

tentials near to the pile head are significantly affected and when the pile-current electrode distance is increased (Fig. 7.6), the distortion between the perforated and unperforated plots are not discernable. Potentials on the surface of the earth are shown in Figures 7.7 and 7.8. As with the reinforcement plots, there exists an equipotential line, approximately mid-way between the pile and current electrode which is neither concave or convex, and this represents the position where the true earthing resistance can be obtained.

Figure 7.9 shows the field distribution when a portion of the paper is left unperforated, i.e. to simulate the case where the concrete has been removed from around the reinforcement and surrounding soil has filled the void. The equipotential surfaces in the vicinity of the fault are displaced away from the pile, implying a decrease in resistance. This displacement of equipotentials is only noticeable for equipotentials close to the pile head, and for large pile-current electrode distances this distortion is not evident - Figure 7.10. The relevance of this to fault detection being that only resistance readings close to the pile head are of importance as these potentials will be significantly altered by faults and other anomalous features.

The field patterns around partially reinforced defective and non-defective piles are shown in Figures 7.11 and 7.12. When the defect is in the unreinforced section of the pile the potential distribution on the ground surface remains unaltered. From this, it may be concluded that only the reinforced section of the pile contributes to the response.

7.3.5 Conclusions

The main conclusions that can be drawn from this study are:

(1) The electric field pattern around a pile is altered by defects which will manifest themselves as a change in resistance measured on the ground surface.

(2) The potential gradient close to the pile head is most affected by defects.

(3) There would appear to be little to be gained in using large pile-current electrode distances.

(4) There exists one equipotential at approximately mid-way between the pile and current electrode where the true earthing-resistance can be obtained. This line occurs when the equi-potential on the ground surface is neither convexnor concave.

(5) The electric field pattern of the pile-soil system is dictated largely by the reinforced section of the pile.

7.4 The Electrolytic Tank - Analogue Design Considerations

Electrolytic tank experiments have been successfully employed by several investigators (106, 107, 108) in connection with laboratory investigation into the electrical resistivity method of geophysical surveying. Experimental graphs and curves can be obtained for

comparison and interpretation of field data particularly when mathematical treatment is difficult. Since the earth-resistance technique involves flow of current through stratified media, the analogue technique would assist the development of a methodology of fault detection and highlight any limitations.

Basically, the analogue comprises a tank of suitable dimensions filled with an electrolyte which simulates the ground. Piles of model dimensions and with typical defects are immersed into the electrolyte and earth-resistance curves obtained for both defective and non-defective piles. This will enable a quantification of the variation in resistance between such piles to be realistically assessed, unlike the previous analogue where only qualitative information could be obtained.

7.4.1 The Electrolytic Tank and Electrodes

The tank used in the experiments was made of fibre reinforced plastic and had dimensions of 1800 x 1200 x 650mm. (Plate 6(a)). The depth (650mm.) in relation to the size of the models was considered sufficient to remove any effects from the tank base, while the other dimensions were large enough to reduce image effects from the sides of the tank to negligible proportions. Brine solution was used as a background medium. This had several advantages over other solid or granular media:

(a) the electrical conductivity of the medium is conveniently variable by the addition of solute. As a result a wide range of both positive and negative reflection coefficients can

be simulated and the influence of this factor on fault detection assessed.

(b) the degree of electrical isotropy and homogeneity is more certain when an electrolyte is used than if a granular material were employed.

(c) longitudinal profiles may be carried out more easily since the position of the electrodes with respect to the model may be changed without disturbance of the background medium.

(d) good electrical contact can be obtained between the electrodes and an electrolyte.

The potential and current electrodes used in the electrolytic tank analogue had to possess the following properties,

(i) their electrical resistivity must be small relative to that of the electrolyte,

(ii) they must not react chemically with the electrolyte,

(iii) they must not be dissolved to any measurable extent by the electrolyte,

(iv) they must present a smooth, well-defined surface, and

(v) they must be easily shaped and cleaned.

Stainless steel or graphite electrodes would fulfil the above requirements - graphite being chosen for this study. The construction of the electrode is shown in Figure 7.13, and consists of a graphite rod 80mm long and 2mm in diameter sheathed with insulation, primarily to prevent damage due to handling. The bottom of the electrode had a rubber grommet glued onto it exposing 4mm of electrode, the reason for which was to ensure correct and consistent depth of immersion each time a profile was carried out. Figure 7.14 shows different depths to which the probes can be immersed, and, as the depth of immersion can influence the resistance readings, consistency was essential. Figure 7.14(b) was used, i.e. when the meniscus level is just touching the bottom of the grommet. The top of the electrode was also exposed to receive a connection from the Terrameter. The electrodes were suspended from a wooden gantry placed across the tank.

7.4.2 Excitation and Instrumentation Considerations

In Chapter 4 several electrical requirements were outlined which any instrumentation had to possess before being considered for use in the field. Likewise, these requirements also apply to electrolytic tank excitation, e.g. reduction in polarisation, elimination of stray currents. The Terrameter described in Section 4.4 was employed for all tank experiments. The use of square wave excitation in electrolytic tank analogues has been shown to be beneficial in reducing stray capacitive and reactive components (109). As accurate determinations were required (to be compared with theory) the wiring arrangement shown in Figure 4.4(b) was used.

7.4.3 Model Piles

As explained in section 7.3 piles come in a variety of shapes and sizes, hence it is only possible to determine field characteristics around a typical pile. However, from these tests, generalisations can be obtained. The longitudinal dimensions of the models were also limited by the depth of the tank, as image effects due to the base of the tank would influence results if the models were too long. Mix requirements for the concrete did not have to be modelled, and only a change in resistivity of the medium around the reinforcement had to be simulated.

Irregularities simulated in the piles are representative of defects normally encountered in cast-in-situ piles. The defects varied,

(a) in their importance - the defect may be over the whole section or over a smaller area; or at the top of the pile head or near the bottom,

(b) in their nature - there may be inclusions of soil, gravel or poor quality concrete in the pile shaft.

A series of models were constructed to simulate such faults. The basic model size had a p/l ratio of 0.1 (14) and an a/l ratio of 0.05 - the length of the model being 300mm. All models were continuously reinforced. The model piles were constructed using a 1:2:4 mix concrete with a 0.6 water-cement ratio, and vibration compacted into plastic tubes. Defective models were constructed by tying pre-shaped polystyrene onto the reinforcement at the quarter points on the

pile, which were subsequently removed. The defect extended over approximately 15 percent of the length. Typical models are shown in Plate 6(b).

An identical series of models was made using a 1:1 sand-cement mix with a 0.5 water-cement ratio. The reason for making these models was two-fold,

(a) to simulate defective concrete in the pile shaft.

(b) to enable large positive reflection coefficients to be obtained. This will in no way affect the general trends as the reflection coefficient, k, is merely a ratio.

After demoulding, the models were immersed in a curing tank (at 13^{o}C) for a period of 40 days before testing. From the work already undertaken on the temporal variation of concrete resistivity, after one month the electrical resistivity increased little with time, i.e. became almost constant. If the models were tested immediately after demoulding then the resistivity of the concrete would be changing quite rapidly over the first two weeks and it would be difficult to ascertain whether changes in resistance for the various models are due to the defects or just a change in the electrical resistivity of the concrete.

Model piles were also constructed to investigate the effect on the earthing resistance of,

(a) changing the diameter of pile to length of pile ratio, i.e. (p/l ratio),

(b) changing the diameter of reinforcement to length of pile ratio, i.e. (a/l ratio), and,

(c) partially reinforced model piles.

Experiments were also undertaken on uncased reinforcement. Control concrete cubes were taken from each concrete batch.

7.4.4 Experimental Procedure

After the tank had been filled with water, sufficient sodium chloride was dissolved to reduce the electrical resistivity of the water to such an extent that a large negative reflection coefficient could be obtained with respect to the concrete model piles. Thereafter, to obtain intermediate negative reflection coefficients and positive reflection coefficients, some of the brine solution was removed and replaced by tap water. In this way a spectrum of reflection coefficients, ranging from -0.9 to +0.7, could be obtained with ease. Before any experiments were carried out in the tank, the surface of the brine solution was skimmed to remove any dust and dirt and then stirred thoroughly for the following reasons,

(a) ensure that thermal equilibrium exists throughout the electrolyte, and,

(b) ensure uniform dispersion of solute.

The electrical resistivity of the brine solution was measured employing

the traditional Wenner four electrode system used for geophysical investigations. In this method four equally spaced, colinear electrodes are lowered into the brine solution - a current is then passed through the two outercurrent electrodes, and the potential drop is measured between the two inner, potential electrodes. Referring to Figure 7.15, if the depth of immersion of the electrodes is d and their spacing is a, then the resistivity, ρ, of the medium is given by (110),

$$\rho = \frac{4\pi a \ \frac{\Delta V}{I}}{\left[1+\frac{2a}{\sqrt{(a^2+4d^2)}}-\frac{2a}{\sqrt{(4a^2+4d^2)}}\right]} \qquad \ldots\ldots (7.4)$$

When d is small in comparison to a this equation reduces to,

$$\rho = 2\pi a \,.\, \frac{\Delta V}{I} \qquad \ldots\ldots (7.5)$$

Since measurements were made using the Terrameter a direct reading of resistance was obtained, i.e. the quotient $\Delta V/I$. The spacing of the electrodes (200mm) was considered adequate to avoid edge effects from the tank boundaries. Several measurements of resistivity were taken over the surface to ensure homogeneity.

The models, current and potential electrodes and Wenner electrode array were suspended from wooden gantries placed over the tank, with the models and electrodes being placed as remote from the tank boundaries as possible. Preliminary experiments showed that only when the models were placed very close to the tank boundaries (100mm), were any noticeable differences in resistance readings observed. The model piles were immersed in the electrolyte so that the top of the pile was at the same elevation as the water level, and connections were made between the projecting reinforcement and Terrameter by means of lightweight cables and crocodile clips.

7.4.5 Discussion of Experimental Results

Referring to Figure 7.16, the results are plotted in the form of Earth-Resistance curves for each model, viz. the voltage-current ratio, in ohms, plotted against distance from the centre line of the pile (increasing d/l ratio) for different pile-current electrode spacings (increasing h/l ratio). Hereafter, this will be referred to as the E-R curve.

7.4.5.1 The E-R Curve for a Pile

Figures 7.17 to 7.23 show the effect of changing the reflection coefficient associated with the pile. Also given on these figures is the E-R curve for the reinforcement on its own, which immediately shows the effect of encasing the reinforcement with a concrete sheath.

As anticipated from the theory in Chapter 3 and the previous analogue, when the reflection coefficient is negative (i.e. the electrical resistivity of the concrete is higher than that of the surrounding medium) then effect is to increase the resistance associated with the reinforcement on its own, and will result in an upward displacement of the E-R curve for the pile. When the reflection coefficient is positive then the E-R curve for the pile is displaced downwards, which is as per theory. It is apparent that the greater the reflection coefficient - either positive or negative - then the greater the displacement of the E-R curve for the pile from that of the reinforcement.

Increasing the background resistivity for both the model pile and reinforcement control will result in an increase in their resistance. This is in agreement with the theory as the reflection coefficient, k, is increased for the pile and the background resistivity increased for the reinforcement. In addition, when the resistivity of the background medium is increased, there is a noticeable change in the shape of the E-R curve. When the reflection coefficient is negative (apparent resistivity of background medium low) then the rate of change of resistance with increasing distance from the pile is small which results in a flat E-R curve. As the reflection coefficient is increased from a negative value to a positive one, then the rate of change of resistance increases and results in a steepening of the E-R curve. This implies that indications as to the nature of the soil around the pile may be inferred from the gradient of the initial portion of the E-R curve, viz. when a low resistivity material is present around a pile the rate of change of resistance with increasing distance from the pile is lower than when a high resistivity material is present.

It is interesting to compare the theoretical earthing resistance (R_∞ on Figs.) for the pile with the experimental resistance (R on Figs.) obtained at the mid-point of the respective E-R curve. The theoretical resistance given by equation (3.35) compares favourably with the experimental values showing that the assumptions made in Chapter 3 were justified.

Also shown in Figures 7.17 - 7.23 is the influence of the h/l ratio on the shape of the E-R curve for a pile. As the h/l ratio is increased

the rate of change of resistance decreases with increasing d/l, and results in the development of a plateau region in the central portion of the curve. As the h/l ratio increases the plateau region becomes more distinctive and is approaching the condition when the return current electrode is removed to infinity.

The resistance obtained at the mid-point of the E-R curve is approximately the same no matter what the h/l ratio. This confirms the postulate that the resistance at infinity (based on the resistivity of the material surrounding the pile) is obtained at the point where d/l = h/2l (i.e. d= h/2).

A theoretical E-R curve for the reinforcement calculated using equation (3.44) is also plotted (dashed curve). For clarity this was only calculated for an h/l ratio of 2.0.

7.4.5.2 The Effect of Partial Reinforcement

The Teledeltos analogue (Section 7.3) indicated that to a large extent the reinforced section of the pile governs the response. In order to investigate this more fully a model pile (400mm in length) was constructed in which the top 25% was reinforced. Lengths were then cut from this pile and the E-R curve plotted for each length. A low resistivity background medium was chosen as this would produce a large reflection coefficient which would then tend to magnify the differences in the E-R curves for the different lengths - if any existed.

Such curves are plotted in Figure 7.24. Decreasing the length of the pile results in a downward displacement of the E-R curve as expected. The maximum displacementoccurring when the length of the pile was equal to that of the reinforced section. The maximum difference in resistance readings was less than 6%. Resistances close to the pile head are virtually unaffected by the change in length. This was taken to confirm the previous finding, namely, that the reinforced section in the main governs the E-R response.

7.4.5.3 Influence of Neighbouring Piles

On site, piles are very rarely isolated and more often than not are laid out in a grid arrangement. For this reason, the influence of neighbouring piles on the earthing resistance of the pile under test was investigated using the electrolytic tank analogue. To simulate such a condition model piles were suspended from the wooden gantry which, supported the model pile under test. The neighbouring piles were then moved with respect to the test pile and the E-R curves plotted for differing positions of neighbouring piles.

Figure 7.25 shows the E-R curves for the non-defective model pile with the neighbouring piles at varying distances from this pile, these distances being multiples of the pile diameter.

From a theoretical point of view, bringing a medium of high resistivity (i.e. higher than the medium surrounding the pile) near to the pile under test would increase the apparent resistivity associated with the reflection coefficient thereby increasing the earthing-resistance of

the pile and vice versa. The experimental results would tend to indicate that only when the neighbouring piles are within 2 pile diameters centre to centre are any noticeable differences observed - the maximum increase being less than 8% when at 1.08 diameters centre to centre.

Applying these findings to the situation on site, it could be assumed that neighbouring piles will have a negligible influence on the pile under test. Furthermore, as every pile tested will be equally affected and only relative magnitudes of results required then the effect of nearby piles can be neglected.

7.4.5.4 Change of Pile Length

Figure 7.26 shows the effect on the E-R curve of changing the length of the pile. In this case the standard model was reduced in length by 33 percent. From Chapter 3, decreasing the length and increasing the p/l ratio will result in an increase in resistance and hence, a resultant upward displacement of the E-R curve. The E-R curve shown in Figure 7.26 is displaced as anticipated.

Initially it may appear that an anomalous result could arise, this being that a short pile in low resistivity soil may give the same E-R curve as a long pile in higher resistivity soil. By considering the findings of section 7.4.5.1 then this possible anomaly can be solved by looking at the overall gradient of the E-R curves.

In Figure 7.26 the resistivity of the soil is the same for both piles

with the rate of change of resistance being the same for both piles. Increasing the background resistivity for the non-defective model will result in a steepening of the E-R curve. Thus, the short pile in low resistivity soil and long pile in high resistivity soil may have the same theoretical earthing-resistance at infinity but the shape of the characteristic E-R curve would indicate which condition obtained.

7.4.5.5 Changing the p/l ratio

Figures 7.27 and 7.28 show the effect of increasing the diameter of the pile (a/l remaining constant) for a positive and negative reflection coefficient. When the reflection coefficient is negative (-0.50) then when the diameter of the pile is increased the earthing-resistance will increase and vice versa for a positive reflection coefficient (+0.46). This will result in a respective upward or downward displacement of the E-R curve from a reference pile.

Theoretical values (R_∞ on Figs.) calculated using equation (3.35) are given, the a/l ratio being 0.005.

7.4.5.6 Changing the a/l ratio

Figure 7.29 shows the effect on the E-R curve of changing the a/l ratio (p/l remaining constant). Decreasing this ratio will result in an increase in the resistance and an upward displacement of the E-R curve from a reference pile. Theoretical values (R_∞ on Fig.) calculated using equation (3.35) are given. The change in resistance due to a change in the a/l ratio is independent of soil resistivity.

7.4.5.7 Effect of Pile Defect on the E-R Curve

E-R curves plotted for the models with simulated defects are shown in Figures 7.30 - 7.37. As discussed in Chapter 3, the effect of a defect is to alter the current density on the reinforcement. The current density will vary as the inverse of the resistivity of the medium in contact with the reinforcement. The total current on the reinforcement, and hence the resistance measured, will be determined by,

(a) the ratio of the resistivity of the concrete to that of the material in the defective section, and,

(b) the extent of the defect.

The greater the ratio in (a) above, the more pronounced the effect on the overall resistance. The model defective piles were tested over a range of such ratios. The simplest way of simulating this was to have the background medium, i.e. the electrolyte, in contact with the reinforcement. On these Figures are E-R curves for,

(a) the case when there is a defective section at the top of the pile (T), and

(b) the bottom of the pile (B), and

(c) the E-R curve for the non-defective pile (G) which is given as a reference datum.

Also shown on Figures 7.30 to 7.36 are E-R curves for a defective pile where the fault does not extend across the whole cross-section (c). The effect of fault position in relation to the auxiliary electrodes was also examined by rotating the electrode array around this pile. It was found, however, that resistance readings were virtually unaffected by fault position in relation to these electrodes.

These Figures clearly indicate that a defective pile will have its E-R curve displaced from that of a non-defective pile; the magnitude of this displacement being dependent upon the resistivity of the material in the defective section and the extent of the defective section. As the ratio ρ_1/ρ_3 (section 3.3.6) approaches unity then the displacement decreases as shown by the experimental data, hence the defect becomes undetectable.

In qualitative terms, the change in the E-R characteristics results in a combination of the local change in $\underset{\sim}{J}$ around the defect and of the change in resistivity, ρ, of the medium surrounding the reinforcement. Both ρ and $\underset{\sim}{J}$ are related to the electric field pattern of the pile-soil system by Ohm's Law,

$$\underset{\sim}{E} = \rho \underset{\sim}{J} \qquad \ldots\ldots (7.6)$$

so a change in the position of equipotentials at the surface of the ground would be expected. Since it is the position of such equipotentials which is the measured variable in the present work, the E-R plot can thus be used for fault detection.

It is apparent that in order to detect defective piles there has to exist a large/small resistivity contrast ratio between defective and

non-defective material. Furthermore, as the size of the defect decreases then the possibility of detection decreases (E-R curve C on Figures).

Figure 7.37 shows the effect of defective concrete, i.e. low resistivity being present over the complete length of the pile (the background resistivity remaining the same). In this case the ratio of the resistivity of non-defective concrete to the resistivity of defective concrete is 2:1. The low resistivity concrete pile has its E-R curve displaced downwards as expected.

The electrolytic tank analogue has shown that faults in the pile shaft have a greater influence on resistance readings close to the pile head than those distant.

7.4.5.8 Validity of Model Experiments

The analysis in Chapter 3 showed that the resistance R, at any point on the E-R curve could be expressed in the form,

$$R = \frac{C\rho_1}{l} \cdot f\left(k, \frac{p}{l}, \frac{l}{a}, \frac{d}{l}, \frac{h}{l}\right) \qquad \ldots\ldots (7.7)$$

Where ρ_1 is the resistivity of the concrete and l, the length of the pile. If the subscripts m and p refer to the model and prototype respectively, then,

$$R_m = \frac{C\rho_m}{l_m} \cdot f\left(k_m, \frac{l_m}{a_m}, \frac{p_m}{l_m}, \frac{d_m}{l_m}, \frac{h_m}{l_m}\right) \qquad \ldots\ldots (7.8)$$

$$R_p = \frac{C\rho_p}{l_p} \cdot f\left(k_p, \frac{l_p}{a_p}, \frac{p_p}{l_p}, \frac{d_p}{l_p}, \frac{h_p}{l_p}\right)$$

If the ratios in the brackets are kept the same for both model and prototype, then,

$$\frac{R_m}{R_p} = \frac{\rho_m}{l_m} \cdot \frac{l_p}{\rho_p} \qquad \ldots\ldots (7.9)$$

and if the resistivities can be made equal, then,

$$R_p = R_m \cdot \frac{l_m}{l_p} \qquad \ldots\ldots (7.10)$$

In order to investigate this analysis a mortar model (resistivity 24Ω-m) and a concrete model (resistivity 46Ω-m) were tested in the electrolytic tank. A reflection coefficient of +0.46 was used - the resistivity of the background medium for the mortar model being 65Ω-m and that for the concrete model being 125Ω-m. All length ratios were kept the same. If the subscripts m and c refer to the mortar and concrete model respectively then,

$$R_m = \frac{\rho_m}{2\pi l_m} \cdot f \text{ (Dimensionless terms)}$$

$$R_c = \frac{\rho_c}{2\pi l_c} \cdot f \text{ (Dimensionless terms)} \qquad \ldots\ldots (7.11)$$

From the above equations the E-R curves can be predicted for one model knowing the E-R curve for the other, i.e.

$$R_c = R_m \cdot \frac{\rho_c}{\rho_m} \cdot \frac{l_m}{l_c} \qquad \ldots\ldots (7.12)$$

the ratio lm/lc was unity due to the influence of tank boundaries if larger ratios existed. Hence,

$$R_c = R_m \cdot \frac{\rho_c}{\rho_m} \qquad \ldots\ldots (7.13)$$

Figure 7.38 shows the E-R curves for both models and the predicted curve for the concrete model using equation (7.13).

The predicted and experimental curve for the concrete model are in good agreement with the maximum deviation of the predicted curve from the experimental curve being less than 7%.

7.4.5 Conclusions

Electrical analogues serve as a useful introduction to the Earth-Resistance method of integrity testing. Extensive experimental programmes have been undertaken which support the theory developed in Chapter 3 and show the methodology of fault detection. The following conclusions can be drawn from this study,

(a) the Earth-Resistance curve for a defective pile will be displaced from that of a non-defective pile. The magnitude of this displacement is dependent upon the resistivity contrast between the defective material and non-defective concrete in the pile shaft and the size of the fault.

(b) piles should be tested when a high reflection coefficient exists as this will tend to eliminate effects such as small fluctuations in near surface geology.

(c) resistance readings close to the pile head are of greater significance to fault detection than those distant. This is especially true when the reflection coefficient is positive.

(d) once a particular pile-current electrode spacing has been chosen it must be maintained throughout the testing programme. If

different pile-current electrode spacings are used then the shape of the E-R curve changes and the relative integrities become difficult to assess. The pile-current electrode distance depends on space availability around the pile head, the h/l ratio should be kept less than unity. Large pile-current electrode spacings are to be avoided.

(e) indications as to the nature of the soil around the pile can be obtained from the overall gradient of the E-R curve. When the apparent resistivity of the soil around the pile shaft is high then the resulting E-R curve will be steep. When the apparent resistivity of the material is low then the E-R curve tends to be flat.

(f) neighbouring piles have negligible influence on the E-R curve.

(g) only the reinforced section of the pile contributes significantly to the response.

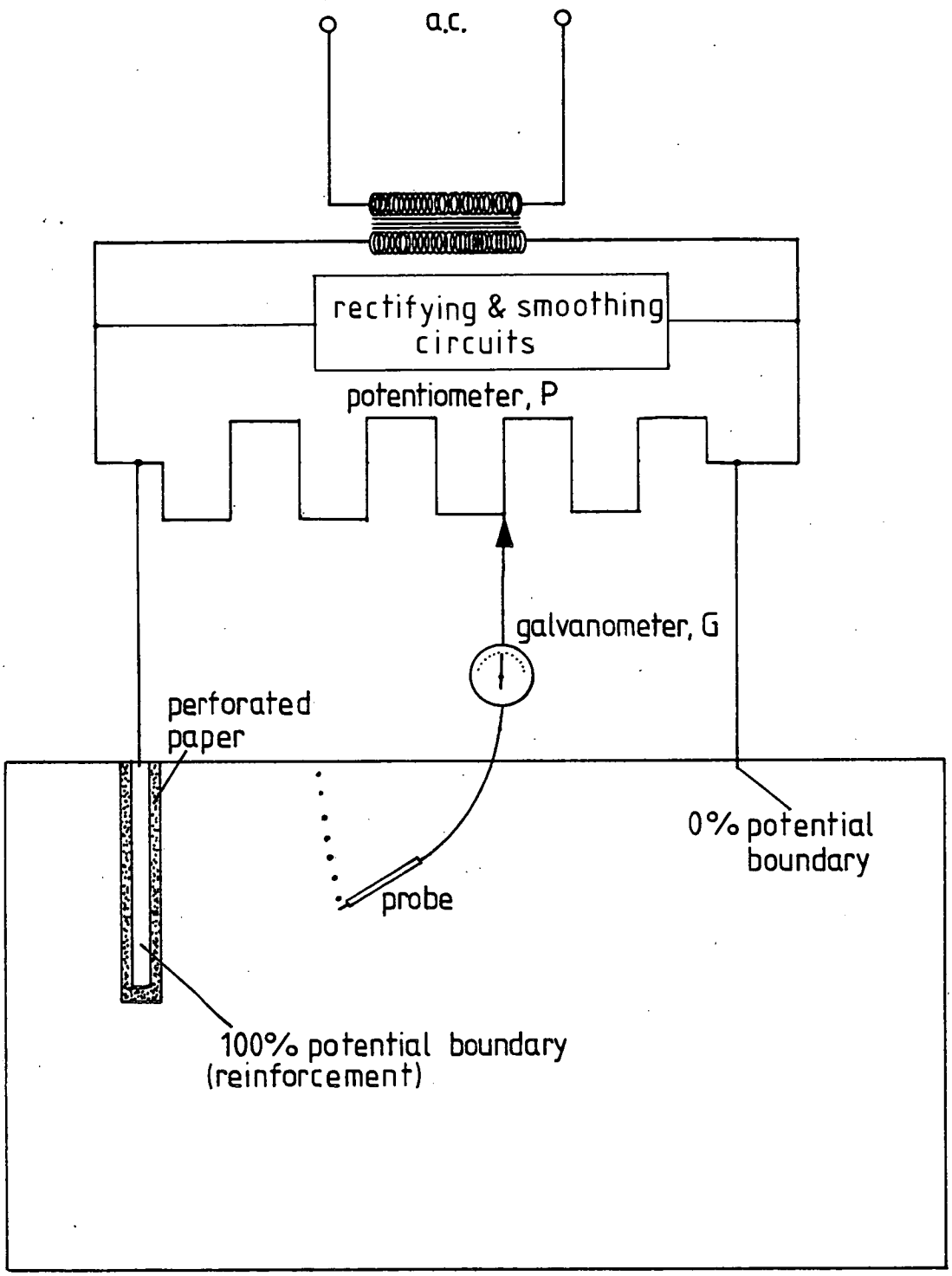

FIG. 7.1 The Teledeltos Analogue

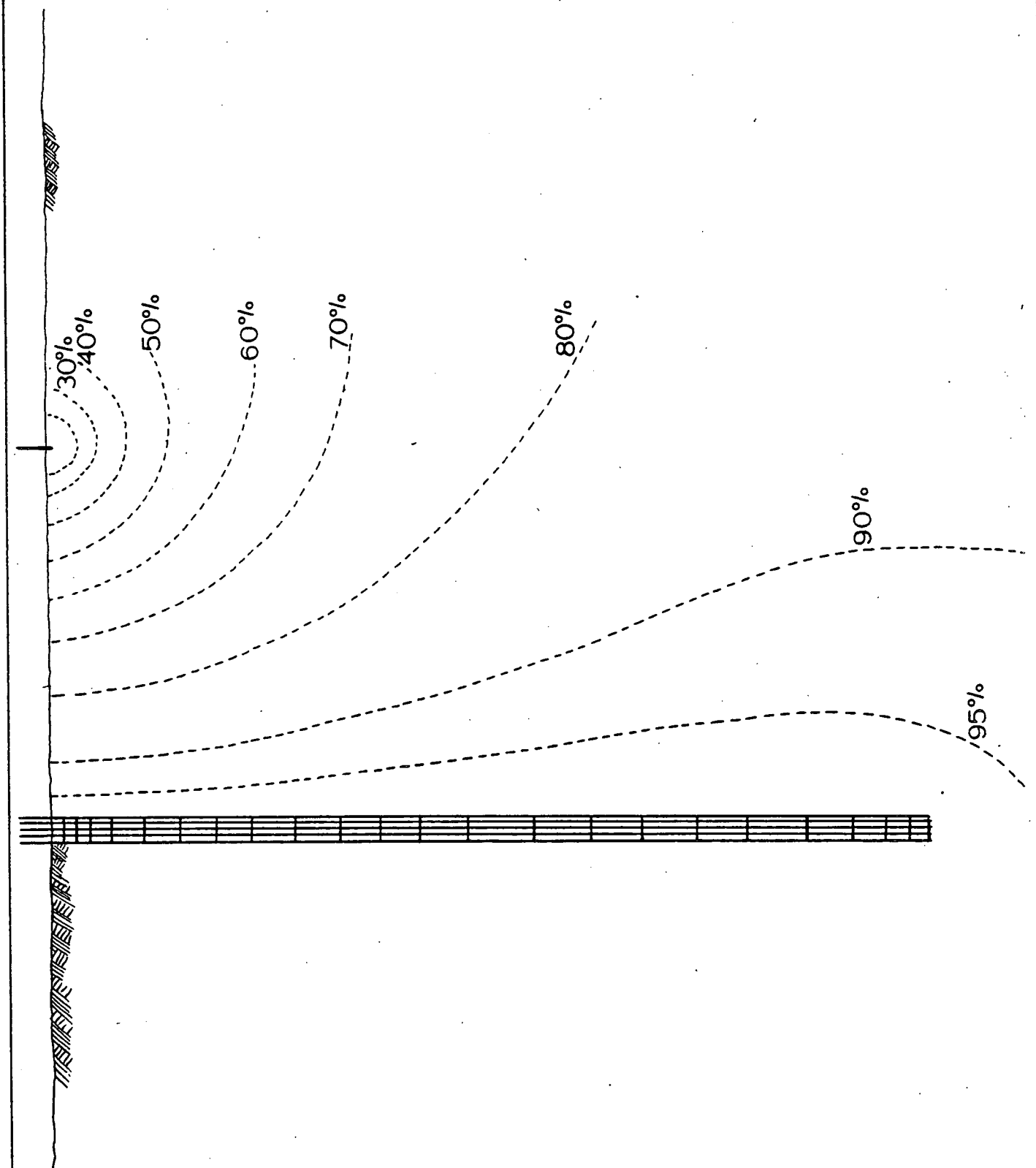

FIG. 7.2

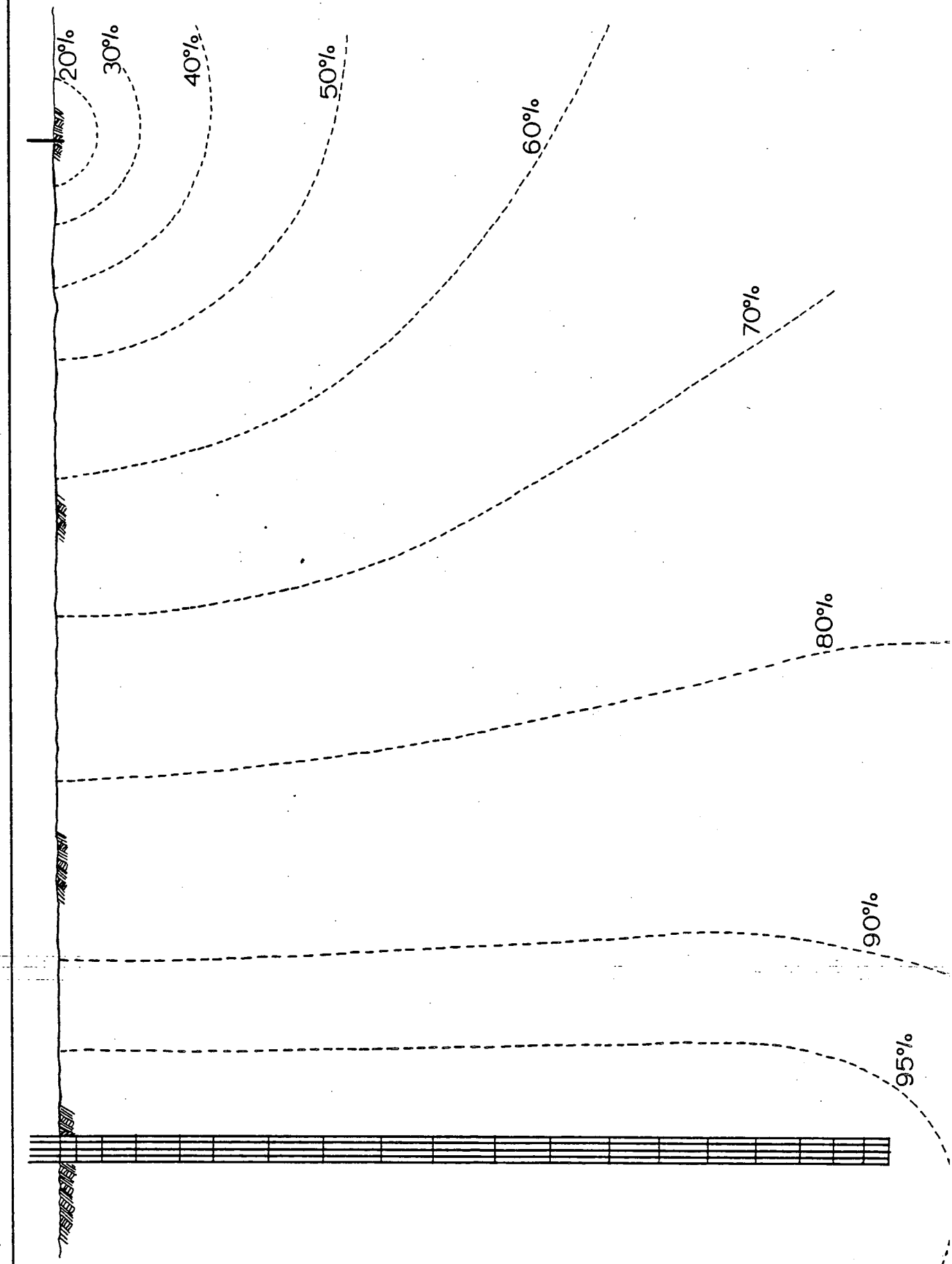

FIG. 7.3

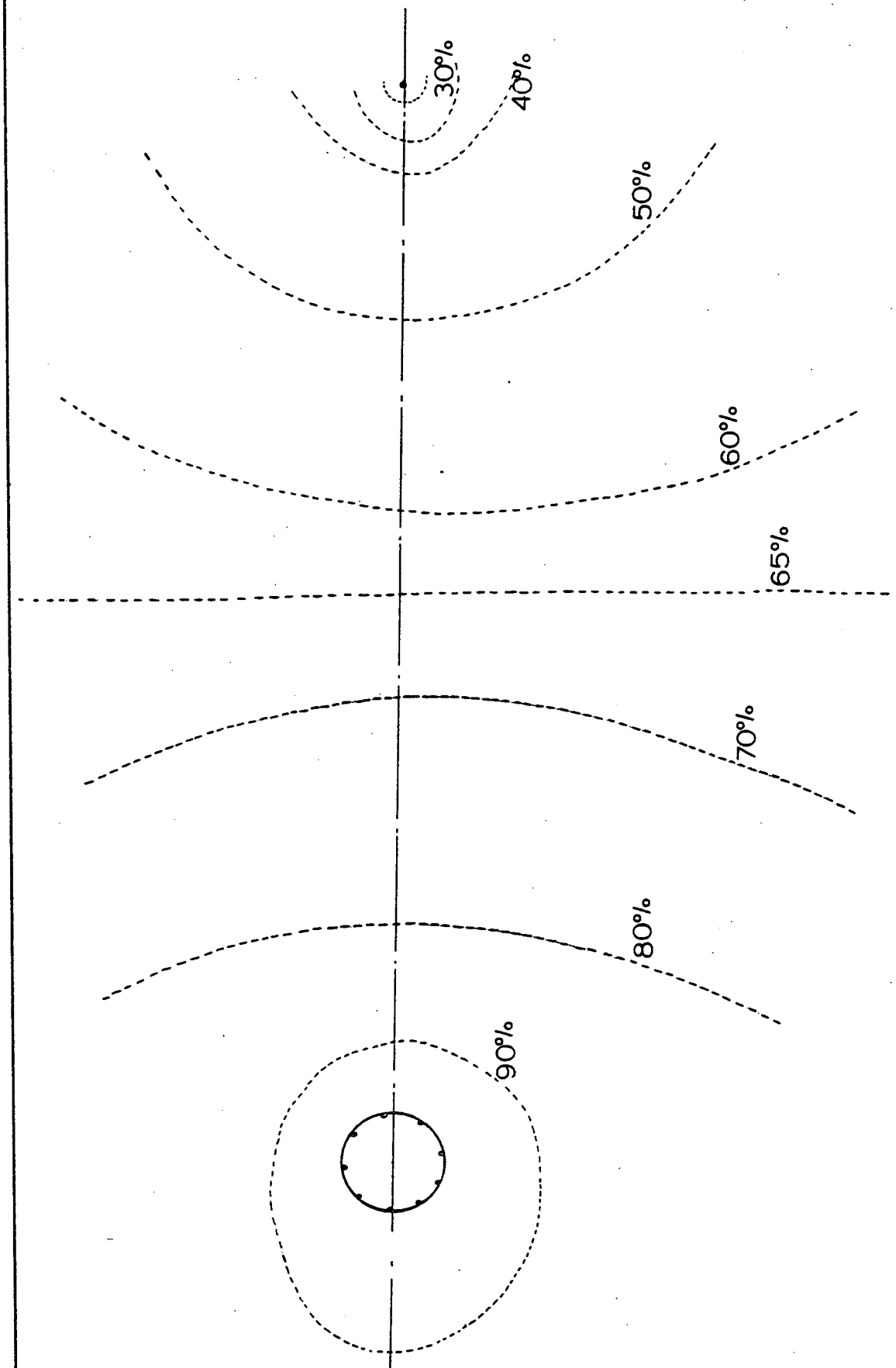

FIG. 7.4

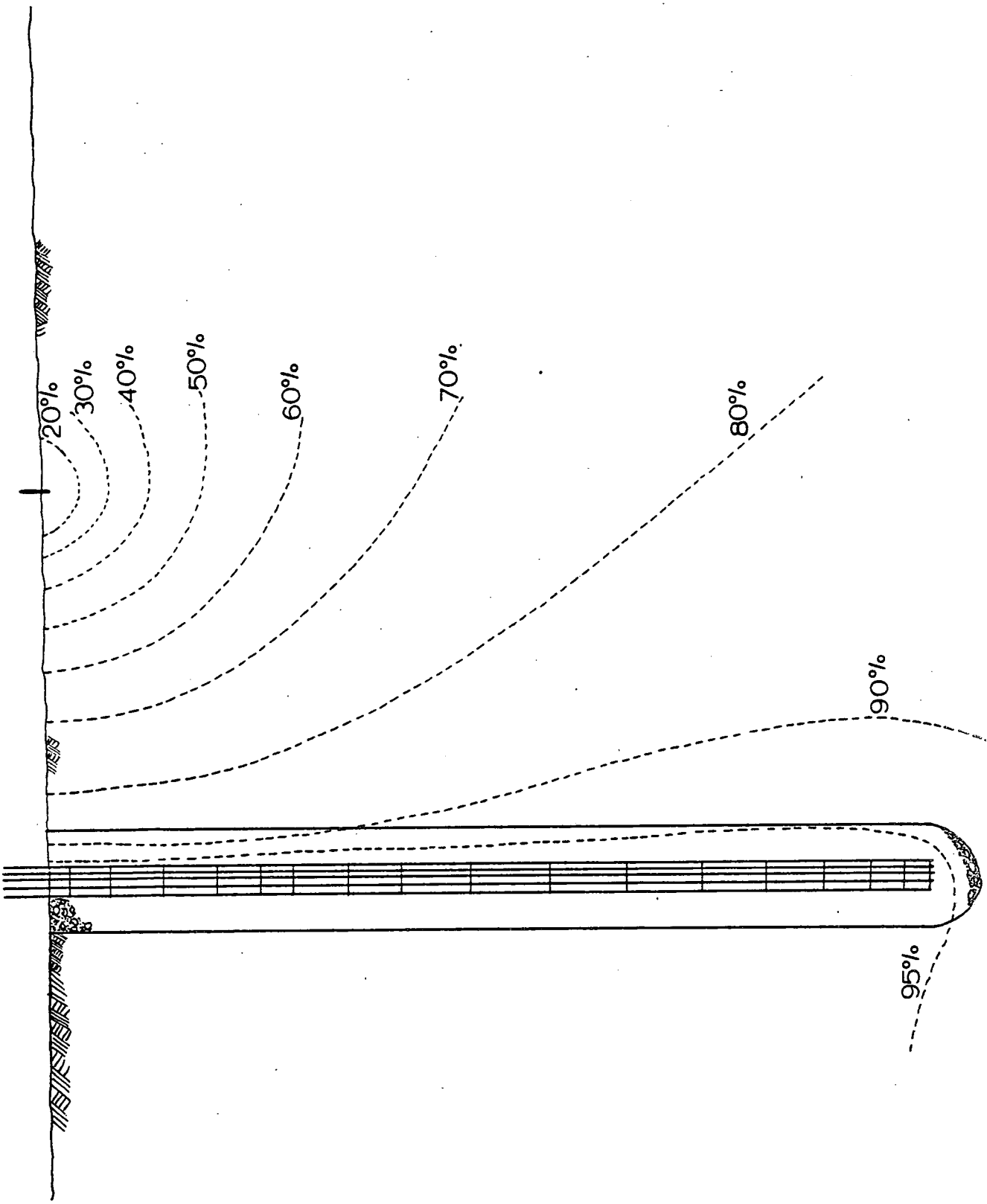

FIG. 7.5

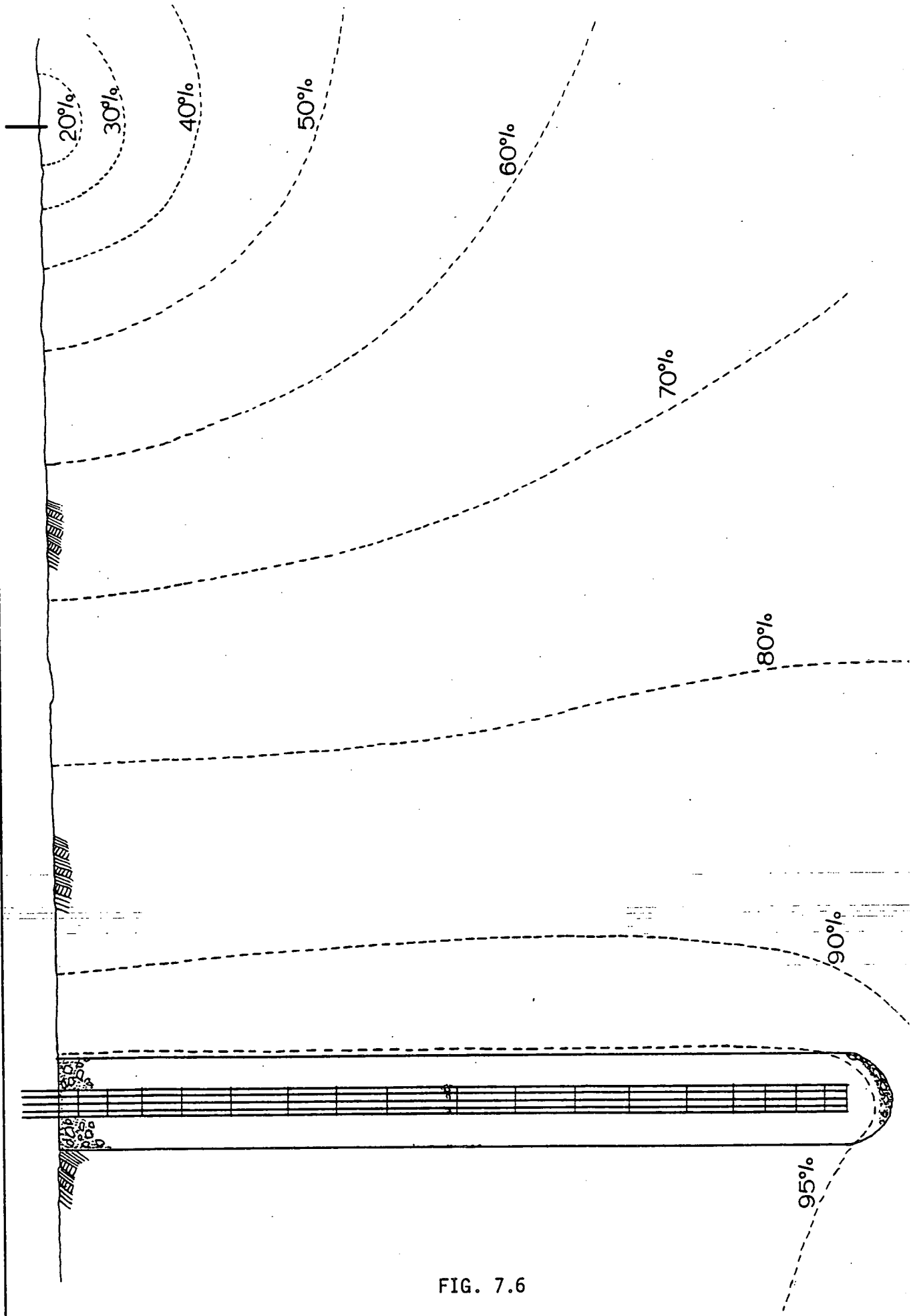

FIG. 7.6

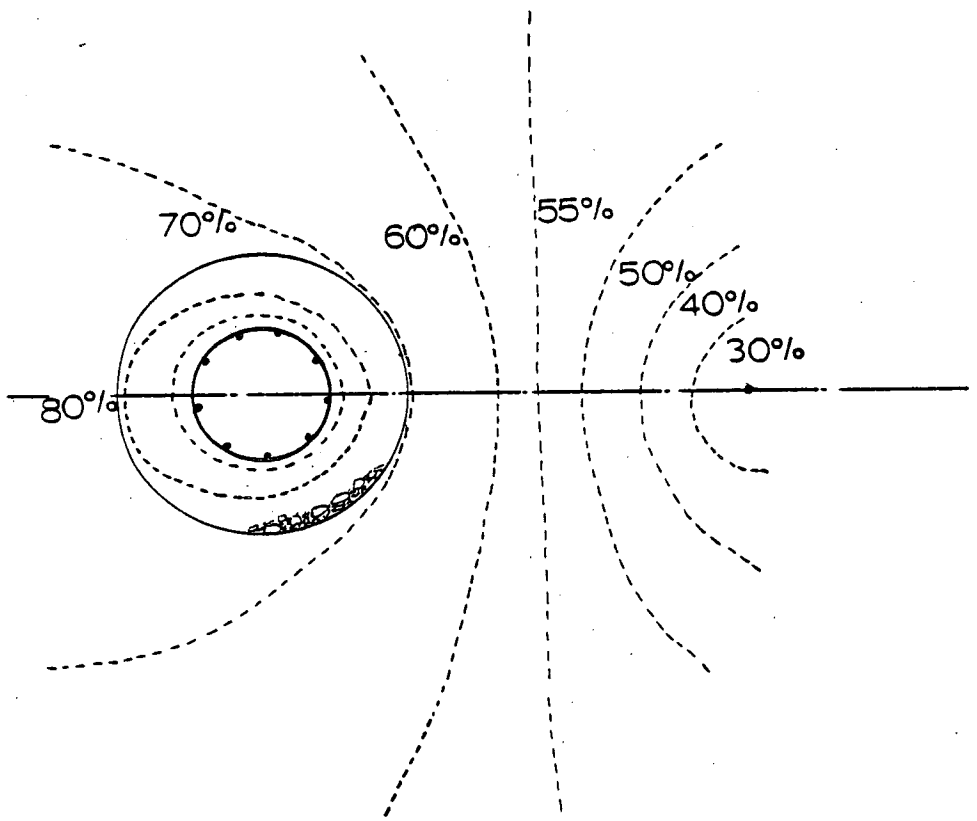

FIG. 7.7

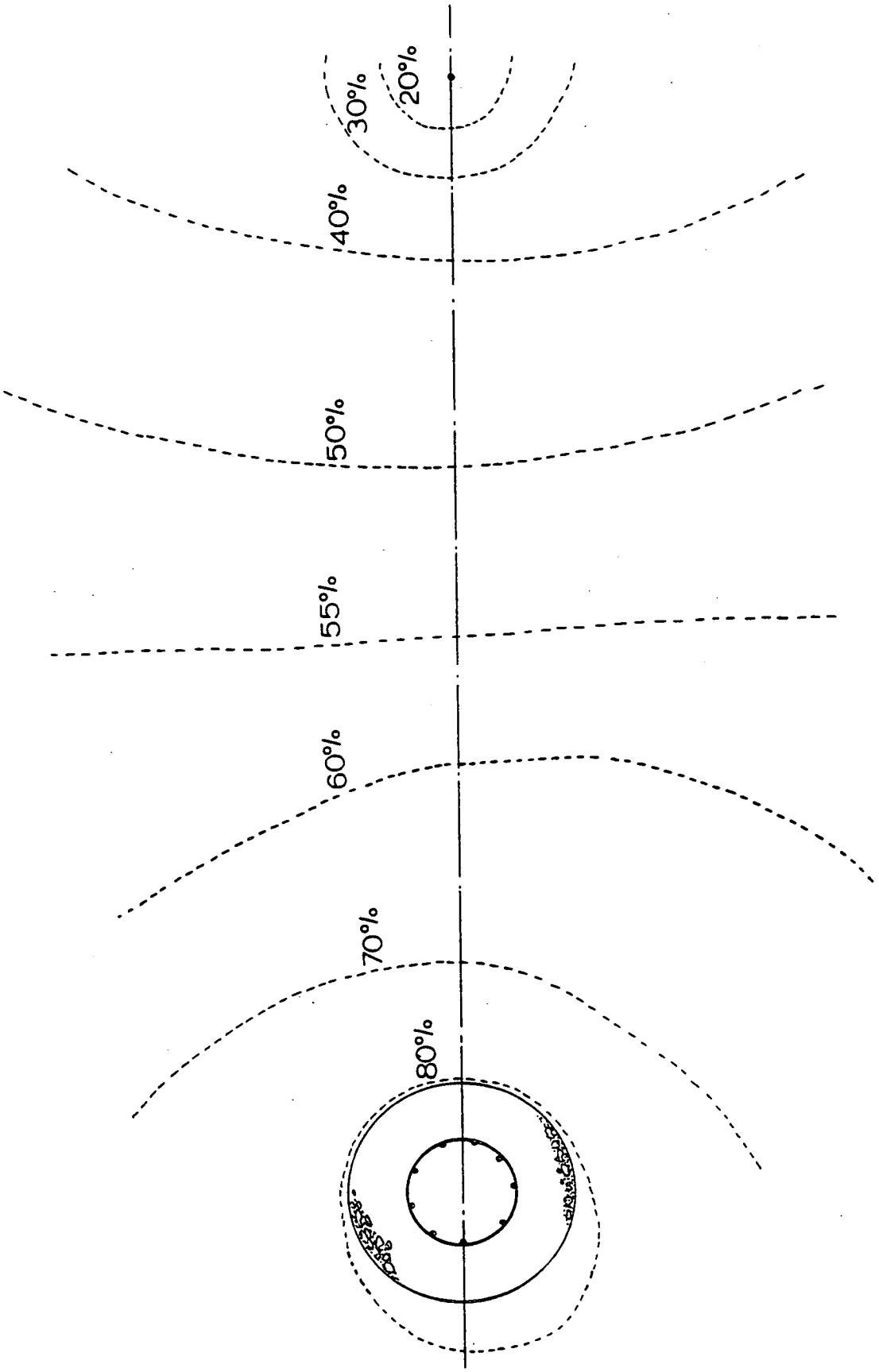

FIG. 7.8

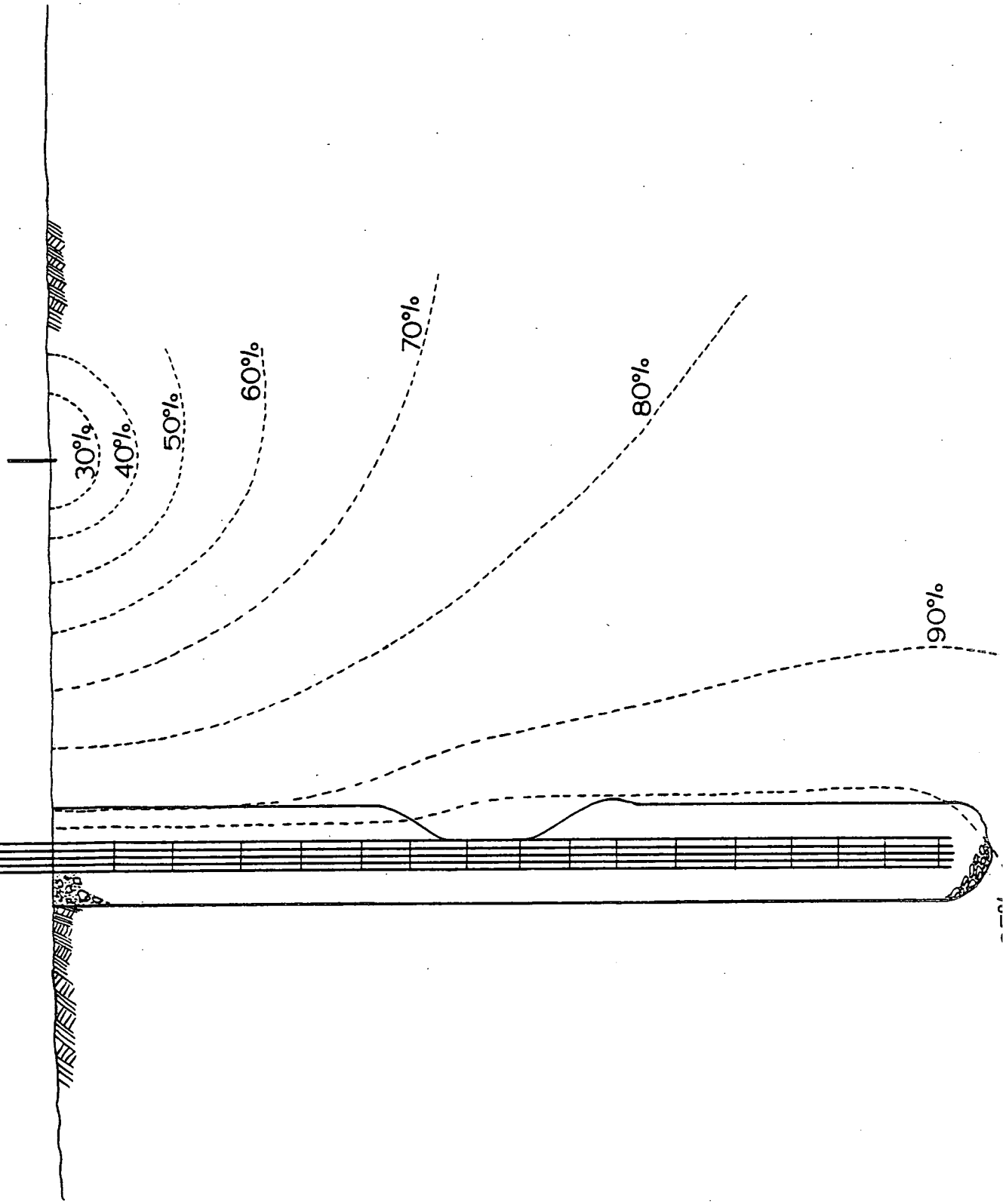

FIG. 7.9

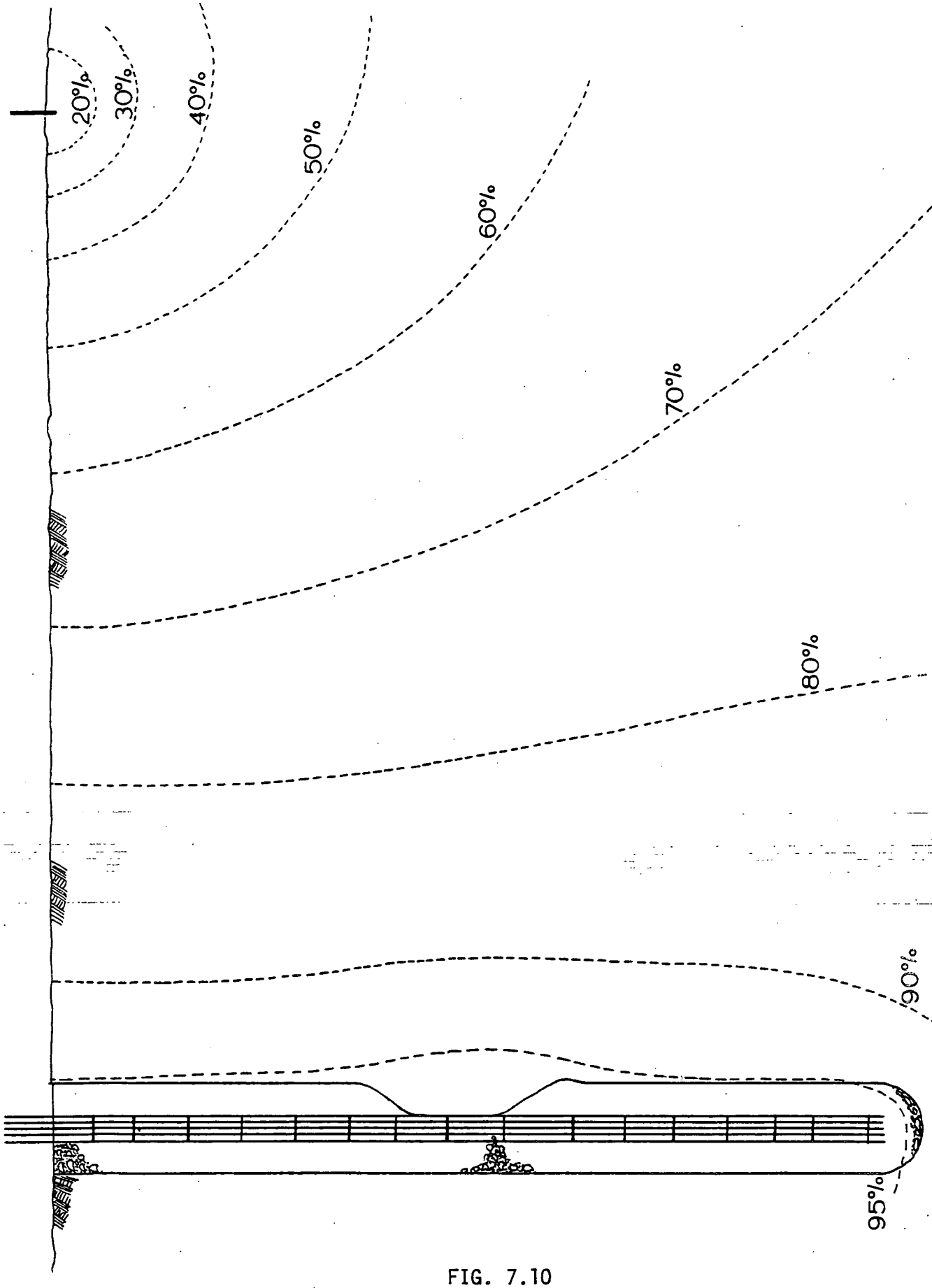

FIG. 7.10

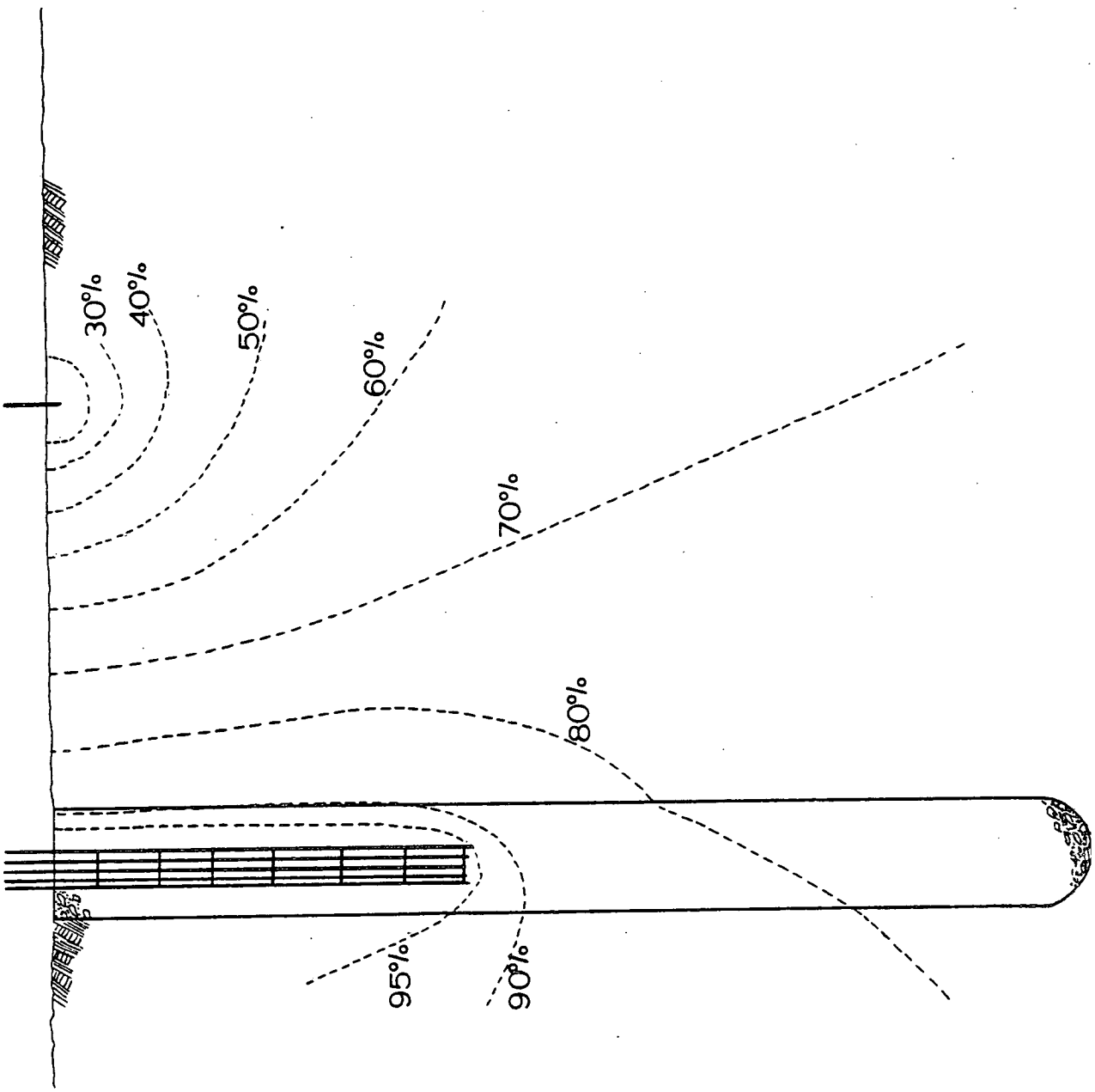

FIG. 7.11

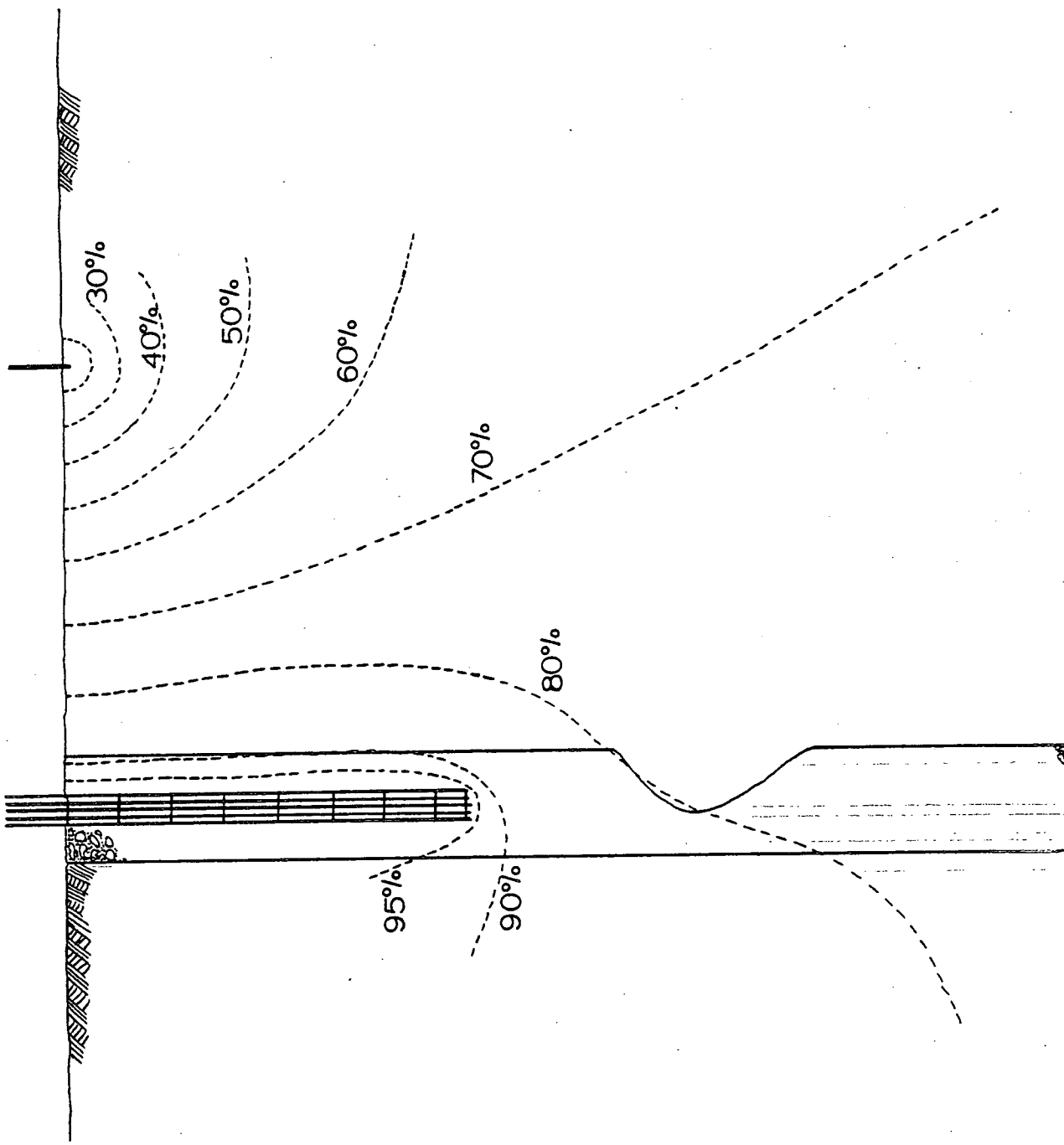

FIG. 7.12

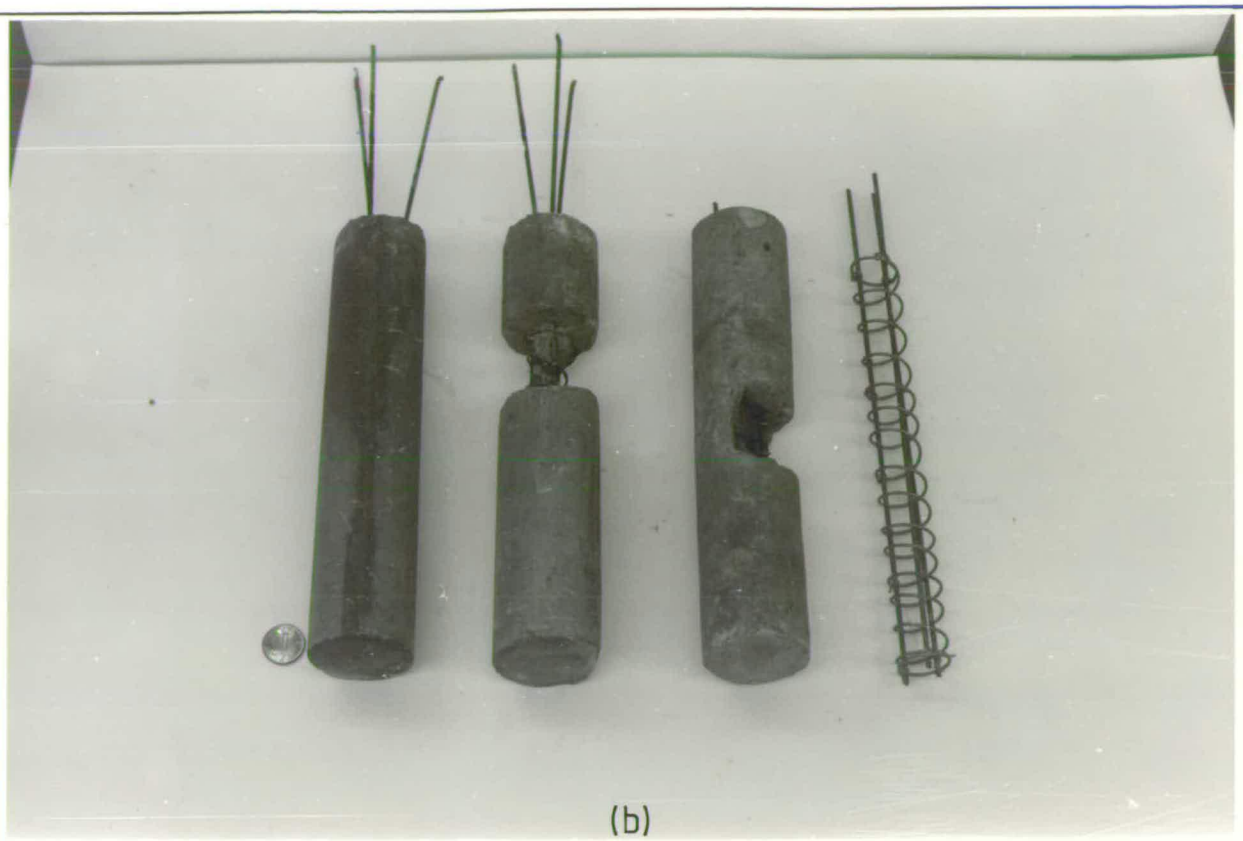

(b)

PLATE 6

(a) The Electrolytic Tank & (b) Typical models

(a)

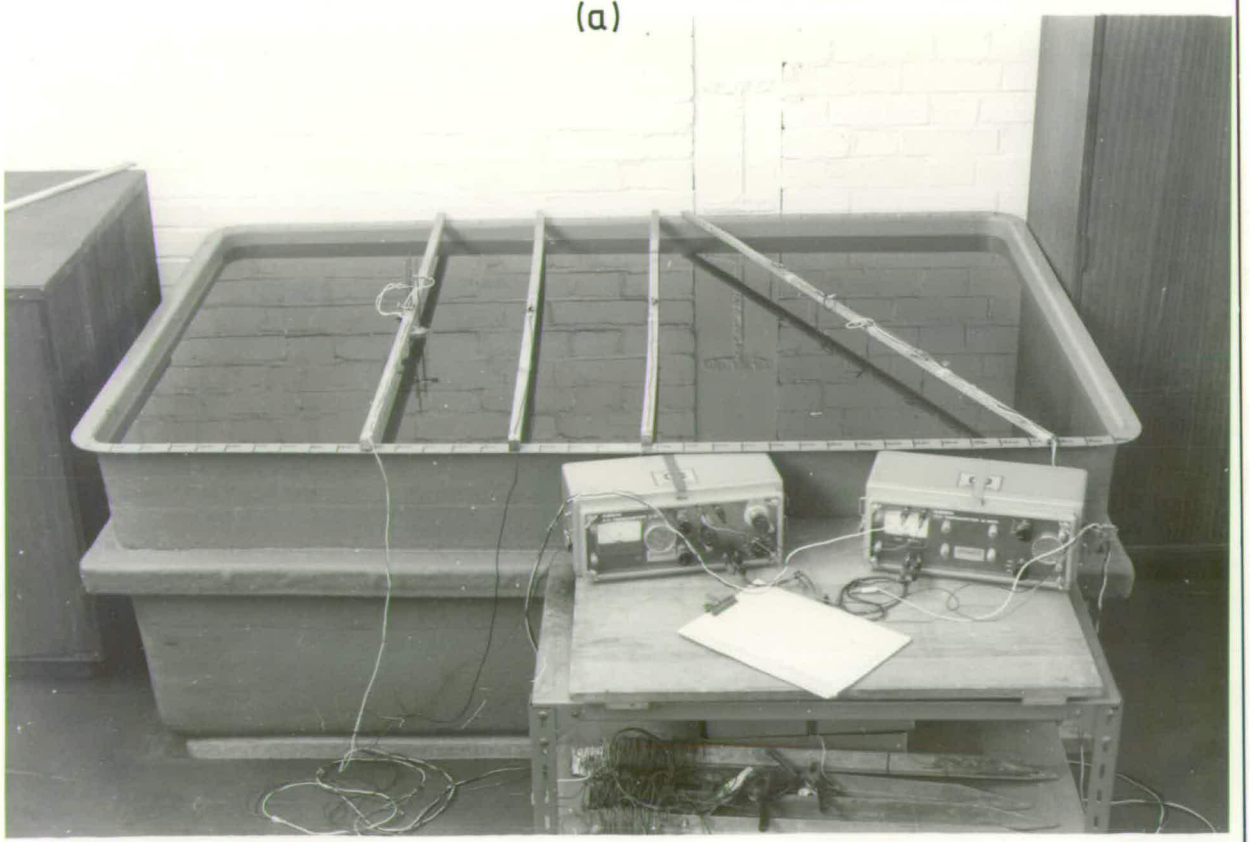

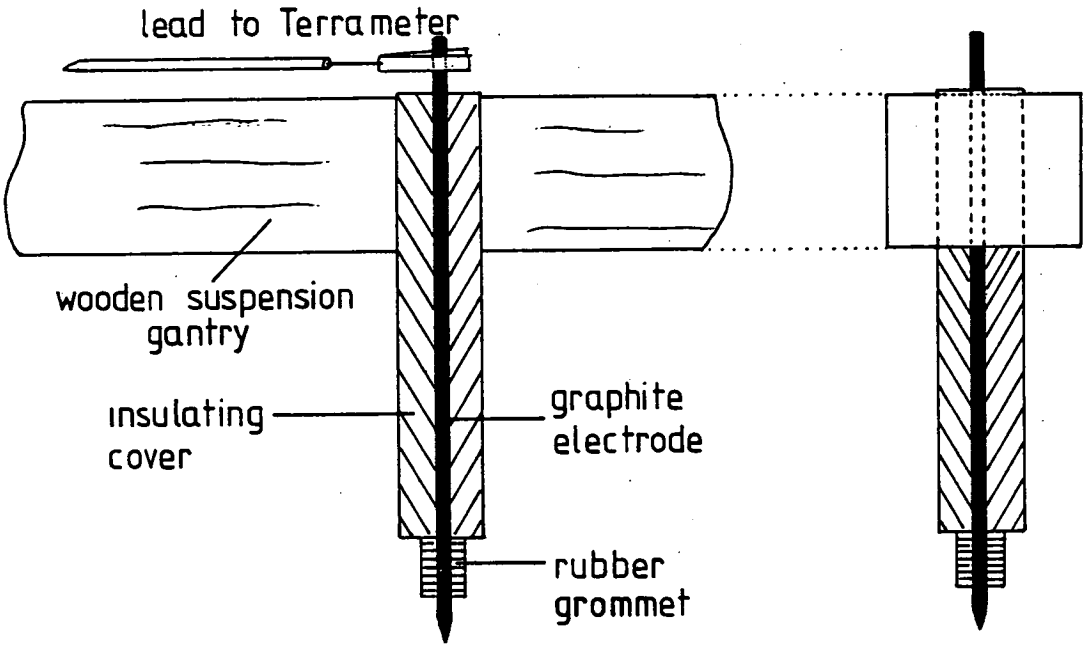

FIG. 7.13 Electrode construction

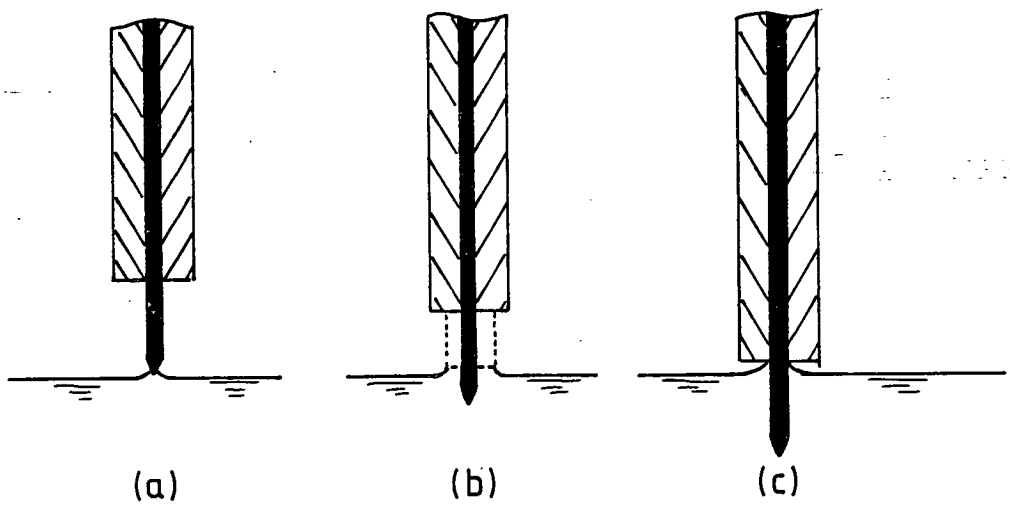

FIG. 7.14 Immersion of electrodes

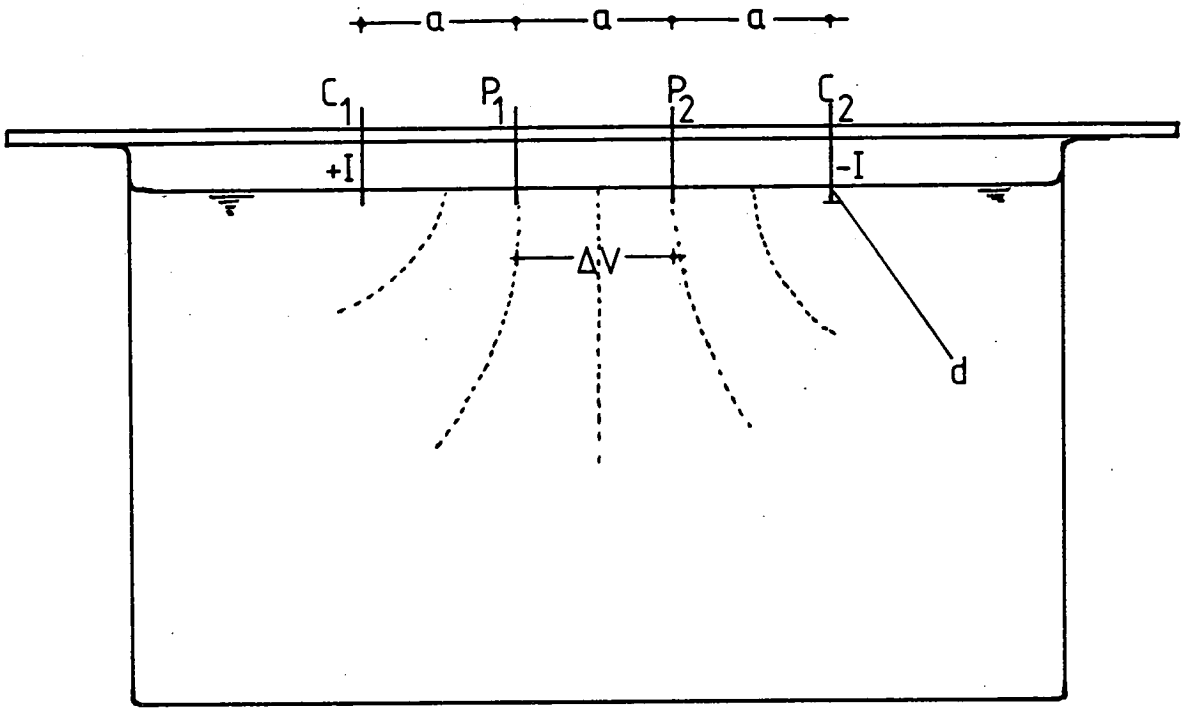

FIG. 7.15 Wenner electrode array for measurement of electrolyte resistivity

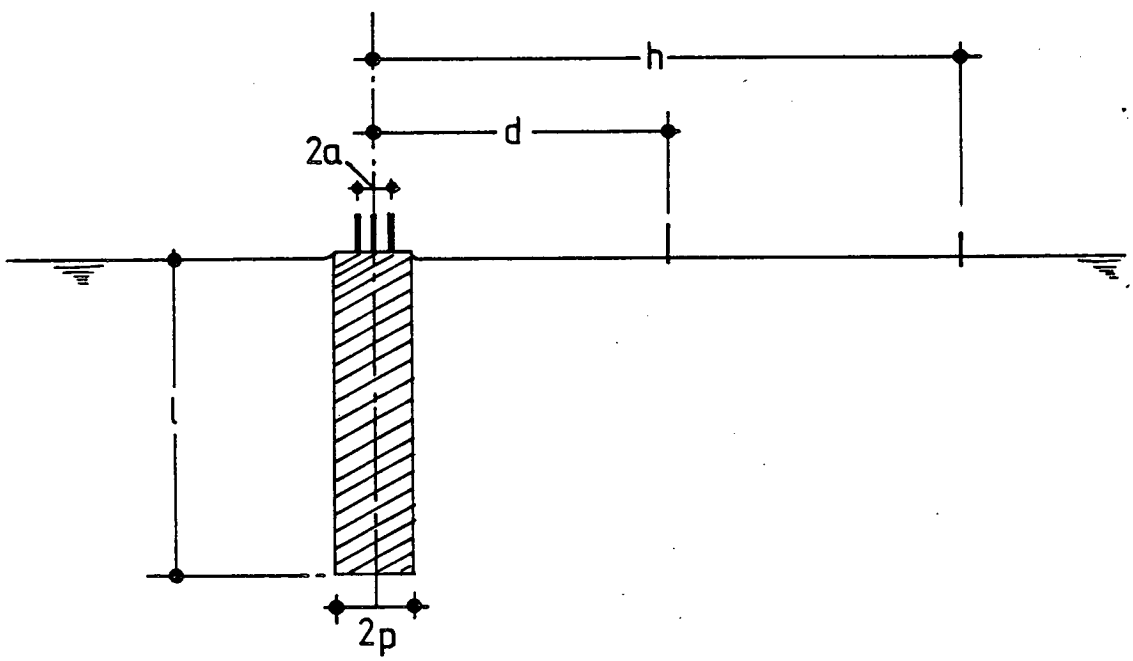

FIG. 7.16 Showing the ratios associated with resistance readings

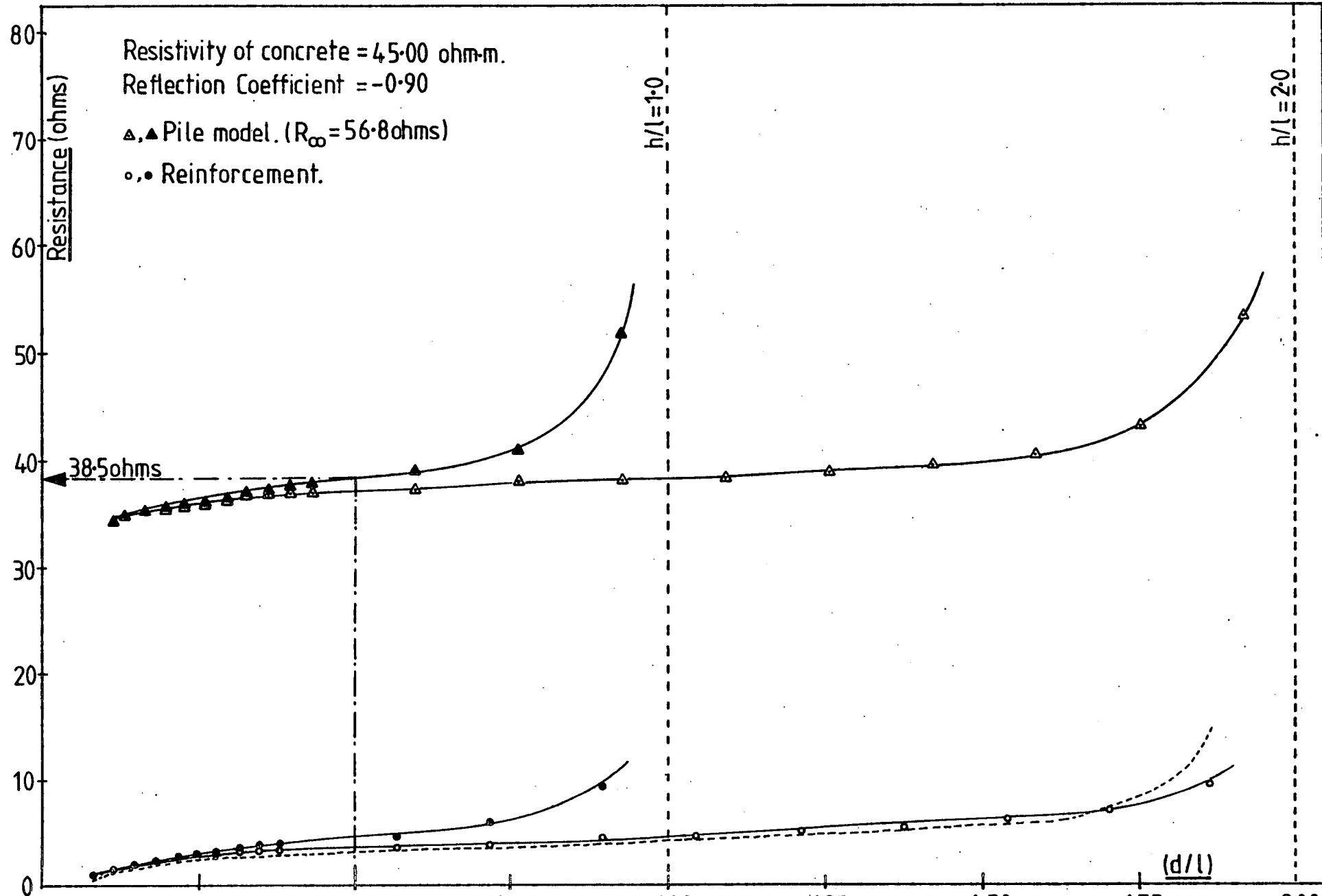
Resistivity of concrete = 45·00 ohm-m.
Reflection Coefficient = -0·90
▲,▲ Pile model. (R_∞ = 56·8ohms)
o,• Reinforcement.
Resistance (ohms)
80
70
60
50
40
30
20
10
0
38·5ohms
h/l=1·0
h/l = 2·0
(d/l)

FIG. 7.17

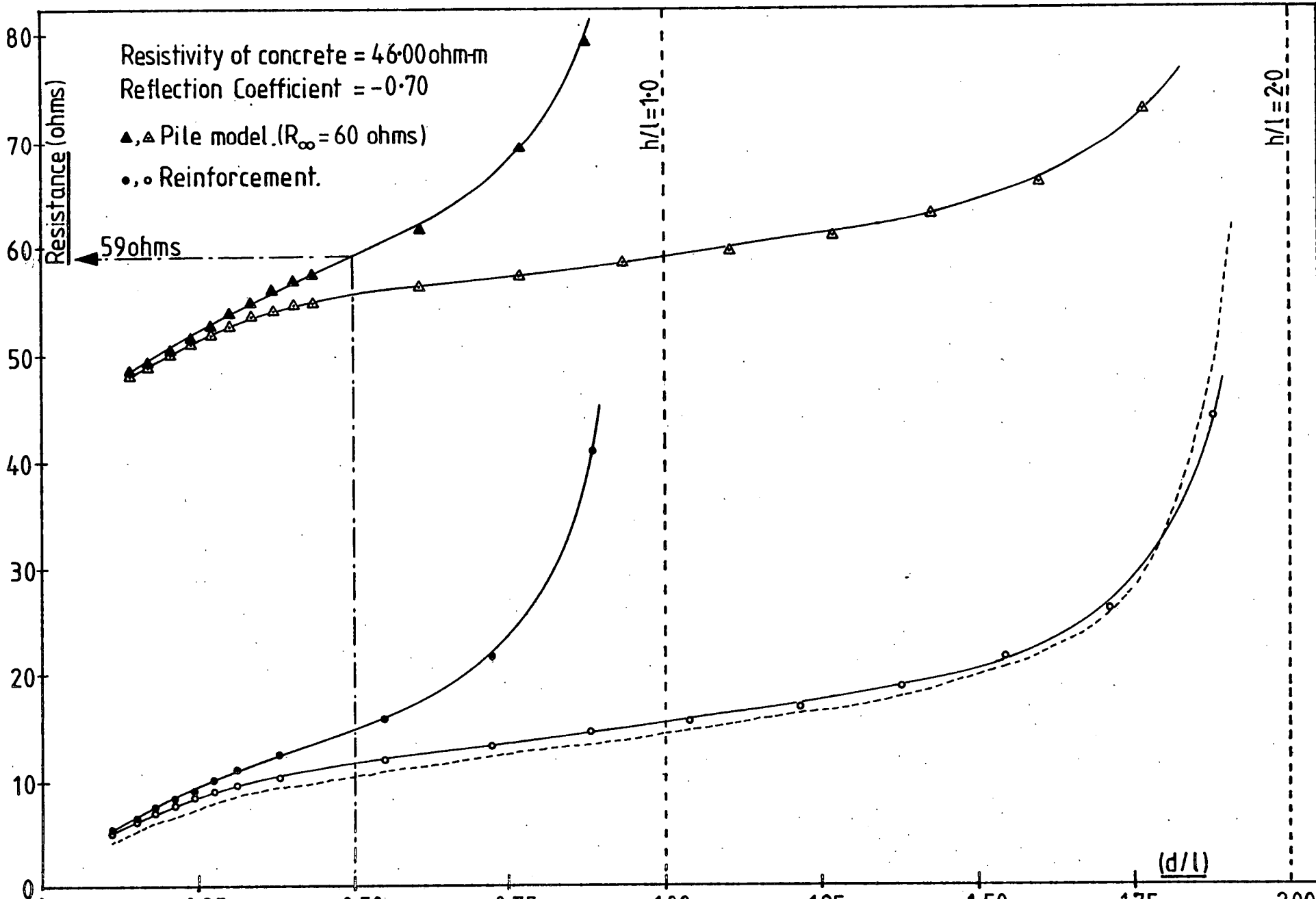
Resistivity of concrete = 46·00 ohm-m
Reflection Coefficient = -0·70
▲,△ Pile model. (R_∞ = 60 ohms)
•,○ Reinforcement.
Resistance (ohms)
59 ohms
h/l = 1·0
h/l = 2·0
(d/l)
0
10
20
30
40
50
60
70
80

FIG. 7.18

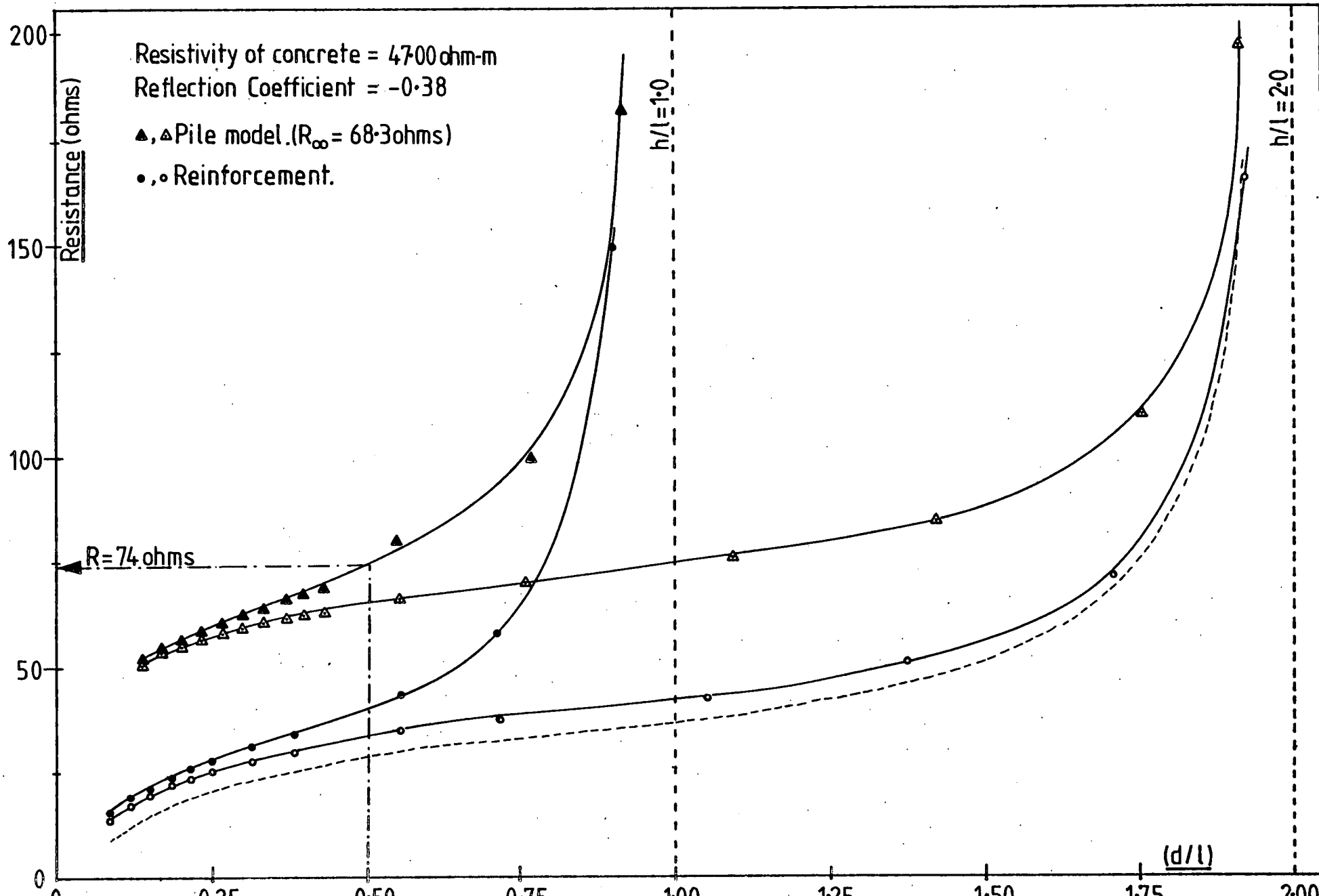
Resistivity of concrete = 4700 ohm-m
Reflection Coefficient = -0·38
▲, △ Pile model. (R_∞ = 68·3 ohms)
•, ○ Reinforcement.
Resistance (ohms)
200
150
100
50
0
R=74 ohms
h/l=1·0
h/l=2·0
(d/l)
0·25
0·50
0·75
1·00
1·25
1·50
1·75
2·00

FIG. 7.19

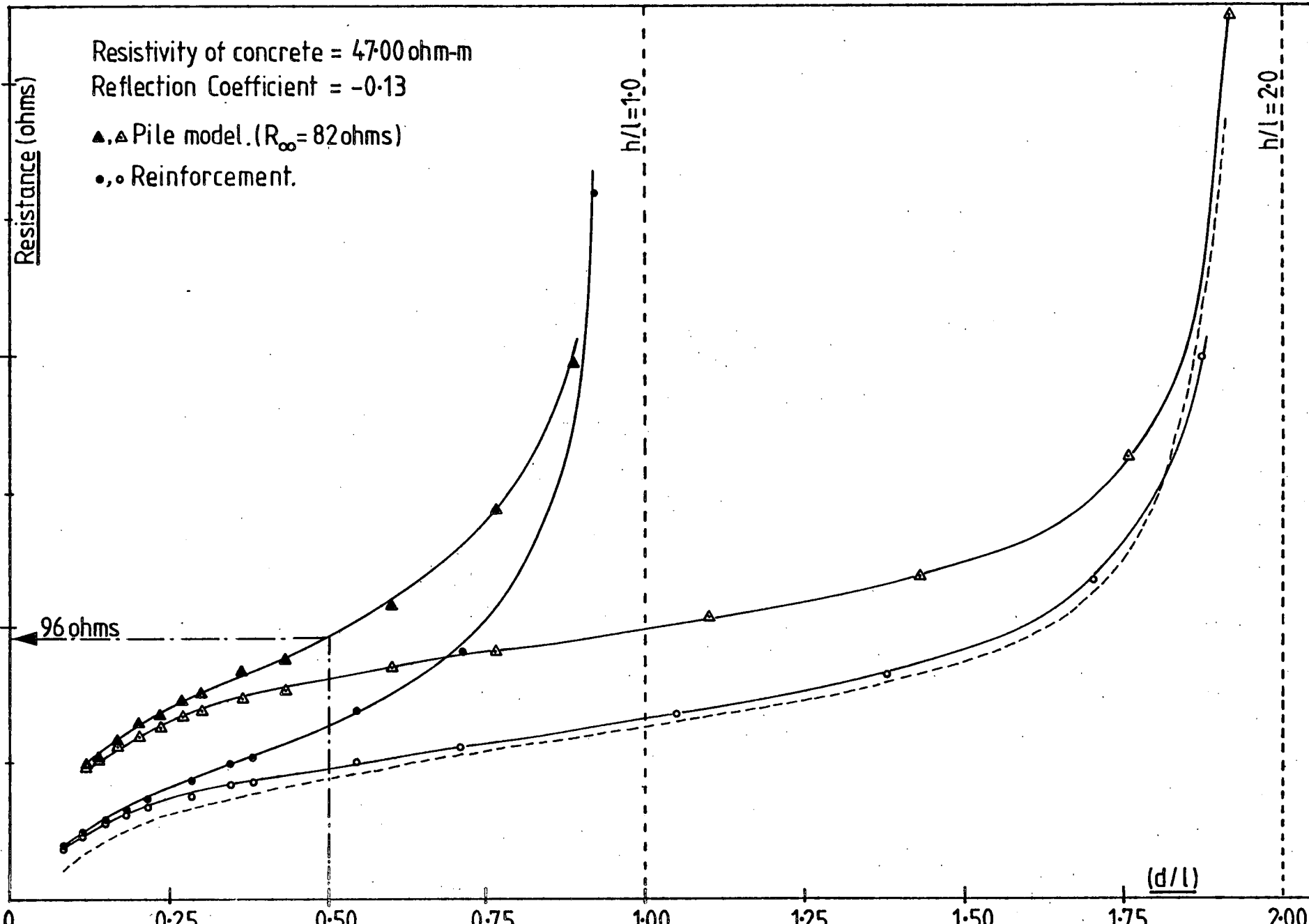
Resistivity of concrete = 47·00 ohm-m
Reflection Coefficient = -0·13
▲,△ Pile model. (R_∞ = 82 ohms)
•,◦ Reinforcement.
Resistance (ohms)
300
200
100
0
96 ohms
h/l=1·0
h/l=2·0
0
0·25
0·50
0·75
1·00
1·25
1·50
1·75
2·00
(d/l)

FIG. 7.20

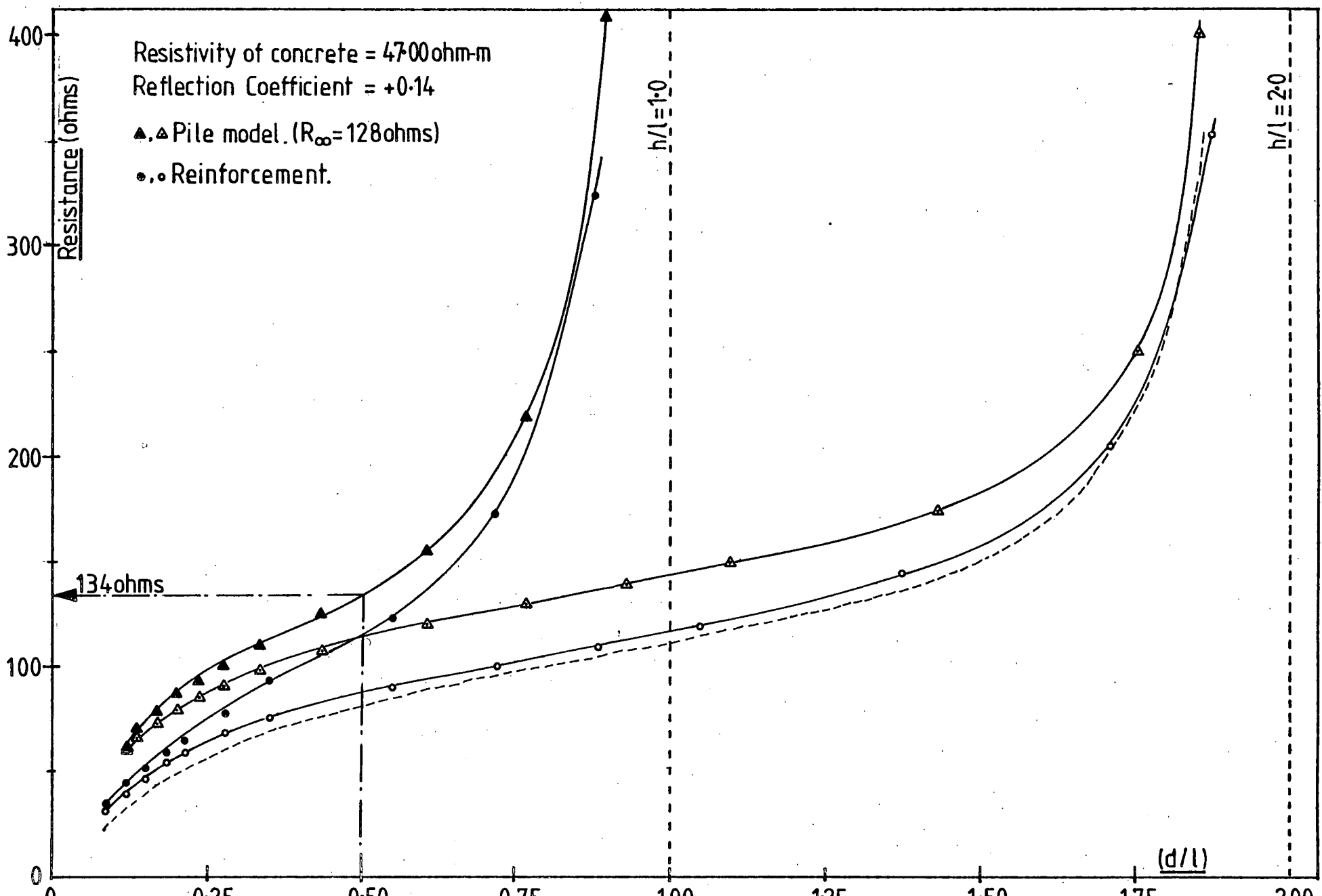
Resistivity of concrete = 4700 ohm-m
Reflection Coefficient = +0·14
▲,△ Pile model. (R_∞ = 128 ohms)
●,○ Reinforcement.
Resistance (ohms)
400
300
200
100
0
134 ohms
h/l = 1·0
h/l = 2·0
(d/l)
0
0·25
0·50
0·75
1·00
1·25
1·50
1·75
2·00

FIG. 7.21

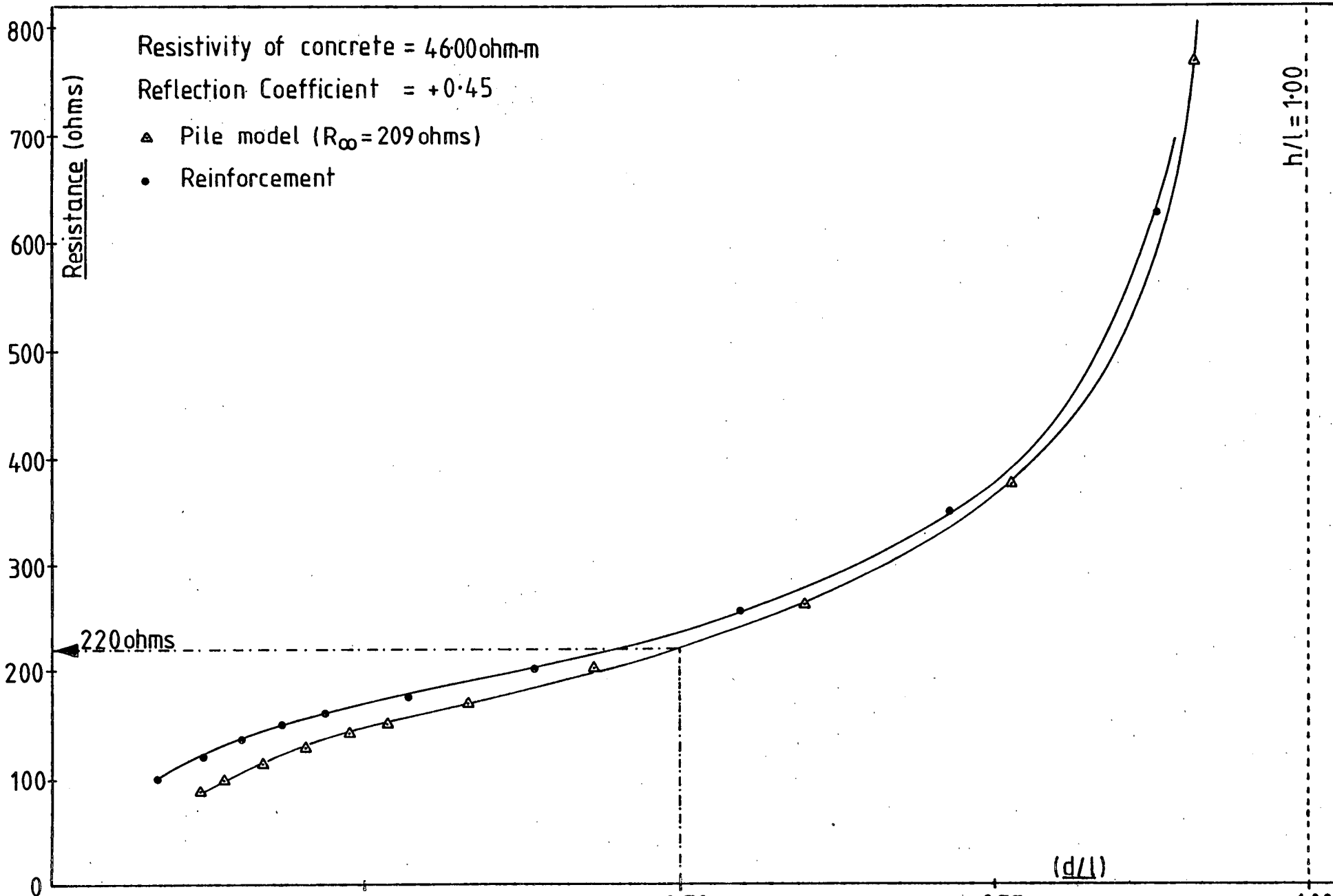
Resistivity of concrete = 4600 ohm-m
Reflection Coefficient = +0·45
Pile model (R_∞ = 209 ohms)
Reinforcement
Resistance (ohms)
800
700
600
500
400
300
220 ohms
200
100
0
h/l = 1·00
(d/l)

FIG. 7.22

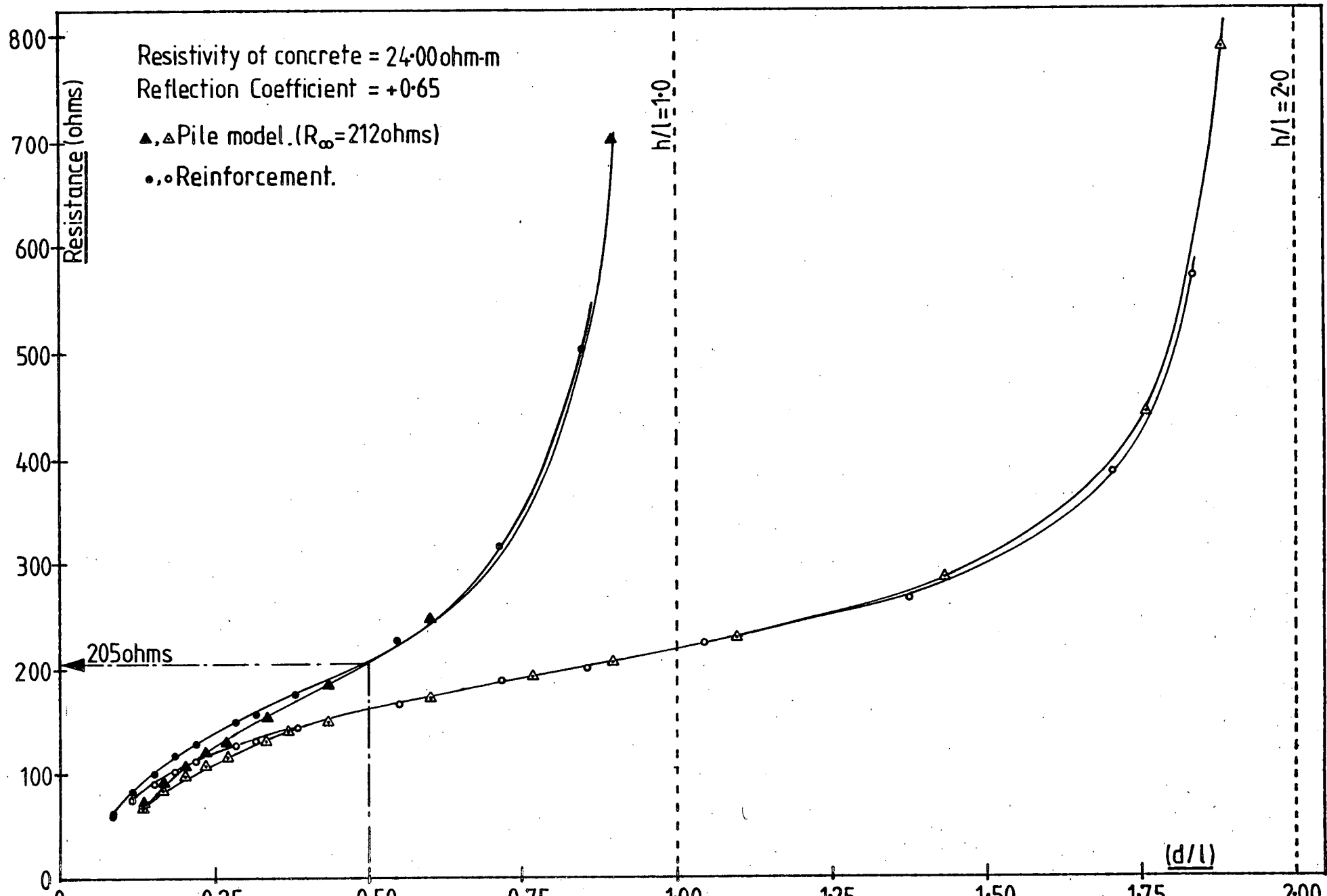
Resistivity of concrete = 24·00 ohm-m
Reflection Coefficient = +0·65
▲,△ Pile model. (R_∞ = 212 ohms)
•,◦ Reinforcement.
Resistance (ohms)
800
700
600
500
400
300
200
100
0
205 ohms
h/l = 1·0
h/l = 2·0
(d/l)
0·25
0·50
0·75
1·00
1·25
1·50
1·75
2·00

FIG. 7.23

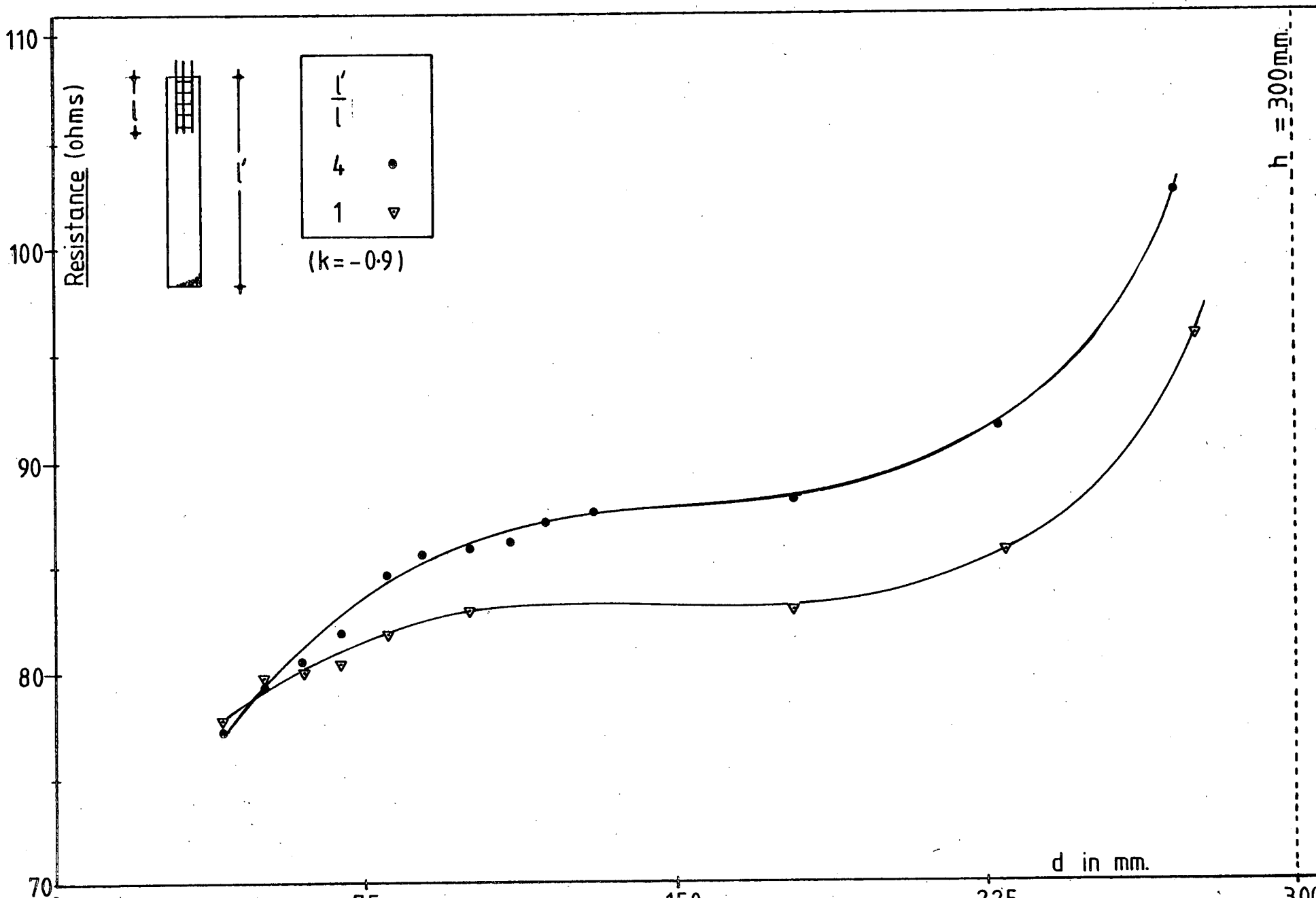

FIG. 7.24

Resistance (ohms)
120
110
100
90
80
70
60
50
40
d'
d
d
d/d'
5
2·5
1·67
1·08
h/l = 1·00
(l/d)
0·25
0·50
0·75
1·00

FIG. 7.25

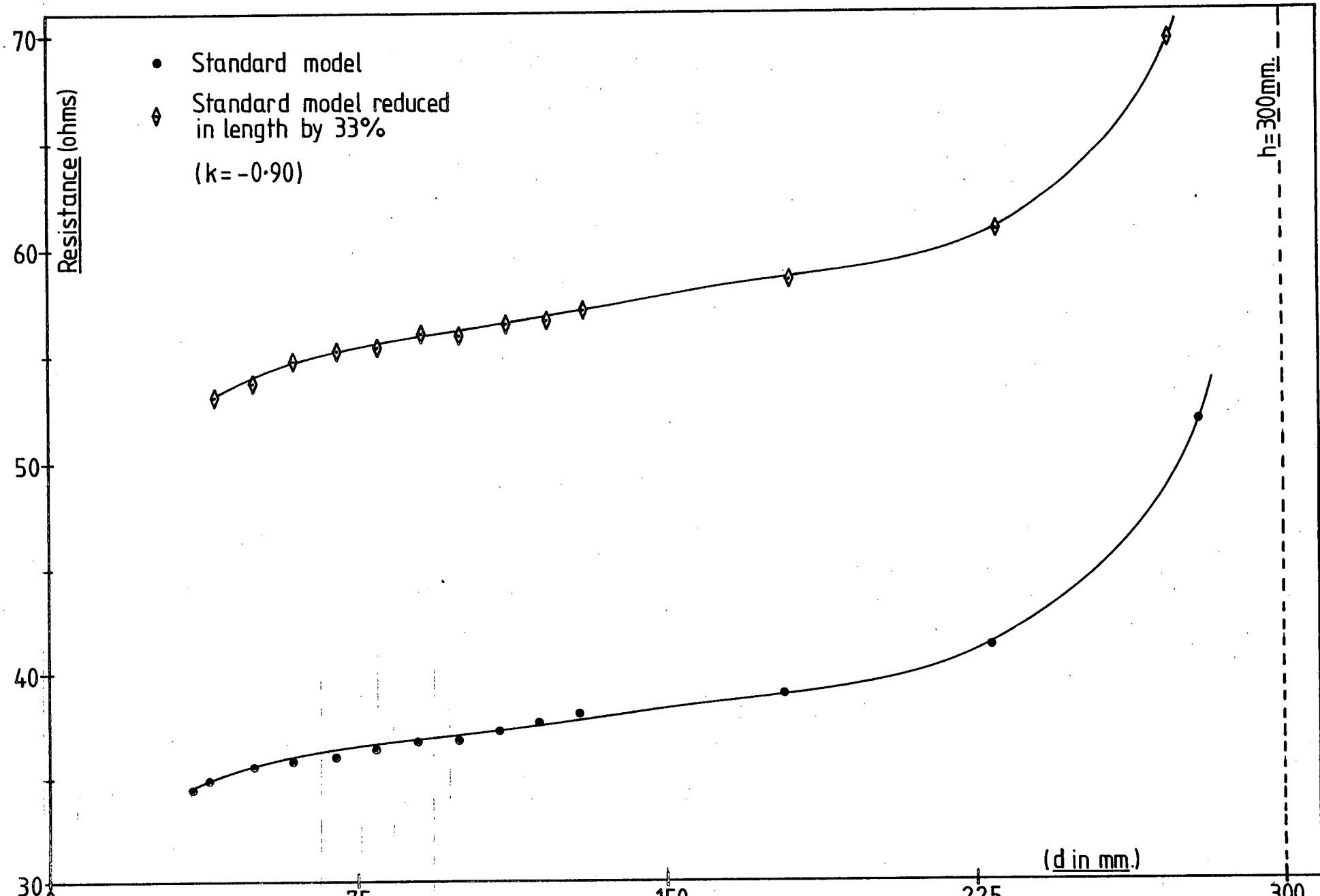
Standard model
Standard model reduced in length by 33%
(k = -0·90)
Resistance (ohms)
70
60
50
40
30
h = 300mm.
(d in mm.)
225
300

FIG. 7.26

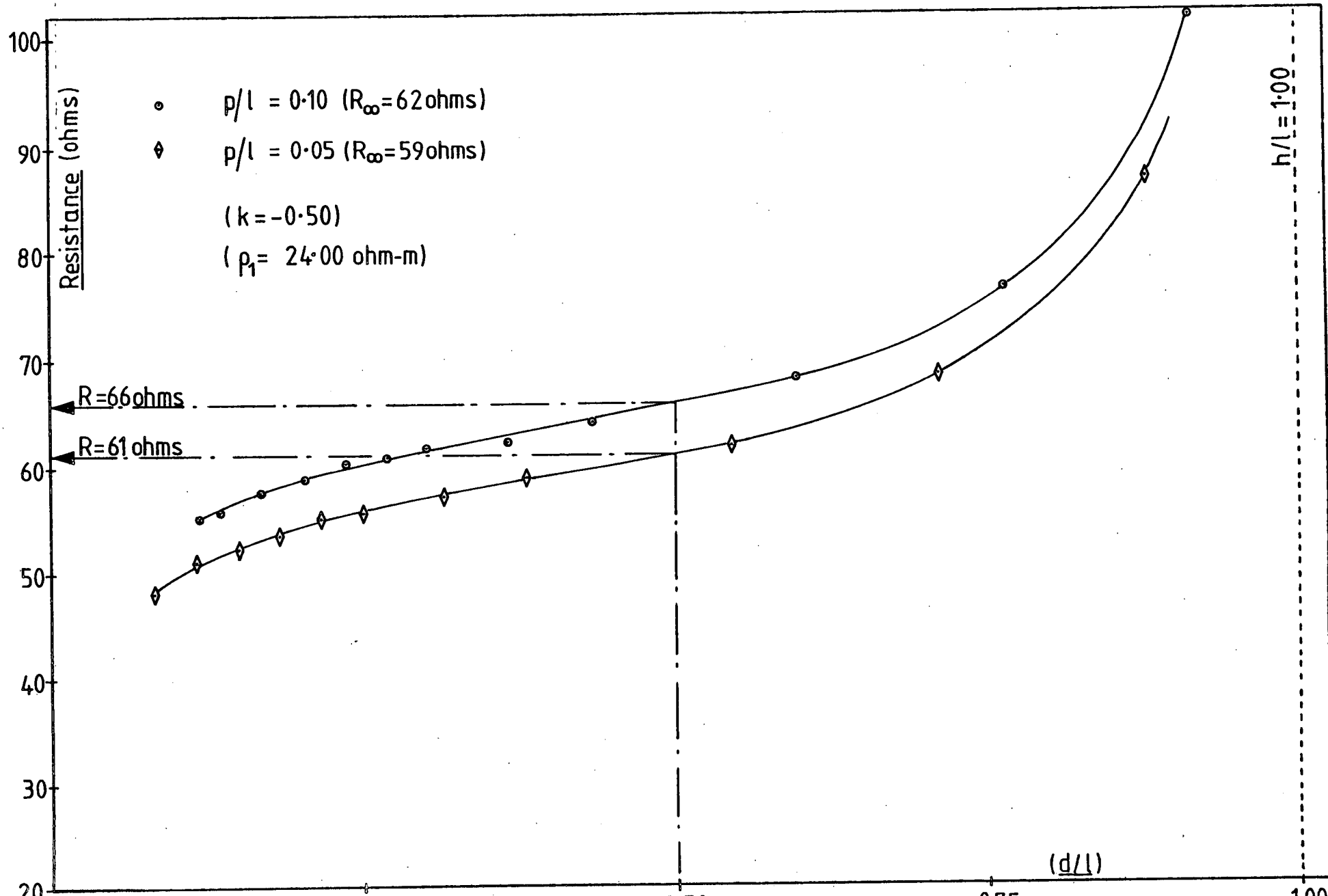
Resistance (ohms)
100
90
80
70
60
50
40
30
20
p/l = 0·10 (R∞=62ohms)
p/l = 0·05 (R∞=59ohms)
(k=-0·50)
(ρ1= 24·00 ohm-m)
R=66ohms
R=61ohms
h/l=1·00
(d/l)

FIG. 7.27

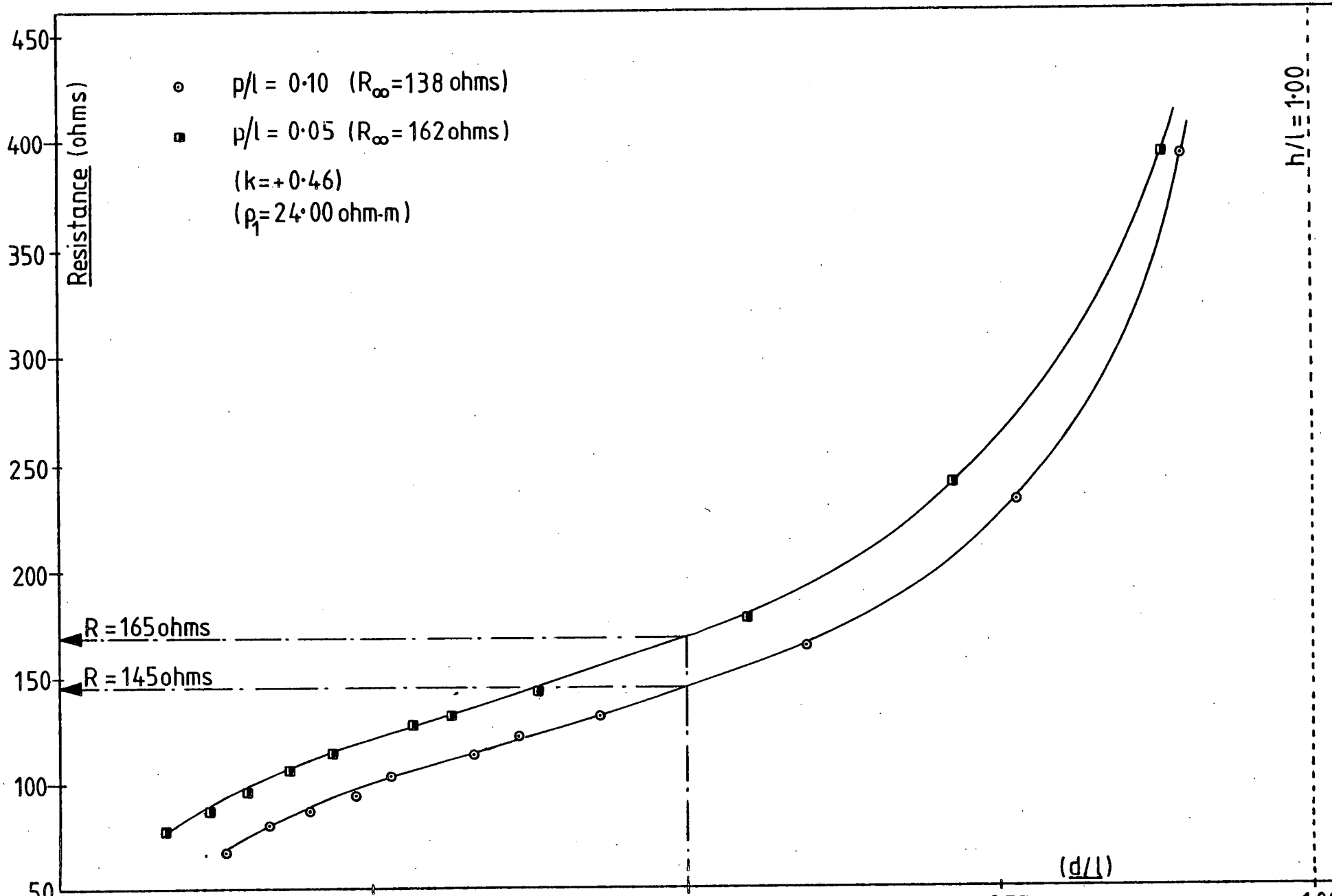
450
400
350
300
250
200
150
100
50
Resistance (ohms)
ρ/l = 0·10 (R∞=138 ohms)
ρ/l = 0·05 (R∞=162 ohms)
(k=+0·46)
(ρ1=24·00 ohm-m)
h/l=1·00
R=165 ohms
R=145 ohms
(d/l)

FIG. 7.28

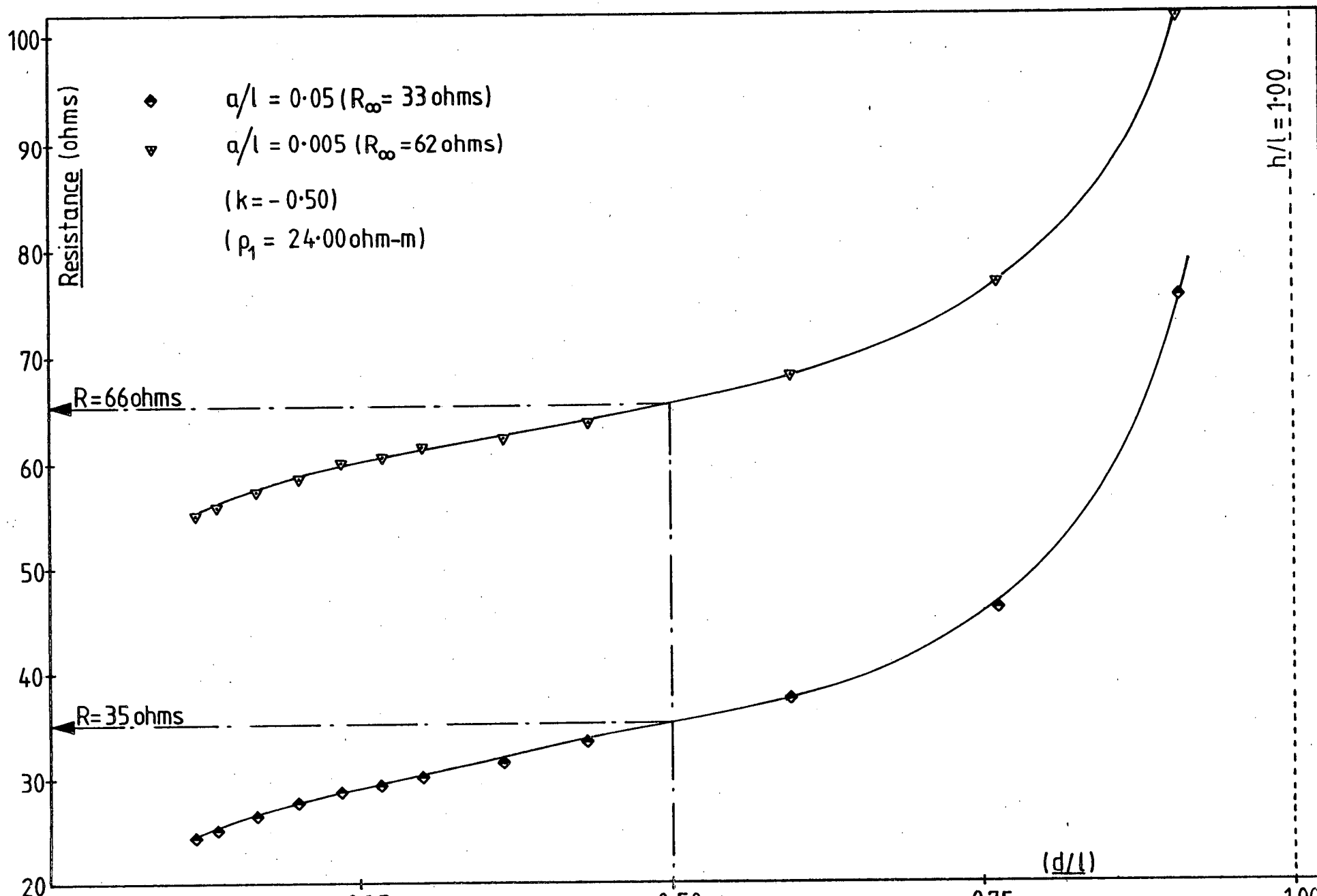
Resistance (ohms)
a/l = 0·05 (R∞= 33 ohms)
a/l = 0·005 (R∞ =62 ohms)
(k = - 0·50)
(ρ1 = 24·00 ohm-m)
R=66 ohms
R=35 ohms
h/l = 1·00
(d/l)
100
90
80
70
60
50
40
30
20

FIG. 7.29

50
40
30
20
10
Resistance (ohms)
T
C
B
G
$\frac{\rho_1}{\rho_3}$ = 19·0
h/l = 1·0
(d/l)
0·25
0·50
0·75
1·00

FIG. 7.30

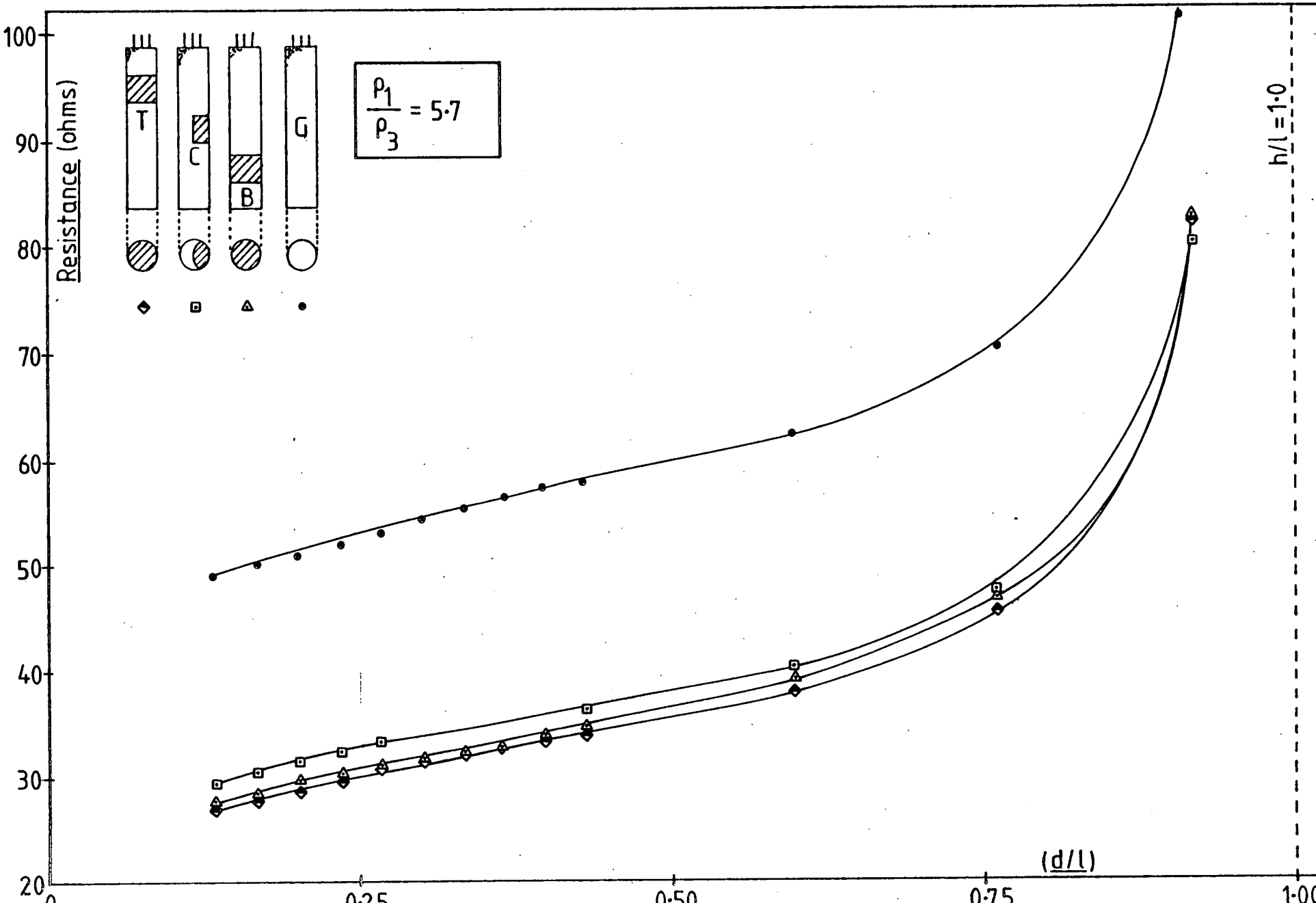
Resistance (ohms)
100
90
80
70
60
50
40
30
20
T
C
B
G
$\frac{\rho_1}{\rho_3} = 5{\cdot}7$
h/l = 1·0
(d/l)
0·25
0·50
0·75
1·00

FIG. 7.31

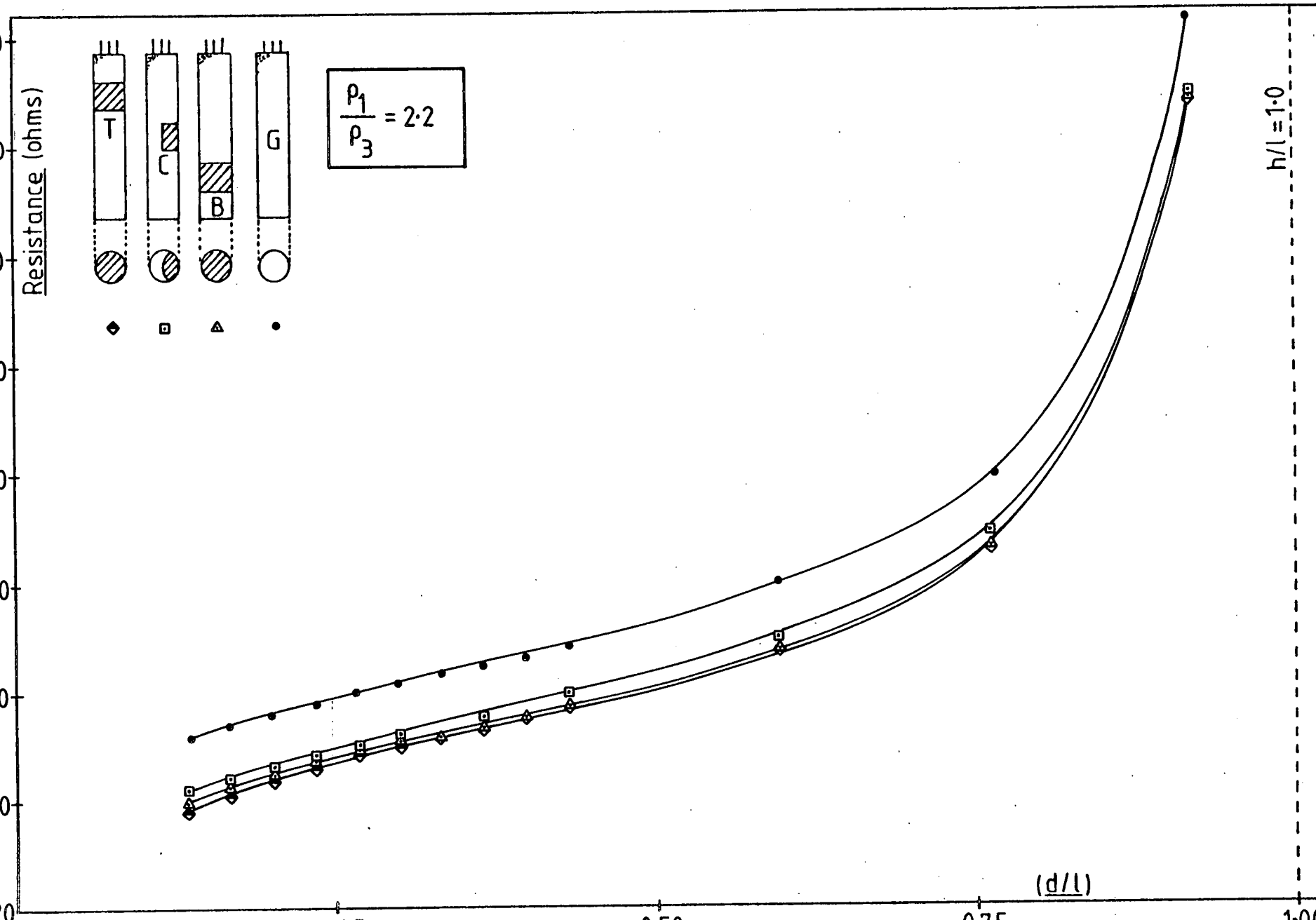
Resistance (ohms)
180
160
140
120
100
80
60
40
20
T
C
B
G
$\frac{\rho_1}{\rho_3} = 2{\cdot}2$
h/l = 1·0
(d/l)
0·75
1·0

FIG. 7.32

Resistance (ohms)
200
180
160
140
120
100
80
60
40
T
C
B
G
$\frac{\rho_1}{\rho_3} = 1{\cdot}27$
h/l = 1·0
(d/l)
0·25
0·50
0·75
1·00

FIG. 7.33

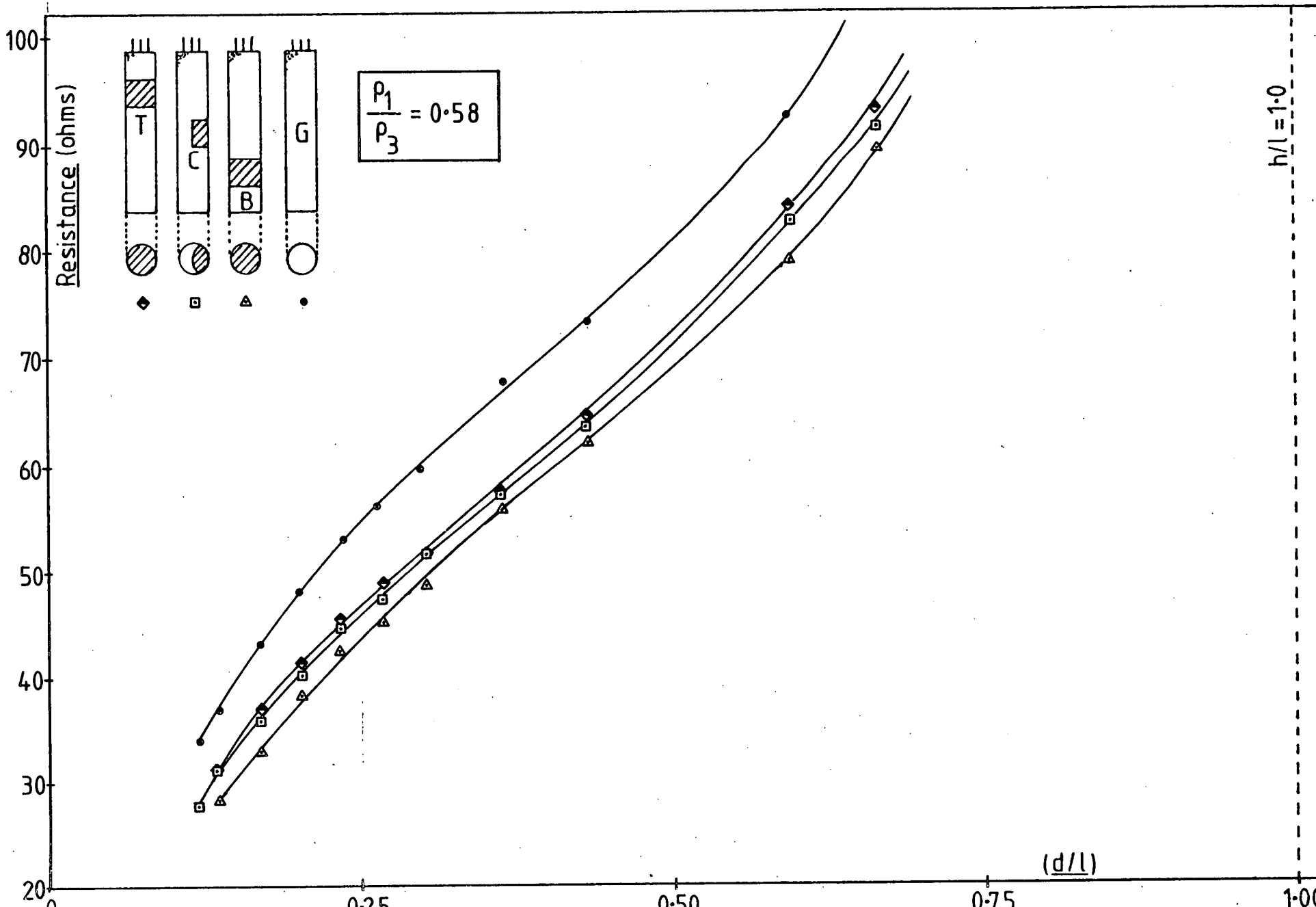
Resistance (ohms)
100
90
80
70
60
50
40
30
20
T
C
B
G
$\frac{\rho_1}{\rho_3} = 0{\cdot}58$
h/l = 1·0
(d/l)
0·25
0·50
0·75
1·00

FIG. 7.34

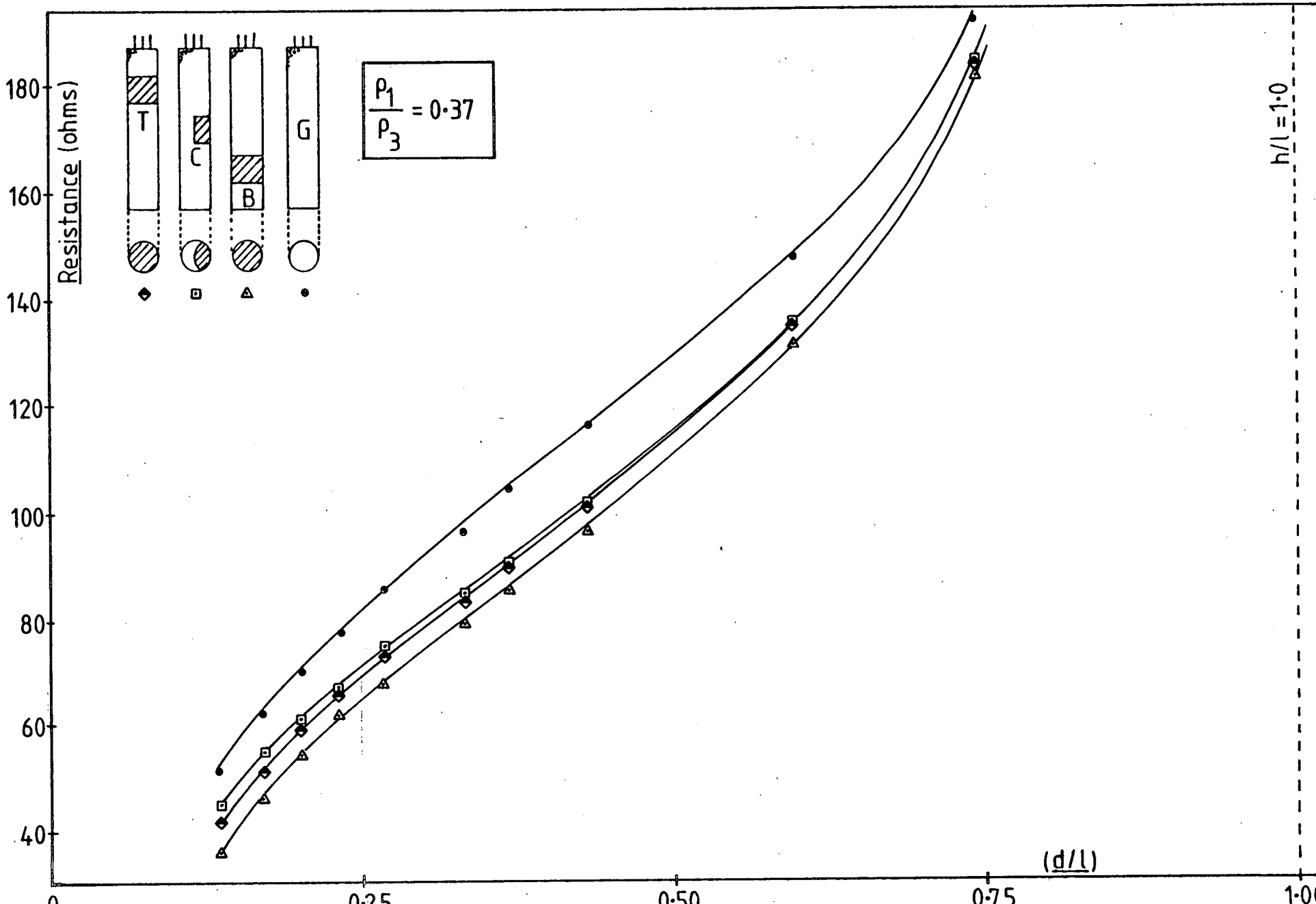
Resistance (ohms)
180
160
140
120
100
80
60
40
T
C
B
G
$\frac{\rho_1}{\rho_3} = 0{\cdot}37$
h/l = 1·0
(d/l)
0
0·25
0·50
0·75
1·00

FIG. 7.35

Resistance (ohms)
300
200
100
0
0·25
0·50
0·75
1·00
(d/l)
h/l = 1·0
T
C
B
G
$\frac{\rho_1}{\rho_3} = 0{\cdot}20$

FIG. 7.36

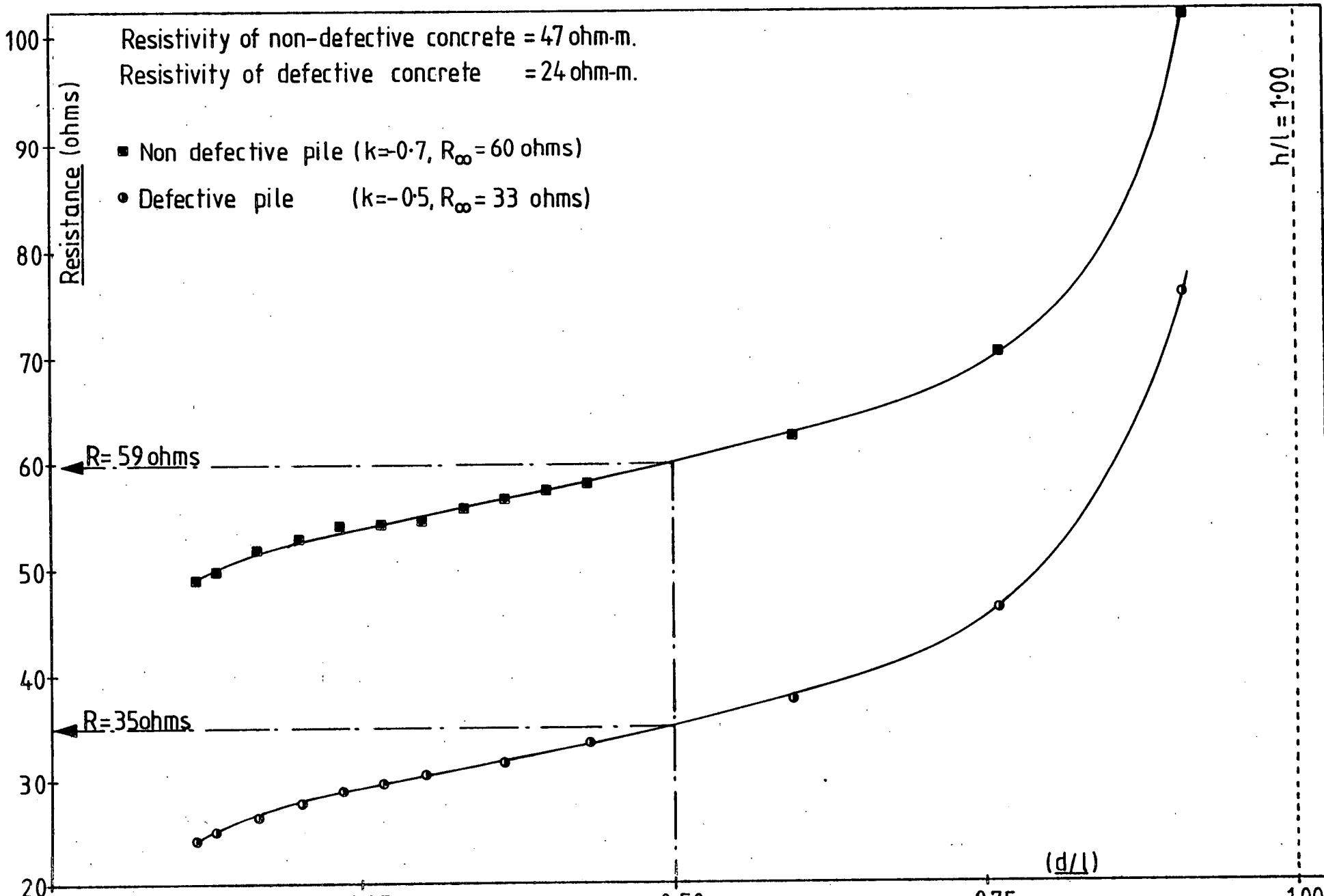
Resistivity of non-defective concrete = 47 ohm-m.
Resistivity of defective concrete = 24 ohm-m.
Non defective pile (k=-0·7, R_∞ = 60 ohms)
Defective pile (k=-0·5, R_∞ = 33 ohms)
Resistance (ohms)
100
90
80
70
60
50
40
30
20
R= 59 ohms
R= 35ohms
h/l = 1·00
(d/l)

FIG. 7.37

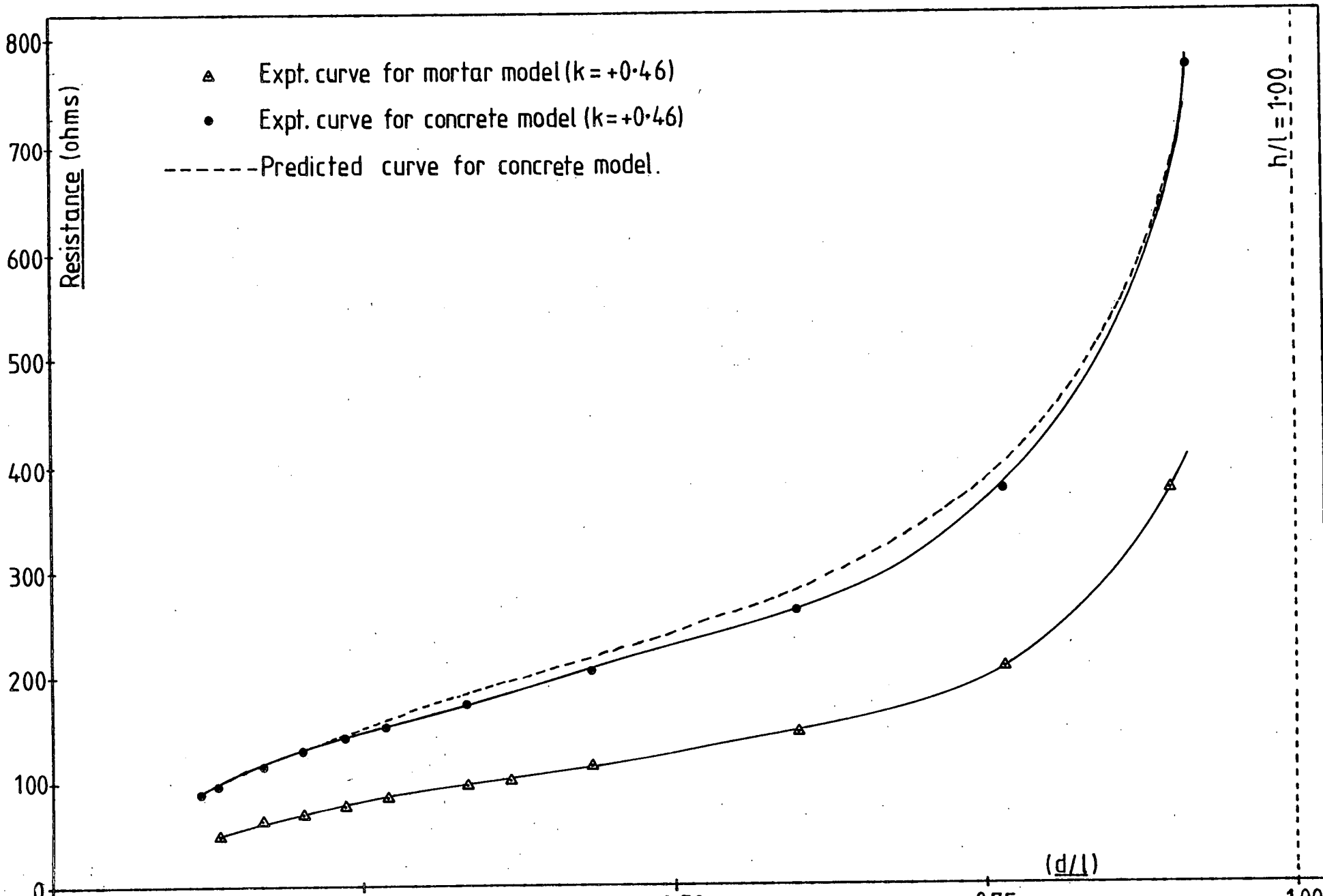
Expt. curve for mortar model (k = +0·46)
Expt. curve for concrete model (k = +0·46)
------Predicted curve for concrete model.
Resistance (ohms)
800
700
600
500
400
300
200
100
0
h/l = 1·00
(d/l)

FIG. 7.38

CHAPTER 8

FIELD TESTS ON PILES

8.1 Introduction

The ultimate proof of any non-destructive technique lies in its operation under field conditions. Although the ability to detect defective piles is the most important attribute many other properties must also be taken into account for a realistic evaluation, among these are portability, reliability, robustness and the speed with which the test may be carried out in the field and assessment made.

8.2 Full Scale Experimental Tests

As a preliminary to site testing, four cast-in-situ piles were constructed at the School of Engineering at the Kings Buildings, Edinburgh. The piles were founded in a boulder clay and were constructed using a shell and auger piling rig (Plate 7), to a depth of 5.0m and diameter of 300mm. Two of these piles were constructed using a tremie tube and were classified as non-defective. Results from these piles could then be used as a reference datum. The reason for constructing two sound piles was to investigate repeatability of results. The remaining piles were constructed as defective - one had defective concrete in the pile shaft, which was achieved by using a concrete with a very high water/cement ratio; the other was constructed one metre shorter than the other three. The concrete used had 1:1½:3 mix proportions with a 0.7 water/cement ratio. All constituents were batched by weight. The sand was grading zone 3 and the maximum size of the coarse aggregate was not greater than 19mm. The piles were continuously reinforced with a 140mm. diameter reinforcing cage.

The electrical resistivity of the boulder clay was obtained using a Wenner electrode configuration with an electrode spacing of 6.0m, this gives an average resistivity to a depth of approximately 6.0m. (Mallot (111) states that the results of 34,000 resistivity soundings and over 4,000 correlation borings have indicated that the depth of current penetration is nearly equivalent to the distance between adjoining electrodes for depths above about 30m).

The piles constructed are summarised below:

Test Pile No.	Length (m)	Diameter (mm)	Nature of defect
TP1	5.00	300	Weak concrete
TP2	5.00	300	Sound
TP3	4.00	300	'Short' pile
TP4	5.00	300	Sound

Field equipment and measurement procedures have been described in Chapter 4.

8.3 Test Results - Discussion

All piles were tested 3 hours after pouring, the electrical resistivity of the concrete at this point in time being 6.50Ω-m. The electrical resistivity of the boulder clay was 62.00Ω-m, giving a reflection coefficient of +0.80.

Figure 8.1 shows typical earth-resistance curves for one of the test piles and also shows the effectofincreasing the pile-current electrode distance from 5m to 10m and 15m.

Figure 8.2 has the earth-resistance curves for all four piles plotted, the pile-current electrode distance being 5m in all cases.

The general shape of the E-R curve for the piles is as anticipated from laboratory studies. Since all piles were tested the same time after placing then the relative integrities can be assessed and it is envisaged that by plotting all curves together then characteristic similarities, as discussed in Chapter 2,can be observed. The theoretical work and experimental programmes undertaken in the laboratory indicate that a defective pile will have its E-R curve displaced either up or down from that of a non-defective pile.

From Figure 8.2, which has all four test pile results plotted, it is evident that the defective piles, TP1 and TP3, have their E-R curves displaced from the non-defective piles, TP2 and TP4. The E-R curves for the non-defective piles show good repeatability as the curves are, for the most part, coincident. Inferring from the electrolytic tank and theoretical work the E-R curves for the defective piles are displaced as anticipated. For TP1, the concrete in the pile shaft will have a much lower resistivity than that in either TP2 or TP4 (due to high water/cement ratio) and, with reference to equation (3.35) and laboratory work on mortar models, will result in a downward displacement of the E-R curve. As the earthing-resistance is inversely proportional to the pile length, then the short pile, TP3, will have its characteristic E-R curve displaced upwards from that of the reference piles. This theoretical deduction is verified by the field data. It is also noticeable that the general gradient of the E-R curves is similar showing that ground

conditions remain reasonably constant.

The work undertaken on these piles has shown that defective piles will have their E-R curve displaced from that of a non-defective pile and has yielded qualitative evidence of pile defects. Furthermore, as site conditions cannot be adequately simulated in a laboratory environment, the use of full-scale experimental piles has helped to develop field procedure and highlighted any problems that could arise on site, for example,

(a) lead lengths should be kept to a miniumum (Plate 8),

(b) the use of bayonet plugs reduces the time taken to set-up equipment,

(c) the auxiliary electrodes need to be hammered into the ground to a depth of approximately 200mm to achieve good grounding.

8.4 Site Testing of Concrete Piles

Work carried out on the full scale piles constructed agreed well with the electrolytic tank predictions; the next stage was to test piles on a construction site. The site tested was at the I.B.M. factory, Inverkip, Greenock. The piles used were West's Shell piles driven to a depth of approximately 6.00m through a compacted clay fill, and were infilled with a 1:1½:3 mix with a 0.6 water/cement ratio, the external diameter of the shells being 400mm. The piles were continuously reinforced with a 200mm diameter reinforcing cage. The

electrical resistivity of the compacted clay fill was approximately 15.00Ω-m, and that of the concrete 70.0Ω-m. The piles had been cast 6 weeks previous to moving onto site and were laid out in a grid formation - the rows were 2.30m apart with the piles in each row at 2.00m centres.

The space availability around the pile head required a 2.0m pile/current electrode distance. The field procedure was to test the piles in groups, with the current and potential electrodes being within the rectangle bounded by the four piles as shown in Figure 8.3. In this way errors introduced due to small changes in soil resistivity will be reduced to a minimum and results can be compared in sets.

The pile reinforcement was cleaned with a wire brush and emery paper and connections made to four of the projecting reinforcing bars. The current electrode was hammered into the ground by means of a small sledge hammer to a pre-measured mark on the stake and securely grounded. The potential electrode was then hammered into the ground at several points intermediate between the current electrode and the pile. The pile, potential electrode and current electrode are kept colinear throughout and measurements are taken from the centre-line of the pile.

8.4.1 Discussion - Field Results

From the limited site testing, results were obtained which are useful in demonstrating how the method can be applied in practice.

The pile-current electrode distance of 2.00m remained the same for all the piles tested and the E-R curves are shown in Figures 8.4 - 8.9, together with the recorded length of the pile and testing configuration. As stated previously, the current electrode was kept within the area bounded by four piles and, hence, the E-R curves can be plotted in groups. In this way, characteristic similarities can be observed, viz. if an individual pile has its E-R curve displaced from its neighbours, then it would indicate that the pile itself is suspect, but if several piles are equally displaced, it may indicate a change in subsoil conditions.

The E-R plots for each group of piles show remarkably good consistency, the E-R curves being plotted in groups of 2,3 and 4. Looking at all the groups collectively, the E-R characteristics of piles tested have the same general shape, showing that subsoil conditions must be reasonably constant.

The E-R curves for the piles within each group are virtually coincident, especially that part of the curve that lies within a radius of 1.40m from the pile head. From laboratory experiments it was shown that the resistance readings close to the pile head are of greater significance in relation to fault detection than those distant. There are two piles, however, that would arouse suspicion, namely 377 and 458. Both piles have their characteristic E-R curve displaced upwards, this upward displacement could be due to,

(a) an increase in the apparent electrical resistivity of the soil,
(b) an increase in the electrical resistivity of the concrete, or
(c) reduction in the length of the pile.

By comparing pile 458 with its neighbour, (a) can be ruled out as deductions as to the subsoil conditions can be inferred from the gradient of the E-R curve. Since pile 458 has the same flat curve as its neighbours, then the same material must be present around the pile shaft. Pile 377, however, has a slightly increased gradient compared to its neighbour and could partly account for the upward displacement of its E-R curve.

Consider pile 458. The resistance readings are increased from its neighbours 449 and 450 by approximately 20%. Since, pile 458 is shorter than 449 and 450 by 1.00m (approximately) then it would be anticipated that its E-R curve will be displaced upwards, the magnitude of this upward displacement being roughly in the ratio of the inverse of their lengths, i.e. by a factor of 1.18 (7.6/6.4). Pile 458 would in consequence not cause concern.

Consider pile 377. If the recorded lengths are correct then the large upward displacement cannot be attributable to a change in length or soil resistivity only, and must be almost solely due to an increase in the electrical resistivity of the concrete. Since the resistance is approximately doubled then the resistivity of the concrete will be nearly twice that of its neighbours. If so, this must mean a decrease in the fractional volume of cement paste hence a weak concrete in the pile shaft.

This assumes, of course, that the recorded length of the pile is correct. At present it would be difficult to ascertain whether an increase in resistance was due to a decrease in pile length or an increase in the

electrical resistivity of the concrete. The E-R method is qualitative in nature and all that is required to raise suspicion is a displacement of its E-R curve from the norm. Such piles should then be subjected to a more quantative testing procedure and clearly pile 377 would fall into this category.

8.4.1.1 Theoretical Earthing Resistance for Greenock Site

Although pre-determined values of earthing resistance are not necessary, a theoretical value can be calculated using the theory of Chapter 3. If the pile is assumed to be 6.00m in length then, $\rho/l = 0.033$, $a/l = 0.017$, $k = -0.65$ and $\rho_1 = 70.0$ ohm-m, this gives R_a a value of -1.713 and a value of the theoretical earthing resistance of 5.7 ohms.

This should be compared to the value obtained at a point midway between the pile and current electrode on the E-R curve associated with each pile, which is, approximately, 5.0 ohms.

8.4.1.2 Influence of Soil Type on the E-R Curve

Figure 8.10 shows the E-R curves for piles in different soil conditions - one for a low resistivity compacted clay fill (I.B.M. Greenock) and one for a high resistivity boulder clay (Edinburgh University). The lengths of the piles are 5.80m (I.B.M.) and 5.00m (Edinburgh) and a pile-current electrode spacing of 2.00m was employed.

This Figure shows clearly the influence of the soil around the pile on the shape of the E-R curve. As the apparent resistivity of the background medium increases then the E-R curve becomes steeper which

is as anticipated from electrolytic tank predications.

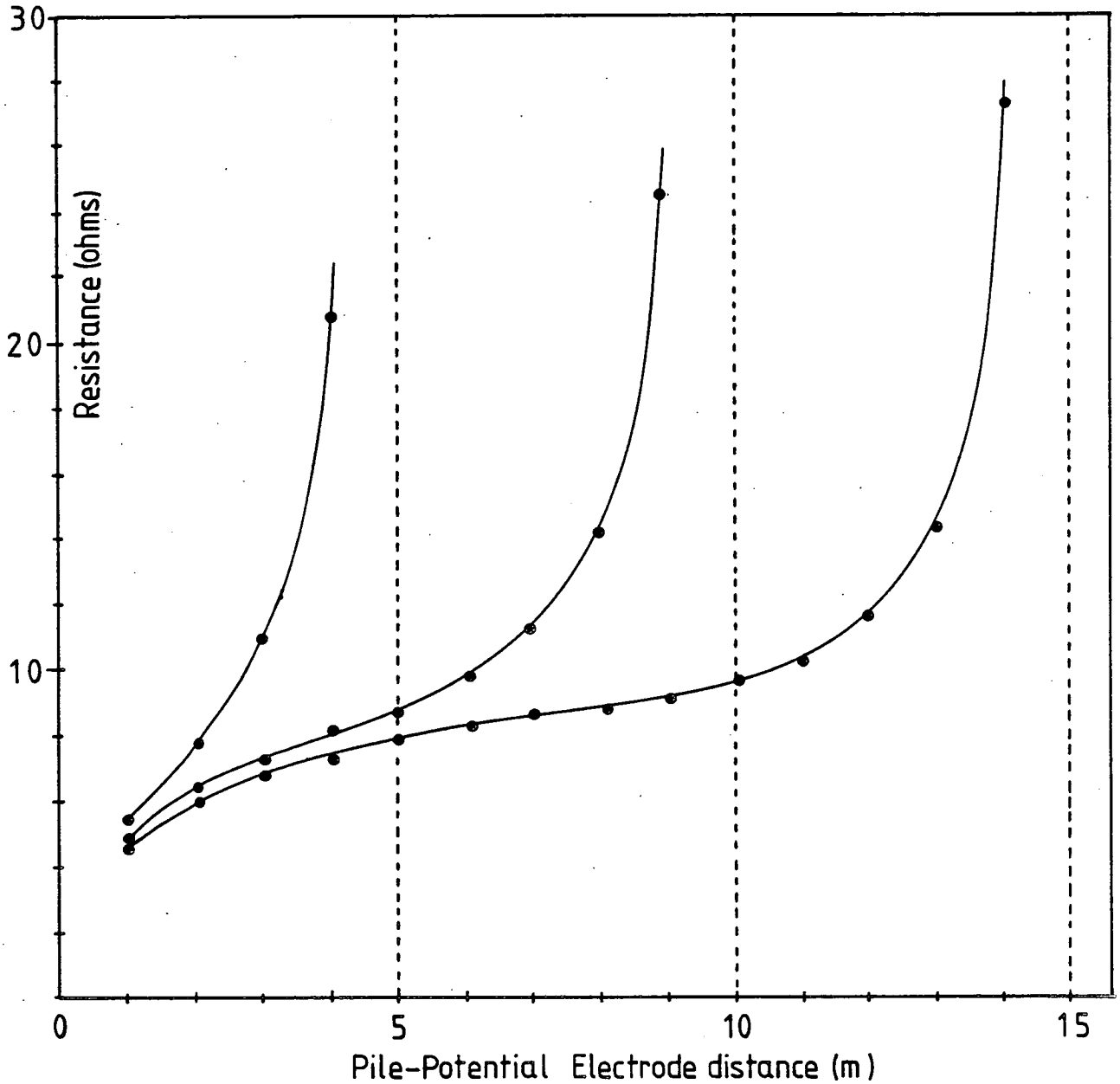

FIG. 8.1 Influence of increasing Pile-Current electrode distance for TP1

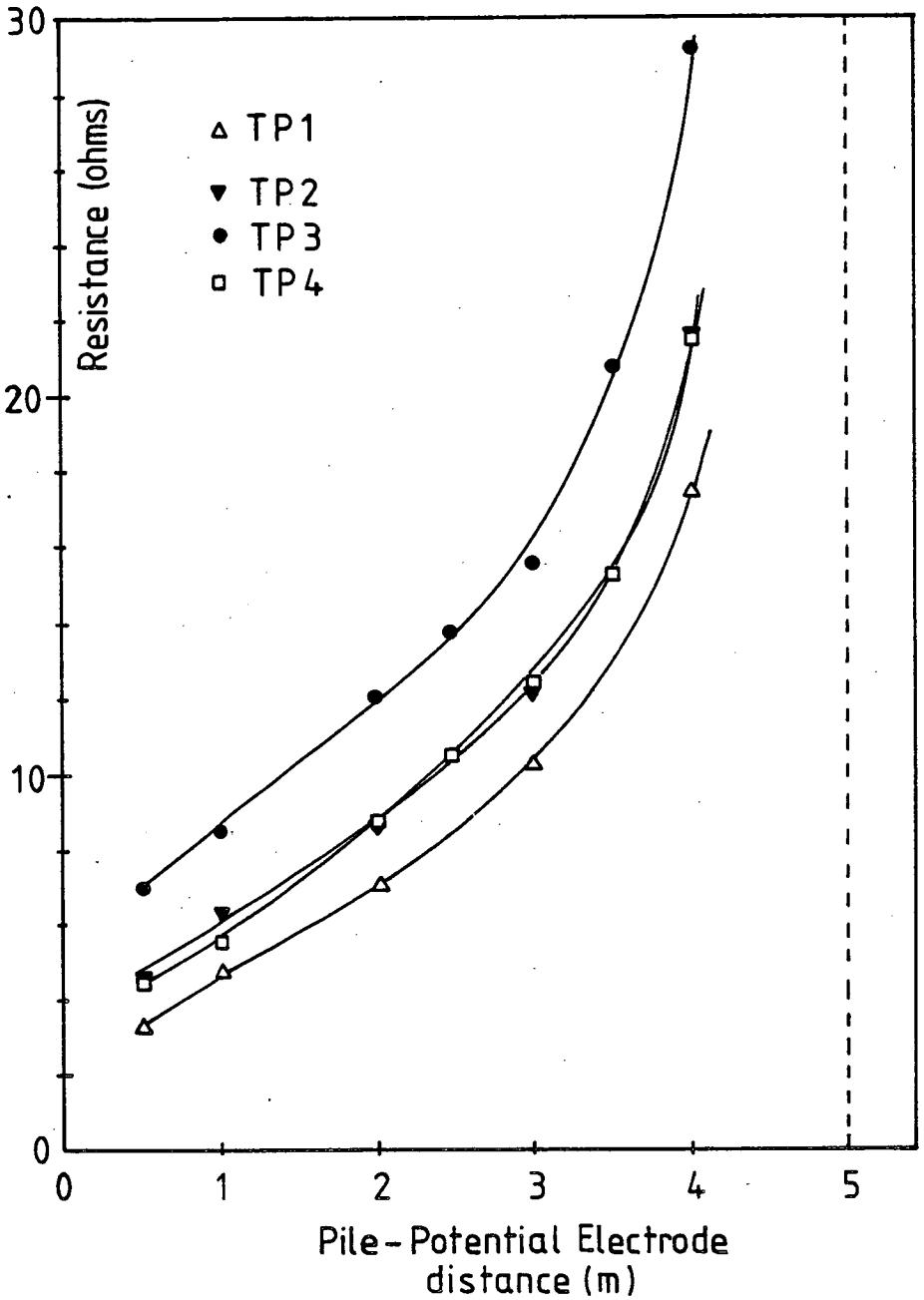

FIG. 8.2 E-R curves for Test Piles

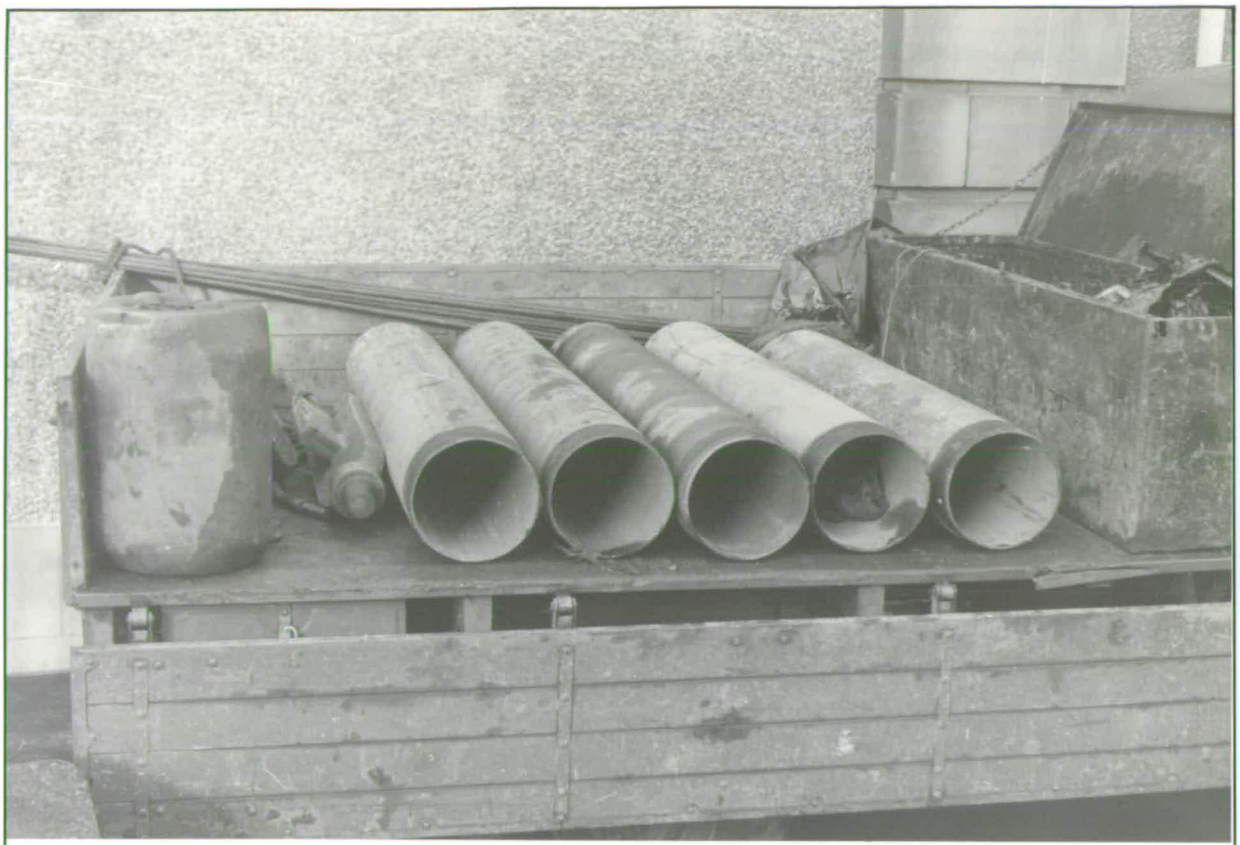

PLATE 7

Piling-rig and steel liners

PLATE 8

Set-up over pile head

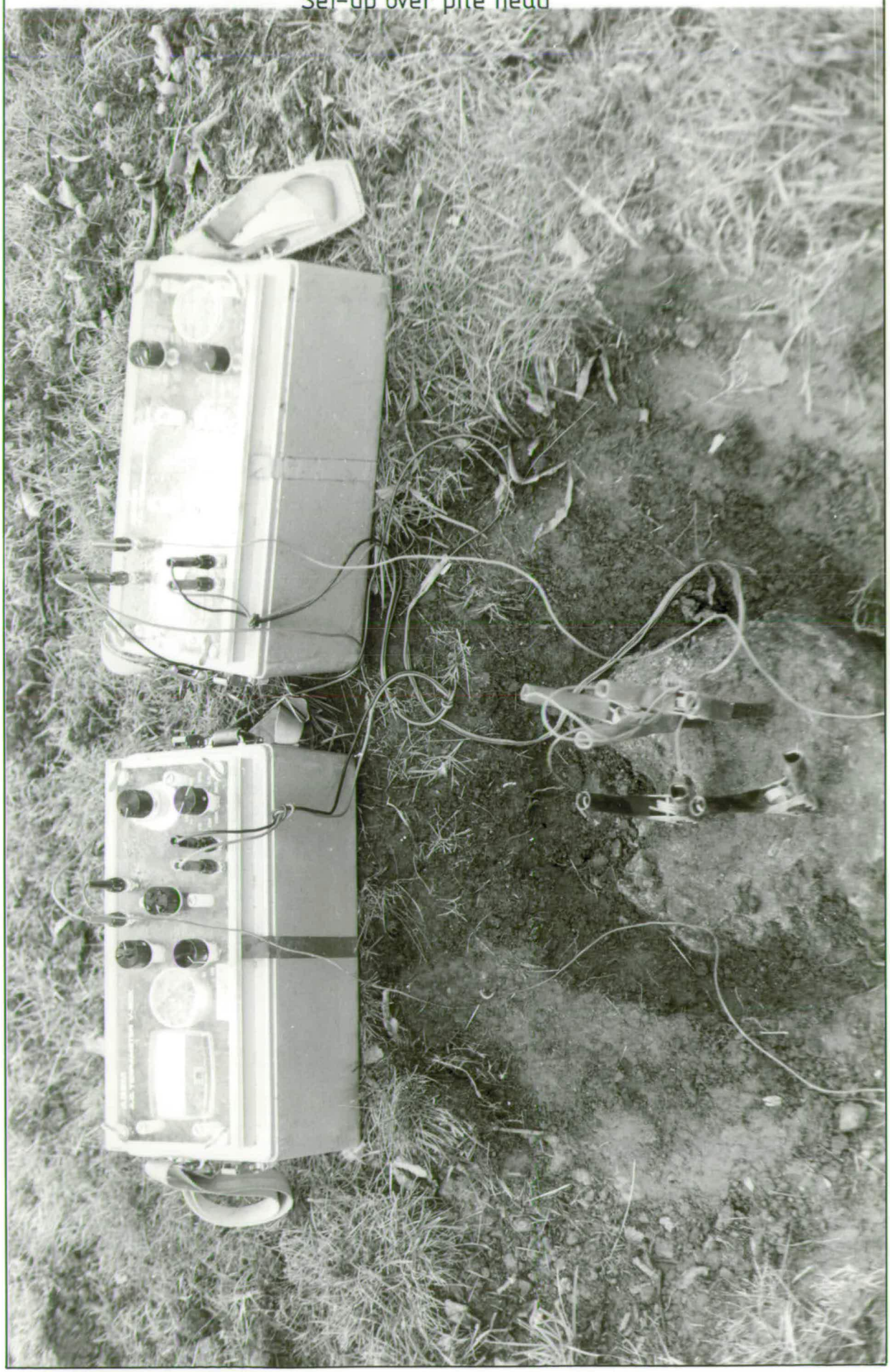

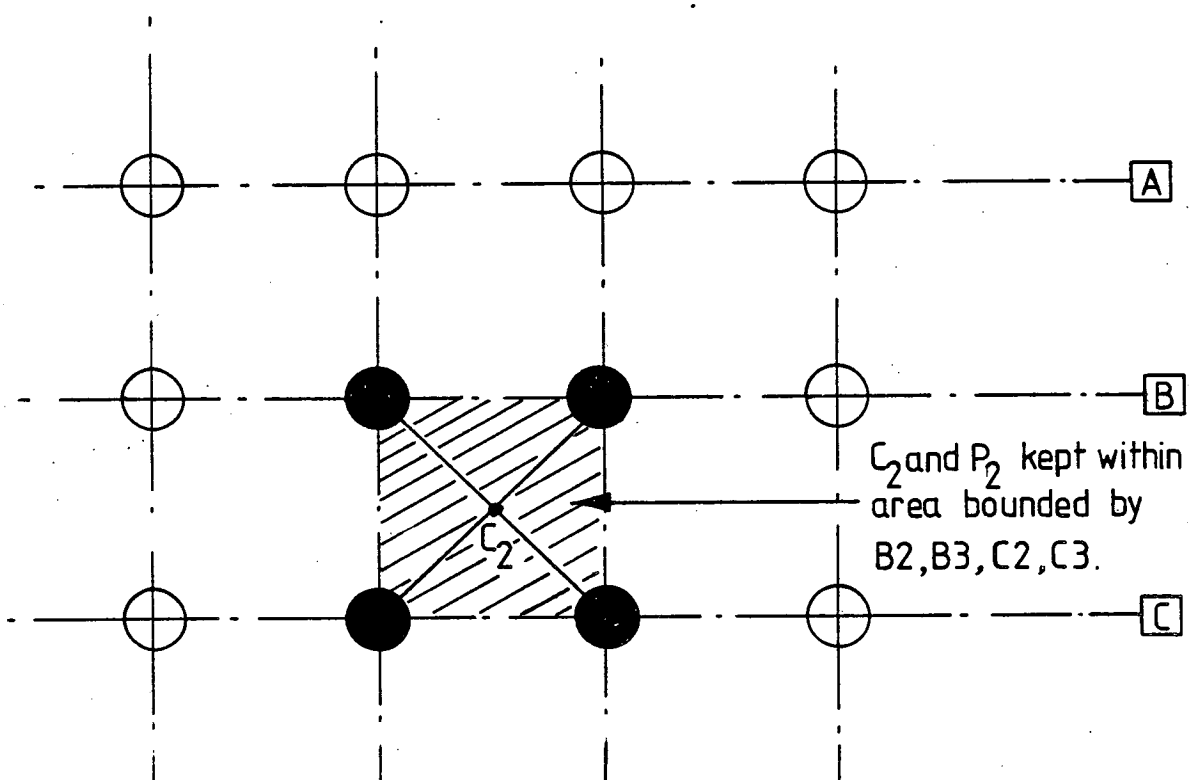

FIG. 8.3 Testing configuration for site environment

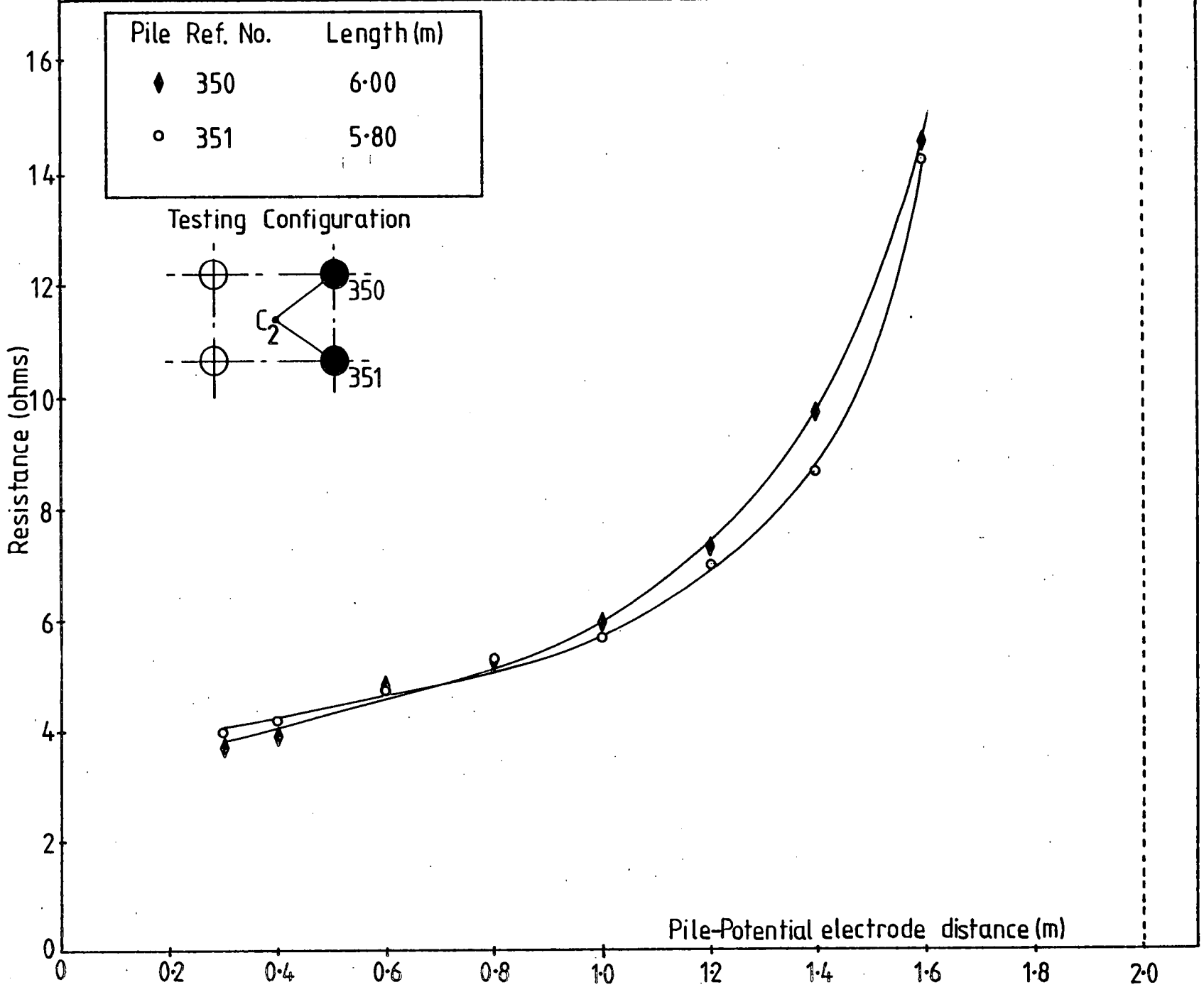
Pile Ref. No.
Length (m)
350
6·00
351
5·80
Testing Configuration
350
C2
351
Resistance (ohms)
0
2
4
6
8
10
12
14
16
Pile-Potential electrode distance (m)
0
0·2
0·4
0·6
0·8
1·0
1·2
1·4
1·6
1·8
2·0

FIG. 8.4

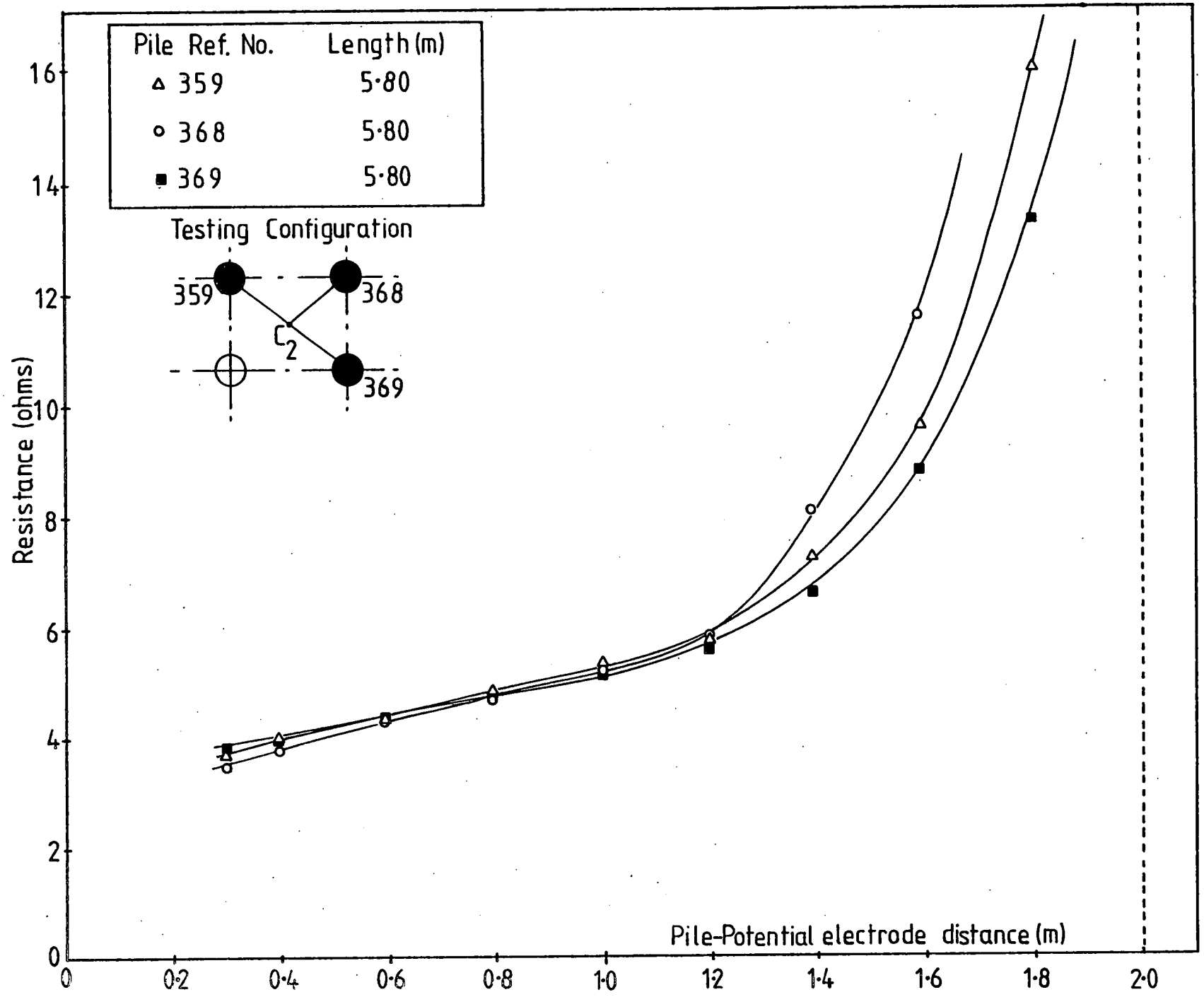
Pile Ref. No.
Length (m)
△ 359
5·80
○ 368
5·80
■ 369
5·80
Testing Configuration
359
368
369
C2
Resistance (ohms)
0
2
4
6
8
10
12
14
16
Pile-Potential electrode distance (m)
0
0·2
0·4
0·6
0·8
1·0
1·2
1·4
1·6
1·8
2·0

FIG. 8.5

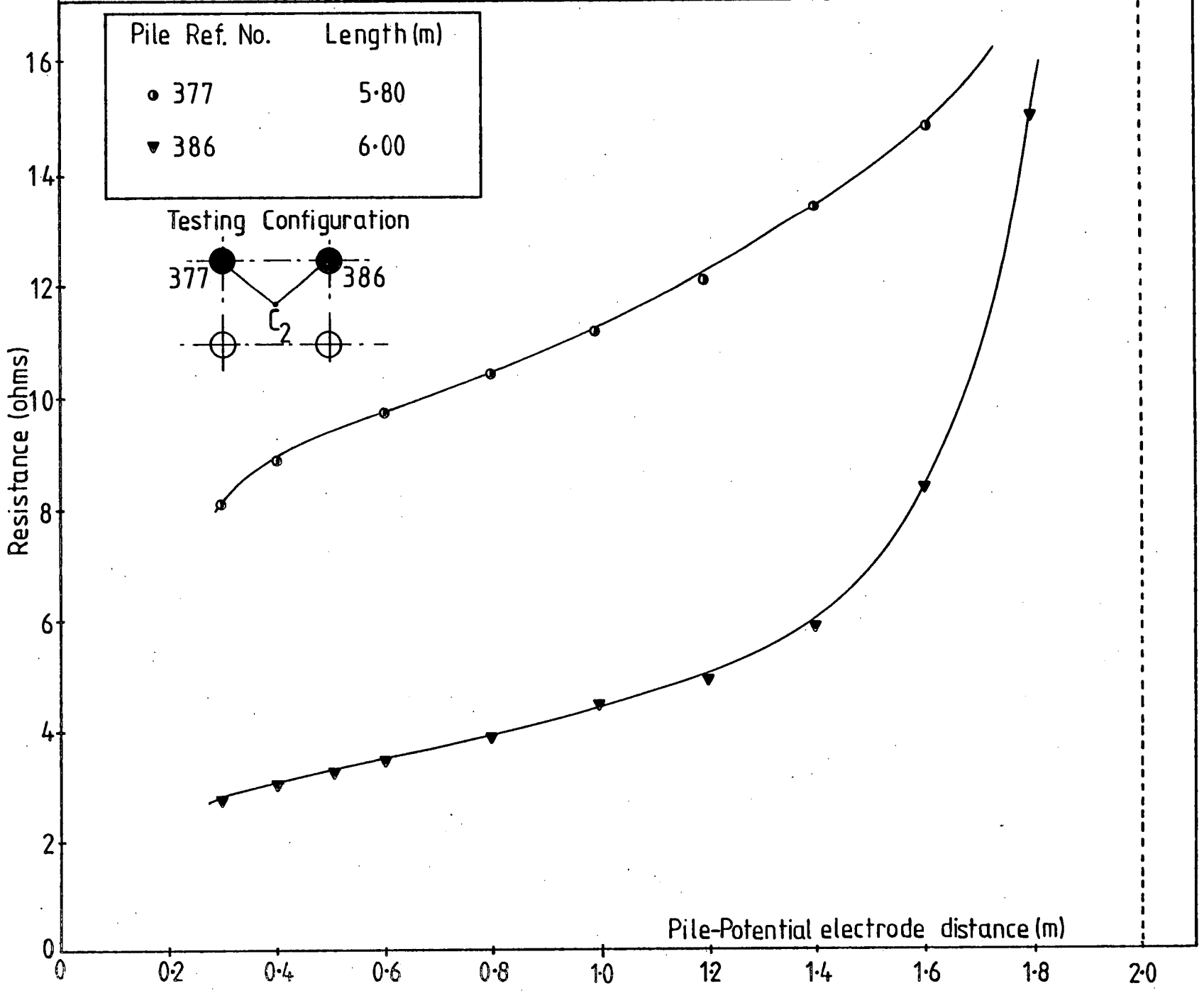
Pile Ref. No.
Length (m)
377
5·80
386
6·00
Testing Configuration
377
386
C2
Resistance (ohms)
Pile-Potential electrode distance (m)
0
2
4
6
8
10
12
14
16
0·2
0·4
0·6
0·8
1·0
1·2
1·4
1·6
1·8
2·0

FIG. 8.6

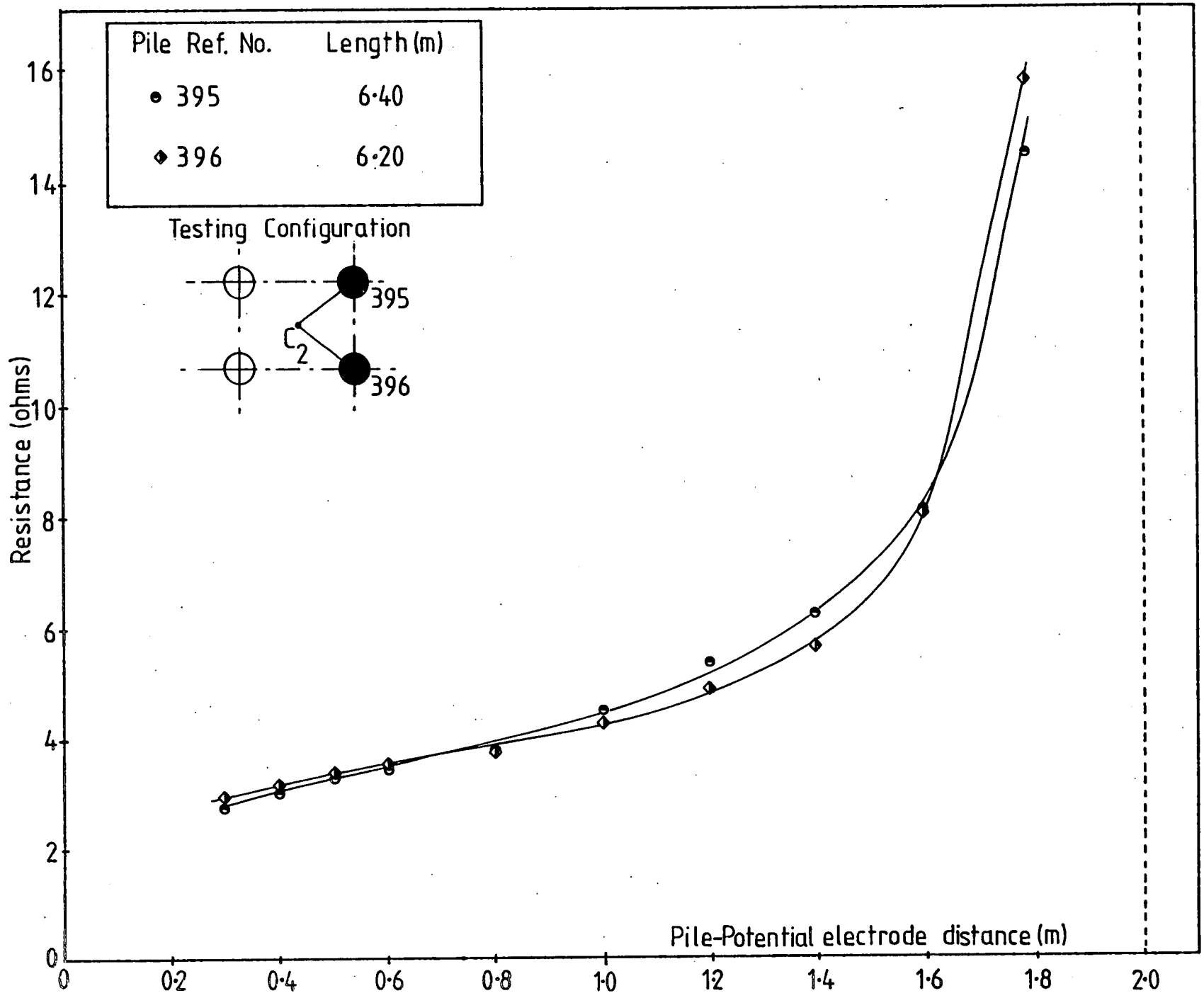
Pile Ref. No.
Length (m)
395
6·40
396
6·20
Testing Configuration
395
396
C2
Resistance (ohms)
Pile-Potential electrode distance (m)
0
2
4
6
8
10
12
14
16
0·2
0·4
0·6
0·8
1·0
1·2
1·4
1·6
1·8
2·0

FIG. 8.7

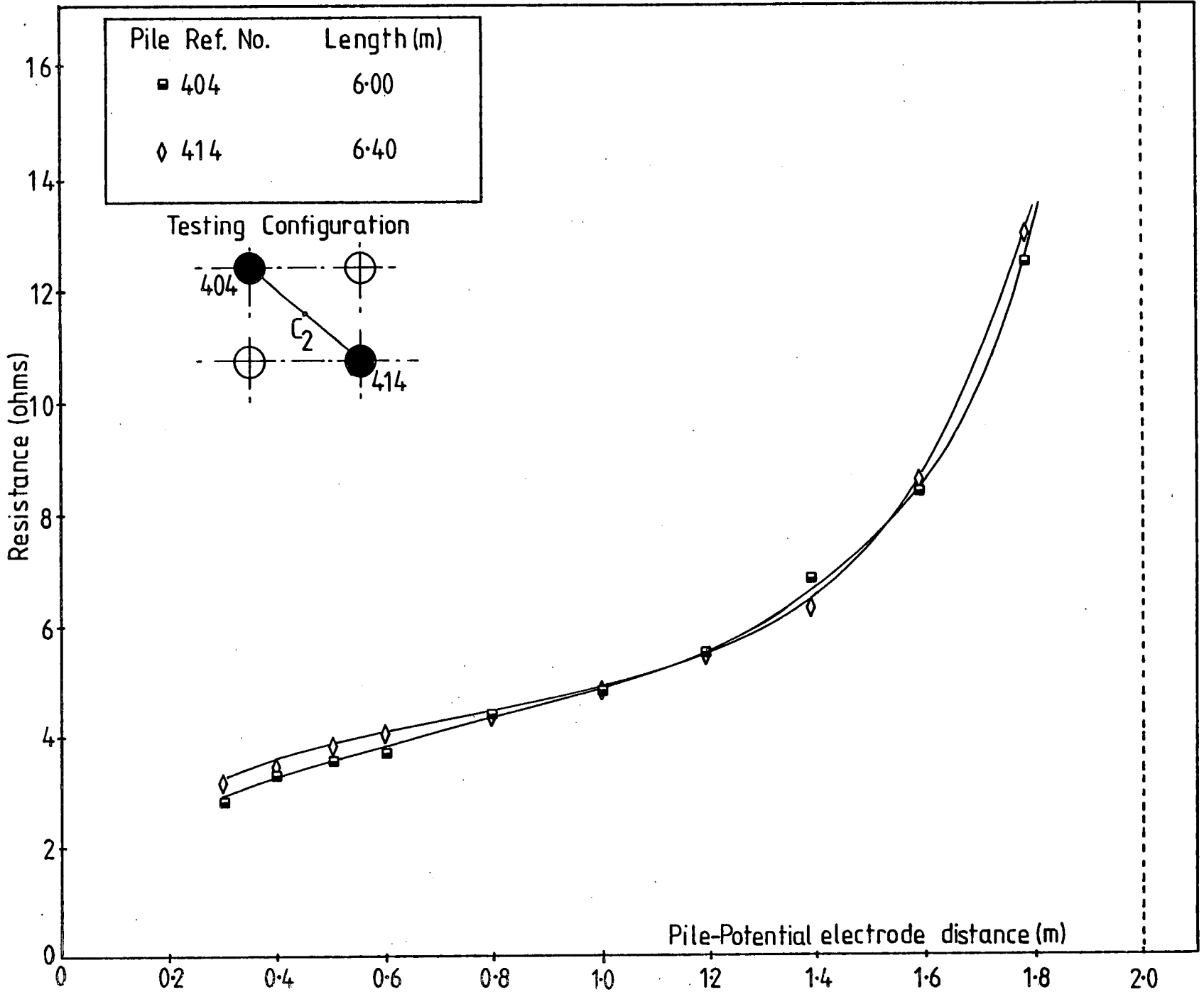
Pile Ref. No.
Length (m)
404
6·00
414
6·40
Testing Configuration
404
C2
414
Resistance (ohms)
0
2
4
6
8
10
12
14
16
0
0·2
0·4
0·6
0·8
1·0
1·2
1·4
1·6
1·8
2·0
Pile-Potential electrode distance (m)

FIG. 8.8

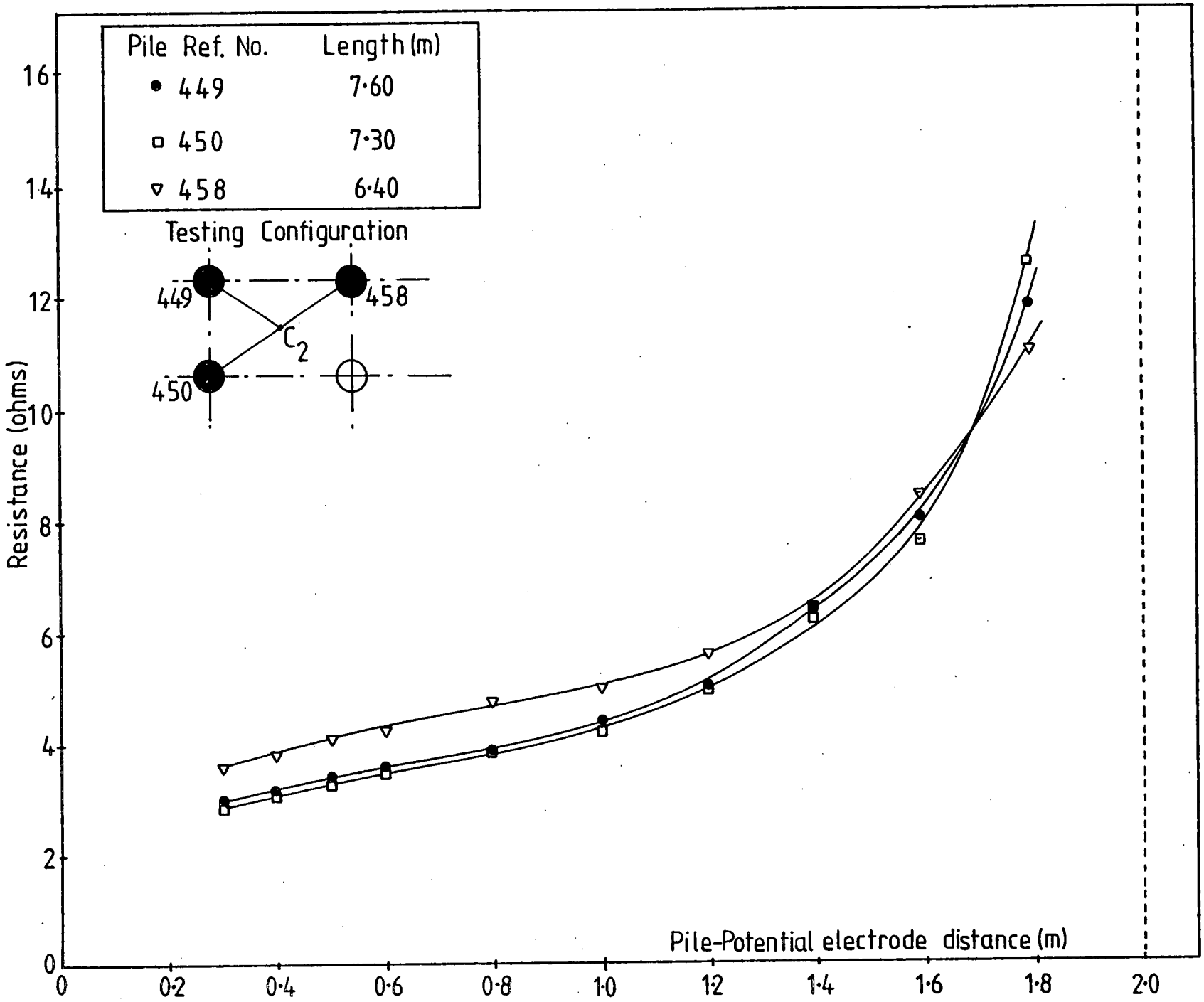
Pile Ref. No.
Length (m)
449
7·60
450
7·30
458
6·40
Testing Configuration
449
458
450
C2
Resistance (ohms)
Pile-Potential electrode distance (m)
0
2
4
6
8
10
12
14
16
0
0·2
0·4
0·6
0·8
1·0
1·2
1·4
1·6
1·8
2·0

FIG. 8.9

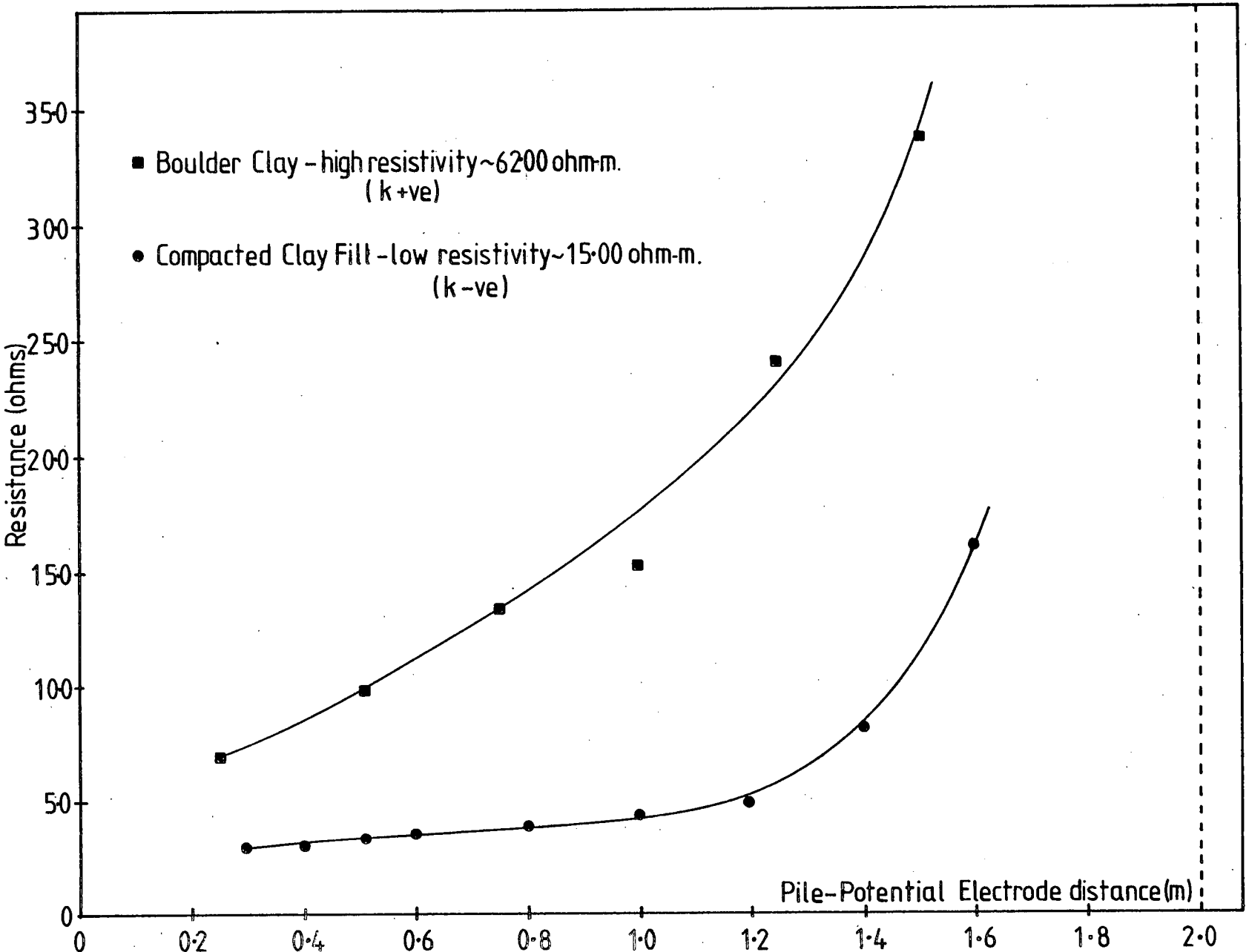

FIG. 8.10 Influence of soil type on E-R curve

CHAPTER 9

CONCLUSIONS AND RECOMMENDATIONS FOR FUTURE RESEARCH

The purpose of this study was to develop the earth-resistance method for the detection of irregularities and imperfections in piled foundations. The theoretical aspects of earthing resistance and testing methodology were first verified in the laboratory by electrical analogue experiments. These experiments show that it is possible to detect discontinuities and abrupt changes in pile cross-sectional areas.

A number of site tests was undertaken showing that the method can be used without any interruption to the construction programme. A minimal amount of preparation to the pile is required and the E-R curves obtained can be used to assess the integrity of the pile-soil system.

The variables which determine the earthing-resistance of a pile have been investigated. Resulting from this investigation certain precautions must be taken to ensure correct interpretation of results. Conclusions have been given at the end of each experimental section. With reference to the context of non-destructive testing the following main conclusions can be drawn from this study,

(a) A new alternative method of testing non-destructively has been investigated. The system variables have been analysed in detail and measurement procedures for pile-testing using this technique proposed. It has been shown that the characteristic E-R curve for a pile gives qualitative indications as to the integrity of the pile-soil system. An approximate theory has been developed showing the inter-relationship between the system variables.

(b) It has been shown that it is best to test a pile when a high reflection coefficient exists, either positive (in the case of cast-in-situ piles) or negative (in the case of precast concrete piles).

(c) The experimental programme undertaken on concrete resistivity indicates that characteristic similarities can be observed only for piles cast on the same day. Alternatively, when the resistivity of the concrete is not changing rapidly (i.e. after 30 days) then several days interval between testing will not significantly change the E-R curves and, as a result, they can be compared.

(d) The pile-current electrode distance is governed by the space limitations of the particular site. It has been shown that the pile-current electrode distance should be kept to within a few metres of the pile head, and once this distance has been decided upon should be kept the same throughout the testing programme. Large pile-current electrode distance should be avoided as anomalies may be due to deeper geological features which would not adversely affect pile performance.

(e) Resistance readings close to the pile head are more important than those distant. Work to-date indicates that faults in the pile shaft will have a greater influence on resistance readings close to the pile head.

(f) Neighbouring piles have a negligible influence on the E-R curve for a pile. In the case where piles are very close (approximately 2 diameter centre to centre) then the true earthing resistance will be altered, but, since all the piles will be equally affected characteristic similarities can still be observed.

(g) Only the reinforced section of the pile will contribute significantly to the E-R curve for a pile and detection of faults depends on the resistivity contrasts between the non-defective concrete, defective concrete and soil around the pile shaft.

(h) The E-R curves for piles should be plotted as a statisticial set and, from this, a defective pile would be noticed by a displacement of its E-R curve from the norm. If the E-R curve of one pile in the group is displaced it would indicate that the pile shaft is suspect. If, however, several piles within the group are displaced from the norm then it may indicate that the soil around the pile group is suspect. By looking at the overall gradient of the E-R curve then possible deductions can be made as to the nature of the soil around the pile.

(i) The electrical resistivity of clays was investigated and their resistivity characteristics established over a large range of consistency indicies. The general shape of the resistivity versus fractional volume of water curve follow the same shape as the resistivity versus moisture content curve established by other researchers.

(j) The resistivity of soils in their natural state will lie in the upper region to the resistivity/fractional volume of water curve, which implies that changes in moisture content will not materially change the resistivity. This fact, coupled with testing the pile with a high reflection coefficient would mean that expected small fluctuations in ground resisitivity will have little influence on resistance readings.

(k) Weak clay soils or soils with a high clay fraction will have a low resistivity and if such material is present the resistance readings will be changed and will result in a E-R curve with a low gradient.

(l) The resistance at infinity of the pile (based on the apparent resistivity of the material around the pile) can be obtained at a point midway between the pile and the current electrode.

The experimental work on concrete has yielded several important conclusions,

(m) The experimental programmes indicate that conduction of current through moist concrete is primarily through the cement paste and, as such, is related to the rate of hydration of the paste.

(n) The electrical resistivity of concrete is dependent upon the fractional volume of cement paste within the concrete and is thus sensitive to any changes in the cement paste, e.g. increase in water-cement ratio.

(o) A model for the conduction of current through concrete was developed and the experimental work would appear to substantiate the model. From this model, explanations can be made which can explain, for example, the general shape of the resistivity versus time curve and the effect of air voids.

Recommendations for Future Work

Many interesting avenues of research have been opened up as a direct result of the work described in this thesis.

(a) Much of the preliminary research, e.g. laboratory investigation, system methodology has been extensively covered in this thesis, hence future developments must be directed towards site testing. Site testing has been undertaken but more is required, especially different types of piles and different subsoil conditions.

(b) Correlation of load-tests and E-R tests.

(c) Further laboratory investigations could employ a deep electrolytic tank analogue (~1.5m - 2.0m in depth) to investigate a wide range of scale ratios. Also to investigate further the effect of defect size, especially for positive reflection coefficients.

(d) It should be possible to develop further the electrical resistivity characteristics of concrete. Since conduction is primarily through the evaporable water in the cement paste then the

electrical conductivity of concrete is a measure of the degree of hydration of the paste and hence indirectly related to its strength. Electrical methods could possibly be developed for quality control of structural concrete.

REFERENCES

(1) THORBURN, S. and THORBURN, J.Q.
Review of problems associated with the construction of cast-in-place piles.
D.o.E. and C.I.R.I.A. Piling Development Group Report PG2, January, 1977.

(2) WEST, A.S.
Piling Practice.
Butterworths, 1972.

(3) BOBROWSKI, J., BARDHAN-ROY, B.K., MAGIERA, R.H. and LOWE, R.H.
The structural integrity of large diameter bored piles.
Behaviour of piles : Proc. Conf. Inst. Civ. Engrs., London, September 1975, pp 179-184.

(4) ANON.
Testing Halts John Hancock Work.
Engineering News Record, August 19, 1966, p 18.

(5) ANON.
Caisson trouble hits Chicago.
Engineering New Record, 1966, 29th September, pp 14-15.

(6) NEW CIVIL ENGINEER.
Essos giant oil tank - a question of more haste the less speed.
N.C.E. 28th February, 1974, pp 28-38.

(7) BARDHAN-ROY, B.K.
J. Bobrowski and Partners, Private Communication.

(8) FARMER, I.W.
Newcastle University, Private Communication.

(9) TOMLINSON, M.J.
Pile design and construction practice.
Viewpoint Publications (Cement and Concrete Association), 1977.

(10) BAKER, C.N. and KHAN, F.
Caisson construction problems and correction in Chicago.
Jnl. Soil Mechanics and Foundation Division, ASCE, February 1971, pp 417-440.

(11) WELTMAN, A.J.
Integrity testing of piles : a review.
D. o. E. and C.I.R.I.A. Piling Development Group, Report PG4, September, 1977.

(12) McCARTER, W.J.
An investigation into the use of resistivity as a non-destructive testing technique in Civil Engineering construction.
University of Edinburgh, Unpublished B.Sc. Thesis, May, 1977.

(13) MITCHELL, J.M.
Assessing large diameter piles.
The Consulting Engineer, December, 1973, pp 37-39.

(14) C.E.B.T.P.
Integrity testing of piles by sonic coring.
12 rue Brancion, 75737 - Paris 15éme, France.

(15) C.E.B.T.P.
Structure sounding methods by non-destructive tests.
12 rue Brancion, 75737 - Paris 15éme, France.

(16) C.E.B.T.P.
Non-destructive testing of structures and piles.
12 rue Brancion, 75737 - Paris 15 éme, France.

(17) LEVY, J.F.
Sonic pulse method of testing cast-in-place concrete piles.
Ground Engineering, May 1970, Vol.3, No.3 pp 17-19.

(18) GARDNER, R.P.M.
Robert Matthew, Johnson-Marshall and Partners, Private Communication.

(19) PRIESS, K. and CAISSERMAN, A.
Non-destructive integrity testing of bored piles by gamma ray scattering.
Ground Engineering, May 1975, Vol.8, No.3.

(20) PAQUET, J.
Etude vibratoire des pieux en béton. Response harmonique et impulsionnelle. Application au contrôle.
Annals. Inst. Tech. Bâtim. 21st year, No.245, June, pp 789-803.

(21) MENOU, J. and VENEC, Y.
Contrôle de la continuité des pieux par la méthode d'auseltation dynamique.
Bull. Liaison Labo. Routiers P. et Ch. 44, March-April, 1970.

(22) STEINBACH, J.
Caisson evaluation by the stress wave propagation method.
Illinois Institute of Technology, Ph.D. Thesis 1971.

(23) STEINBACH, J. and VEY, E.
Caisson evaluation by the stress wave propagation method.
Jrnl. of the Geotechnical Division, A.S.C.E. April 1975, 101 (No.GT4) pp 361-378.

(24) WHITTINGTON, H.W., FEGEN, I. and FORDE, M.C.
Signal processing of ultrasonic pulses for non-destructive testing of concrete piles.
Proc. Conf. Ultrasonics International, Graz, Austria, May 1979, pp 351-359.

(25) FEGEN, I., FORDE, M.C. and WHITTINGTON, H.W.
The detection of voids in concrete piles using sonic methods.
Proc. 4th Int. Conf. on N.D.T., Grenoble, France, Sept. 1979, pp 40-46.

(26) DVOŘÁK, A.
Correlation of static and dynamic pile tests.
Proc. 3rd Asian Regional Conf. on Soil Mechanics and Foundation Engineering, Haifa, 1967, pp 193-195.

(27) DAVIES, A.G. and DUNN, C.S.
From theory to field experience with non-destructive vibration testing of piles.
Proc. Instn. Civ. Engrs. Part 2, 1974, 57, December. pp 571-593.

(28) GARDNER, R.P.M. and MOSES, G.W.
Testing bored piles in laminated clays.
Civil Eng. and Pub. Wks. Rev. May 1972, 67, pp 60-63.

(29) HIGGS, J.S.
Integrity testing of concrete piles by a shock method.
Concrete, October 1979, pp 31-33.

(30) MOON, M.R.
A test method for the structural integrity of bored piles.
Civil Eng. and Pub. Wks. Rev. May 1972, 67, pp 476-480.

(31) GRIFFITHS, D.H. and KING, R.F.
Applied geophysics for engineers and geologists.
Pergamon Press, 1965.

(32) HIGGINBOTTOM, I.E.
The use of geophysical methods in engineering geology.
Ground Engineering, March 1976, Vol 9. No.2, pp 34-38.

(33) BRUCKSHAW, J.M.
Electrical methods of geophysical prospecting.
Jrnl. Inst. Elect. Engrs. 1933, Vol.73, pp 521-533.

(34) PALMER, L.S.
Examples of geoelectric surveys.
Proc. of Inst. Elect. Engrs. Vol.106, Pt.A, 1959, pp 231-244.

(35) TOMLINSON, M.J.
Foundation Design and Construction.
Pitman Pub. Co., 1969.

(36) McCARTER, W.J., WHITTINGTON, H.W. and FORDE, M.C.
Application of electrical resistivity to integrity testing of concrete load-bearing piles.
Proc. 4th Int. Conf. on N.D.T., Grenoble, France, Sept. 1979, pp 185-192.

(37) HAUSMAN, D.A.
Electrochemical behaviour of steel in concrete.
Jrnl. Amer. Conc. Inst., 1964, Vol.61, No.2, pp 171-188.

(38) HEILAND, C.A.
Geophysical Exploration.
Hafner Pub. Co., 1968.

(39) WENNER, F.
Method of Measuring Earth Resistivity.
N.B.S. Scientific Paper No.258, Vol.12, No.3 (1915-1916), pp 469-478.

(40) KELLER, G.V. and FRISCHKNECHT, F.C.
Electrical Methods in Geophysical Prospecting.
Pergamon Press Inc., New York, 1970.

(41) TAGG, G.F.
Earth Resistances.
George Newnes Ltd., London, 1964.

(42) RYDER, R.W.
Earthing principles and practice.
Pitman and Sons Ltd., 1952.

(43) FINK, G.D. and CARROLL, J.M.
Standard Handbook for Electrical Engineers.
McGraw Hill Book Co., 10th Edition, 1969.

(44) VITKOVITCH, D.
Field Analysis : Experimental and Computational Methods.
D. Van Nostrand Co., Ltd., London, 1966.

(45) WATSON, G.N.
Theory of Bessel Functions.
Cambridge Univ. Press, 1952 (2nd Edition).

(46) KING, L.V.
On the flow of electric current in semi-infinite stratified media.
Proc. Royal Soc., Vol.139, pp 237-277, 1933.

(47) MAXWELL, J.C.
A treatise on Electricity and Magnetism.
Oxford University Press, 1904 (3rd Edition).

(48) GISH, O.H. and ROONEY, W.J.
Measurement of resistivity of large masses of undisturbed earth.
Terr. Magn. and Atmos. Elect., December 1925, Vol. 30, No.4,
pp 161-188.

(49) WHITEHEAD, S. and RADLEY, W.S.
Experiments relating to the distribution of alternating electric current in the earth and the measurement of the resistivity of the earth.
Proc. Phy. Soc. of London, 47, pp 589-614, 1935.

(50) GISH, O.H.
General description of the earth-current measuring system at the Watheroo magnetic observatory.
Terr. Magn. and Atmos. Elect. September 1923, Vol.28, No.3,
pp 89-108.

(51) E.L.E. Limited
Technical literature : Standard A.C. Terrameter.
Hemel Hempstead, Hertfordshire, England.

(52) BAIRE, M.G.
Sur le contrôle de la prise des cements au moyem d'courant électrique.
Revue des Materiaux de Construction et de Travaux Publics (Paris) No.272, 1932, p 182.

(53) PETIN, N., HIGEROVITSCH, M. and GAJSINOVITCH, E.
A study of the setting process of cement paste by electrical conductivity methods.
Jrnl. of Gen. Chem. U.S.S.R., 1932, No.2 pp 614-629.

(54) KIND, V.A. and ZHURALER, V.F.
Electrical conductivity of setting Portland cements.
Tsement, Vol.5, No.9, 1937, pp 21-26.

(55) DORSCH, K.E.
The hardening and corrosion of cement-IV.
Cement and Cement Manufacture, April, 1933, pp 131-142.

(56) BOAST, W.B.
A conductometric analysis of portland cement pastes and mortars and some of its applications.
Jrnl. A.C.I. Vol.33, pp 131-146, Nov-Dec 1936.

(57) MICHELSEN, S.
Beitrag zur Bindezeitbestimmung.
Zement, Vol.22, 1933, pp 457-461.

(58) ASCHAN, N.
Determining the setting time of cement paste, mortar and concrete with a copper-lead electrode.
Mag. of Conc. Res., Vol.18, No.56, Sept., 1968, pp 153-160.

(59) JESSER, L.
Die ehärtung der zementmörtel-ein electrostatisches phänomen.
Zement, Vol.23, 1934, pp 514-518.

(60) CALLEJA, J.
New techniques in the study of setting and hardening of hydraulic materials.
Jrnl. Amer. Conc. Inst., 1952, Vol.23,7, pp 525-536.

(61) WATERS, E.H.
New techniques in the study of setting and hardening of hydraulic materials.
Jrnl. Amer. Conc. Inst. Vol.24,4, 1952, pp 536-1-10.

(62) MAGUIRE, D. and OLEN, M.
Report on an investigation into the electrical properties of concrete.
Trans. S.A. Inst. of Elect. Engrs. Vol.31,11, November 1940, pp 301-313.

(63) DECOUX, R. and BARREE, J.
Étude de la conductibilité electrique des bétons.
Institut Technique du Batiment et des Travaux Publics.
12 rue Brancion, Paris. Circulaire Série F.No.3, 1st March, 1941.

(64) CIGNA, R.
Measurement of electrical conductivity of cement mortars.
Annali di Chimica, 66, January 1966, pp 482-494.

(65) OHAMA, F.
A research for curing of concrete by means of electricity.
Jap. Soc. Civ. Engrs.,Vol.36, 4, April 1951, pp 186-190.

(66) YAMADA, J.
Studies on concrete electrically heated.
Jap. Soc. Civ. Engrs., Vol.36, 2, February 1951, pp 72-77.

(67) SPENCER, R.W.
Measurement of moisture content of concrete.
Jrnl. Amer. Conc. Inst., 1937, Vol.34, 1, 1937, pp 45-61.

(68) HAMMOND, E. and ROBSON, T.D.
Comparison of Electrical Properties of various cements and concretes.
The Engineer, 1955, Vol.199, January 21, pp 78-80; January 28, pp 114-115.

(69) GANIN, V.P.
Electrical resistance of concrete as a function of its composition.
Beton i Zhelezobeton, No.10, 1964, pp 462-465.

(70) MONFORE, G.E.
The electrical resistivity of concrete.
Jrnl. of the P.C.A. Res. and Develp. Labs., May, 1968, pp 35-48.

(71) HENRY, R.L.
Water vapour transmission and the electrical resistivity of of concrete.
Technical Report, R314 (U.S. Naval Civ. Engng. Lab., Port Hueneme, California, 25 June 1964).

(72) FARRAR, J.R.
Electrically conductive concrete.
G.E.C. Jrnl. of Sci. and Tech., Vol.45, 1, 1978, pp 45-48.

(73) NIKKANNEN, P.
On the electrical properties of concrete and their application.
Valtion Teknillinen Tutkimuslaitos, Tiedotus, Sarja III Rakennus 60, 1962. (In Finnish with English summary).

(74) HANCOX, N.L.
An electrical measurement of the effective cross-sectional area for conduction or flow processes in cement paste.
Mag. Conc. Res., Vol.20, No.64, September 1968, pp 171-175.

(75) SAUER, M.C., SOUTHWICK, P.R., SPIEGLER, K.S. and WYLLIE, M.R.J.
Electrical conductance of porous plugs.
Industrial and Engng. Chemistry, Vol.47 (Oct) 1955, pp 2187-2193.

(76) SACHS, S.B. and SPIEGLER, K.S.
Radiofrequency measurements of porous plugs.
Jrnl. of Phy. Chem. (Ion Exchange Resins Solution Systems),
Vol.68(1) 1964, p 1214.

(77) WHITTINGTON, H.W.,McCARTER, W.J. and FORDE, M.C.
The conduction of electricity through concrete.
Mag. Conc. Research Vol.33. No.114. March 1981 pp 48-60.

(78) McCARTER, W.J., FORDE, M.C. and WHITTINGTON, H.W.
Resistivity characteristics of concrete.
Proc. Inst. of Civ. Engrs., Pt.2, March, 1981, Vol. 71, pp 107-117.

(79) DOBRIN, M.B.
Introduction to Geophysical Prospecting.
McGraw-Hill Book Co., 1960 (2nd Edition).

(80) NEVILLE, A.M.
Properties of Concrete
Pitman Pub. Co. (1972).

(81) WYLLIE, M.R.J. and GREGORY, G.H.F.
The generalised Kozeny-Carmen equation - Part 2, a novel
approach to problems of fluid flow.
World Oil, April, 1958, 146, 5, pp 210-228.

(82) SELIGMAN, P.
Nuclear Magnetic resonance studies of water in hardened cement paste.
Jrnl. of P.C.A. Res. and Devel. Labs., January 1968, pp 52-65.

(83) RAYLEIGH, LORD.
On the influence of obstacles arranged in rectangular order upon the properties of a medium.
Phil. Mag., 1892 , 34, p 481.

(84) FRICKE, H.
The electric conductivity and capacity of disperse systems.
Physics, 1931 , 1, pp 106-115.

(85) FRICKE, H.
The electric conductivity of a suspension of homogeneous spheriods.
Physics Review, Vol.24, 1924, pp 678-681.

(86) FRICKE, H. and MORSE, S.
An experimental study of the electrical conductivity of disperse systems. I. Cream.
Physics Review, Vol.25, 1925, pp 361-367.

(87) SLAWINSKI, A.
Conductivity of an electrolyte containing dielectric bodies.
Jrnl. de Chemie Physique, Vol.23, 1926, pp 710-727.

(88) ARCHIE, G.E.
The electrical resistivity log as an aid in determining some reservoir characteristics.
Trans. A.I.M.E., 1942, 146, pp 54-62.

(89) PIRSON, S.J.
Factors which affect true formation resistivities.
Oil and Gas Journal. 1947, 46, Nov., pp 76-81.

(90) ATKINS, E.R. and SMITH, G.H.
The significance of particle shape in formation resistivity factor-porosity relationships.
Trans. Amer. Inst. Mining Engrs. 1961, 222 pp 285-291.

(91) WINSAUER, W.O., SHEARIN, H.M., MASSON, P.H. and WILLIAMS, M.
Resistivity of brine-saturated sands in relation to pore geometry.
Bull. A.A.P.G., 1952, 36,2, pp 253-277.

(92) Aggregates from natural sources for concrete (including granolithic).
B.S. 882, 1201, Part 2,1973.

(93) MITCHELL, J.K.
Fundamentals of Soil Behaviour.
John Wiley & Sons, Inc., N.Y. 1976.

(94) ATTEWELL, P.B. and FARMER, I.W.
Principles of Engineering Geology.
Chapman and Hall Ltd., London, 1976.

(95) McCOLLUM, B. and LOGAN, K.H.
Electrolytic Corrosion of Iron in Soils.
Bureau of Standards Technologic. Paper No.25.

(96) HIGGS, P.J.
An investigation of earthing resistances.
Jrnl. Inst. Elect. Engrs. 1930, Vol.68, pp 736-750.

(97) SMITH-ROSE, R.L.
Electrical measurements on soil with alternating current.
Jrnl. Instn. of Elect. Engrs., Vol.75, 1934, pp 221-237.

(98) SMITH-ROSE, R.L.
The electrical properties of soil at frequencies up to 100 megacyles/sec. with a note on the resistivity of soil in the UK.
Proc. Phy. Soc. of London, Vol.47, 1935, pp 923-931.

(99) SMITH-ROSE, R.L.
The electrical properties of soil for alternating currents at radio frequencies.
Proc. Royal Soc., Vol.140, 1933, pp 359-377.

(100) CAMPBELL, I.
An investigation into the variation of resistivity with moisture content and compaction.
University of Edinburgh, Unpublished B.Sc. Thesis, May 1976.

(101) CRONEY, D. and COLEMAN, J.D.
Pore pressure and suction in soils.
Butterworths, 1961.

(102) CARPENTER, E.W.
Application of electrical resistivity for the determination of depths to geological horizons.
Leeds University, Ph.D. Thesis, 1955.

(103) KĚZDI, A.
Handbook of soil mechanics: soil physics.
Elsevier Pub. Co., London, 1974.

(104) ROAD RESEARCH LABORATORY
Soil mechanics for road engineers.
H.M.S.O. (London), 1957.

(105) SOILTEST INC.
The earth-resistivity manual.
Soiltest Inc., 2205 Lee Street, Evaston, Illinois.

(106) BURNETT, W.R.
The Earth-Resistivity method of geophysical surveying.
Heriot-Watt University, Ph.D. Thesis, 1953.

(107) LYNAM, J.T.
Techniques of geophysical prospecting as applied to near surface structure determination.
Bradford University, Ph.D. Thesis, 1970.

(108) WIGHTMAN, W.E.
The use of the resistivity method in shallow depth mineral prospecting.
Leeds University, Ph. D. Thesis, 1971.

(109) SANDER, K.F. and YATES, J.K.
The accurate mapping of electric fields in an electrolytic tank.
Proc. Inst. Elect. Engrs. Pt. II, Vol.100, pp 167-183, 1953.

(110) RIMES, R.E.
Some aspects of earthing.
Post Office Elect. Engrs. Jnl., October 1947, 40, pp 130-134.

(111) MALLOT, D.F.
The application of geophysics to highway engineering in Michigan.
Highway Research Record, No.81, 1965, pp 20-41.

(112) BENJAMIN, J.R. and CORNELL, C.A.
Probability, Statistics and Decision for Civil Engineers.
McGraw-Hill Book Co.,1970.

APPENDIX 1

A NOTE ON SAMPLING FROM A POPULATION

A note on sampling from a population

Load testing piles at random on a site corresponds to sampling without replacement and the probability of finding a given number of defective piles in the sample is obtained from the hypergeometric distribution,

$$P(x) = \frac{\begin{bmatrix} M \\ x \end{bmatrix} \begin{bmatrix} N-M \\ n-x \end{bmatrix}}{\begin{bmatrix} N \\ n \end{bmatrix}} \qquad \ldots\ldots \text{(A .1)}$$

where,

N = number of piles on site,

M = number of N which are defective,

n = number of load-tests carried out,

x = number of defective piles found in sample size, n.

Table A1.1 shows the probability of selecting at least one defective pile on a site of 100 piles containing 2%, 5% and 10% defective units, with various sample sizes.

Equation A .1 gives the probability of exactly x failures and (n-x) successes in the sample of n. The probability of at least one failure in a sample size n is,

$$P(x) = \sum_{r=o}^{x} \frac{\begin{bmatrix} M \\ r \end{bmatrix} \begin{bmatrix} N-M \\ n-r \end{bmatrix}}{\begin{bmatrix} N \\ n \end{bmatrix}} \qquad \ldots\ldots \text{(A .2)}$$

Development and application of Bayesian decision theory to the field of Civil Engineering has been given extensive treatment by Benjamin and Cornell (112).

No. of Piles not meeting Specification	No. of Piles Tested	Probability of selecting at least one defective Pile
2	2	0.0398
2	5	0.0980
2	10	0.1909
5	2	0.0980
5	5	0.2304
5	10	0.4162
10	2	0.1909
10	5	0.4162
10	10	0.6695

TABLE A1.1

APPENDIX 2

CALCULATION OF PROPORTION OF CURRENT FLOWING THROUGH THE CEMENT PASTE IN A CONCRETE

As an example, consider the mix 1:1:2 with a water cement ratio of 0.4 (by weight); the fractional volume of cement paste in this mix is 0.38. The resistivity of a paste with a water cement ratio of 0.4 is 13 Ω-m, while the resistivity of the concrete at the same age is 41.2 Ω-m. Let an average value for the resistivity of aggregate be 500 Ω-m (perhaps an underestimate). By using a unit cube, then the resistance, R, of each path can be determined by its dimensions and using equation (5.1), i.e.

$$R_{a,b,c} = \rho L/A \qquad \ldots\ldots \text{(A.1)}$$

Referring to Figure A2.1(a) then,

$$R_a = \frac{13 \times 1}{z \times 1}\ \Omega,$$

$$R_b = \frac{500 \times 1}{x \times 1}\ \Omega \text{ and,} \qquad \ldots\ldots \text{(A.2)}$$

$$R_c = \frac{500\ (w)}{y \times 1} + \frac{13(1-w)\Omega}{y \times 1}$$

where the subscripts refer to the path taken.

The equivalent circuit is shown in Figure A2.1(b) and, using simple circuit theory, the resistance, R_m, of the composite model system is given by

$$\frac{1}{R_m} = \frac{1}{R_a} + \frac{1}{R_b} + \frac{1}{R_c} \qquad \ldots\ldots \text{(A.3)}$$

It should be noted that R_m will be numerically equal to the resistivity of the composite system as a unit cube is assumed, thus R_m will have a value of 41.2 Ω-m units. For practical purposes path (b) can be

neglected as the surfacearea at the point of contact between the aggregate particles will be very small resulting in a very high contact resistance. Consequently, using (A.2) and (A.3) above,

$$\frac{1}{41.20} = \left(\frac{13}{z}\right)^{-1} + \left(\frac{500w}{y} + \frac{13(1-w)}{y}\right)^{-1} \quad \ldots\ldots \text{(A.4)}$$

Furthermore,

$$(1-w)y + z.1 = 0.38 \quad \ldots\ldots \text{(A.5)}$$

and

$$z + y = 1.0$$

Substituting equation (A.5) into (A.4) results in,

$$\frac{1}{41.20} = \frac{z}{13} + \frac{(1-z)^2}{500(0.62) + 13(0.38-z)} \quad \ldots\ldots \text{(A.6)}$$

Solving (A.6) gives a value of z equal to 0.295 thus approximately 77% of the paste is available for path (c). The proportion of the total current flowing through each branch of the network is $R_m/R_{a,b,c}$, resulting in 93% of the current being conducted through the continuous interstitial path.

By assuming different values of w,x,y and z and using the simplified model, the overall resistance and hence the resistivity of the model can be computed. For resistivities to lie in the region of concretes, most of the current will pass through the cement paste i.e. through the path of least resistance.

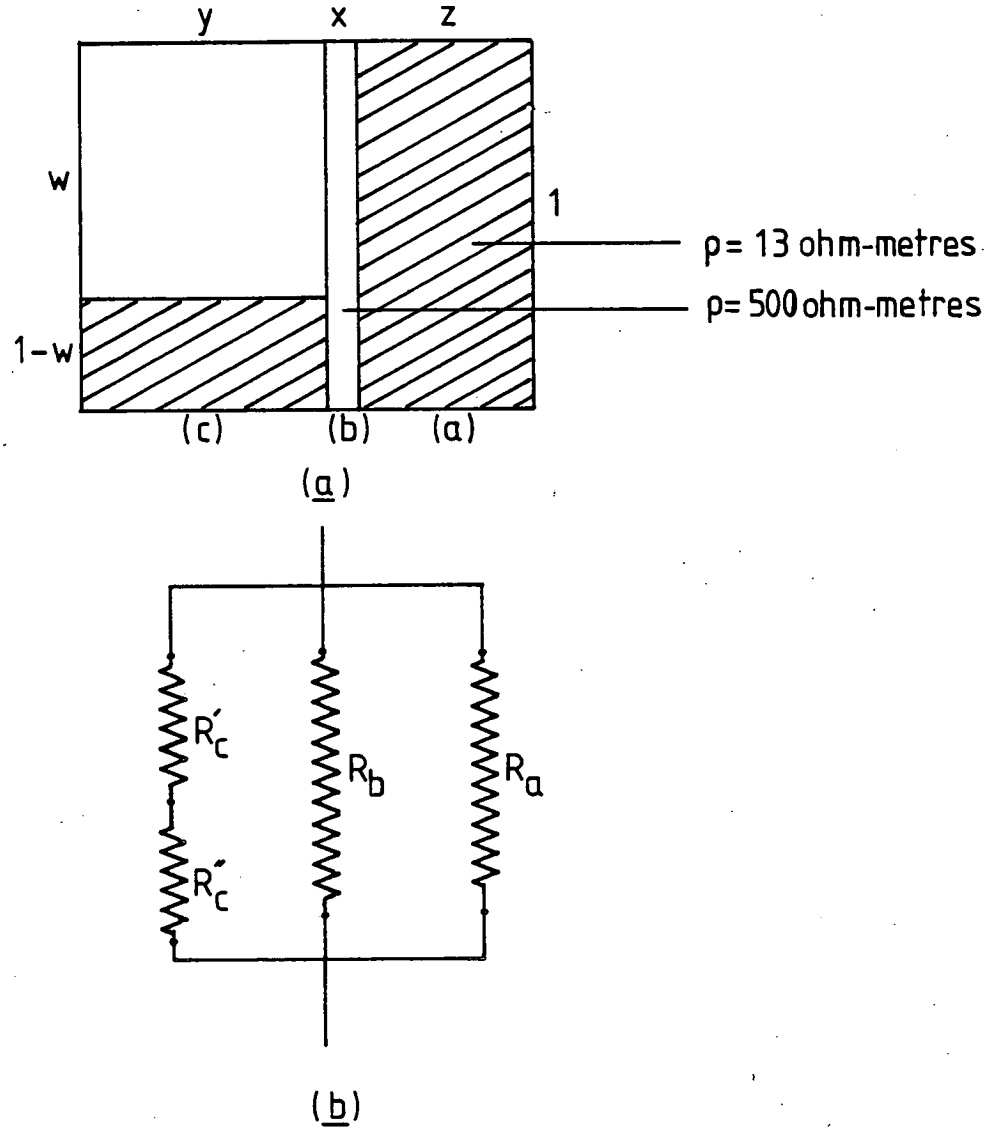

FIG. A2.1 (a) Resistivity of constituents of concrete and
(b) the equivalent electrical circuit